Developing Novel Technologies to Model the Effects of Therapies on Microbial Biofilms

Jennifer Adams

BSc, MSc

Advanced Therapies Group

Thesis presented for the degree of Doctor of Philosophy

2023

Acknowledgments

Firstly, I would like to express my gratitude and thanks to my supervisors Professor David Thomas, Dr. Katja Hill and Dr. Manon Pritchard. Thank you for your never-ending support, advice, and guidance that you have provided throughout my PhD both inside and outside of the lab, for making me be a better scientist, and for pushing me to get to the end. I would also like to acknowledge Algipharma AS and KESS2 for funding my PhD and allowing me to pursue my research.

I am thankful to everyone at Cardiff University who have always been there if I needed any help and to all my colleagues and friends within the ATG group; Jing, Priyanka, and Ghaida – special thanks to Dr. Lydia Powell for all your help with the confocal and in getting my first paper published! A million thanks to Dr. Joana Stokniene and Dr. Wenya Xue both for your help in the lab when I first started and throughout my PhD, and for your companionship in the office and the laughter we shared.

I would like to acknowledge the work of others who have helped me with experiments presented in this Thesis – Dr. Lydia Powell for setting up the permeabilisation assay (Chapter 2), Dr. Chris von Ruhland for the TEM imaging (Chapter 2), Dr. Georgina Menzies for the FTIR analysis (Chapter 3), and Dr. Anne Tøndervik for the ATP cell viability assay set up (Chapter 3).

To Brogan, Ella, and Justine - I will forever cherish the joy and the laughter that your friendship has brought to my life. Thank you for always being there to support me throughout the lows and celebrating with me all the highs. Thank you to my family for their support– I couldn't have done it without you. And many thanks to Josh, Eva, and Freddie(!) who have helped and supported me in getting this Thesis written in its final months.

Finally, to Dan. Thank you for everything over the last six years. I am eternally grateful for you. I can't wait to see what the next chapter will bring. I love you.

Summary

The development of antimicrobial resistance against multiple antibiotic and antifungal classes in bacterial and fungal pathogens respectively is of global clinical concern. With “last resort” antibiotics and antifungal treatments having associated toxicity issues and with a drying-up of new antimicrobials in the development pipeline, (especially for Gram-negative organisms), the development of novel therapies is urgently needed. OligoG CF-5/20 is a low molecular weight alginate oligosaccharide that has been shown to have antimicrobial and anti-biofilm properties against a range of multi-drug resistant pathogens.

OligoG CF-5/20 was tested against a range of *Candida* spp., in addition to being used as a combination therapy with the antifungal nystatin. Minimum inhibitory concentration (MIC) assays and growth curves showed that OligoG CF-5/20 synergistically enhanced the effect of nystatin against planktonic cells. Furthermore, confocal laser scanning microscopy (CLSM) and COMSTAT analysis showed that it was also effective at preventing biofilm formation, as well as disrupting established biofilms. This study demonstrated that OligoG CF-5/20 can act as a stand-alone treatment against *Candida* spp., as well as showing enhanced effectiveness when used as a combination therapy with the antifungal nystatin ($P < 0.0001$).

To investigate the contribution of calcium (Ca^{2+})-binding in its antimicrobial activity, G-block (OligoG CF-5/20) and an M-block alginate oligosaccharide (OligoM) with comparable average size (DPn 19) and contrasting Ca^{2+} binding properties (that of OligoG being greater), were compared. The tailored alginate OligoM was shown to be comparable to OligoG CF-5/20 at reducing planktonic and biofilm growth of *P. aeruginosa*; also demonstrating similar reductions in virulence

factor production of pyocyanin ($P < 0.05$), elastase ($P < 0.0001$), and protease ($P < 0.0001$) when tested at 6%. Compared to OligoM, OligoG CF-5/20, exhibited a significantly stronger inhibitory effect on quorum sensing (QS) signaling, and displayed increased potentiation of the antibiotic azithromycin in MIC and biofilm assays. These results with OligoM highlight the fact that the antimicrobial effects of alginate oligosaccharides were not purely dependent upon Ca^{2+} binding.

Colistin is often referred to as the antibiotic of last resort for the treatment of e.g., carbapenem-resistant *Enterobacteriaceae*. The discovery of the plasmid-encoded colistin resistance, *mcr*, and its rapid dissemination into the environment in recent years heralds the risk of a post-antibiotic era. The resistance profiles associated with the *mcr-1* and *mcr-3* genes were apparent in MIC and minimum biofilm eradication concentration (MBEC) assays, and the associated fitness costs of *mcr* plasmid carriage were highlighted in the growth curves with *mcr-1* strains showing significantly lower growth rates than those carrying *mcr-3*. A bead biofilm model was adapted to monitor the stability of *mcr-1* and *mcr-3* genes over time, using isogenic *E. coli* J53 hosts. After serial passage (every 2 days for a month), the *mcr-1* gene was lost by day 23, while the *mcr-3* gene was stably maintained for up to 31 days. CLSM and COMSTAT analysis demonstrated the antibiofilm effect of OligoG CF-5/20 against *mcr* carrying *E. coli* ($P < 0.05$), whilst also showing changes in extracellular polymeric substance (EPS) such as a reduction of proteins ($P < 0.05$) and the release of eDNA.

These results suggest that OligoG CF-5/20 has considerable potential as an antimicrobial agent, either as a stand-alone treatment or in combination with existing therapies, such as colistin or nystatin, to treat multidrug resistant pathogens that are responsible for hard-to-treat chronic infections.

Published papers from Thesis to date

Powell, L.C., **Adams, J.Y.M.**, Quoraishi, S., Py, C., Oger, A., Gazze, S.A., Francis, L.W., von Ruhland, C., Owens, D., Rye, P.D., Hill, K.E., Pritchard, M.F. & Thomas, D.W. 2022. Alginate oligosaccharides enhance the antifungal activity of nystatin against candidal biofilms. *Frontiers in Cellular and Infection Microbiology*. doi: 10.3389/fcimb.2023.1122340.

Powell, L.C., Cullen, J.K., Boyle, G.M., Ridder, T.D., Yap, P., Xue, W., Pierce, C. J., Pritchard, M.F., Menzies, G.E., Abdulkarim, M., **Adams, J.Y.M.,** Stokniene, J., Francis, L.W., Gumbleton, M., Johns, J., Hill, K.E., Jones, A.V., Parsons, P.G., Reddell, P. & Thomas, D.W. 2022. Topical, immunomodulatory epoxy-tiglianes induce biofilm disruption and healing in acute and chronic skin wounds. *Science Translational Medicine* doi:10.1126/scitranslmed.abn3758

Pritchard, MF., Powell, L.C., **Adams, J.Y.M**., Menzies, G., Khan, S., Tøndervik, A., Sletta, H., Aarstad, O., Skjak-Brak, G., McKenna, S., Buurma, NJ., Farnell, D., Rye, P.D., Hill, K.E. & Thomas, D.W. 2023. Structure-activity relationships of low molecular weight alginate oligosaccharide therapy against *Pseudomonas aeruginosa*. *Biomolecules* doi: 10.3390/biom13091366

Abbreviations

3-D	3-Dimensional
3-oxo-C12-AHL	N-(3-oxododecanoyl)-1-AHL
μM	Micromolar
ABC	ATP-Binding Cassette
AFM	Atomic Force Microscopy
AHLs	*N*-acyl Homoserine Lactones
AIs	Autoinducers
ALS	Agglutinin-Like Sequence
AmB-D	Amphotericin B Deoxycholate
AMR	Antimicrobial Resistance
ANOVA	Analysis of Variance
AQs	Alkyl-4-Quinolones
ASL	Airway Surface Liquid
ATCC	American Type Culture Collection
ATP	Adenosine Triphosphate
ATR	Attenuated Total Reflection
A.U.	Arbitrary Unit
BA	Blood Agar
BM2	Basal Medium 2
C4-AHL	N-Butyryl-1-AHL
C4BP	C4b-Binding Protein
C12-AHL	3-Oxo-C12-AHL
C. albicans	*Candida albicans*
C. auris	*Candida auris*
C. glabrata	*Candida glabrata*
C. krusei	*Candida krusei*
C. parapsilosis	*Candida parapsilosis*
C. tropicalis	*Candida tropicalis*

C. violaceum	*Chromobacterium violaceum*
CF	Cystic Fibrosis
CFTR	Cystic Fibrosis Transmembrane Regulator
CFU	Colony Forming Units
CLSI	Clinical and Laboratory Standards Institute
CLSM	Confocal Laser Scanning Microscopy
CMS	Colistimethate Sodium
COL^{R}	Colistin Resistant
COL^{sens}	Colistin Sensitive
CSP	Competence Stimulating Peptide
CTL	C-Type Lectin Receptor
CV	Crystal Violet
CWPs	Cell Wall Proteins
Cyclic di-GMP	Cyclic Diguanylate
CYP51	Cytochrome P450- Dependent Enzyme 14α-Lanosterol Demethylase
dH_2O	Distilled Water
ddH_2O	Double-Distilled Water
DMSO	Dimethyl Sulfoxide
DNA	Deoxyribonucleic Acid
DPn	Degree of Polymerization
E. coli	*Escherichia coli*
eDNA	Extracellular Deoxyribonucleic Acid
EDTA	Ethylenediaminnetetraacetic Acid
EMA	European Medicines Agency
ENaC	Epithelial Sodium Channel
EPS	Extrapolymeric Substance
ESKAPE	*Enterococcus faecium, S. aureus, Klebsiella pneumoniae, Acinetobacter baumannii, P. aeruginosa,* and *Enterobacter* spp.
EtOH	Ethanol

Ex/Em	Excitation/Emission
FDA	Food and Drug Administration
FEV1	Forced Expiratory Volume in 1 Second
Fig	Figure
FTIR	Fourier Transform Infrared Spectroscopy
g	G-force ($g = rpm^2 \times r \times 1.118 \times 10^{-5}$)
GI	Gastrointestinal
GlcNAc	N-Acetylglucosamine
H_2O_2	Hydrogen Peroxide
H	Hour(s)
HAIs	Hospital-Acquired Infections
HCA	Hierarchical Cluster Analysis
HHQ	2-Heptyl-4-quinolone
HPAEC-PAD	High-Performance Anion-Exchange Chromatography with Pulsed Amperometric Detection
ICU	Intensive Care Unit
IFI	Invasive Fungal Infection
IM	Inner Membrane
Inc	Incompatibility
IPA	Propan-2-ol
IQS	Integrated Quorum Sensing
ITC	Isothermal Titration Calorimetry
KO	Knockout
LB	Luria-Bertani
LPS	Lipopolysaccharides
LTA	Lipoteichoic Acids
M	Molar
MATE	Multidrug and Toxin Extrusion
MBEC	Minimum Biofilm Eradication Concentration
MCR	Mobilized Colistin Resistance

MD	Molecular Dynamics
MDR	Multidrug Resistance
MFS	Major Facilitator Superfamily
MHB	Mueller-Hinton Broth
MIC	Minimum Inhibitory Concentration
Mins	Minutes
mM	Millimolar
MOPS	3-[N-Morpholino] Propanesulfonic Acid
MRSA	Methicillin Resistant *Staphylococcus aureus*
MSD	Minimum Significant Difference
MurNAc	*N*-Acetylmuramic Acid
Mw	Molecular Weight
NaCl	Sodium Chloride
NaOH	Sodium Hydroxide
NCAC	Non-*Candida albicans* Candida
Nm	Nanometer
NYS	Nystatin
OD	Optical Density
OM	Outer Membrane
OMPs	Outer Membrane Proteins
O/N	Overnight
P. aeruginosa	*Pseudomonas aeruginosa*
PABA	P-Aminobenzoic Acid
PAMP	Pathogen Associated Molecular Pattern
PBPs	Penicillin-Binding Proteins
PBS	Phosphate Buffered Saline
PCA	Phenazine-1-Carboxyclic Acid
PCR	Polymerase Chain Reaction
PDR	Pan-Drug Resistant
pEtN	Phosphoethanolamine

PG	Peptidoglycan
pH	Power of Hydrogen Concentration
PI	Propidium Iodide
PL	Phospholipase
PMB	Polymyxin B
Pra1	pH-regulated Antigen 1
PQS	*Pseudomonas* Quinolone Signal
PRR	Pattern Recognition Receptor
QS	Quorum Sensing
QSIs	Quorum Sensing Inhibitors
QSM	Quorum Sensing Molecule
QQs	Quorum Quenchers
Ra	Average Roughness
RND	Resistance Nodulation Division
ROS	Reactive Oxygen Species
ROUT	Robust Regression and Outlier Removal
rpm	Revolutions Per Minute
RPMI	Roswell Park Memorial Institute
RT-qPCR	Real-Time Quantitative Polymerase Chain Reaction
SAP	Secreted Aspartyl Proteinases
SAR	Structure Activity Relationship
SEM	Scanning Electron Microscopy
SCV	Small Colony Variant
SD	Standard Deviation
SDA	Sabouraud Dextrose Agar
SEM	Standard Error of the Mean
SMR	Small Multidrug Resistance
Spp.	Species
TEM	Transmission Electron Microscope

TER	TAAB Embedding Resin
TLR	Toll-Like Receptor
TSA	Tryptone Soy Agar
TSB	Tryptone Soy Broth
UV	Ultraviolet
UV/Vis	Ultraviolet/Visible
v/v	% Volume in Volume
VVC	Vulvovaginal Candidiasis
WHO	World Health Organisation
XDR	Extensively Resistant

Table of Contents

List of Figures

Chapter 1

Chapter 2

Chapter 3

Chapter 4

List of Tables

Chapter 2

Chapter 4

Supplementary

Chapter 1

General Introduction

1.0 Introduction

The exponential rise in antimicrobial resistance (AMR), combined with the lack of both new antibiotic and anti-fungal treatments currently in development, poses a serious global health issue, resulting in high patient mortality and huge cost implications (Antimicrobial Resistance Collaborators 2022). This situation is compounded by the fact that bacteria in a biofilm state are known to be responsible for the majority of hard-to-treat chronic infections, which confers increased antimicrobial tolerance, adding another layer of complexity to possible patient treatment options. Furthermore, current antifungal treatments for invasive fungal infections are limited by their toxicity, as are current "last resort" treatments for multidrug resistant pathogens, thereby limiting their use. Therefore, there is an urgent demand for less toxic alternatives. This could be achieved through new drug formulations or through the use of combined therapies which could potentially reduce drug toxicity, as well as improving the efficiency of treatments currently in clinical use (Tøndervik et al. 2014).

1.1 Bacterial cell wall

The bacterial cell wall can be broadly categorised into one of two groups, Gram-positive and Gram-negative **(Figure 1.1)**. The major cell wall component of Gram-positive bacteria is a thick layer of peptidoglycan; composed of alternating *N*-acetylglucosamine (GlcNAc) and *N*-acetylmuramic acid (MurNAc) subunits which are cross linked by β-(1-4) glycosidic bonds (Vollmer et al., 2008). Peptidoglycan is essential for a strong, but elastic scaffold, protecting the cell from stress such as osmotic pressure, and dictating the shape of the cell (Scheffers and Pinho 2005). Attached to this peptidoglycan are accessory molecules, such as carbohydrates, teichoic and lipoteichoic acids. Lipoteichoic acid is a polymer that is linked to the cell

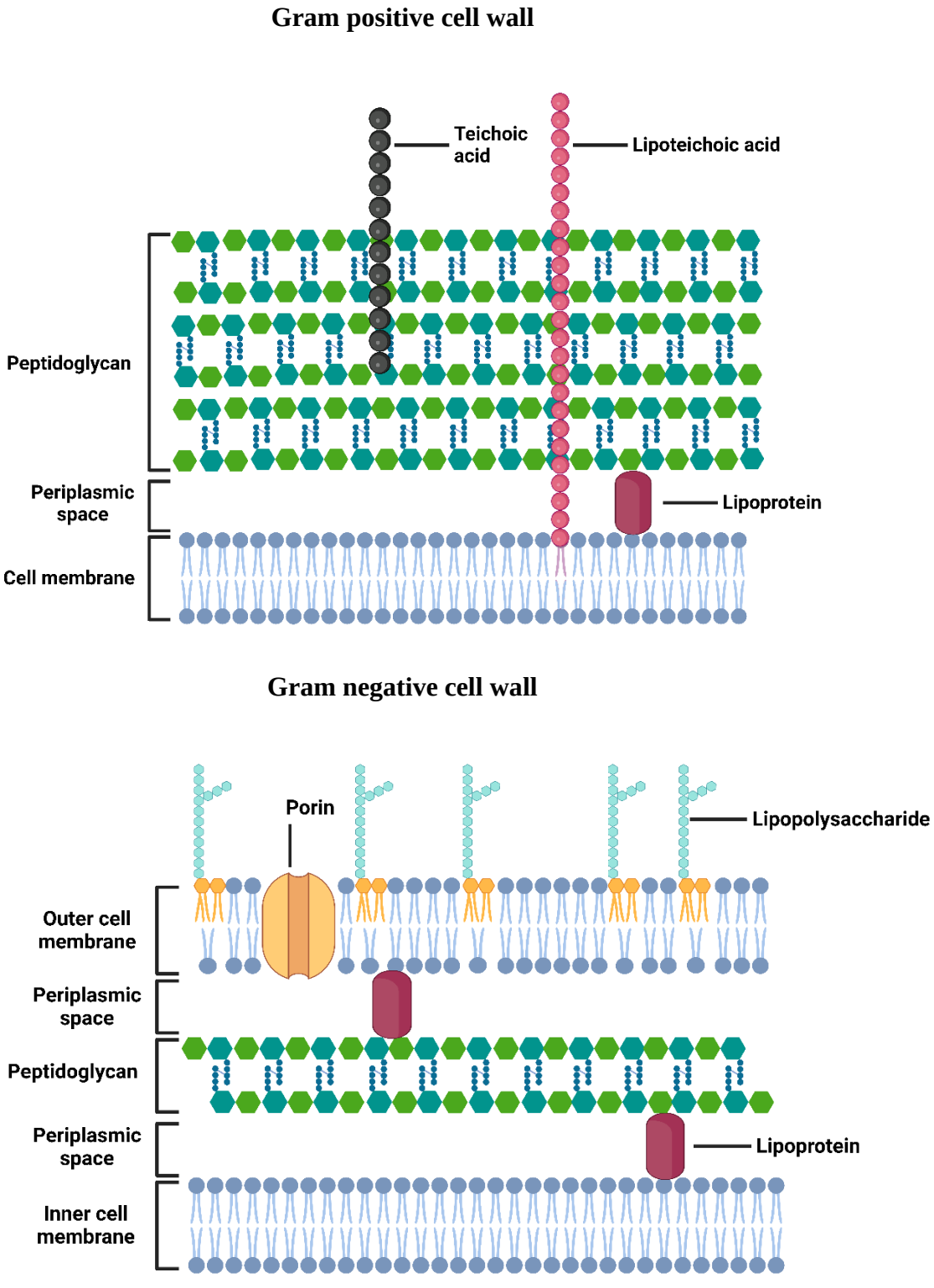

Figure 1.1. Diagrammatic representation of the cell walls of Gram-positive and Gram-negative bacteria.

membrane via a lipid anchor (Percy and Gründling 2014). Similar to Gram-positive bacteria, Gram-negative bacteria also have a peptidoglycan layer, although it is considerably thinner (~3-6 nm thick compared to 10-40 nm) and lies between the inner and outer lipid membrane in the periplasmic space (Scheffers and Pinho 2005; Egan et al. 2017). The Gram-negative cell wall has sufficient physical strength to withstand turgor pressure, and extreme pH, and temperature (Beveridge 1999). It has two membranes; an inner membrane and an outer membrane, while Gram-positives have only one. Situated in the outer membrane of Gram-negative bacteria are outer membrane proteins (OMPs), such as porins, which form pores allowing the uptake of nutrients and the release of waste (Galdiero et al. 2012). These pores are also important for the emergence of antibiotic resistance in pathogenic strains. Lipopolysaccharides (LPS) are present on the surface of the outer membrane, as well as being released into the environment. LPS is made up of three regions: the core polysaccharide, an O-antigen and lipid A. LPS causes an overall negative electrostatic charge on the surface of Gram-negative bacteria, playing a role in adhesion and in the initiation of biofilm formation (Beveridge 1999). Lipid A varies amongst bacterial species and its structure strongly defines the degree of immune activation.

1.2 The antibiotic development pipeline

Although there is an urgent need for new antimicrobials, the number of new drugs currently in development is actually very low. The WHO has stated (as of September 2021), that there are 217 antimicrobial products in preclinical (phase I-III) stages of development (mostly in Western countries with high GDP) and that only 49 of these target the WHO “priority pathogens” (WHO 2021, 2022a). Since 2017, the Food and Drug Administration (FDA) has approved eight new antibiotics, and only a

few new classes of antimicrobials (including oxazolidinone and cyclic lipopeptides), have been introduced into clinical practice targeting Gram-positive pathogens (Coates et al. 2011; Hutchings et al. 2019; Terreni et al. 2021; Chahine et al. 2022).

Despite the prediction that deaths caused by MDR will surpass cancer-related deaths by 2050, many pharmaceutical companies are not focused on antibiotic development. This is due to financial, economic, and regulatory issues compared to other more lucrative treatments, such as anticancer drugs (AMR-review.org 2015). To get a new drug to market, the cost to pharmaceutical companies is estimated to be up to $2.5 billion, taking around 10-15 years to get through clinical trials and into clinic use (Plackett 2020; Wouters et al. 2020; Brown et al. 2022). Consequently, the financial return in investment for companies developing new antibiotics is poor, especially in comparison to other treatments. Ideally, any new antimicrobials effective against MDR pathogens should be saved as "last resort" drugs, meaning that their use should be heavily restricted to ensure that they remain effective, as high prescribing rates contribute to resistance. However, this is not commercially viable, as limiting antibiotic prescribing, ultimately limits the likely financial profit (Luepke et al. 2017).

The increasing length of time taken for new drugs to get to clinical trial, the lack of outside investment and high failure risks are all barriers to new product development. This makes it increasingly difficult for pharmaceutical companies to recoup their costs, so that antibiotic research is no longer viewed as a profitable investment (Nelson 2003). Interestingly however, there are potential alternatives to antibiotics for treating resistance, such as bacteriophage therapies and immunomodulation (Cook and Wright 2022; WHO 2022a).

1.3 Antimicrobials

1.3.1 Discovery

The discovery of penicillin (the first β-lactam antibiotic) in 1928 and its introduction to clinical use in the 1940's, along with the discovery of streptomycin in 1943 (the first aminoglycoside), resulted in the greatest decline in mortality by infectious disease ever witnessed (Fleming 1929; Aminov 2017). This started the "golden age" of antibiotic discovery, with the majority of novel classes of antimicrobials being discovered within a couple of decades. However, since this initial momentum of antimicrobial discovery and development, there has been a steady decline in discovery rates and a worrying lack of new antimicrobials in the development pipeline, referred to as a "discovery void" (Davies 2006).

1.3.2 Antibiotic classification and targets

Antibiotics can be described as having either narrow or broad-spectrum activity and being either bactericidal (if they kill bacteria) or bacteriostatic (if they slow down/inhibit their growth; **Figure 1.2**) (Grada and Bunick 2021). Antibiotics which have a narrow spectrum of activity are specific to certain types of bacteria which they can kill or inhibit. For example, vancomycin is effective against only Gram-positive bacteria including methicillin resistant *Staphylococcus aureus* (MRSA) and *Clostridium difficile*, in comparison broad-spectrum antibiotics, such as amoxicillin (a penicillin derivative) which target a wider range of both Gram-positive and Gram-negative bacteria (Kaur et al. 2011; Álvarez et al. 2016).

Although broad-spectrum antibiotics can treat a wider range of pathogens compared to narrow spectrum antibiotics, which can be beneficial when treating

unknown infections, their widespread use is more likely to select for antibiotic resistance and allow the spread of multidrug resistant pathogens (Cižman and Plankar Srovin 2018; Melander et al. 2018). Furthermore, the indiscriminate use of broad-spectrum antibiotics can lead to disruption of the host microbiome, leading to increased susceptibility to colonisation by pathogens such as *C. difficile*, causing issues with nutrient absorption, diarrhoea, and colitis, thereby leading to higher levels of morbidity and mortality (Sears et al. 2013).

1.3.2.1 Antibiotics targeting cell wall synthesis

Due to the unique composition of the bacterial cell wall, many antimicrobials are specifically able to target it, disrupting its synthesis. The mechanism of action of the β-lactam family of antibiotics (including penicillins, carbapenems, monobactams and cephalosporins) targets cell wall synthesis, ultimately leading to cell death, which occurs via inhibition of the final step of peptidoglycan synthesis (Tooke et al. 2019; Lima et al. 2020). Normal peptidoglycan synthesis involves around thirty enzymes, where typically, penicillin-binding proteins (PBPs) bind to the D-alanyl-D-alanine segment of the GlcNAc peptide chain, allowing cross-linking by glycine residues between the glycan chains, which are then incorporated into the growing peptidoglycan structure forming the cell wall (Sauvage et al. 2008; Bush and Bradford 2016). The antibiotic β-lactam ring mimics the D-alanyl D-alanine segment, so is able to bind PBPs, interrupting terminal transpeptidation and, effectively terminating the final steps in the peptidoglycan synthesis pathway (Kapoor et al. 2017). Glycopeptides (such as vancomycin) similarly also inhibit cell wall synthesis. However, the target molecule is different to β-lactams, as it binds directly to the D-alanyl D-alanine

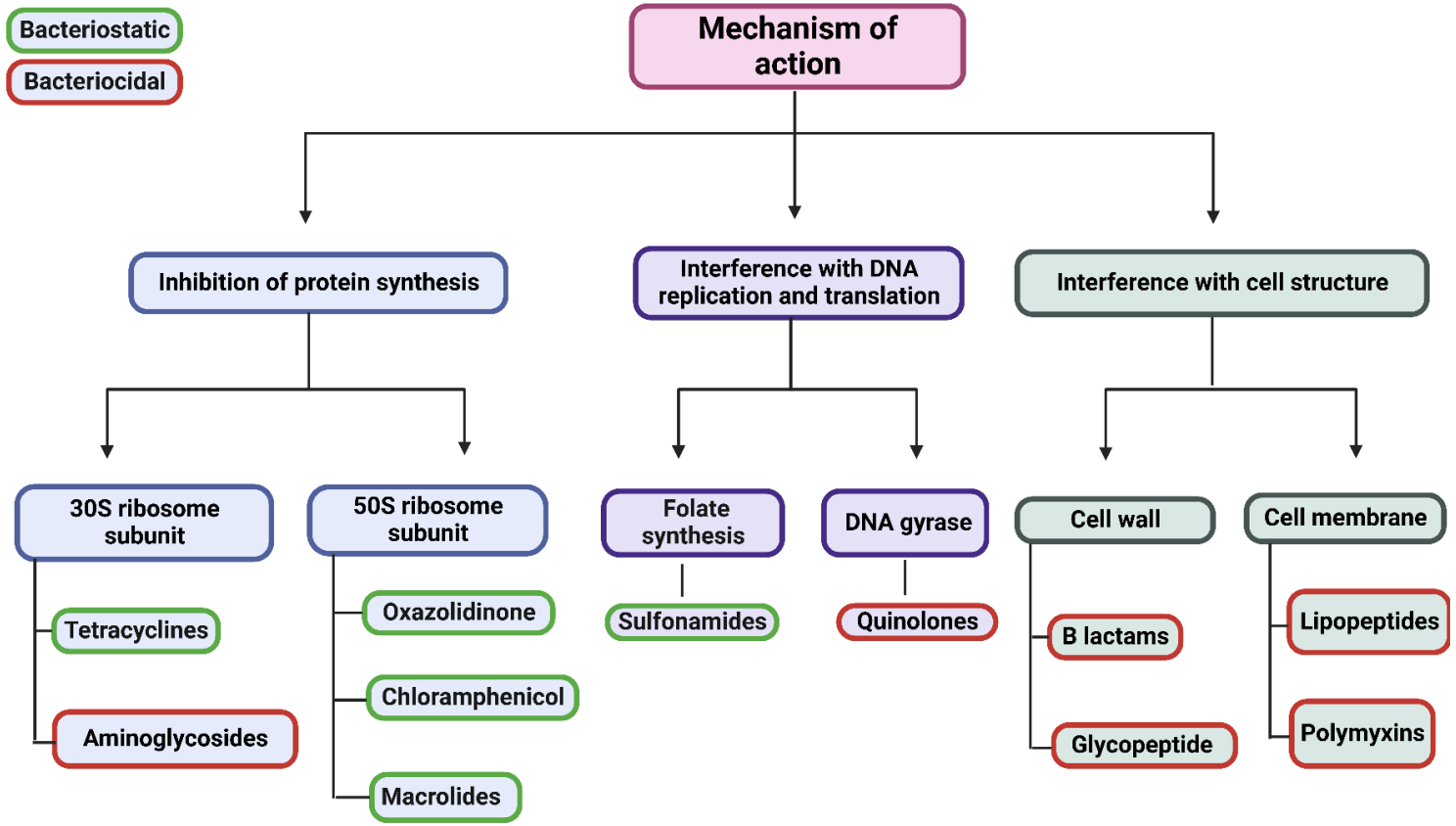

Figure 1.2. The mechanism of action of different classes of antibiotic.

in the peptidoglycan precursor, forming hydrogen bonds and sequestering it, thereby shielding the peptide from transpeptidase activity (Jovetic et al. 2010; Zeng et al. 2016; Acharya et al. 2022).

Daptomycin is a thirteen amino acid cyclic polypeptide belonging to the lipopeptide class of antibiotics that also targets the bacterial cell membrane (Bush 2012). Both Ca^{2+} ions and the phospholipid phosphatidylglycerol are essential for daptomycin activity, with daptomycin complexing with Ca^{2+} to form micelles. When these small micelles come into close proximity with the bacterial membrane, (comprised at least in part of phosphatidylglycerol) its structure is altered, allowing daptomycin to become inserted into it (Miller et al. 2016; Kreutzberger et al. 2017). This insertion into the membrane leads to potassium efflux and rapid membrane depolarization, resulting in cell death (Steenbergen et al. 2005).

Polymyxins, such as polymyxin E (colistin), also target the bacterial (Gram-negative) cell membrane. In this case, the cationic peptide region of colistin binds to the LPS, while the hydrophobic fatty acid tail interacts with the lipid A component of bacterial LPS, displacing divalent cations, leading to outer membrane permeabilisation and subsequent cell death (Andrade et al. 2020).

1.3.2.2 Inhibitors of nucleic acid synthesis

Folate, (the natural form of vitamin B9), is important for many cellular processes in bacterial cells, including DNA synthesis and methylation, as well as DNA repair (Sobczyńska-Malefora and Harrington 2018). Sulfonamides are analogues of p-aminobenzoic acid (PABA), which can competitively inhibit dihydropteroate synthetase, an enzyme essential for dihydropteroic acid production (and similarly

dihydrofolic acid and tetrahydrofolic acid synthesis), Hence, sulfonamides directly inhibit DNA replication, stopping both cell growth and division (Ovung and Bhattacharyya 2021).

1.3.2.3 Inhibitors of protein synthesis

Protein synthesis in eukaryotes occurs on ribosomes with 40S and 60S subunits, while in prokaryotes this occurs on 30S and 50S ribosome subunits. Tetracyclines are broad-spectrum protein synthesis inhibitors. They target the 30S subunit, preventing binding of aminoacyl tRNA to the acceptor site on the ribosome, resulting in failure of protein chain elongation and synthesis (Shutter and Akhondi 2022). Aminoglycosides similarly bind to the 30S subunit (specifically the A site on the 16S ribosomal RNA), promoting incorrect protein translation and assembly, resulting in production of faulty proteins which are then released to cause cell damage (Krause et al. 2016).

The 50S ribosome subunit is also the target of several antibiotic classes including, oxazolidinones, chloramphenicol and macrolides. Oxazolidinones bind to the 23S portion of the 50S subunit, preventing protein synthesis at a very early stage, whilst also preventing formation of the 70S initiation complex (Foti et al. 2021). Chloramphenicol prevents chain elongation through inhibition of peptide bond formation (Dinos et al. 2016). Macrolides also bind to the 23S portion of the 50S subunit, although they prevent protein synthesis through inhibition of transpeptidation or the translocation step, leading to premature detachment of incomplete peptide chains (Uddin et al. 2021).

1.4 Multidrug resistant pathogens

Antimicrobials are used in many aspects of life, with animal husbandry, veterinary medicine, and the medical industry each using tonnes of antibiotics each year (Ventola 2015). The overuse of antibiotics has been a huge contributing factor to the observed rise in levels of bacterial resistance, with the emergence of MDR pathogens, such *Staphylococcus aureus* and *Pseudomonas aeruginosa,* becoming increasingly more prevalent.

Bacteria can be classed as multidrug resistant (MDR), extensively resistant (XDR) or pan-drug resistant (PDR; i.e. showing resistance to all antibiotic classes). This creates huge limitations as to which antimicrobial agent can be used for treatment of specific MDR bacteria (Magiorakos et al. 2012). Rapidly emergent MDR pathogens pose a global threat to public health, with a recent government review predicting that by the year 2050, 10 million people annually will die from antimicrobial resistance (AMR), at an estimated cost to the economy of $100 trillion (O'Neill 2014). There is, therefore, a pressing need to develop new antibiotics to keep ahead of the development of AMR.

The so called "ESKAPE" pathogens (*Enterococcus faecium*, *S. aureus, Klebsiella pneumoniae, Acinetobacter baumannii, P. aeruginosa*, and *Enterobacter* spp.) display high levels of MDR, limiting treatment options for patients with ESKAPE pathogen infections. They are responsible for substantial numbers of hospital-acquired infections (HAIs), contributing significantly to patient mortality and morbidity. Hence, they have 'priority' status, to which new antimicrobial agents should be urgently targeted. New products in the antibacterial drug pipeline are currently

directed against the top three pathogens namely, *P. aeruginosa*, *S. aureus* and *Mycobacterium tuberculosis* (WHO 2021).

1.4.1 Intrinsic antibiotic resistance

Antimicrobial resistance can occur intrinsically as part of the normal characteristics that bacteria may already possess (**Figure 1.3**). This can be mediated by the bacterial outer membrane (stopping hydrophobic compounds from entering), active efflux (transporting the drug out of the Gram-negative cell outer membrane), or additional genes/genetic loci already within the host cell which contribute to this phenotype rendering them immune to the mechanism of action of a drug (Rosenblatt-Farrell 2009; Cox and Wright 2013). *Pseudomonas* spp. are a clinical issue due to intrinsic resistance that confers protection from antibiotics. Their outer membrane has low permeability which slows down the uptake of antibiotics, while they also possess enzymes, such as β-lactamases, which inactivate antibiotics and express efflux pumps which can actively remove antibiotics (Alvarez-Ortega et al. 2011). This intrinsic resistance is independent of antibiotic selective pressure and therefore, does not arise as a consequence of antibiotic overuse.

1.4.2 Acquired antibiotic resistance

Antibiotic resistance can also be acquired through random mutations in existing genes leading to the creation of new characteristics (genotypes/phenotypes). The frequency of spontaneous mutations occurring within the chromosome is rare (~1 in 10^6 - 10^9) (Silver 2011). This can be caused by several mechanisms, such as point mutations altering the antibiotic target or bacterial inactivation of the antibiotic through modification, such as hydrolysis (Blair et al. 2015).

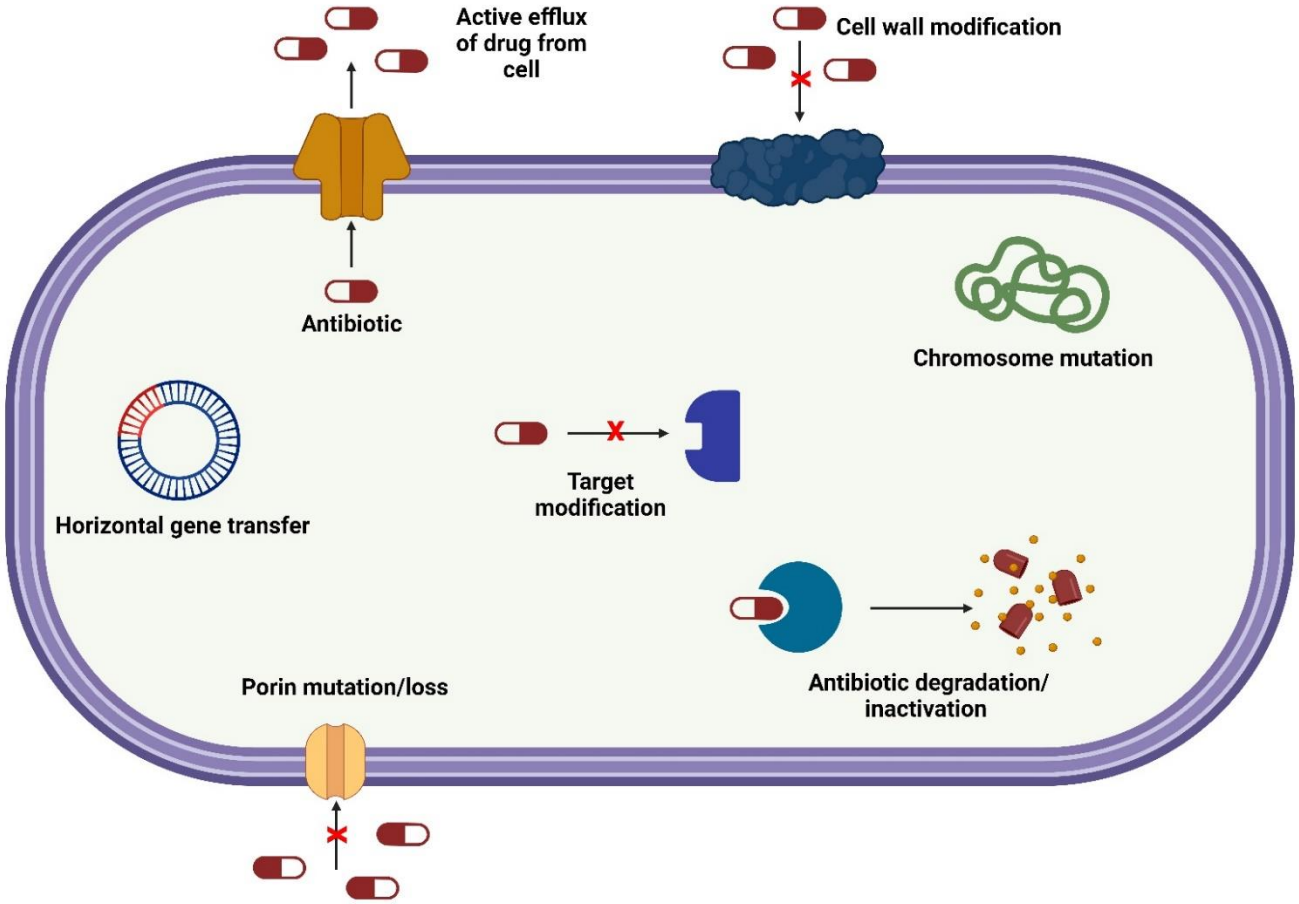

Figure 1.3. Mechanisms of antibiotic resistance in bacteria.

Resistance can also be acquired through the transfer of genetic material. For example, mobile genetic elements, such as transposons or plasmids, can transfer resistance genes via horizontal gene exchange to neighbouring bacteria or indeed, the whole biofilm population (van Hoek et al. 2011). Plasmid-mediated colistin resistance through mobilised colistin resistance (*mcr*) genes has been noted in recent years, with their ability to be disseminated worldwide through horizontal transfer posing a severe global threat to last resort antibiotics (Hussein et al. 2021).

The main mechanisms of horizontal gene transfer are conjugation, transformation, and transduction. Conjugation requires cell-to-cell contact (for example through adhesins or a pilus), that allows the transfer of plasmid DNA from a donor to a recipient cell through a formed pore (Graf et al. 2019). The transfer machinery for this to occur is encoded by the conjugative plasmid itself. Transformation is the process, whereby a competent cell (a cell that has the ability to uptake foreign DNA) takes up naked DNA from the surrounding environment and integrates it into their own chromosome or into its cell, in the case of plasmid recircularization in the new host (von Wintersdorff et al. 2016). *Streptococcus* spp. can produce a competence stimulating peptide (CSP) encoded by the *comCDE* operon and is released in response to environmental stress and cell density, and aids in inducing bacteria competent by binding to receptors (Baig et al. 2021). *Streptococcus* spp. use the CSP as a virulence factor, allowing the formation of MDR persisters and affecting the formation of biofilms with mutants producing biofilms with a reduced biomass and less structural architecture compared to wild types (Leung et al. 2015; Matsumoto-Nakano 2018).

Phage-mediated transduction is the transfer of DNA by bacteriophage. Generalised transduction occurs when DNA has been up taken from a previously infected host and packaged in the phage capsid before delivering it to a recipient cell through lysis, with homologous recombination facilitating the transfer of resistance and virulence genes into the new host genome (Colavecchio et al. 2017). Specialised transduction is more limited and is only able to transfer specific sets of genes (Chiang et al. 2019).

1.5 Biofilms

A biofilm is a natural state that bacteria can exist in which is distinct from their free-living planktonic lifestyle. It can be described as communities of microbes attached to a surface and encapsulated in a self-produced extracellular polymeric substance (EPS) matrix (Mann and Wozniak 2012). Biofilms are found in the environment on both natural (rivers and streams) and nosocomial surfaces such as on domestic appliances, on the teeth as dental plaque, on indwelling medical devices and on live tissue (Gattlen et al. 2010). *P. aeruginosa* has previously been described as the model organism for biofilm formation **(Figure 1.4)** (Mann and Wozniak 2012). The transition of a planktonic cell to a biofilm state involves the expression of adhesins, allowing for attachment to a surface and the production of EPS (Fazli et al. 2014). During the formation of a biofilm, bacteria can change their phenotypic and genotypic characteristics in response to environmental conditions, resulting in development of a mature biofilm which can be genetically distinct from its isogenic planktonic cells. Biofilms are often made of heterogeneous species, rarely being formed from one species of bacteria (Costerton et al. 1995). Biofilms often form in the periodontal pocket leading to inflammation and damage to the surrounding tissue,

more than 700 different species of bacteria have been found in the oral cavity (Zijnge et al. 2010). In polymicrobial chronic wounds it has been found that *S. aureus* mainly colonises the upper region closer to the surface while *P. aeruginosa* colonises deeper regions (Fazli et al. 2009).

1.5.1 Stages of biofilm development

1.5.1.1 Conditioning film

The formation of a conditioning film is considered the first step in biofilm formation. The conditioning film is comprised of organic and inorganic particles. The surface conditions including charge, roughness and hydrophobicity are altered, due to the adsorption of molecules onto the substrate which favours bacterial attachment and allows the start of biofilm formation (Lorite et al. 2011). This surface conditioning can occur in the bloodstream when a catheter is inserted, or in the saliva on dentures with the particles providing nutrients for the microbial cells (Dunne 2002; Garrett et al. 2008). In oral plaque, this is referred to as the acquired pellicle (Marsh et al. 2016).

1.5.1.2 Attachment and adhesion

When planktonic bacteria are brought into close contact with the target (<1 nm), they interact with the conditioning film. This initial attachment is determined by weak, non-specific interactions including van der Waals forces and hydrogen bonds. This attachment is loose and is reversible by gentle rinsing, although the presence of bacterial flagella can greatly improve the chances of successful attachment and adhesion, as they allow bacteria to come into close proximity, overcoming repulsive forces of both the bacterium and the target surface (Donlan 2001; Dunne 2002).

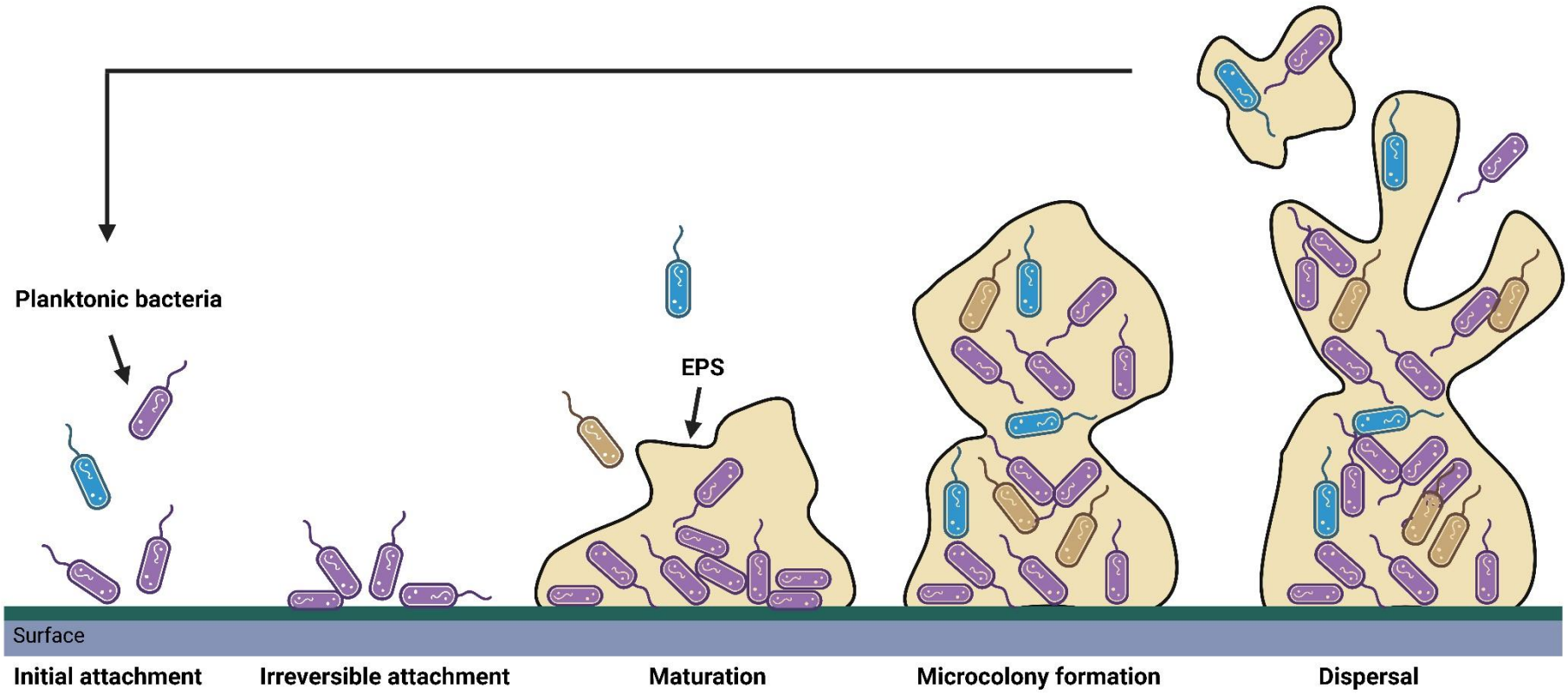

Figure 1.4. Diagrammatic representation of the various stages of biofilm formation on a surface.

Adhesion is an irreversible attachment step and is mediated through specific mechanisms, such as pili, flagella, bacterial surface proteins and ligands, which allow the bacteria to firmly anchor to the surface. It has also been suggested that the signalling second messenger molecule, cyclic diguanylate (cyclic di-GMP), has a role in bacteria 'sticking' to surfaces and transforming from a motile to a sessile state (Prüß 2017). In a biofilm state, higher levels of cyclic di-GMP are observed which leads to suppression of flagellar synthesis and increases matrix production (Römling et al. 2013).

1.5.1.3 Maturation and microcolony formation

Once firmly bound, bacteria replicate, spreading upwards and outwards forming intricate 3-dimensional (3D) "mushroom like" clusters, termed microcolonies, with a variety of different shapes ranging from "mushroom like" to "corn cobs" with numerous water channels, which allow nutrients to move deep within a biofilm (Garrett et al. 2008; Zijnge et al. 2010). An increase in the synthesis of EPS, including extracellular DNA (eDNA), proteins, polysaccharides, and glycolipids (which make up the biofilm matrix) is also seen, which acts as a scaffold for biofilm formation, keeping cells in close proximity to each other and allowing cell-cell interactions (Flemming et al. 2007; Flemming and Wingender 2010). Extracellular polysaccharides make up a majority of bacterial EPS, which are species-specific. For example, *P. aeruginosa* produces alginate, an exopolysaccharide which is over overproduced when the *mucA* gene is mutated leading to a mucoid phenotype. *Pel* and *Psl* are both required for biofilm formation in non-mucoid *P. aeruginosa*, encoding a mannose- and a glucose-rich exopolysaccharide, respectively (Ramsey and Wozniak 2005; Price et al. 2020).

Depending on species composition, the microcolony can be composed of 75-90% EPS matrix and 10-25% bacterial cells, with the matrix material being densest closest to the core (Costerton 1999). This EPS coating provides protection of cells in a biofilm state from disinfectants and antimicrobials (Zhao et al. 2016). During this stage of maturation, other secondary species of bacteria and other planktonic bacteria can co-aggregate to the biofilm through interactions between specific adhesions and receptors (Kerr et al. 2003).

1.5.1.4 Dispersal and reversal to planktonic state

Cells can detach from a biofilm by means of sloughing, seeding or erosion which are all thought to be passive processes that may occur due to external shear forces (Faria et al. 2020). Sloughing is the rapid detachment of larger parts of the biofilm in the later stages of biofilm development, whilst seeding refers to the hollowing of microcolonies where cells can escape from the interior, with erosion being the continuous detachment of cells from the biofilm (Kaplan 2010). Cells can also escape through desorption early in the formation process, reversing the attachment of the bacteria to a surface (Petrova and Sauer 2016). A sub-population of cells can be dispersed from the growing biofilm due to quorum sensing signalling molecules, as well as environmental cues, such as temperature and nutrient availability (Guilhen et al. 2017). Interestingly, these dispersed cells can possess distinct phenotypes before reverting back to their planktonic state, with genes which are important for motility being upregulated, while those characteristic of a sessile biofilm lifestyle become downregulated (McDougald et al. 2012). This allows the cells to become disseminated, resulting in their spread to secondary sites, thereby facilitating the

establishment of new biofilms in other locations. This has implications in the spread of infection.

1.5.2 Antibiotic tolerance and resistance of biofilms

Bacteria present in a biofilm can be up to 1000-fold more resistant to individual drug treatment and combination therapy, than when growing in a planktonic state (Mulcahy et al. 2008). There are several hypotheses for the resistance mechanisms in biofilms. The first is that the bacterial cells embedded in an EPS act as a physical barrier slowing down or leading to incomplete penetration or even sequestration of the antibiotic deep within the biofilm (Mah 2012). The second is that microenvironments may arise within the biofilm associated with differences in pH or oxygen depletion which may alter the activity of the antibiotic (Stewart 2002). Lastly, nutrient and oxygen limitation may cause the cells to go into a 'dormant but culturable state', described as a hibernation state with decreased metabolic activity (Lambert 2002). As most antibiotics act on actively growing cells, they are ineffective against such cells which are not metabolically active, called persister cells (Høiby et al. 2010a). Multi-species biofilms also allow survival through interspecies interactions increasing the collective tolerance of the biofilm to treatment. For example, *P. aeruginosa* can inhibit the growth of *S. aureus*, therefore increasing its tolerance against the action of vancomycin, while *S. aureus* promotes aggregation and alters the biofilm structure, providing protection against tobramycin (Zhang and Cheng 2022).

Biofilms can form on indwelling medical devices, such as implants and catheters, on teeth as dental plaque, as well as in the lungs of cystic fibrosis (CF) sufferers, resulting in persistent chronic infections. These chronic infections persist despite the host immune response and antimicrobial treatments, contributing to both

AMR and chronic inflammation (Chen and Wen 2011). For indwelling medical devices, this ultimately may require removal and replacement. However, this is not always possible for all cases of persistent infection. Biofilm resistance increases the economic burden on healthcare systems, with AMR infections estimated to prolong hospital stays from 6.4 to 12.7 days and could lead to a decrease of up to 3.5% in world GDP by 2050 (O'Neill 2014; Ventola 2015).

1.5.3 Quorum sensing (QS) systems

Quorum sensing is a cell-density detection system present in bacteria and fungi that allows for coordinated activity and gene expression of a multicellular group through cell-cell communication and detection of signalling molecules (Miller and Bassler 2001). Bacteria release chemical signalling molecules called autoinducers (AIs), which accumulate as cell density increases to a "quorate" threshold concentration, which causes a change in gene expression and allows bacteria to act in unison (Ng and Bassler 2009). Gram-positive bacteria use small (<10 amino acids in length) extracellular peptides as AIs, while *N*-acyl homoserine lactones (AHLs) are the main group of autoinducers released from Gram-negative bacteria (Waters and Bassler 2005). The first quorum sensing molecule discovered in eukaryotes was farnesol. In *C. albicans,* farnesol stops the switch of yeast into their filamentous form. The aromatic alcohol, tyrosol, is another quorum sensing molecule (QSM), which affects morphogenesis and aids biofilm formation as it promotes germ tube and hyphae production (Padder et al. 2018). Other QSM have been identified in fungi, including tryptophol and phenylethanol, that similarly affect morphology, induce apoptosis, and when in combination with antifungal agents show to increase the efficacy of the drug (Wongsuk et al. 2016).

1.5.4 Experimental biofilm models

The effectiveness of new therapies is often performed using laboratory experiments with planktonic bacteria. While the results can reflect what may happen during an acute infection, in many chronic diseases (e.g., CF), where most of the bacteria are in a sessile biofilm form, a biofilm model may be more representative of antimicrobial therapies, as well as the development and diversity of chronic infections (Steenackers et al. 2016). Long-term evolutionary models reproduce many of the characteristics seen in CF patients, with cells being exposed to antibiotic treatment while allowing the formation, maturation and dispersal of biofilms (Poltak and Cooper 2011).

1.6 Fungal infections

The scale of severity in fungal disease can range from common superficial infections, such as ringworm and athletes' foot caused by *Trichophyton* spp., to systemic infections, such as candidemia or pneumonia. Around 25% (~1.7 billion) of the world population has been affected by a fungal infection of the skin, hair, or nail. However, these are relatively easy to treat and rarely lead to mortalities (Bongomin et al. 2017). Dermatophytes are the main cause of superficial fungal infections, colonising keratinous tissue which they encounter, with the infection risk increasing if there are breaks in the skin (Havlickova et al. 2008).

Serious invasive fungal infections (IFIs) can occur in those with predispositions, such as cancer, immunosuppression, HIV/AIDS, and neutropenia (Aly and Berger 1996; Viscoli et al. 1999; Eggimann et al. 2003). In recent years, there has been an increase in IFIs, such as aspergillosis and candidiasis. While

incidence rates are much lower compared to those of superficial infections, the mortality rate is much higher, despite the availability of antifungal treatments. The reasons suggested for this increase in IFIs include the use of broad-spectrum antibiotics, immunosuppressants, and the increased use of implanted medical devices (Enoch et al. 2006). Fungal species have also become frequent biofilm colonisers of voice prosthesis, reducing the lifespan of the device to around 3-6 months before replacement is required (Somogyi-Ganss et al. 2017).

1.7 Cystic fibrosis

1.7.1 Background

CF is a rare inherited autosomal recessive genetic disorder characterised by mutations in the cystic fibrosis transmembrane conductance regulator (CFTR) gene on chromosome 7, which encodes a chloride ion channel present on the surface of secretory epithelial cells (**Figure 1.5**). The airway surface liquid (ASL) is a thin fluid layer that spans over two layers; the top mucus layer that trap inhaled particles that can then be removed and the periciliary layer below that surrounds cilia (Iram et al. 2016). The ASL has antimicrobial properties and aids with ciliary function and mucociliary clearance. However, in CF patients, the ASL is dehydrated and significantly more acidic (Lewis et al. 2019).

CF affects around 1 in 4000 newborns in the USA and 1 in 3000 in Europe, while around 3-4% of the population are carriers of the mutated CFTR gene (Corriveau et al. 2018; Martin and Burgel 2020; Scotet et al. 2020b; NHS 2021a). CF requires mutations in both copies of the CFTR gene (i.e., a copy from each parent). The CFTR protein facilitates the transport of chloride and bicarbonate ions, and (with the epithelial sodium channel) maintains the balance of salts and water in cells

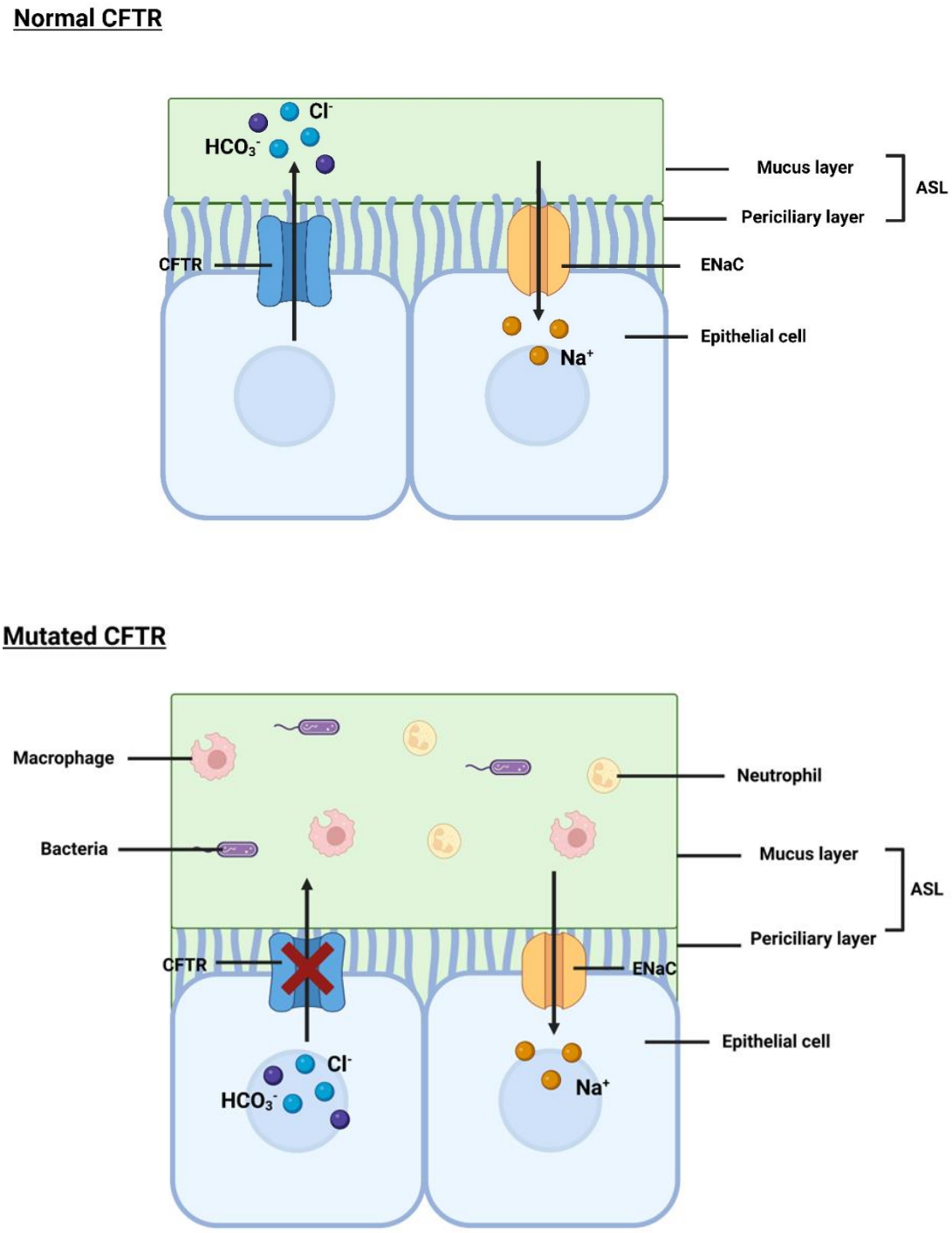

Figure 1.5. Schematic diagram showing a functional CFTR protein in healthy individuals and a mutated CFTR in a cystic fibrosis patient. (ASL, airway surface liquid; CFTR, cystic fibrosis transmembrane conductance regulator; ENaC, epithelial sodium channel).

(Tang et al. 2009; Bell et al. 2020). The CFTR protein was first discovered in 1989 and is part of the ATP-binding cassette (ABC) transporter family, that uses energy from ATP binding and hydrolysis to move ions across the membrane (Kerem et al. 1989; Liu et al. 2017a). There are over 2000 mutations known to result in a CF phenotype, which result in differing extremes of disease/symptoms. The mutations can be split into six classes depending on their phenotype including: Class I, defective protein synthesis resulting in reduced or completely absent CFTR; Class II, defective maturation; Class III, defective channel regulation; Class IV, defective conductance; Class V, reduced quantity of CFTR and Class VI, reduced CFTR stability (Veit et al. 2016). The most common mutation is ΔF508 (a class II mutation caused by a phenylalanine deletion at position 508), seen in around 90% of CF cases in Europe and North America, which causes impaired folding of CFTR and compromised plasma membrane expression (Mall and Hartl 2014). Life expectancy for CF patients has increased dramatically over the last 70 years, with the average life expectance now being 34 and 38 in the US and the UK respectively, compared to the 1950's where children were not expected to live past 5 years of age (Cystic Fibrosis Foundation 2022; McBennett et al. 2022; UK Cystic Fibrosis Registry 2022).

1.7.2 Diagnosis and treatment

Screening of newborn babies for CF is widely implemented worldwide, with the heel prick test occurring 5 days after birth in the UK (NHS 2021b). If this test shows a patient may have cystic fibrosis, the sweat test (chloride concentrations above 60 mmol/L) and genetic testing can be used to look for symptoms, mutations and to confirm diagnosis (De Boeck et al. 2017). These tests have led to the majority of CF cases now being diagnosed before the patient turns one year of age, and can also be

used to test older children or adults who did not have the heel prick test as a newborn (Cystic Fibrosis Foundation 2022).

Mutations in the CFTR protein can cause a diverse array of symptoms (ranging from malnutrition to infertility) in a wide number of organs, causing severe damage to the lungs, the digestive system and other organs in the body (**Figure 1.6**, Castellani and Assael 2017; Naehrig et al. 2017). The mutated CFTR protein affects the consistency of mucus within the CF lung, with epithelial cells unable to regulate Cl^- secretions (Mall and Galietta 2015). Without this flow of chloride and other anions, the movement of water is reduced, leading to accumulation of a hard-to-clear, thick mucus, causing airway obstruction and chronic bacterial infection in the lungs, which is responsible for morbidity and mortality in up to 95% of CF patients (Stoltz et al. 2015). Normal mucus is mostly comprised of water (~90-95%) with 1-5% mucin and other materials making up the rest of its composition, however, in CF patients the mucin to water ratio is much higher, with mucin levels being 5-10 fold higher (Bansil and Turner 2018; Morrison et al. 2019; Okuda et al. 2022). Divalent cations, such as Ca^{2+} and Mg^{2+}, can be found in significantly higher concentrations in the sputum of CF patients (102 and 30 mg/L respectively) compared to 45 and 4 mg/L respectively in healthy patients. This discrepancy is thought to arise as a result of tissue damage within the lung causing the release of metal ions from immune cells (Smith et al. 2014). Magnesium has been shown to be protective against the disruption of established biofilms, while the presence of calcium is thought to enhance cellular adhesion leading to bacterial biofilms being at least 10-fold thicker (Wang et al. 2019a).

Early diagnosis allows disease symptoms to be monitored and prophylactic measures or treatments to begin sooner (Scotet et al. 2020a). There is currently no

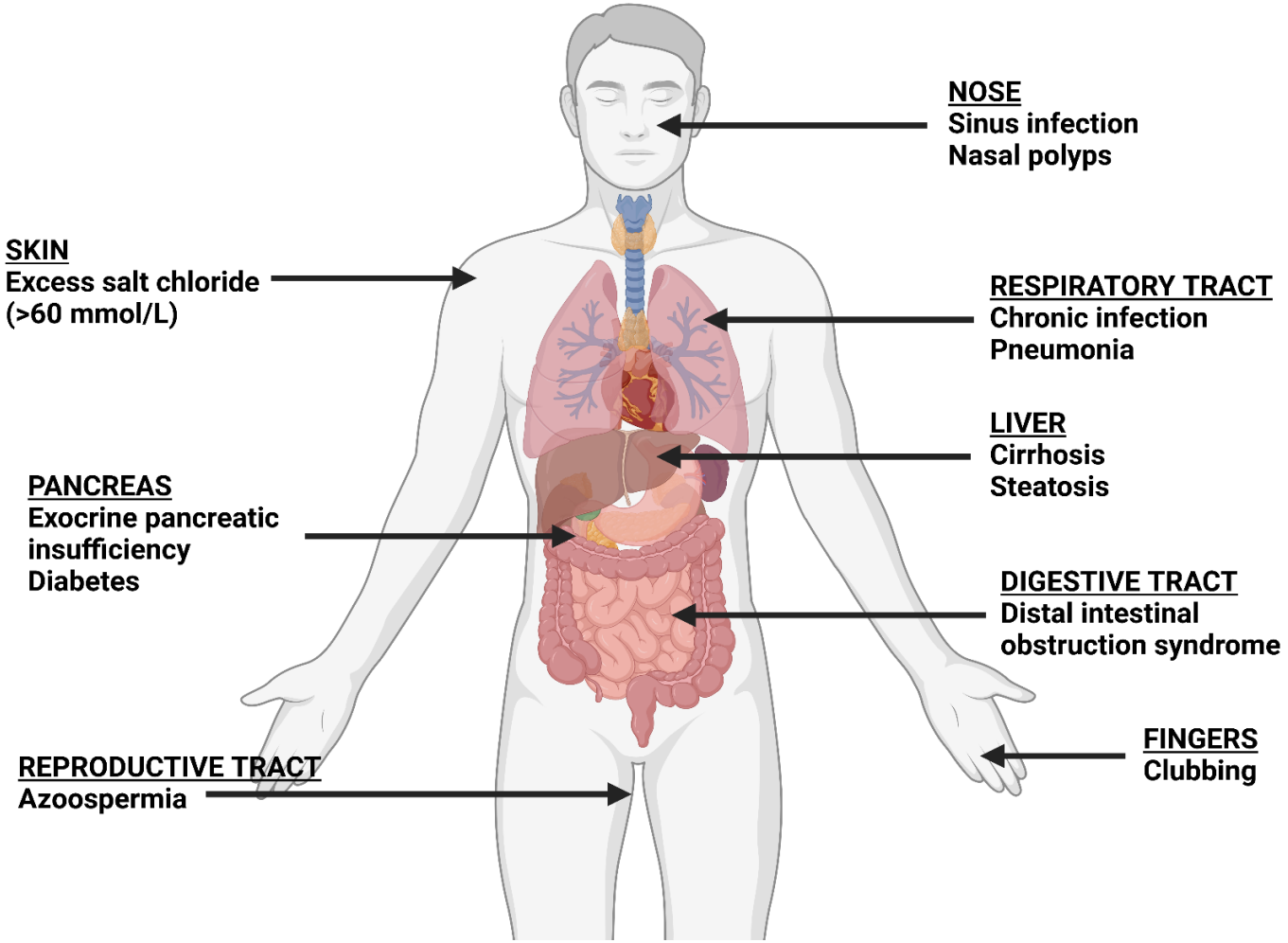

Figure 1.6. Symptoms of cystic fibrosis and affected organs.

cure for CF, although there are treatments available to manage symptoms, preventing complications arising and helping to improve quality of life. Symptoms of CF patients with chronic *P. aeruginosa* can be maintained with inhaled antibiotics (such as colistin, tobramycin and aztreonam), aiming to prevent acute pulmonary exacerbations, while mucus thinners can help clear excess mucus build up (Taccetti et al. 2021). Patients may also require daily physiotherapy to prevent the build-up of lung mucus. Other treatments include modulators that target the causative dysfunctional CFTR protein; correcting CFTR processing and facilitating ion delivery to the cell surface or potentiating ion flow through the CFTR protein (De Boeck and Amaral 2016). Orkambi® (lumacaftor/ivacaftor), Symkevi® (tezacaftor/ivacaftor) and Kalydeco® (ivacaftor), all targeting ΔF508 mutation are currently available on the NHS. Kaftrio®, a triple therapy composed of two CFTR modulators, elexacaftor and tezacaftor, repairs ΔF508 by increasing availability of the CFTR protein on the cell surface, and ivacaftor (a chloride channel opener), has shown promising *in vivo* efficacy (Aspinall et al. 2022).

The microbiome in CF patients is dynamic and can affect the progress of disease (**Figure 1.7**). Lung infection in patients can occur from infancy, with species such as *S. aureus* (and clinically important methicillin resistant *S. aureus*) and *Haemophilus influenzae* colonising epithelial surfaces (Goss and Muhlebach 2011). As the child grows older, a shift is seen in the colonising species, with *P. aeruginosa* becoming dominant by the time the patient enters early adulthood (Turcios 2020). The CF lung is polymicrobial, with fungi such as *Aspergillus fumigatus* and *C. albicans* commonly found as co-colonisers with bacteria in up to 57% and 70% of cases respectively (King et al. 2016; Haiko et al. 2019). This fungal colonisation is of clinical relevance due to its link with a decline in patient lung function and the development

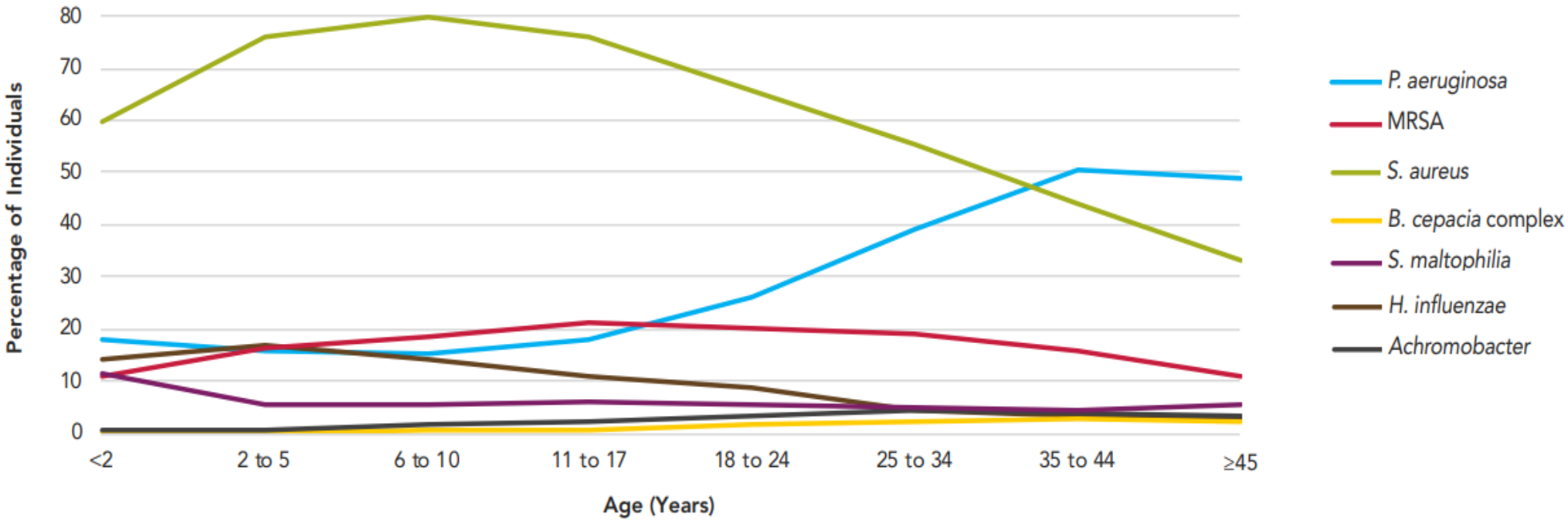

Figure 1.7. Bacterial colonisation and prevalence in the cystic fibrosis lung with patient age (Cystic Fibrosis Foundation 2022).

of pulmonary disease (Liu et al. 2013). Specific microbe-microbe interactions between *P. aeruginosa* and *C. albicans* have been noted, with *P. aeruginosa* producing quorum sensing substances, which can modulate the growth of *C. albicans* (Delhaes et al. 2012; Méar et al. 2013). Farnesol produced by *Candida* can also affect *P. aeruginosa*, inhibiting virulence factors and reducing swarming in *P. aeruginosa* PAO1(Li et al. 2020b).

In CF patients, increased tolerance of *P. aeruginosa* to antibiotics occurs due to bacterial biofilm development in the CF lung and the high doses of antibiotics used daily, with growth and infection facilitated due to the thick CF mucus polymer matrix. *P. aeruginosa* in the CF lung can mutate from a non-mucoid bacterial morphology (which predominates in earlier childhood infections) to a mucoid one (more common in older patients). Mucoid *P. aeruginosa* have the ability to overproduce mucoid exopolysaccharide which has distinct roles in the evasion of host defences and in protection from antibiotic threats (Hengzhuang et al. 2011; Goltermann and Tolker-Nielsen 2017). Mucoid, alginate producing *P. aeruginosa* are responsible for the chronic lung infections seen in a high proportion of CF patients and have been linked to a poorer long-term clinical prognosis exemplified by declining lung function and increased mortality (Høiby et al. 2010b). Other phenotypes of *P. aeruginosa* that have been recognised in the CF lung are small colony variants (SCVs), which are colonies 1-3 mm in diameter that can auto aggregate. SCVs have been linked to the use of inhaled antibiotics and contribute to poor lung function, augmenting inflammation and displaying strong attachment to surfaces, thereby enhancing biofilm-forming ability and persistence in CF patients (Malone 2015; Pestrak et al. 2018).

1.8 Alginate oligomers

Alginates are a family of linear polysaccharides which can be harvested from brown algae or are produced by bacteria, such as *Pseudomonas* and *Azotobacter* species as an exopolysaccharide, the main component of their biofilms (Ueno and Oda 2014). Alginates consist of 1-4 linked α-L-guluronic acid (G) and β-D-mannuronic acid (M) residues, with the monomers arranged into homopolymeric regions of mannuronate residues (M blocks), guluronate residues (G blocks) or alternating residues (MG blocks). Alginate composition varies between algal species, as well as tissue type (leaves, stem, etc), growth conditions, plant age, all of which directly affects their physical properties (Donati and Paoletti 2009; Fertah 2017).

The genes involved in alginate synthesis are similar between *Pseudomonas* and *Azotobacter*, with twelve (out of 13) genes making up the *alg* operon with one gene (*algC*) present elsewhere on the chromosome (Ertesvåg et al. 2017). Alginates produced by *Pseudomonas* spp. are characterised by a lack of continuous G residues, with alginates initially being synthesised as polymannuronic acid, before being modified by acetylation and epimerisation (Remminghorst and Rehm 2006). Alginates are commonly used as gelling, stabilising, and thickening agents in the food industry, often added to provide extra nutrients, as well as being used in the pharmaceutical industry as a wound dressing material (Rashedy et al. 2021).

1.9 OligoG CF-5/20

OligoG CF-5/20 (OligoG) is an alginate oligosaccharide prepared from the stem of the brown seaweed, *Laminaria hyperborea*, a species known for having a high guluronic acid content. Following purification and fractionation, low molecular

weight oligomers are prepared (mean Mn 3200 g/mol^{-1}), with >85% of the monomer residues being G residues (**Figure 1.8**). Charcoal filters were used in the final purification step, followed by spray drying to create a dry powder form. OligoG is soluble in water up to around 15%, with an increase in viscosity seen at higher concentrations (Khan et al. 2012). Tailored alginate oligosaccharides can be created through epimerisation technology, allowing the engineering of alginates with known M:G composition and degree of polymerization (DPn). The repeat G-blocks bind to Ca^{2+} ions forming structures which represent eggs in an egg box. However, M blocks cannot form the characteristic gels that G blocks do when binding to divalent cations, such as Ca^{2+} (Lee and Mooney 2012; Borgogna et al. 2013).

1.9.1 Initial toxicity studies in rodents

Preclinical studies in rats showed that the majority of OligoG (82.6%) was eliminated by the gastrointestinal (GI) tract in 24 h of being administered orally. This study showed that both formulations were tolerated, although the dry powder formulation demonstrated higher whole lung deposition (38.6% cf. 17.1%), along with lower deposition (11.3% cf. 19.9%) in the extra-pulmonary region (i.e., the stomach and oropharyngeal), compared to the nebulised solution (Pritchard et al. 2016). Furthermore, when labelled with tritium OligoG CF-5/20 showed excretion in faeces when administered orally and in the urine when administered intravenously, displaying no toxicity. Following inhalation studies using aerosolized OligoG over fourteen days before rats were screened for pathological, biochemical, and clinical changes. To compare the nebulized formulation with the dry powder formulation, rats were dosed with OligoG in dry powder formulation daily for four weeks with

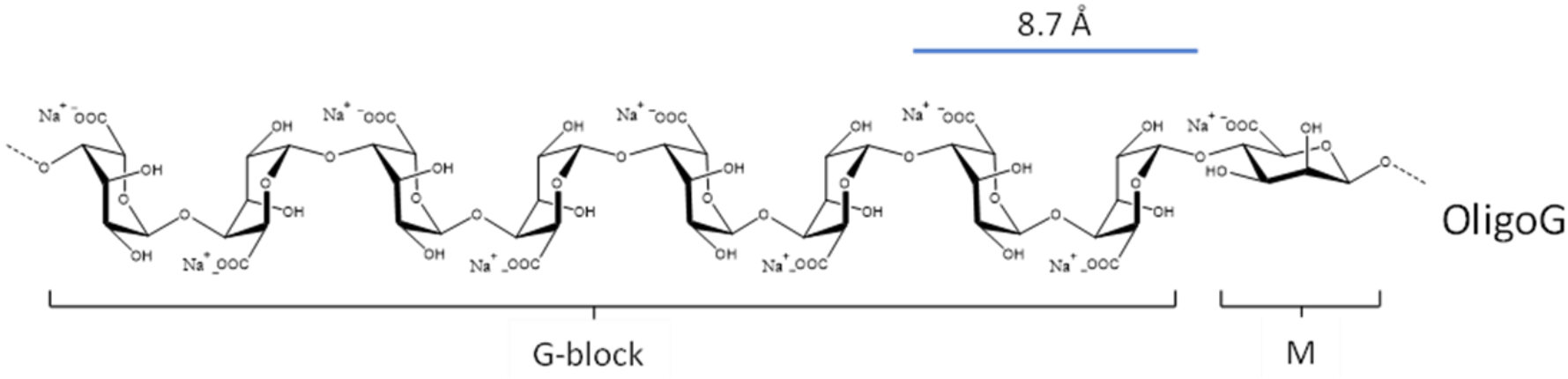

Figure 1.8. Molecular structure of β -L-guluronic acid (G) and β -D-mannuronic acid (M) components making up OligoG CF-5/20.

histopathology, toxicokinetic, condition, food consumption, urinalysis and body weight analysed.

1.9.2 Human clinical trials

OligoG CF-5/20 has, to date, completed multiple clinical trials in humans (AlgiPharma 2020). The first in 2009, was a randomised, phase I trial to determine the safety, tolerability and efficacy of OligoG as an inhaled nebulised therapy in 26 healthy individuals over three consecutive days (clinicaltrials.gov identifier: NCT00970346). The study demonstrated that concentrations up to 10% were safe to use and working concentrations of 2-10% were, therefore, used in subsequent studies investigating the *in vitro* properties of OligoG (Khan et al. 2012; Tøndervik et al. 2014; Pritchard et al. 2017a; Pritchard et al. 2017c).

A phase IIa human clinical trial followed in 2013 to evaluate dosing with 6% OligoG CF-5/20 in water (compared to a saline placebo) over 28 days in patients with CF and chronic *P. aeruginosa* infections. This study further showed that OligoG was safe in humans and was well tolerated after multiple doses (clinicaltrials.gov identifier: NCT01465529). Inhaled OligoG demonstrated no adverse effects or significant changes in urinalysis, vital signs, biochemistry, or haematology (Pritchard et al. 2017c).

A study used Gamma Scintigraphy to investigate lung deposition of radiolabelled OligoG was performed in 2014 (clinicaltrials.gov identifier: NCT01991028). The dose administered to patients was 186 mg OligoG over two doses, compared to previous studies which used 540 mg/day, and which showed that the treatment was well tolerated, with no reported adverse issues. For this study,

OligoG was developed in a dry powder formulation, allowing administration using a more practical inhaler instead of a nebuliser.

Two more recent phase IIb clinical trials in 2017 involved dry powder OligoG as an inhalation therapy for CF patients (65 patients), or CF patients with *Burkholderia* spp. colonisation (15 patients) to check efficacy after multiple doses, measured by forced expiratory volume in 1 second (FEV1) and efficacy at reducing microbial load (clinicaltrials.gov identifier: NCT02157922 or NCT02453789 respectively). No significant improvement in FEV1 was noted, although a decrease in microbial load of *Burkholderia cepacia* was noted after treatment, along with improved quality of life scores (van Koningsbruggen-Rietschel et al. 2020; Weiser et al. 2021; Fischer et al. 2022).

1.9.3 *In vitro* studies

Previous research investigating the *in vitro* properties of OligoG CF-5/20 has shown it to be effective at significantly inhibiting the growth of multiple Gram-negative bacterial and fungal species (Khan et al. 2012). Furthermore, it has been shown to inhibit the ability of biofilm formation as well as promoting biofilm disruption as a stand-alone treatment with the mechanism of action thought to be due to the chelation of calcium ions and the subsequent EPS modification (Powell et al. 2013; Pritchard et al. 2023). Studies have investigated the effects of OligoG CF-5/20 as a combination therapy, with potentiation effects seen when combined with treatments which are currently limited by either toxicity and growing antimicrobial resistance, Khan et al (2012) showed OligoG increased the efficacy of conventional antibiotics by up to 512-fold in minimum concentration assays.

1.10 Aims

The main objectives of this project were to further investigate the use and effectiveness of the alginate oligosaccharide, OligoG CF-5/20, as an antibiofilm treatment and to look at potentiation when used in combination with current therapies which are limited by the development of multidrug resistance and toxicity.

Specific aims of the study were:

- To investigate the effect of OligoG CF-5/20 on planktonic and biofilm *Candida* spp. in combination with nystatin, and to further elucidate its antifungal mode of action.
- To investigate the effect of OligoG CF-5/20 and tailored OligoM alginate oligomers on mucoid and non-mucoid *P. aeruginosa* biofilms, and compare their effects (similarities and differences) on bacterial virulence and quorum sensing signalling.
- To characterise colistin resistant (Col^R) *Escherichia coli mcr* strains by assessing their stability and fitness in an evolutionary model and examining the effect of OligoG CF-5/20 on biofilm disruption.

Chapter 2

Characterising the ability of OligoG CF-5/20 to enhance the effect of nystatin

2.1 Introduction

2.1.1 Candidal structure and morphology

Fungi, such as *Candida,* exist as either "yeast like" cells or as a filamentous hyphal form, which is linked to its virulence (Staniszewska et al. 2012). Pseudo-hyphae and hyphae are both filamentous forms of *Candida* that grow in a polarised manner. Hyphae form either from other hyphae or from a mother yeast cell. This occurs when a germ tube protrudes from the yeast cell and elongates from the tip, forming hyphae with parallel sided walls along its whole length (Sudbery 2011). In contrast, pseudo-hyphae are the result of incomplete budding. These cells remain elongated and attached to yeast cells or hyphae, and due to this, they have constrictions at septal junctions (Thompson et al. 2011).

Fungal species which are restricted to either yeast or filamentous forms have been shown to have attenuated virulence compared to strains which exhibit dimorphism (Cheng et al. 2012). Several environmental cues can induce *Candida* to switch between its dimorphic states. For example, *Candida albicans* at low pH (pH <6), temperatures < 30°C, and high cell densities tends to favour the yeast form, while hyphal growth is induced at pH >7, low cell densities and temperatures > 30°C (Sudbery et al. 2004; Mayer et al. 2013).

The cell wall of *C. albicans* is composed of an outer and inner layer (**Figure 2.1**). The inner skeletal layer is made of chitin and β-glucan. This is a glycan made of β-(1-3) or β-(1-6) linkages of glucose, which provides a strong scaffold and represents the structural component of the cell, which can withstand pressure exerted on the wall (Gow et al. 2017). The outer layer is made up of high levels of mannans,

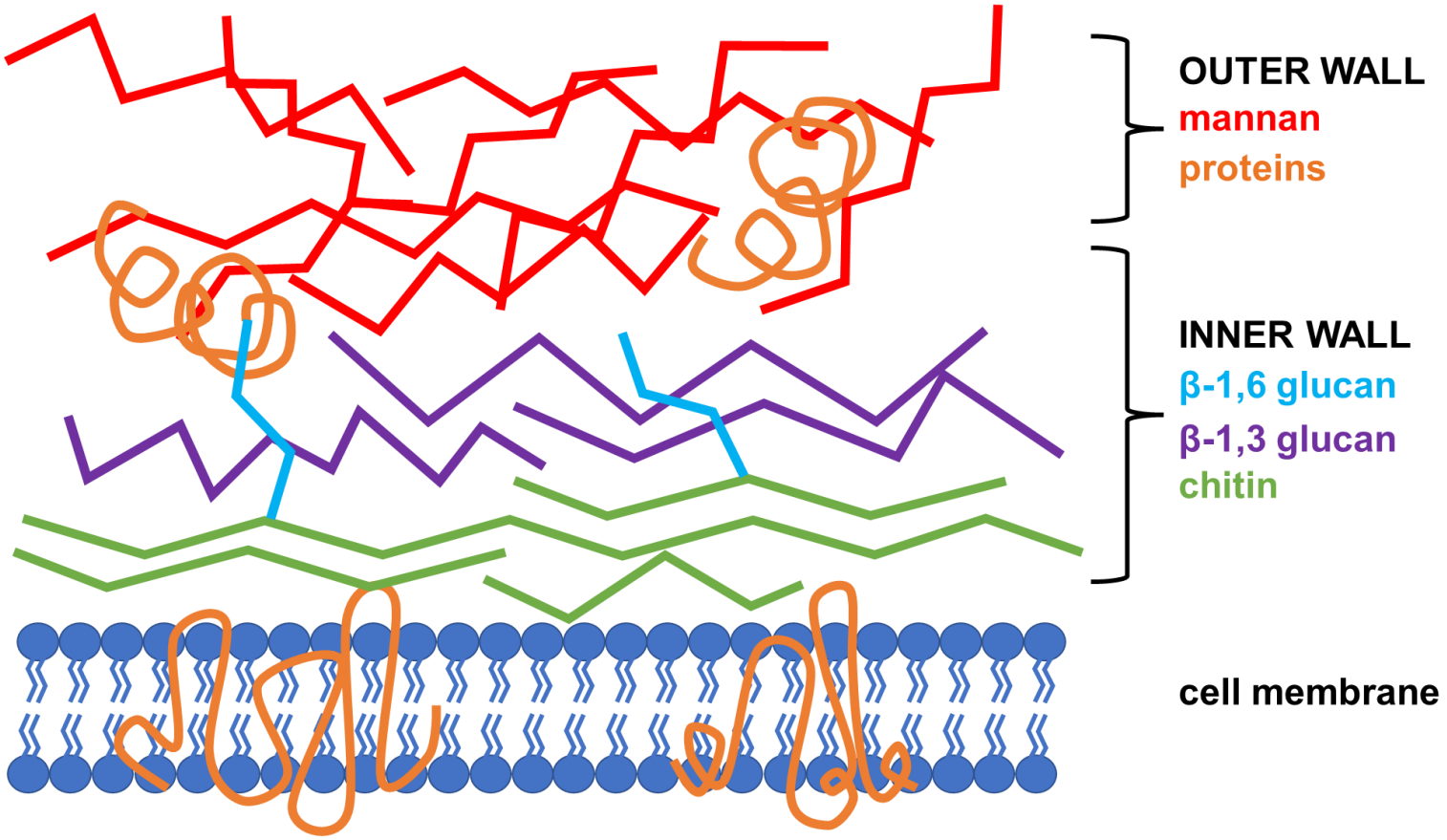

Figure 2.1. Structure of the *Candida albicans* cell wall.

linear O- and branched N-linked mannose polymers, making up 40% and 20% of the dry weight of the cell wall respectively (Gow et al. 2012). Cell wall proteins (CWPs) have roles in interacting with the environment, adherence and in disguising the cell from recognition by phagocytes. However, many of the proteins in the cell wall are not found in humans, making them desirable targets for antifungals and triggers of the host immune response (Chaffin 2008; Hall and Gow 2013).

2.1.2 *Candida* spp.

Candida colonise most mucosal surfaces, such as the gastrointestinal (GI) tract of humans, as well as the skin, and is currently the most common cause of fungal and yeast infections worldwide (Brown et al. 2012). While found as a commensal organism, *Candida* can cause opportunistic infections in those who are immunosuppressed or when the mucosal membrane has become compromised. The use of antibiotics can promote the presence of *Candida*, leading to overgrowth of the fungal microflora, while suppressing the growth of the commensal bacterial flora. This can lead to infections, such as vulvovaginal candidiasis (VVC), which is predicted to affect 75% of women at least once during their life, with 40-45% experiencing it at least twice, with predisposing factors ranging from hormones and pregnancy to contraception (Achkar and Fries 2010). Although *Candida* spp. are present in the oral cavity of up to 60% of the population, most people will experience no adverse effects. However, host factors, such as diet, age, denture use, and use of inhaled corticosteroids can lead to oral candidiasis (Pankhurst 2009).

2.1.3 *Candida albicans*

In the 1990's *Candida albicans* was responsible for over two thirds of *Candida* infections, but has since declined to around 50%, with other *Candida* species recently becoming more prevalent (Maschmeyer 2006; Cuenca-Estrella et al. 2008). This may partly be due to better identification of different species, as well as the increased use of immunosuppressive therapy (Silva et al. 2009). As already stated, *Candida albicans* is dimorphic, with the ability to switch between filamentous (pseudo)hyphae and unicellular budding yeast forms. Generally, dimorphic fungi exist in the environment in their filamentous form, and switch to their yeast form in diseased tissue, where they can replicate and become disseminated in the bloodstream. A reversible "phenotypic switch" is responsible for this change in morphology and the subsequent up-regulation of virulence factors, allowing colonisation of new environmental niches and the ability to evade the immune system (Sudbery et al. 2004; Luo et al. 2013). Clearly, therefore, the hyphal form of growth provides a distinct fitness advantage, facilitating tissue damage and invasion, as well as access to the blood stream (Sudbery 2011). This switch can be induced by changes in environmental conditions, such as temperature, pH, and nutrient availability (e.g., serum addition), as well as the cell density of *C. albicans*, which is regulated via quorum sensing signalling (Molero et al. 1998; Sudbery et al. 2004).

2.1.4 Non-*Candida albicans Candida* (NCAC)

In the last 20 years, there has been a clear epidemiological shift from *C. albicans* to non-*Candida albicans Candida* (NCAC) species, such as *Candida tropicalis, Candida glabrata, Candida krusei* and *Candida parapsilosis*, as the key aetiological agents of human disease (Hajjeh et al. 2004; Silva et al. 2012). This shift

may be due to resistance to treatment being more common in NCAC than *C. albicans*, giving these species an advantage when part of a heterogenous infection.

Compared to the other *Candida* species, *C. glabrata* is a haploid, non-dimorphic yeast, which lacks the ability to form pseudo-hyphae (Fidel et al. 1999). Importantly, *C. glabrata* is intrinsically less susceptible to the azole class of antifungals, giving it an evolutionary advantage over another *Candida* spp. Molecular reasons for decreased azole resistance include increased ergosterol production; drug sequestration; mutations leading to decreased affinity to the target enzyme, as well as decreased drug accumulation due to an enhanced efflux pump system caused by gene upregulation (Sanguinetti et al. 2005; Xiang et al. 2013). Consequently *C. glabrata* now has a mortality rate much higher (~49%) than those of other NCAC spp. (Maschmeyer 2006; Deorukhkar et al. 2014a).

Candida auris was first isolated in 2009 from the ear canal of a hospitalised patient in Tokyo, Japan (Satoh et al. 2009). Since then, it has become an increasingly clinically relevant pathogen due to strains often being multidrug resistant, with some resistant to all three main antifungal classes: azoles, echinocandins and polyenes (Arendrup and Patterson 2017). Combined with the previous misidentification of *C. auris* infections, and its ability to cause serious invasive fungal infections (IFIs) associated with high mortality, it poses an emerging threat to public health, and has already caused severe invasive infections in nosocomial settings across five continents (Jeffery-Smith et al. 2018; Cdc 2019; Du et al. 2020).

Candida dubliniensis was first identified as a novel species in 1995, being isolated from a HIV patient with oral candidiasis attending Dublin Dental Hospital (Sullivan et al. 1995). *C. dubliniensis* is very closely related to and shares similar

characteristics to *C. albicans,* such as the production of germ tubes, often leading to its previous misidentification as *C. albicans* in samples dating back as far as 1957 (Sullivan et al. 1993; Coleman et al. 1997).

Although widely distributed around the globe, *C. tropicalis* is more prevalent in countries with tropical climates i.e., increased humidity and temperature (Negri et al. 2012). It possesses many virulence factors which aids invasion into host tissues, such as formation of true hyphae (like *C. albicans* and *C. dubliniensis*) and the production of enzymes, such as proteases (Ann Chai et al. 2010; Deorukhkar et al. 2014b). These factors all contribute to the ability of *C. tropicalis* to form strong biofilms and increase the pathogenesis of candidiasis.

C. parapsilosis (unlike *C. albicans* and *C. tropicalis*) is unable to produce true hyphae, existing in either a yeast or pseudo-hyphal form (Trofa et al. 2008). Before 2005, *C. parapsilosis* was divided into three sub-groups (I to III) but has since been reclassified into three distinct species due to clear genetic differences at the sequence level: *C. parapsilosis* (I), *Candida orthopsilosis* (II) and *Candida metapsilosis* (III) (Tavanti et al. 2005). The clinical importance of *C. parapsilosis* infections has increased in recent years due to their ability to form biofilms on indwelling medical devices, such as catheters, as well as spreading easily through nosocomial settings leaving neonates and those in intensive care units (ICU) vulnerable to infection (Silva et al. 2012; Tóth et al. 2019).

The importance that *Candida* pose to public health and the need for antifungal treatments has been highlighted by the recent World Health Organisation (WHO) list of fungal priority pathogens which were categorised into three groups; critical, high and medium (WHO 2022b). *C. auris* and *C. albicans* were categorised as ‘critical

threat' pathogens with *C. parapsilosis*, *C. glabrata*, and *C. tropicalis* classed as being a high priority.

2.1.5 Immune evasion

Pathogens and hosts are in a constant "arms race" to survive, to evolve and to gain a reproductive advantage. As a result, *Candida* has evolved a myriad of immune evasion strategies to avoid host innate and adaptive immunity. Host pattern recognition receptors (PRR) recognise 'non-host' ligands (referred to as pathogen associated molecular patterns, PAMPs), which triggers the innate immune response via cytokine and chemokine production, inflammation, phagocytosis and complement activation. There are many PAMPs in the *Candida* cell wall, such as β-glucan and O-linked mannan, which are recognised by their respective PRRs, namely Dectin-1 and the macrophage mannose receptor, respectively (Netea et al. 2010; Cheng et al. 2012). However, *Candida* has adapted to mask PAMPs from recognition by PRRs, β-glucan in the cell wall can be shielded from Dectin-1 by an outer layer of mannoproteins and mannan, which has been shown to promote invasion *in vivo*, as well as an extracellular exoglucanase, Xog1, being expressed which has been shown to "shave" off β-glucan (Gow et al. 2017; Pradhan et al. 2019; Childers et al. 2020). Furthermore, *Candida* cells can escape macrophages (and neutrophils) following phagocytosis. Hyphae formed inside the immune cells can puncture the cell wall from inside, leading to the immune escape of *Candida* (Mayer et al. 2013).

Once activated, the complement system causes a cascade of proteins to be generated which can opsonise pathogens, marking them for phagocytosis. This also increases recognition by the immune system, degranulation of mast cells, as well as cytolysis. The pH-regulated antigen 1 (Pra1) is a surface protein found on both forms

of *C. albicans*, which can regulate complement activation through binding to the inhibitor C4b-binding protein (C4BP). However, it is also a ligand recognised by the host CR3 receptor, and as such, can trigger phagocytosis (Zipfel et al. 2011; Cheng et al. 2012).

2.1.6 Virulence

C. albicans is a commensal organism found in healthy hosts with the ability to become an opportunistic pathogen in a diverse array of situations. For colonisation to occur, the initial event needed is adhesion. Receptor ligands, such as adhesins and invasins, expressed on the surface of *Candida* play a vital role in primary attachment onto biotic and abiotic surfaces. The agglutinin-like sequence (ALS) gene family was first identified in *C. albicans*, of which eight glycoproteins (ALS1-7 and ALS9) have now been described (Hoyer et al. 2008; Hoyer and Cota 2016). In ALS3 knock-out mutants, a reduction in epithelial adhesion was observed alongside a decreased pro-inflammatory cytokine response (a marker of epithelial activation), demonstrating that ALS3 plays a vital role in host interaction and invasion (Murciano et al. 2012).

The invasion of host cells by *Candida* spp. occurs via two contrasting mechanisms: namely, induced endocytosis and active penetration (Maza et al. 2017). An additional function of the ALS3 adhesin is its ability to bind to the host surface proteins, E-cadherin and N-cadherin, via its N-terminal region, mimicking the action of host cadherins and triggering induced endocytosis (Phan et al. 2007). Alternatively, *C. albicans* hyphae exert pressure as the tip begins to extend, penetrating epithelial cells or allowing growth between them, which is aided by the presence of hydrolytic enzymes, thereby facilitating further tissue invasion (Naglik et al. 2011). On connection with the epithelium, hyphae-associated genes including *ALS3*, *pra1*, and

hwp, have been shown to be upregulated, suggesting they may be pivotal to cell penetration (Cheng et al. 2012). Hydrolytic enzymes are important for multiple stages of the infection process, and contribute to both superficial mucosal and systemic infections; their presence greatly enhancing the pathogenicity of *Candida* spp. *Candida* possess several families of hydrolytic enzymes, including phospholipases (PLs), which are further broken down into four classes; A-D and secreted aspartyl proteinases (SAPs) (Mayer et al. 2013). PLs can degrade the cell membrane of the host, hydrolysing phospholipids into fatty acids and exposing expressed surface receptors, which *Candida* is able to exploit for adhesion (De Bernardis et al. 1999). There are currently ten genes in the SAP enzyme family (SAP1-10), which have been observed in *C. albicans*, as well being found in several NCAC species, including *C. tropicalis* and *C. parapsilosis*, which are thought to express at least four and three SAP genes, respectively (Calderone and Fonzi 2001; Silva et al. 2012). SAPs 1-8 are secreted, while SAPs 9-10 remain surface bound (Naglik et al. 2011). SAP enzymes contribute to tissue damage, degrading molecules in the extracellular matrix, such as keratin and collagen, while evading immune system components by degrading complement and cathepsin D (Naglik et al. 2003).

2.1.7 Antifungals

The treatment of fungal infections is more complex than bacterial infections, due to the eukaryotic nature of fungal cells. This means that therapeutic targets for yeasts are often shared with those in human cells (Campoy and Adrio 2017). There are four commonly used classes of antifungals: polyenes, azoles, echinocandins and allylamines. Polyenes, azoles and echinocandins are used intravenously, topically, and

orally for infections, while allylamines are mainly used for treating superficial infections caused by dermatophytes (Campoy and Adrio 2017).

Polyenes, azoles, and allylamines all interact with ergosterol, a major component found in the cell membrane of fungi, either by interrupting its synthesis or by directly interacting with it (Ghannoum and Rice 1999). Polyenes, such as amphotericin B and nystatin (NYS), bind to ergosterol, forming a complex able to form pores in the membrane, thereby causing leakage of the cytoplasm contents and fungal death (Odds et al. 2003). The polyene, amphotericin B deoxycholate (AmB-D), has broad spectrum antifungal activity and has been considered the gold standard for severe and systemic IFIs (severe and systemic) (Hahn-Ast et al. 2010). However due to the common occurrence of side-effects, such as nephrotoxicity in 50-90% of cases, other antifungals such as azoles and echinocandins with reduced toxicity are often used as alternatives (Enoch et al. 2006).

The polyene, nystatin, is obtained from *Streptomyces noursei*, and was first discovered in 1951 and is the most frequently used treatment for voice prosthesis failures caused by *Candida* spp., and is often prescribed for oral candidiasis (Bauters et al. 2002; Ameye et al. 2005; Garcia-Cuesta et al. 2014; Quindós et al. 2019). It has additional benefits, including low cost and high efficacy, which is beneficial in low economic countries as it can be prescribed to pregnant and breastfeeding mothers and it's been shown that through autooxidation further cell damage can occur (Quindós et al. 2019). Allergy and intolerances to nystatin are rare, due to poor absorption through the skin and GI tract (Martínez et al. 2007; Scheibler et al. 2017). However, amphotericin B has immunomodulatory responses that can lead to increased levels of

cytokines, prostaglandins and chemokines, which have shown to be associated with toxic side effects (Mesa-Arango et al. 2012; Faustino and Pinheiro 2020).

Azoles can be divided into two groups namely, triazoles and imidazoles, depending on whether they have three or two nitrogen's in the azole ring, respectively. Triazoles, such as fluconazole, have replaced imidazoles and display a broader spectrum of antifungal activity against superficial infections and IFIs, being deemed safer for use due to their greater affinity for fungal (as opposed to mammalian) cytochrome P450 enzymes (Sheehan et al. 1999). Fluconazole is used for prophylaxis, as well as being prescribed for clinical cases of *Candida*, although it remains ineffective against filamentous fungi (Enoch et al. 2006). Azoles inhibit the cytochrome P450-dependent enzyme, 14α-lanosterol demethylase (CYP51). This results in inhibition of lanosterol to ergosterol conversion, thereby interrupting synthesis of the cell membrane (Ami et al. 2008).

Echinocandins act as inhibitors of the enzyme complex β-1,3-D-glucan synthase, preventing the production of β-(1-3) glucan in the cell wall (Canuto and Rodero 2002). This leads to a weaker cell wall and cell death through lysis (Denning 2003). They are used for the treatment of invasive infections and for patients with neutropenia (Grover 2010).

2.1.8 Resistance to antifungals

The treatment of fungal infections is becoming increasingly difficult, due to the development of resistance to antifungal therapies. Resistance to azoles can occur through mutations or overexpression of the *ERG11* gene that encodes for the enzyme, cytochrome P-450 lanosterol 14α-demethylase (Eliopoulos et al. 2002). This can lead

to modifications in the quantity of the enzyme produced, the affinity of drug binding, as well as access of the drug to the target. The presence and overexpression of drug efflux pumps can also lead to an intracellular reduction of the enzyme (Ghannoum and Rice 1999). Resistance to polyenes such as AmB-D and nystatin are less common than azole resistance, partly due to their associated toxicity, although they are often used for shorter treatments, suggesting that resistance may emerge from cells which possess resistance naturally (Ghannoum and Rice 1999; Lupetti et al. 2002). It is suggested that these naturally resistant cells have a lower affinity for polyenes, due to them producing modified sterols (Anderson et al. 2014)

The use of a combination of antifungal therapies can often overcome some of the limitations of using individual antifungals and may improve treatment outcomes. They can broaden the spectrum of antifungal activity, prevent emergence of resistance to antifungals, as well as increase potency, meaning that doses of individual antifungals can be reduced, thereby minimising any toxic side effects (Baddley and Poppas 2005).

2.1.9 Aims and objectives

The hypothesis of this study was that OligoG CF-5/20 is a suitable and effective alternative treatment for fungal infections, particularly in combination with the antifungal nystatin.

The specific aims of this study were:

- To investigate the effect of OligoG CF-5/20 on planktonic growth of *Candida* spp., using growth curves and minimum inhibitory concentration (MICs) assays.
- To examine the effect of OligoG CF-5/20 on biofilm formation and biofilm disruption of *Candida* spp., using confocal laser scanning microscopy (CLSM) and COMSTAT image analysis.
- To determine whether cell permeabilisation is the antifungal mode of action for OligoG CF-5/20 using sorbitol and ergosterol assays, and transmission electron microscopy.

2.2 Materials and methods

2.2.1 Microbial strains and growth media

A total of thirteen *Candida* strains were selected; eight of which were *Candida albicans* and five non-*Candida albicans Candida* (NCAC), as shown in **Table 2.1**. However, for several assays, a selected four strains (*C. albicans* ATCC 90028, *C. albicans* GBJ13/4A, *C. parapsilosis* W23, and *C. auris* NCPF 8971), were used due to labour intensive techniques being used, as well as being of great clinical concern with them being listed in the "critical" or "high" priority group by the WHO (WHO 2022b). Strains were stored at -80°C using Microbank bead vials (Pro-Lab Diagnostics), until required. The identification of the *Candida* species used in this study was confirmed using MALDI-TOF mass spectrometry.

For all assays, *Candida* spp. were grown on Sabouraud Dextrose (SAB; Lab M) agar at 37 °C and Roswell Park Memorial Institute (RPMI 1640; Sigma-Aldrich), buffered with 0.165 mol/L MOPS (3-[N-morpholino] propanesulfonic acid; Sigma-Aldrich) for overnight (O/N) liquid culture. Unless otherwise stated, strains were grown at 37 °C (120 rpm shaking) and adjusted with RPMI 1640 to a standardised cell suspension of $5x10^6$ cells/mL, as determined by an OD_{600} absorbance reading of 0.37 for all experiments. All RPMI 1640 medium was filter-sterilised and stored at 4 °C prior to use.

The antifungal nystatin (Sigma-Aldrich) was prepared in dimethyl sulfoxide (DMSO) at a stock concentration of 5 mg/mL, and aliquots were stored at -20 °C until required. When using nystatin within an assay, plates were wrapped in tinfoil to prevent exposure to light. OligoG CF-5/20 was obtained from AlgiPharma AS and prepared, purified, and characterised, as previously described (Khan et al. 2012).

Table 2.1. Summary of *Candida* strains used in this study.

Isolate	Isolation Source	MALDI-TOF ID Score[a]	Reference
C. albicans ATCC 90028	Blood	2.21	
C. albicans GBJ 13/4A	Failed tracheoesophageal prosthesis	2.27	(Elving et al. 2000)
C. albicans SC5314	Clinical specimen (human)	2.24	
C. albicans CCUG 39343	Human faeces	2.3	
C. albicans 480/00	SCC, oral mucosa	2.06	(Bartie et al. 2004)
C. albicans PB1/93	Normal oral mucosa	1.96	(Bartie et al. 2004)
C. albicans LR1/93	Normal oral mucosa	1.98	(Bartie et al. 2004)
C. albicans Ptr/94	CHC, buccal mucosa	2.19	(Bartie et al. 2004)
C. parapsilosis W23	Clinical specimen (human, oral)	2.09	(Powell et al. 2023)
C. auris NCPF 8971	Wound swab	1.99	
C. tropicalis 519468	Urinary tract	2.25	(Silva et al. 2009)
C. glabrata ATCC 2001	Faeces	2.14	
C. dubliniensis 40/01[b]	PMC, palate	2.03	(Bartie et al. 2004)

CHC; chronic hyperplastic candidosis, SCC; squamous cell carcinoma, PMC; pseudomembranous candidosis, ATCC; American Type Culture Collection, NCPF; The National Collection of Pathogenic Fungi; CCUG; Culture Collection University of Gothenburg.
[a]a score value ≥2 indicates species identification; a score value between 1.7 and 1.9 indicates genus identification, and a score value <1.7 indicates no identification. [b] Formally known as *C. albicans* 40/01.

Clinical grade silicone sheets of the same material used in the manufacture of Provox tracheo-esophageal prostheses were obtained from Atos Medical.

2.2.2 Minimum inhibitory concentration (MIC) assay

MIC assays for *Candida* strains were performed, according to the Clinical and Laboratory Standards Institute (CLSI, 2008) guidelines. In a sterile, flat-bottomed 96-well microtiter plates (100 µL/well), two-fold serial dilutions of nystatin were prepared in RPMI-1640 ± OligoG CF-5/20 (0.5, 1, 2, 4, and 6%), with a starting concentration of 16 µg/mL. Five colonies of each *Candida* strain were taken from a freshly sub-cultured SAB plate and adjusted in phosphate buffered saline (PBS) to an optical density (OD_{600}) between 0.08-0.1 (0.5 McFarland standard ~$1x10^6$ colony forming units; CFU/mL). The adjusted culture was further diluted 1:50 in PBS and then diluted again 1:1 in RPMI-1640 medium. A 5 µL inoculum of the adjusted cultures was then added to each well and plates were incubated statically for 48 h at 37 °C (n=3). The MIC values were determined as the modal value of the lowest concentration, at which there was no visible growth.

2.2.3 Candidal growth curve analysis

To study the effect of antifungals in combination with OligoG CF-5/20 on planktonic *Candida*, growth curves were set up in a sterile flat-bottomed 96-well microtiter plate (200 µL/well). Liquid overnight cultures of *C. albicans* ATCC 90028, GBJ 13/4A, *parapsilosis* W23 and *auris* NCPF 8971 were adjusted in RPMI-1640 medium to $1x10^6$ cells/mL, before being diluted at a ratio of 1:10 in RPMI-1640 ± OligoG CF-5/20 (0.5, 1, 2, 4, 6%) ± ½ MIC nystatin of the respective strain (1-2 µg/mL). The absorbance measurements were taken hourly at OD_{600} using a FLUOstar

Omega plate reader (BMG Labtech) after shaking the plate at 200 rpm for 3 seconds. Each growth curve was performed in triplicate and results presented as mean values for 48 h at 37 °C. The minimum significant difference (MSD) was calculated using the Tukey-Kramer method, using Minitab 17.2.1 (Minitab Inc, State College, PA, USA).

2.2.4 ATP cell viability assay

2.2.4.1 Biofilm disruption assay

Adjusted ($5x10^6$ cells/mL) overnight cultures (n=3) were added to a sterile black walled, flat-bottomed 96-well plate, followed by pre-warmed (37 °C) RPMI 1640, in a 1:10 ratio (200 µL/well) and incubated for 45 mins at 37°C, with 20 rpm rocking. After incubation, the resultant biofilms were gently washed with pre-warmed RPMI-1640 (x3), before adding a further 200 µL of fresh medium and reincubating for 24 h (37 ^{o}C, 20 rpm). Half of the well supernatant was removed and replaced with fresh RPMI-1640 ± 4% OligoG CF-5/20 (v/v) ± MIC nystatin for each respective strain (v/v;1-4 µg/mL), followed by a further 24 h incubation (37 °C, 20 rpm). To assess biofilm disruption, the BacTiter-Glo^{TM} Microbial Cell Viability Assay (Promega) was used according to the manufacturer's instructions for Candida, to determine luminescence (600 nm) as a measure of viable bacterial cell number using a FLUOstar Omega plate reader.

2.2.5 Confocal laser scanning microscopy (CLSM)

2.2.5.1 Biofilm formation assay

Adjusted O/N *C. albicans* ATCC 90028, GBJ 13/4A, *parapsilosis* W23 and *auris* NCPF 8971 cultures ($5x10^6$ cells/mL) were incubated in a sterile black, glass-

bottomed 96-well plate (Greiner) for 45 mins at 37 ºC with 20 rpm rocking, with prewarmed RPMI-1640 medium in a 1:4 ratio. After incubation, biofilms were gently washed with prewarmed RPMI-1640 (x3), all medium was then removed from wells before adding fresh RPMI-1640 ± 4% OligoG CF-5/20 ± MIC nystatin (1 µg/mL) and the plate was re-incubated for 24 h (37 °C, 20 rpm). After biofilm formation, all the supernatant was gently removed, and biofilms were stained with 7 µl of LIVE/DEAD® stain (BacLight™ Bacterial Viability kit; Invitrogen; diluted (1:1) using 2 µL SYTO 9 and 2 µL propidium iodide in 1 mL phosphate buffered saline (PBS)) for 3 minutes. Samples were covered in foil to prevent exposure to light. A further 43 µL of PBS was added to prevent the biofilms from drying-out before imaging by CLSM. The green SYTO 9 stain was used to visualise LIVE cells (excitation/emission 480/500 nm), while red propidium iodide (excitation/emission 490/635 nm) was used to visualize dead/dying cells.

2.2.5.2 Biofilm disruption assay

C. albicans ATCC 90028, GBJ 13/4A, *parapsilosis* W23 and *auris* NCPF 8971 O/N cultures were adjusted to $5x10^6$ cells/mL and incubated, as described above (**Section 2.2.5.1**). After incubation, all supernatants were gently removed and well contents were replaced with 200 µL fresh RPMI-1640 medium and incubated for 24 h (37 ºC, 20 rpm). After incubation, half of well volume was removed and replaced with 100 µL of fresh RPMI-1640 ± 4% OligoG CF-5/20 (v/v) ± 2xMIC nystatin (2 µg/mL; v/v), and the plate was reincubated for a further 24 h (37 °C, 20 rpm; n=3). After 24 h, all the supernatant was gently removed, and biofilms were stained with 7 µL of LIVE/DEAD® stain, as described above (**Section 2.2.5.1**), before imaging by CLSM using a Leica TCS SP5 CLSM.

2.2.5.3 COMSTAT image analysis

Experiments were performed in triplicate with five Z-stack images taken of each sample using a Leica SP5 CLSM on x63 magnification oil lens, resolution of 512 x 512, zoom x1, line average of 1 and step size of 0.67 µm and step number 50. Las-X software was used for exporting images as well as processing data. CLSM Z-stack images were analysed using COMSTAT software for quantification of the 3-D biofilm structure (biomass volume, thickness, surface roughness and LIVE/DEAD biomass ratio) (Heydorn et al. 2000).

2.2.6 Sorbitol assay

Sorbitol acts as a cell wall osmotic protective agent, so that in its presence, osmotic pressure in the cell is maintained, allowing biosynthesis of the cell wall (Frost et al. 1995). Sorbitol (Sigma-Aldrich) was added and dissolved in RPMI-1640 medium (to a working concentration of 0.8 M), and the assay was set up similarly to the MIC assays (**Section 2.2.2**), with MIC values compared to a control assay (performed without sorbitol). Plates were set up for *C. albicans* ATCC 90028, GBJ 13/4A, *parapsilosis* W23 and *auris* NCPF 8971, before being incubated at 37 ^{o}C, and readings were taken after 1, 2, and 7 days (n=3). Due to the protective effects of sorbitol, an increase in MIC in the presence of added sorbitol was, therefore, taken as indicative that the mechanism of action for the test agent was linked to disruption of the cell wall.

2.2.7 Ergosterol assay

This assay was used to determine OligoG CF-5/20 binding to ergosterol present in the fungal cell wall. A positive interaction showing binding to exogenous ergosterol

present in the medium was denoted by an observed increase in MIC compared to the no ergosterol control (Leite et al. 2015). *C. albicans* ATCC 90028, GBJ 13/4A, *parapsilosis* W23 and *auris* NCPF 8971 overnight cultures were adjusted and set up as performed for the MIC assays (**Section 2.2.2**). *Candida* MICs were repeated in the presence and absence of ergosterol (Escalante et al. 2008). Ergosterol (Sigma-Aldrich) was dissolved in DMSO (with 1% Tween 80, Sigma-Aldrich, prior to being diluted to a final concentration of 400 µg/mL in RPMI-1640). Plates were read after 1, 2, and 7 days of incubation at 37 ^{o}C (n=3). The antifungal amphotericin B was used as a positive control (starting concentration of 128 µg/mL).

2.2.8 Germ tube assay

Overnight cultures of *C. albicans* ATCC 90028, GBJ 13/4A, *parapsilosis* W23 and *auris* NCPF 8971 were set up in SAB broth. *Candida* cells were then washed (x2) with PBS and the resulting pellet was re-suspended in 500 µL of PBS (~5x10^{6} CFU/mL) (Tøndervik et al. 2014). Then, 1 mL of donor horse serum (ThermoFisher Scientific) ± 4% OligoG CF-5/20 ± 1 µg/mL nystatin was inoculated with 100 µL of the washed candidal suspensions, and incubated for 2 h at 37 °C. After incubation, the suspension was washed with 0.9% Sodium Chloride (NaCl) (x3) to remove OligoG CF-5/20 and resuspended in 200 µL PBS. The percentage number of cells with hyphal growth was calculated using a Neubauer haemocytometer, under phase contrast microscopy. *C. glabrata* (ATCC 2001) was used as a negative control, due to its inability to form germ tubes.

2.2.9 Permeabilisation assay

Adjusted O/N cultures of *C. parapsilosis* W23 ($1x10^7$ cells/mL) was first added to a sterile glass-bottomed 96-well plate (Greiner), followed by pre-warmed RPMI-1640 at a ratio of 1:10 and incubated shaking for 24 h at 20 rpm at 37 ºC (200 µL/well). After incubation, each well was washed with dH_2O, after which 200 µL of RPMI-1640 ± OligoG CF-5/20 (4%) ± nystatin (1 µg/mL) was added to each well and incubated for 3 h at 37 ºC (n=3). Samples were then washed and exposed to propidium iodide (PI, 1 mg/mL) for 15 min at 37 ºC, washed and mounted using Vectashield® (Vector Laboratories), prior to examination by Leica TCS SP5 CLSM microscopy. Fungal membrane permeability was assessed through measuring the fluorescence intensity of propidium iodide from CLSM Z-stack imaging using IMARIS software. With thanks to Dr. Lydia Powell for set up and imaging.

2.2.10 Transmission electron microscopy (TEM) imaging of the cell wall

An adjusted O/N culture of *C. parapsilosis* W23 ($5x10^6$ cells/mL) were grown on Thermanox™ glass cover slips (ThermoFisher Scientific) in a sterile 6-well microtiter plates for 45 mins (37 ºC, 20 rpm rocking). After incubation, biofilms were gently washed with prewarmed RPMI-1640 (x3), before removing all medium and adding 2 mL of RPMI-1640 ± 4% OligoG CF-5/20 ± nystatin (1 µg/mL). Plates were then reincubated on a rocker for 24 h (37 ºC, 20 rpm), after which, the supernatant was removed, and cells were fixed with 1% glutaraldehyde for 1 h before replacing the fixative with PBS.

Cells were fixed and imaged by Dr. Christopher Von Ruhland. Fixed cells were centrifuged at 100 *g* for 10 mins, before the pellet was mixed with 4% molten agarose in equal volumes and was cooled to room temperature. The blocks were cut into 1 mm

cubes and washed in double distilled water (ddH_2O) for 10 mins, before being processed into resin in a rotary mixer at room temperature by the following steps: post-fixed for 1 h in 2% (w/v) osmium tetroxide in ddH_2O, 10 min wash in ddH_2O (x3), block stained for 1 h in 2% uranium acetate in ddH_2O, 10 min wash in ddH_2O (x3), 15 mins in 50% (v/v) propan-2-ol (IPA) in ddH_2O, 15 mins in 70% (v/v) IPA in ddH_2O, 15 mins in 90% (v/v) IPA in ddH_2O, 15 mins in IPA (x2), 30 mins in 50% (v/v) hard grade TAAB Embedding Resin (TER) in IPA, 1 h in TER (x4). Blocks were transferred into truncated polypropylene BEEM capsules, and the capsules filled with fresh TER resin. Capsules were placed in a 60 °C oven and curing allowed to proceed for 24 h. Semi-thin (0.35 mm thick) sections were cut with glass knives on an Ultracut E ultramicrotome (Leica Microsystems), placed on droplets of water on a glass slide and dried on a hot plate. Sections were stained with 1% toluidine blue, washed in tap water, dried, and mounted with Gurr's Neutral Mountant. Thin (100 nm thick) sections were cut with a diamond knife on an Ultracut E ultramicrotome, collected onto 300 mesh copper grids and allowed to air dry. Sections were stained with Reynold's lead citrate for 15 mins, washed in ddH_2O for 1 min (x3) and allowed to air dry. Samples were examined in a Hitachi HT7800 TEM (Hitachi High Tech Ltd) at 100 kV and images captured with Radius software (EMSIS GmbH).

2.2.11 Statistical analysis

GraphPad Prism® was used for all data analysis. Any outliers were identified and removed by the robust regression and outlier removal (ROUT) method, with the Q coefficient set to between 1-10%. One-way analysis of variance (ANOVA) test was used to calculate any significant changes between treatments ($n > 2$), followed by the Tukey multiple comparison test. For analysis of *C. albicans* ATCC 90028 (formation

assay) mean thickness COMSTAT data and *C. albicans* GBJ 13/4A (formation assay) roughness coefficient COMSTAT data, group wise comparisons were analysed using Kruskal-Wallis nonparametric one-way analysis of variance. *C. albicans* GBJ 13/4A (formation assay) biovolume COMSTAT data was transformed to be normally distributed using Y=cos(Y). A $P < 0.05$ was considered significant.

2.3 Results

2.3.1 Antifungal effect of nystatin and OligoG CF-5/20 against *Candida* spp.

The combination treatment of OligoG CF-5/20 with nystatin was shown to increase the antimicrobial effect of nystatin against a range of *Candida* species (**Table 2.2**). The greatest dose-dependent effect was seen for *C. dubliniensis* 40/01, showing a five-fold dilution decrease in MIC value, when nystatin was used in combination with 6% OligoG CF-5/20. In contrast, *C. albicans* ATCC 90028 and *C. parapsilosis* W23 showed a two-fold change, two strains (*C. auris* 8971 and *C. albicans* Ptr/94) showed no change, and all other strains showed only a non-significant (one-fold) reduction in MIC value between 0% and 6% OligoG CF-5/20.

2.3.2 Effect of OligoG CF-5/20 on planktonic growth of *Candida* species

The growth curves of *Candida* strains revealed that OligoG CF-5/20 (tested at 0 and 6%), showed a significant dose-dependent inhibition of growth for *C. auris* NCPF 8971 and *C. parapsilosis* W23 (MSD=0.12 and 0.20 respectively), although this was not evident for *C. albicans* ATCC 90028 or *C. albicans* GBJ 13/4A (MSD=0.12 and 0.32 respectively) (**Figure 2.2)**. Untreated controls showed a 3–5-h lag phase is seen before an exponential phase of 7 h for *C. albicans* ATCC 90028, 8 h for *C.*

Table 2.2. Minimum inhibitory concentration (MIC;[μg/mL]) of nystatin alone and with increasing concentrations of OligoG CF-5/20 after 48 h incubation.

***Candida* strains**	**Nystatin MIC (μg/mL) at indicated OligoG CF-5/20 concentration (%)**					
	0	**0.5**	**1**	**2**	**4**	**6**
C. albicans ATCC 90028	2	2	2	1	1	0.5
C. albicans GBJ 13/4A	2	2	2	2	1	1
C. albicans SC5314	1	1	1	1	0.5	0.5
C. albicans CCUG 39343	2	2	2	1	1	1
C. albicans 480/00	2	4	4	2	1	1
C. albicans PB1/93	2	2	4	2	1	1
C. albicans Lr1/93	1	2	2	1	0.5	0.5
C. albicans Ptr/94	2	2	2	2	2	2
C. parapsilosis W23	4	2	2	2	1	1
C. auris NCPF 8971	2	4	4	4	2	2
C. tropicalis 519468	2	2	1	1	1	1
C. glabrata ATCC 2001	4	8	4	4	2	2
C. dubliniensis 40/01	2	2	2	0.5	0.25	0.063

Shaded areas represent decrease in MIC (nystatin potentiation) with increasing OligoG CF-5/20 concentration.

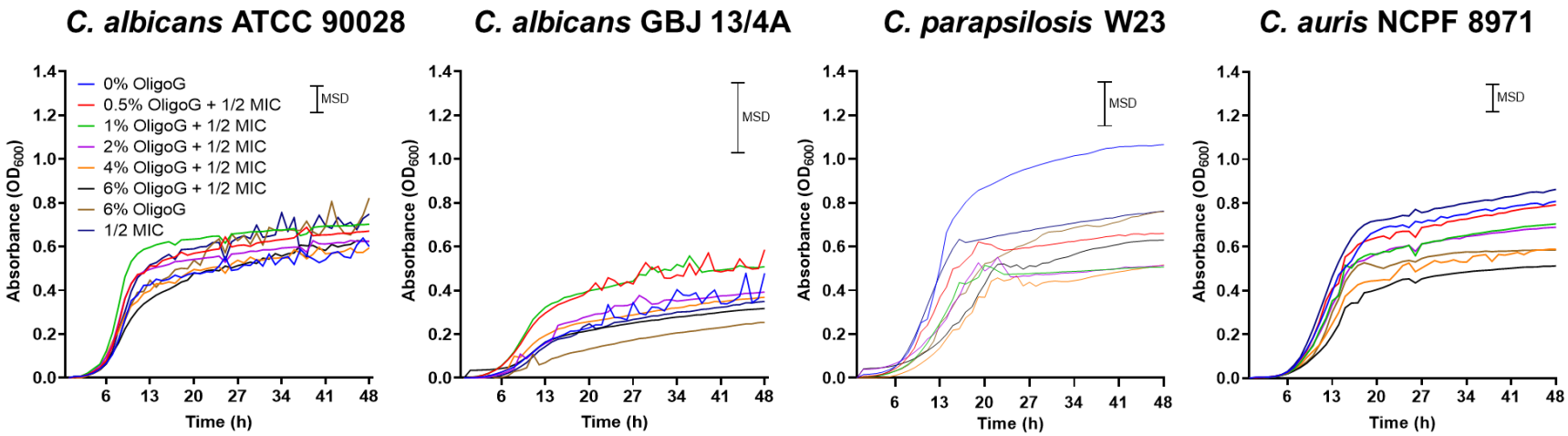

Figure 2.2. Growth curves for *C. albicans* ATCC 90028, *C. albicans* GBJ 13/4A, *C. parapsilosis* W23 and *C. auris* NCPF 8971 and treated with ½ MIC nystatin (1-2 µg/mL) with increasing concentrations of OligoG CF-5/20 (0, 0.5, 1, 2, 4, 6 %) and OligoG CF-5/20 alone (6%). Minimum significant difference (MSD) for absorbance was calculated in MiniTab using the Tukey-Kramer method (n=3): *C. albicans* ATCC 90028 (MSD=0.12); *C. albicans* GBJ 13/4A (MSD=0.32); *C. parapsilosis* W23 (MSD= 0.20); and *C. auris* NCPF 8971 (MSD=0.12).

albicans GBJ 13/4A, 15 h for *C. parapsilosis* W23, and 13 h for *C. auris* NCPF 8971. Between 24 h and 48 h, only *C. parapsilosis* W23 showed significant decreases for all treatments, compared to the untreated control. Over the same period, *C. auris* NCPF 8971 demonstrated a significant decrease in growth for 6% OligoG CF-5/20 alone, 4% OligoG CF-5/20 and nystatin and 6% OligoG CF-5/20 and nystatin treatments, resulting in prolonged lag-phase and reducing overall growth at 48 h. For strains *C. albicans* ATCC 90028 and GBJ 13/4A, the observed decreases in growth were not significant.

2.3.3 Effect of OligoG CF-5/20 in combination with nystatin on cellular viability

ATP viability assays showed that the combination therapy of 4% OligoG CF-5/20 and nystatin at the MIC value significantly reduced the cellular viability of pre-established biofilms, compared to untreated controls for twelve of the *Candida* strains tested, including all *C. albicans* strains and four of the five NCAC strains (*C. dubliniensis* 40/01 being the exception; **Figure 2.3**). Interestingly, OligoG CF-5/20 showed to significantly reduce cell viability within an established biofilm for all thirteen strains, compared to only eight of the thirteen strains when treated with NYS only, with was only significant at reducing 1 out of 5 of the NCAC strains (*C. glabrata* ATCC 2001). Furthermore, comparison of NYS with combination treatment and NYS with OligoG CF-5/20 showed significant reductions for all strains **(Supplementary Table 1**).

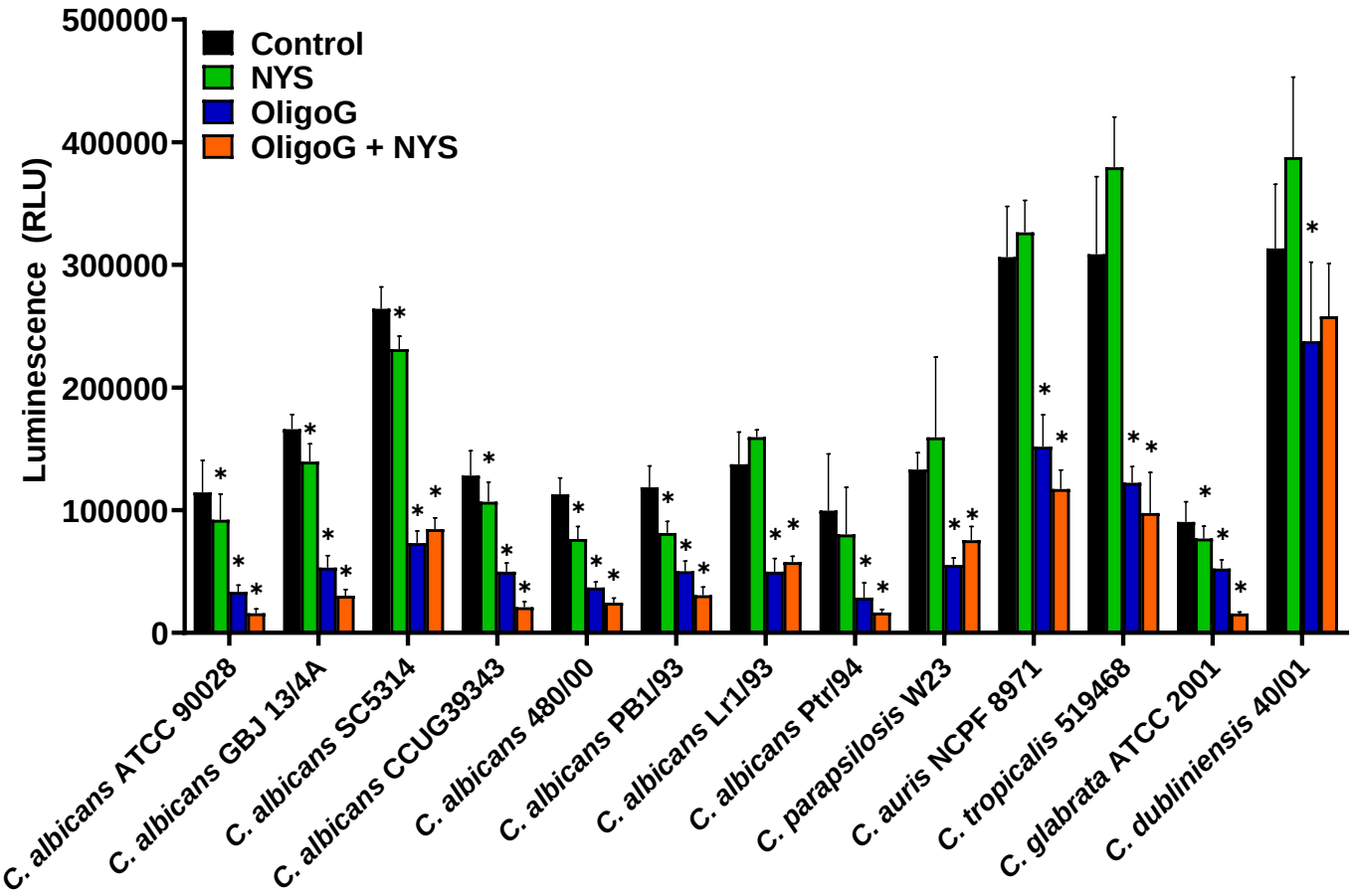

Figure 2.3. ATP cell viability assay for biofilms of thirteen *Candida* spp. grown for 24 h prior to treatment with ± 4% OligoG CF-5/20 ± nystatin (NYS; at MIC, 1-4 μg/mL) for a further 24 h showing mean ± S.D (n=3). Group wise comparisons were analysed using one-way ANOVA followed by Tukey's post-hoc tests; * $P < 0.05$ compared to an untreated control. (All P values are shown in **Supplementary Table 1**).

2.3.4 Confocal laser scanning microscopy and COMSAT analysis of therapies on *Candida* biofilm formation and disruption

CLSM imaging and COMSTAT image analysis following treatment with OligoG CF-5/20 and/or nystatin were performed on four *Candida* strains of clinical importance, namely *C. albicans* ATCC 90028, *C. albicans* GBJ 13/4A, *C. parapsilosis* W23, and *C. auris* NCPF 8971 (**Figures 2.4 to 2.11**). In the biofilm formation assay, COMSTAT analysis showed that the combination treatment (4% OligoG CF-5/20 and nystatin at MIC value [1 μg/mL]) demonstrated a significant reduction in both biovolume and the biofilm thickness (**Figures 2.5, 2.7, 2.9 and 2.11**), in addition to significant increases in roughness coefficient and ratio of DEAD cells (red) to LIVE (green) cells, compared to the untreated controls and nystatin only treatments for all four *Candida* strains. The inhibitory effects on strains *C. albicans* GBJ 13/4A and *C. parapsilosis* W23 were particularly striking, with almost no biofilm formation having occurred (**Figures 2.7 and 2.9**). Interestingly, OligoG CF-5/20, when used as a stand-alone treatment was highly effective against *C. auris* NCPF 8971, demonstrating disrupted biofilm formation, with COMSTAT analysis revealing significant reductions in biofilm biomass and thickness, as well as an increase in biofilm roughness and ratio of DEAD to LIVE cells (**Figure 2.11**).

In the biofilm disruption assay, confocal imaging showed that combination therapy of 4% OligoG CF-5/20 and 2 μg/mL nystatin (two-fold MIC) visibly altered the architecture of the biofilms formed by all *Candida* spp., causing a more porous structure to form (**Figures 2.4, 2.6, 2.8 and 2.10**). However, COMSTAT analysis did not show any significant structural alterations in biovolume, when compared to an untreated control. OligoG CF-5/20 treatment alone of *C. albicans* ATCC 90028 did show a significant decrease in both biofilm biovolume and mean thickness, with a

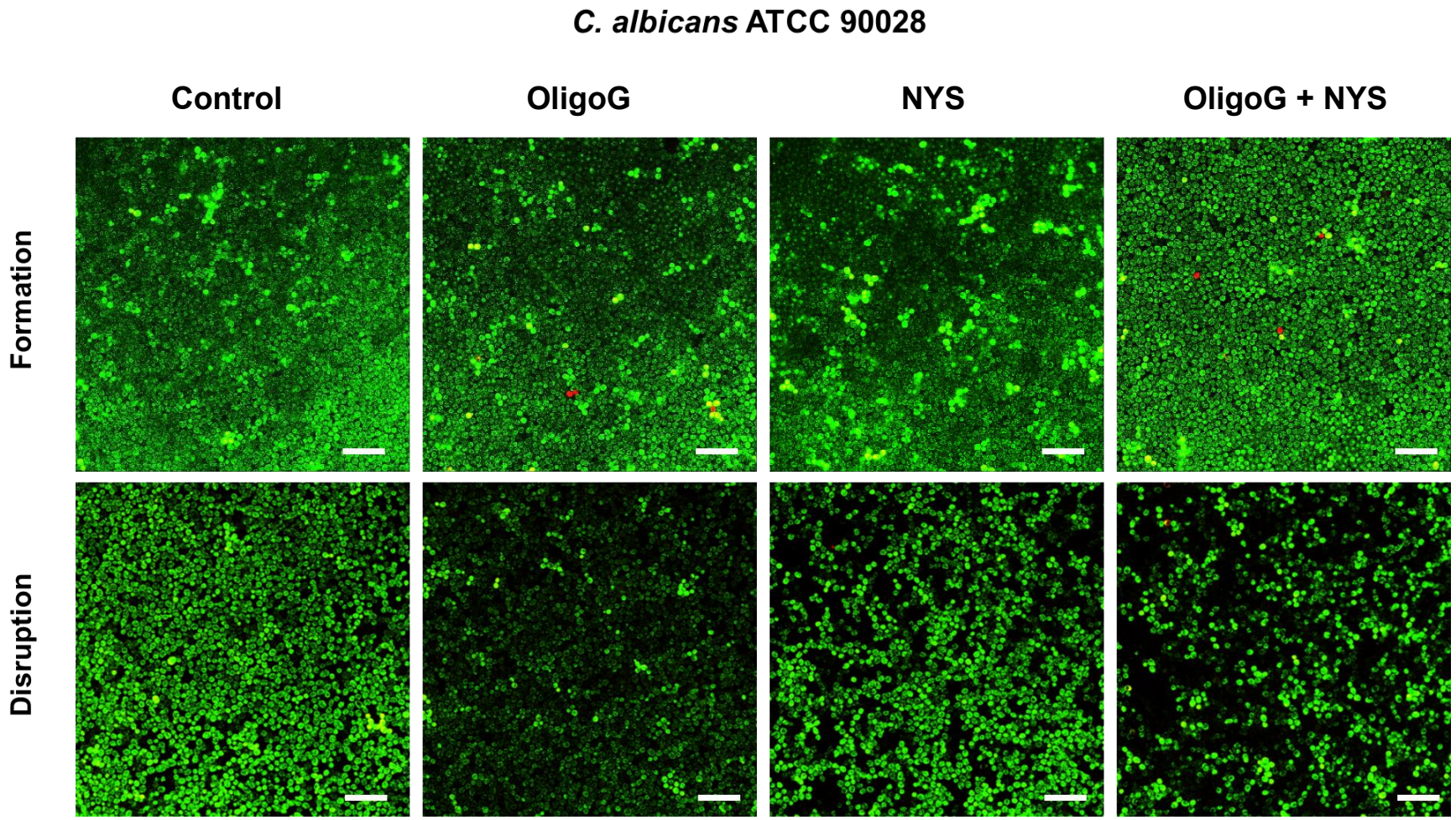

Figure 2.4. CLSM maximum projection of a Z-stack of *C. albicans* ATCC 90028 biofilms with LIVE/DEAD® staining. For the biofilm formation assay, biofilms were grown for 24 h ± 4% OligoG CF-5/20 ± nystatin at MIC value (1 µg/mL) and for the biofilm disruption assay. Biofilms were grown for 24 h, before a 24 h treatment ± 4% OligoG CF-5/20 ± 2-fold MIC nystatin (2 µg/mL); scale bar = 30 µm.

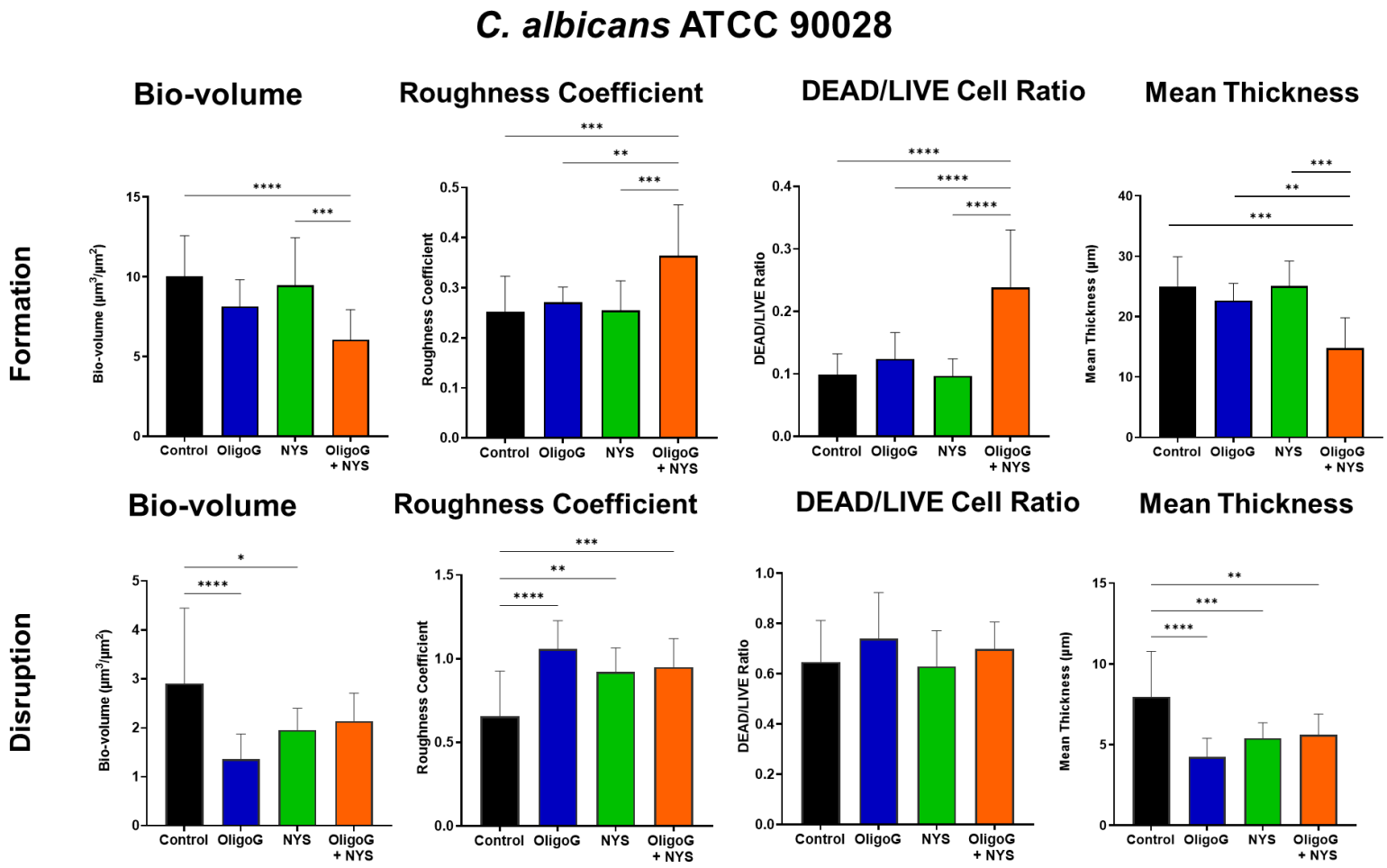

Figure 2.5. COMSTAT image analysis of *C. albicans* ATCC 90028 formation and disruption assays (**Figure 2.4**), showing bio-volume ($\mu m^3/\mu m^2$), roughness coefficient, DEAD/LIVE cell ratio and mean thickness (µm) ± S.D; n=15. Group wise comparisons were analysed using one-way ANOVA, followed by Tukey's post hoc tests *P<0.05 **P<0.01 ***P<0.001****P<0.0001 denotes significance.

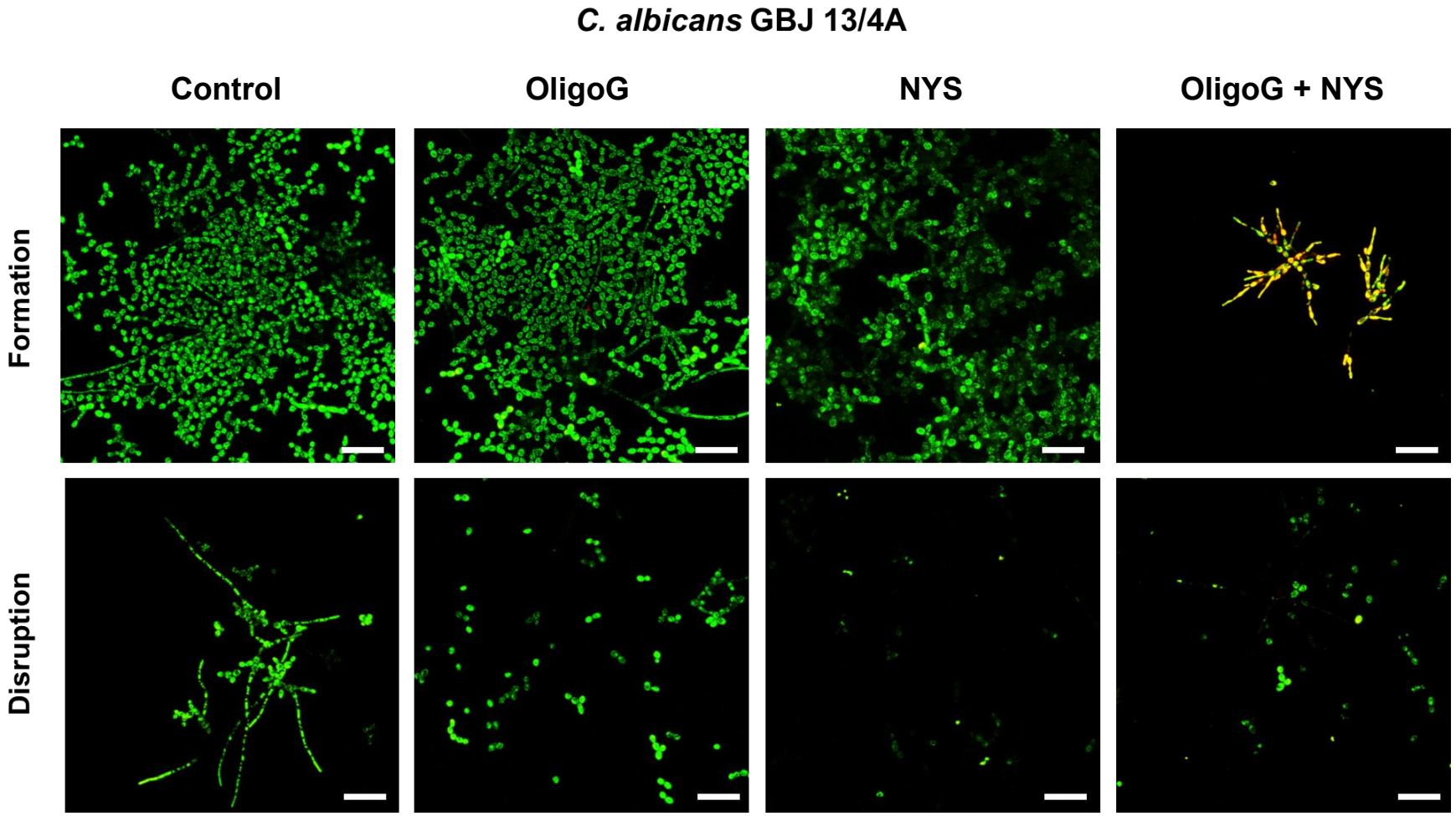

Figure 2.6. CLSM Z-stack imaging of *C. albicans* GBJ 13/4A biofilms with LIVE/DEAD® staining. For the biofilm formation assay, biofilms were grown for 24 h ± 4% OligoG CF-5/20 ± nystatin at MIC value (1 μg/mL) and for the biofilm disruption assay. Biofilms were grown for 24 h, before a 24 h treatment ± 4% OligoG CF-5/20 ± 2-fold MIC nystatin (2 μg/mL); scale bar = 30 μm.

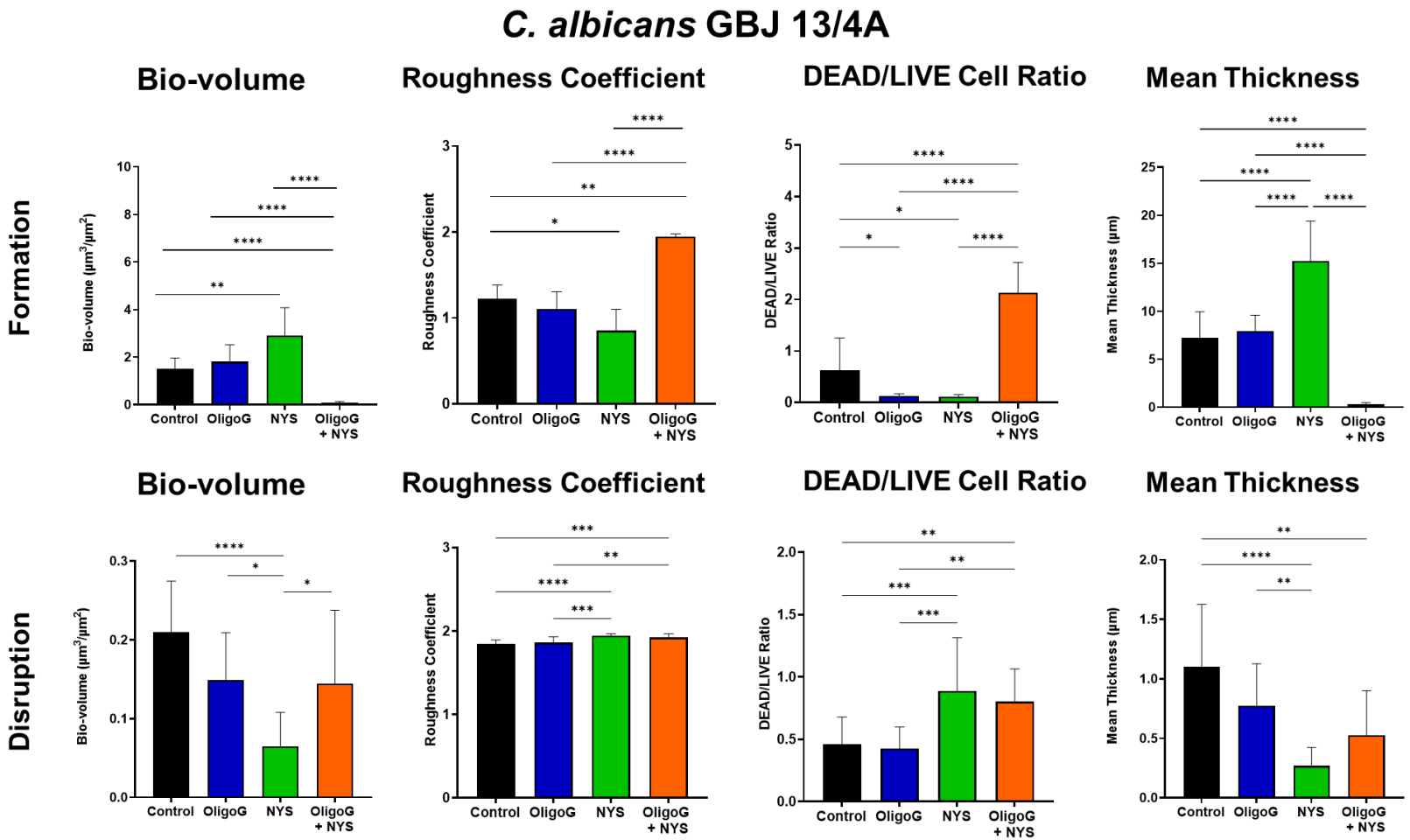

Figure 2.7. COMSTAT image analysis of *C. albicans* GBJ 13/4A formation and disruption assays (**Figure 2.6**) showing bio-volume ($\mu m^3/\mu m^2$), roughness coefficient, DEAD/LIVE cell ratio and mean thickness (µm) ± S.D; n=15. Group wise comparisons were analysed using one-way ANOVA, followed by Tukey's post hoc tests *P<0.05 **P<0.01 ***P<0.001****P<0.0001 denotes significance.

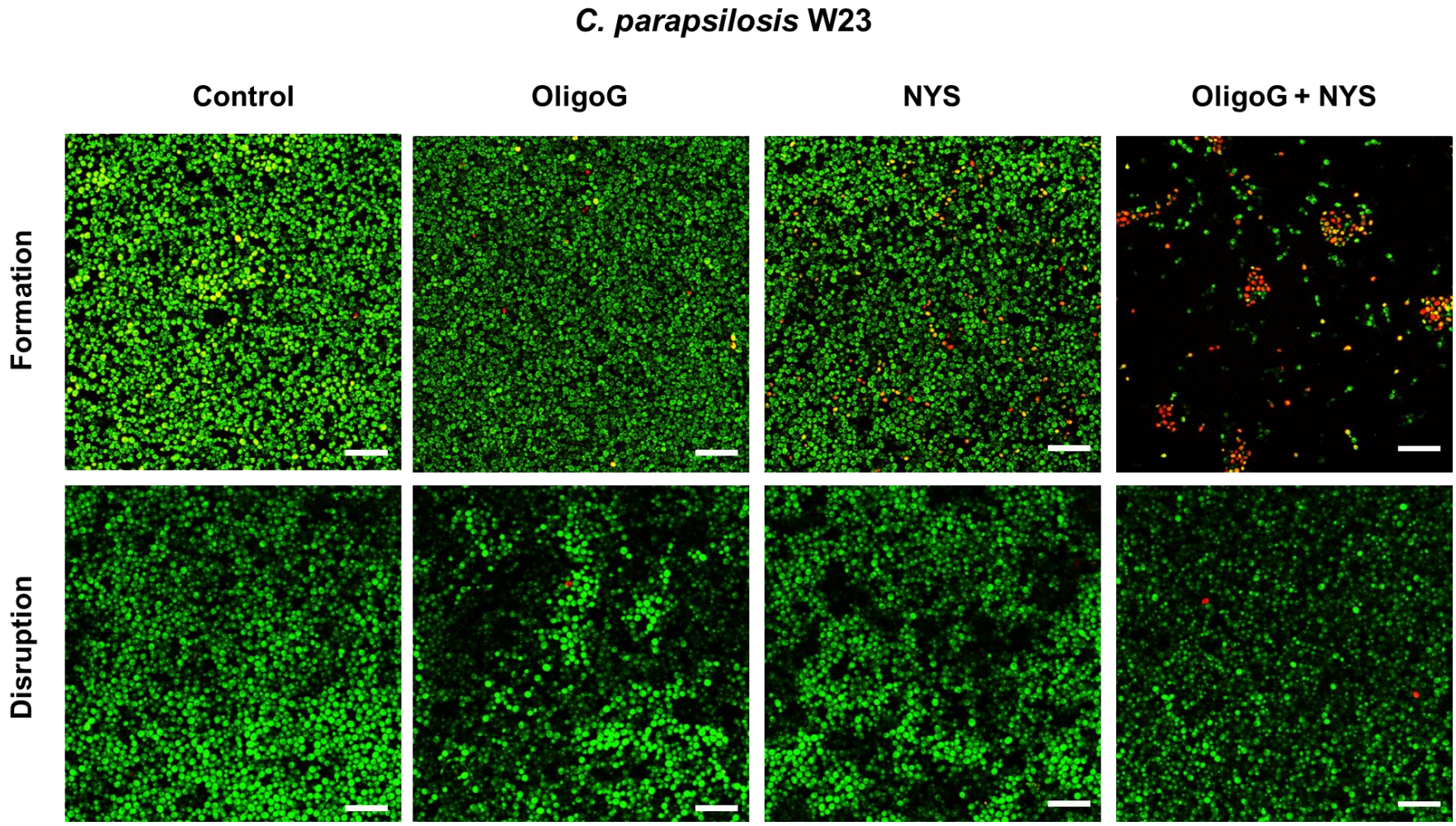

Figure 2.8. CLSM Z-stack imaging of *C. parapsilosis* W23 biofilms with LIVE/DEAD® staining. For the biofilm formation assay, biofilms were grown for 24 h ± 4% OligoG CF-5/20 ± nystatin at MIC value (1 µg/mL) and for the biofilm disruption assay. Biofilms were grown for 24 h, before a 24 h treatment ± 4% OligoG CF-5/20 ± 2-fold MIC nystatin (2 µg/mL); scale bar = 30 µm.

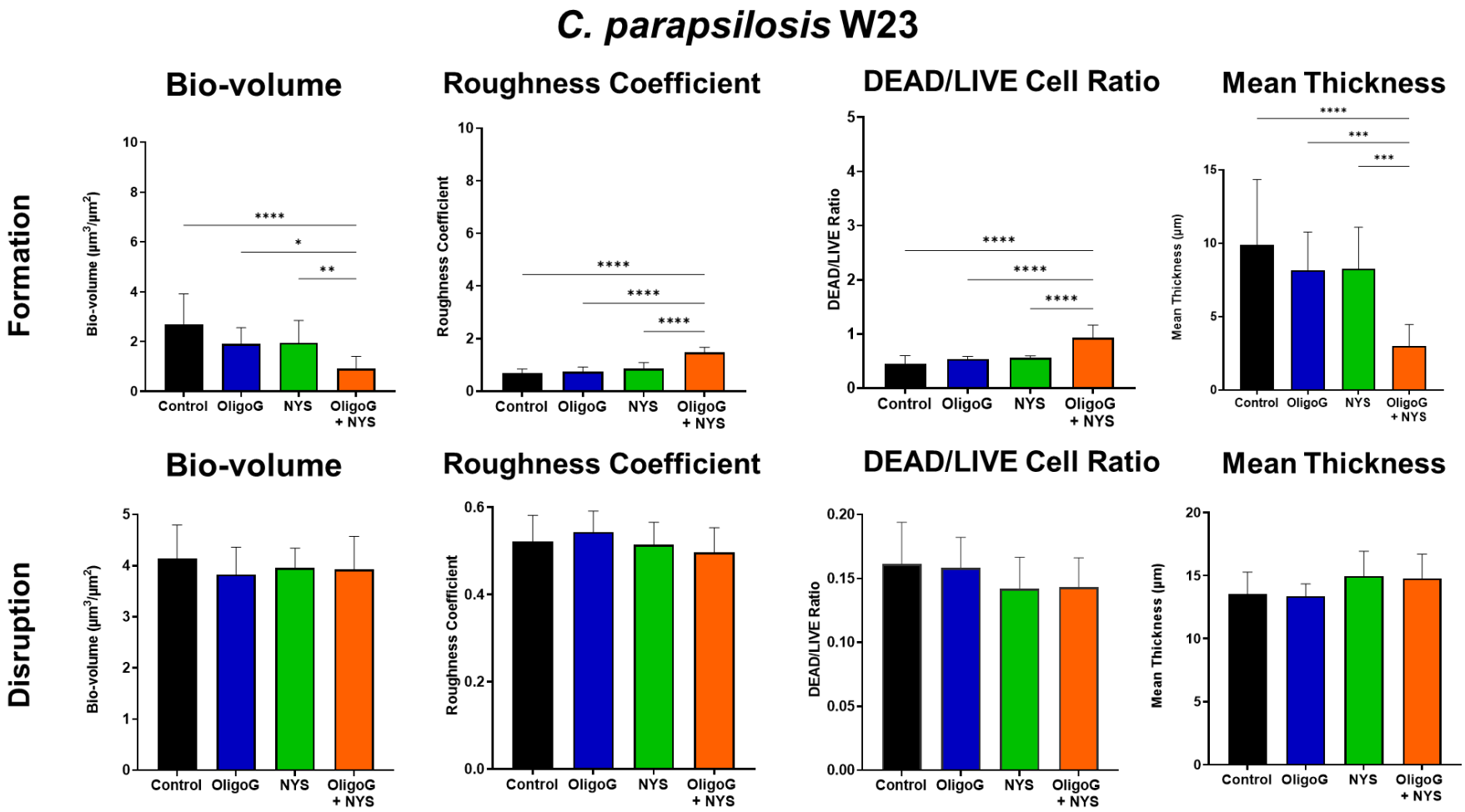

Figure 2.9. COMSTAT image analysis of *C. parapsilosis* W23 formation and disruption assays (**Figure 2.8**), showing bio-volume ($\mu m^3/\mu m^2$), roughness coefficient, DEAD/LIVE cell ratio and mean thickness (µm) ± S.D; n=15. Group wise comparisons were analysed using one-way ANOVA, followed by Tukey's post hoc tests *P<0.05 **P<0.01 ***P<0.001****P<0.0001 denotes significance.

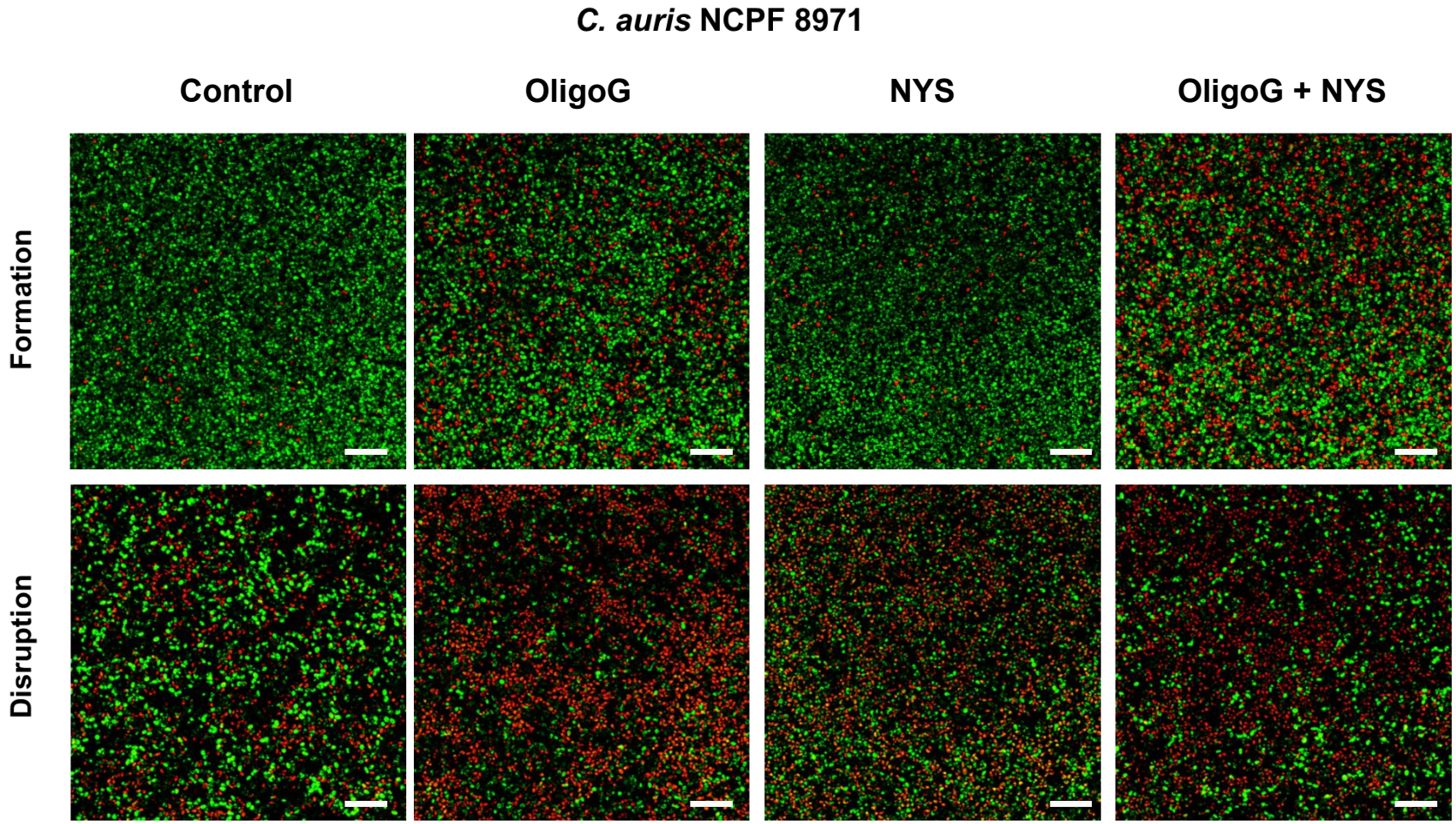

Figure 2.10. CLSM Z-stack imaging of *C. auris* NCPF 8971 biofilms with LIVE/DEAD® staining. For the biofilm formation assay, biofilms were grown for 24 h ± 4% OligoG CF-5/20 ± nystatin at MIC value (1 µg/mL) and for the biofilm disruption assay. Biofilms were grown for 24 h, before a 24 h treatment ± 4% OligoG CF-5/20 ± 2-fold MIC nystatin (2 µg/mL); scale bar = 30 µm.

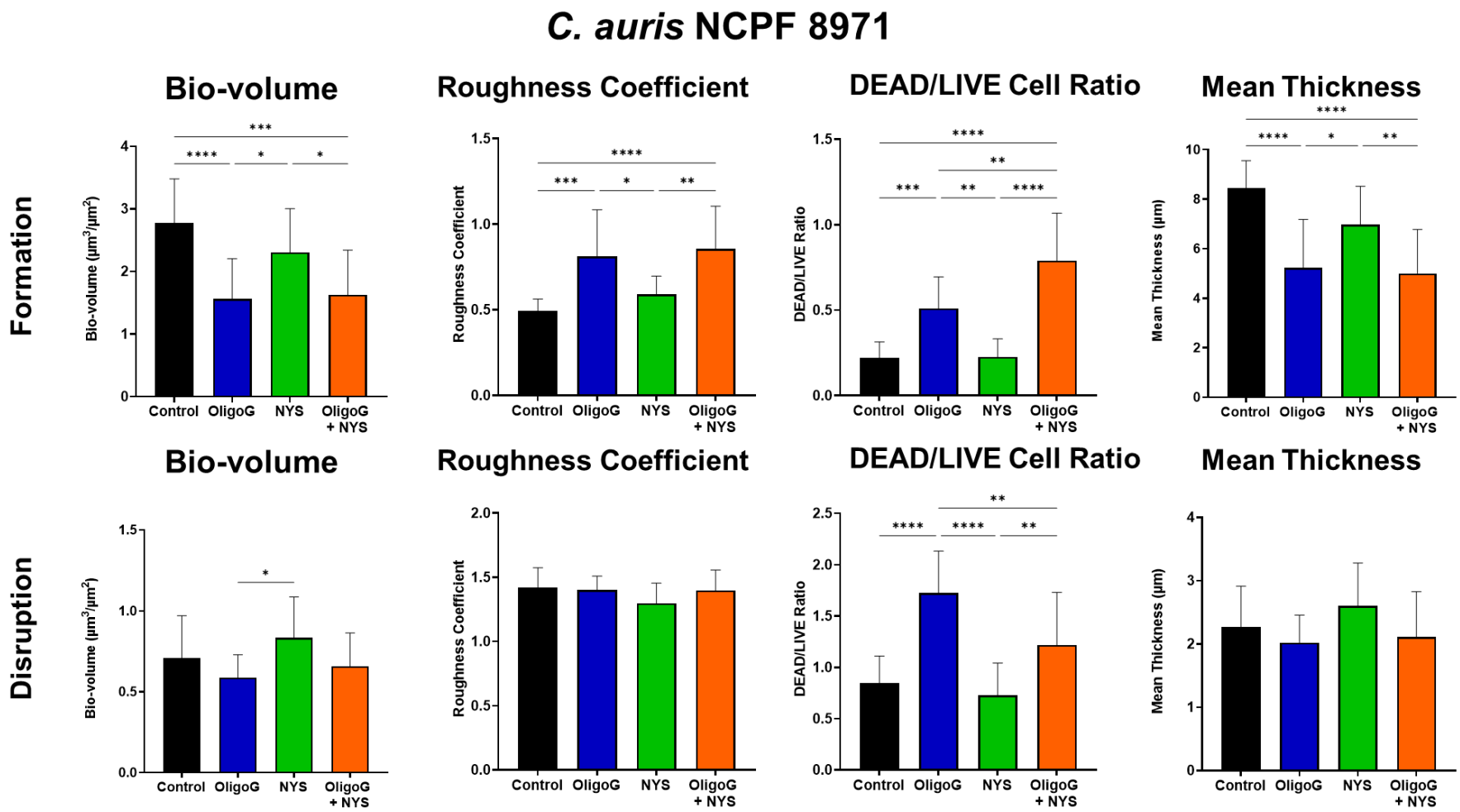

Figure 2.11. COMSTAT image analysis of *C. auris* NCPF 8971 formation and disruption assays (**Figure 2.10**), showing bio-volume ($\mu m^3/\mu m^2$), roughness coefficient, DEAD/LIVE cell ratio and mean thickness (µm) ± S.D; n=15. Group wise comparisons were analysed using one-way ANOVA, followed by Tukey's post hoc tests *P<0.05 **P<0.01 ***P<0.001****P<0.0001 denotes significance.

simultaneous significant increase in surface roughness. Combination treatment showed a significant decrease in biofilm thickness, while also displaying a significant increase in surface roughness (**Figure 2.5**). Similarly, when treated with the combination therapy, *C. albicans* GBJ 13/4A showed a marked increase in the roughness coefficient, DEAD/LIVE cell ratio with a significant reduction in the mean biofilm thickness, compared to the untreated control. However this was not significant when compared to the nystatin only treatment (**Figure 2.7**). Interestingly, *C. parapsilosis* W23 showed no significant changes in biofilm disruption compared to the untreated control (**Figure 2.9**). OligoG CF-5/20 showed significant effects on *C. auris* NCPF 8971 biofilm disruption with increased levels of DEAD to LIVE cells, indicating that this treatment had anti-biofilm effects (on biofilm formation and disruption) when used alone (**Figure 2.11**).

2.3.5 Germ tube formation

Light microscopy showed that of five strains tested only two (*C. albicans* ATCC 90028 and *C. albicans* GBJ13/4A) formed germ tubes, with *C. auris* NCPF 8971 and *C. parapsilosis* W23 not found to form any under the conditions used (**Figure 2.12**). *C. glabrata* ATCC 2001 was the negative control for this assay. For the two *Candida albicans* strains, all treatments were shown to reduce hyphal production compared to the untreated control, although this was not significant. The percentage of cells with germ tubes produced in the untreated control was shown to vary considerably between these two strains, with the majority of *C. albicans* ATCC 90028 producing hyphae, compared to *C. albicans* GBJ 13/4A, which had very low numbers in comparison.

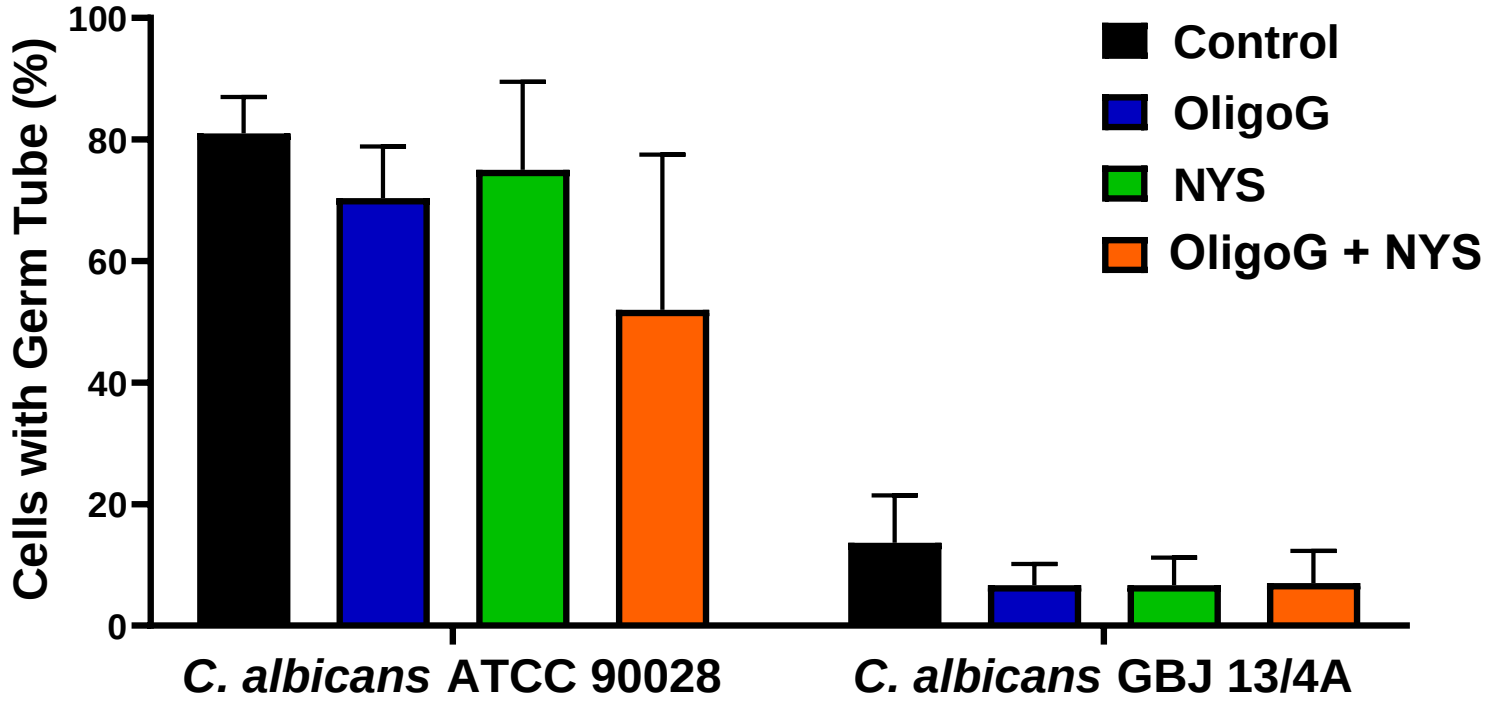

Figure 2.12. Percentage of *Candida* cells producing hyphae in *C. albicans; C. auris* NCPF 8971 and *C. parapsilosis* W23 (data not shown) were also tested, but also did not form hyphae.

2.3.6 Antifungal mechanism of action of OligoG CF-5/20

The MICs of four *Candida* strains were performed with and without the presence of 0.8 M sorbitol and read at day 1, day 2, and day 7 (Leite et al. 2015), (**Table 2.3**). At day 7, (except for one reading), no significant changes in MIC were observed, regardless of the presence or absence of sorbitol, in this case, suggesting that the cell wall was not one of the possible anti-microbial cell targets for nystatin and OligoG CF-5/20. To assess if the enhancement of nystatin by OligoG CF-5/20 is due to ergosterol binding, MICs were also performed with and without exogenous ergosterol (**Table 2.4**). In contrast to the sorbitol assay, for three out of four strains (apart from *C. parapsilosis* W23), the ergosterol assay showed a slight increase (two-fold dilution maximum) in MIC with the addition of ergosterol to the culture medium, compared to the no ergosterol control. A one-fold change was taken to represent experimental error and not an actual increase in MIC. In comparison, the positive control, amphotericin B, demonstrated an increase in MIC for 3/4 of the strains from <0.065 μg/mL to 16 μg/mL (equivalent to an 8-fold increase), in the presence of ergosterol. Hence, nystatin demonstrated low interaction with ergosterol (binding to fungal membrane sterols), although this was far less than that observed for amphotericin B (used at a concentration of ≥128 μg/mL), which was much higher than the concentrations used for nystatin (≥16 μg/mL). The concentration of OligoG CF-5/20 used in the assay had a minimal effect on the MICs obtained, similar to those observed earlier where many strains showed only a one- or two-fold change in MIC at 6% OligoG CF-5/20 (**Table 2.2**). Furthermore, if OligoG CF-5/20 enhanced the affinity of nystatin for ergosterol binding, the presence of exogenous ergosterol in these assays should minimize changes in the MIC value of the combination treatment,

in comparison to nystatin only (plus ergosterol) treatment. However, this was not the case, as the MIC of the combination treatment (6% OligoG CF-5/20 plus nystatin) in the presence of additional ergosterol demonstrated a decrease (up to three-fold), compared to the nystatin-only (plus ergosterol) treatment. This data suggests that a secondary mechanism of action, (other than ergosterol binding), contributes to the antifungal effect of the combination treatment of OligoG CF-5/20 and nystatin.

2.3.7 Permeabilisation of *Candida* spp. cells by OligoG CF-5/20

The fungal membrane permeability assay, unsurprisingly, revealed nystatin treatment significantly increased cell permeabilization, when compared to an untreated control. A significant difference in cell permeabilisation was evident when comparing the combination treatment of OligoG CF-5/20 and nystatin to the untreated control. However, no significant difference was seen when comparing the combination treatment to the nystatin treatment alone **(Figure 2.13 A)**. These results were mirrored in TEM imaging, with reorganisation of the *Candida* cell membrane observed when treated with nystatin only or a combination treatment of OligoG CF-5/20 and nystatin (**Figure 2.13 B**). This structural reorganisation was not evident in untreated, or OligoG CF-5/20 treated *Candida* cells.

Table 2.3. MIC values (µg/mL) of the antifungal nystatin at indicated OligoG CF-5/20 concentration in the absence (-) and presence (+) of sorbitol (0.8 M) against 4 *Candida* strains measured after 1- (D1), 2- (D2) and 7-days (D7) incubation.

Isolate		Antifungal MIC (µg/mL at indicated OligoG CF-5/20 Concentration (%)											
		0		0.5		1		2		4		6	
		-	+	-	+	-	+	-	+	-	+	-	+
C. parapsilosis W23	D1	1	0.5	1	0.5	1	0.5	0.5	0.5	0.5	0.5	0.5	0.25
	D2	4	2	4	2	4	2	4	2	4	2	2	2
	D7	4	2	4	2	4	2	4	2	4	2	2	2
C. albicans GBJ13/4A	D1	1	<0.0156	1	<0.0156	1	<0.0156	0.25	<0.0156	0.25	<0.0156	0.125	<0.0156
	D2	2	1	2	2	2	2	2	1	1	1	0.5	0.25
	D7	8	1	2	8	4	4	4	4	4	2	2	2
C. albicans ATCC 90028	D1	2	1	2	1	2	1	2	0.5	1	0.5	1	0.25
	D2	4	2	4	2	4	2	4	2	2	1	2	1
	D7	4	4	8	4	8	4	8	4	8	4	4	2
C. auris NCPF 8971	D1	2	2	2	2	2	2	2	2	2	2	2	2
	D2	4	4	4	4	4	4	4	2	4	2	2	2
	D7	4	4	8	4	4	4	4	4	4	4	4	4

Shaded area represents an increase in MIC with sorbitol, compared to the no sorbitol control.

Table 2.4. MIC values (µg/mL) of the antifungal nystatin at indicated OligoG CF-5/20 concentration in the absence (-) and presence (+) of ergosterol (400 µg/mL) against 4 *Candida* strains measured after 1- (D1), 2- (D2) and 7-days (D7) incubation.

Isolate		Antifungal MIC (µg/mL) at indicated OligoG CF-5/20 Concentration (%)													
		0		0.5		1		2		4		6		Amphotericin B	
		-	+	-	+	-	+	-	+	-	+	-	+	-	+
C. parapsilosis W23	D1	1	1	1	1	1	1	0.5	0.5	0.5	0.5	0.5	0.125	<0.0625	<0.0625
	D2	4	4	4	4	4	4	4	4	4	4	2	2	<0.0625	2
	D7	8	16	16	16	16	16	16	16	16	16	8	16	0.5	4
C. albicans GBJ13/4A	D1	1	4	1	2	1	1	0.25	0.5	0.25	0.5	0.125	0.03125	<0.0625	4
	D2	2	8	2	8	2	8	2	8	0.5	4	0.5	1	<0.0625	16
	D7	8	8	2	8	4	8	4	16	4	8	2	2	<0.0625	16
C. albicans ATCC 90028	D1	2	8	2	8	2	4	2	2	1	0.5	1	0.5	<0.0625	16
	D2	4	8	4	8	4	8	4	8	2	2	2	2	<0.0625	16
	D7	4	16	8	16	8	16	8	16	8	8	4	8	<0.0625	16
C. auris NCPF 8971	D1	2	8	2	8	2	8	2	8	2	4	2	4	<0.0625	16
	D2	4	16	4	16	4	16	4	16	4	8	2	4	<0.0625	16
	D7	4	16	8	16	4	16	4	16	4	8	4	8	<0.0625	16

Shaded area represents a significant increase in MIC with ergosterol, compared to the no ergosterol control.

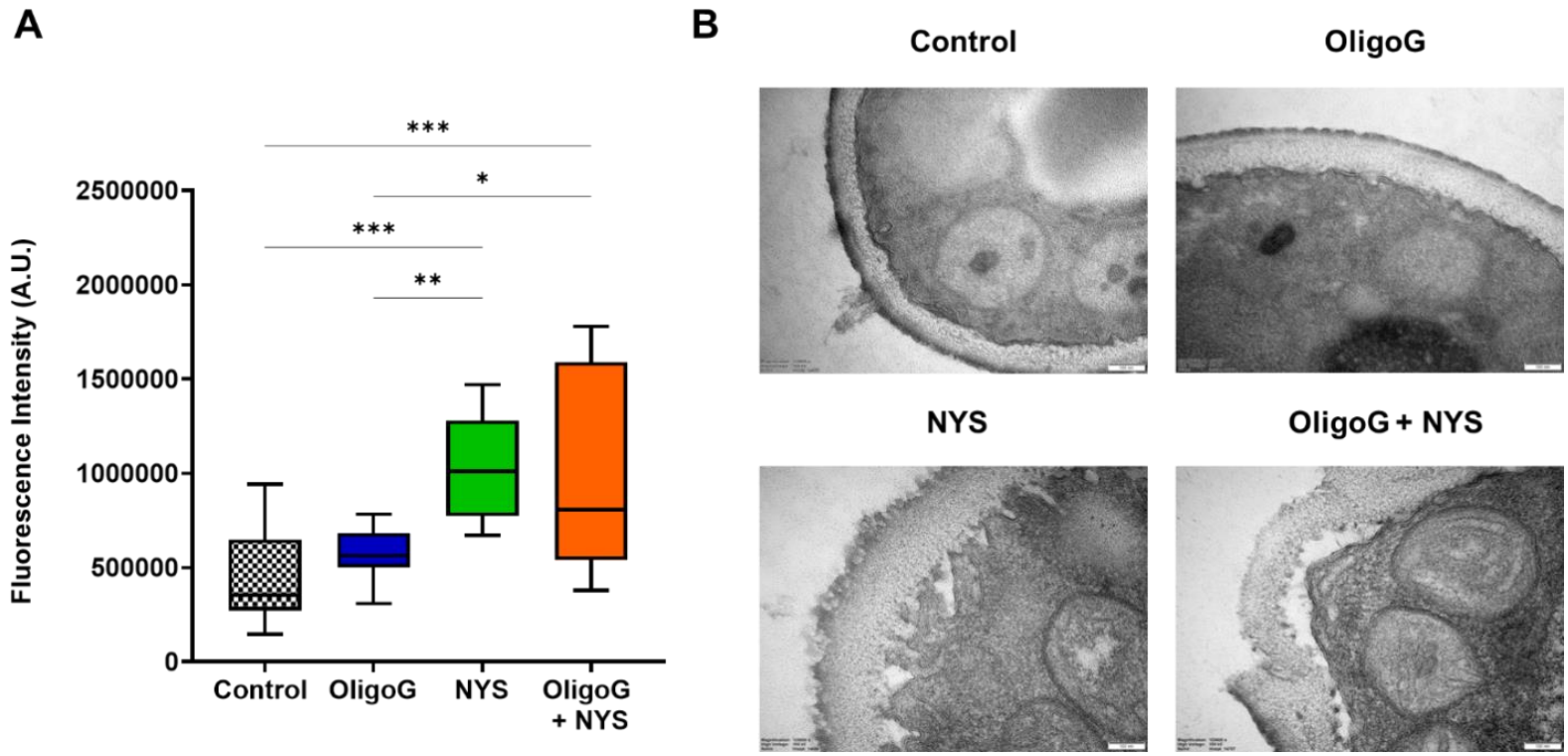

Figure 2.13 (A) Fluorescence intensity data derived from PI staining used in the fungal membrane permeability assay of *C. parapsilosis* W23 treated ± 4% OligoG CF-5/20 ± 1 µg/mL nystatin (NYS; n=3). **(B)** TEM imaging of *C. parapsilosis* W23 treated ± 4% OligoG CF-5/20 ± 1 µg/mL nystatin: scale bar 100 nm (n=1) *<0.05. Group wise comparisons were analysed using one-way ANOVA, followed by Tukey's post hoc tests *P < 0.05; **P < 0.01; ***P < 0.001; ****P < 0.0001

2.4 Discussion

Biofilm-related infections in a clinical setting pose a significant challenge to treatment. With up to 65% of all chronic infections likely to be associated with the presence of biofilms and AMR levels continuing to rise, it is perhaps unsurprising that current therapies often lead to treatment failure and recurrence of infection (Wolcott and Ehrlich 2008). Serious IFIs have increased in recent years, especially in a clinical setting, due to the overuse of antifungals, invasive surgery, and the greater use of immunosuppressive drugs and indwelling medical devices (Enoch et al. 2006). Patients with underlying health conditions have increased risk of fungal infections caused by *Candida* spp. They are responsible for around 70-90% of IFIs in healthcare-associated infections, being ranked as the fourth most common pathogen in bloodstream infections in the US (Delaloye and Calandra 2014). IFIs such as candidemia have a mortality rate of around 50% depending on the population and *Candida* species involved (Muñoz et al. 2011). Hence, there is a critical need for new and effective antifungal treatments.

Treatment of fungal infections has been made more complicated due to the emergence of resistance to many of the currently used antifungals. The increase of mucosal infections in patients with a suppressed immune system has been attributed to the emergence of azole resistance (Rodrigues et al. 2017). Resistance to azoles can occur through defective ergosterol biosynthesis, most commonly in the essential *ERG3* gene which encodes for sterol Δ5,6-desaturase (Silva et al. 2012). ERG3 converts 14α-methylated sterols into toxic 14α-methylergosta-8,24(28)-dien-3β,6α-diol during biosynthesis, inactivation of ERG3, therefore, results in suppressed toxicity and resistance to azoles as cells bypass the toxic sterol. Furthermore, it confers resistance

to polyenes, such as nystatin, as the cells are devoid of ergosterol (Vale-Silva et al. 2012). Additionally, mutations in *ERG11* or *ERG6* can also lead to polyene resistance, some of which have been noted in *C. glabrata* strains (Vandeputte et al. 2007). *ERG11* gene encodes for the main target for azoles, 14α-lanosterol demethylase, this can be mutated to upregulate the gene or mutated to reduce the affinity towards azoles (Morio et al. 2012). Intrinsic and acquired resistance to antifungals may be responsible for the observed shift in the more recently recorded cause of nosocomial infections moving from *C. albicans* to NCACs, such as *C. glabrata* and *C. tropicalis* (Eliopoulos et al. 2002).

The biofilm matrix restricts the access of antimicrobials into the 3D structures of the biofilm extracellular polymeric substance (EPS), with studies showing treatments using 20-fold the MIC value being inefficient at clearing *C. albicans* biofilms (Baillie and Douglas 1998). It has been shown that *FKS1*, the gene responsible for β-1,3 glucan synthase, is needed for resistance to triazole drugs when in a biofilm state though not when in a planktonic state, through radio labelling of fluconazole it is shown that resistance occurs via sequestration by the EPS (Nett et al. 2010a). β-glucan present in the matrix allows the drug to be absorbed, preventing its initial target from being reached and allowing cells to evade exposure to high levels of antifungal agents; *in vitro* studies have shown that up to 70% of fluconazole is sequestered and retained within the EPS of *Candida* species including those of *C. auris* (Nett et al. 2010b; Dominguez et al. 2018).

The growth state of bacterial cells was thought to be important for drug resistance. Planktonic *Candida* cells have been shown to only exhibit resistance to AmB-D at a low growth rate, while those in a biofilm growth state were resistant at all

growth rates, implying that both a low growth rate and biofilm state are important for resistance (Douglas 2003). However, it has been shown that varying rates of growth within a *Candida* biofilm plays no effect on resistance to Amphotericin B (Baillie and Douglas 1998). Other environmental factors, such as temperature, pH, and nutrient conditions, influence the biofilm structure and consequently may confer resistance to treatments (Pettit et al. 2010; Ramage et al. 2012).

Biofilms are often polymicrobial. For *C. albicans*, polymicrobial biofilms displayed higher microbial loads and AMR compared to single species biofilms (Qu et al. 2016). Studies have shown that *C. albicans* acts as a scaffold for *S. aureus* to form microcolonies on the biofilm surface (Harriott and Noverr 2009). This creates additional challenges when treating fungal or bacterial biofilms as extracellular matrix belonging to *Candida* can provide cross-resistance to microbial treatments, and due to the biological differences between species makes it hard to find relevant compounds that can target both pathogens. This highlights the need for the development of new (broad-spectrum) antimicrobial pharmaceuticals to treat these conditions (Harriott and Noverr 2011).

OligoG CF-5/20 has previously been shown to reduce the growth of both *Candida* and *Aspergillus* species in a dose-dependent manner, with cell density in the presence of 10% OligoG CF-5/20 being reduced by up to 50% after 48 h (Tøndervik et al. 2014). Furthermore, the authors also showed that OligoG CF-5/20 could potentiate antifungal agents, notably causing a decrease in the MIC of both nystatin (up to 16-fold) and fluconazole (by up to 8-fold). In this study, OligoG CF-5/20 was shown to slightly potentiate the effect of the polyene antifungal, nystatin, against

Candida strains (one-fold dilution), though this effect was most notable against *C. dubliniensis*.

The antifungal potential of a combination therapy utilising OligoG CF-5/20 and nystatin against planktonic growth was also demonstrated by the growth curves of four *Candida* strains over the course of 48 h. A significant dose-dependent effect (at 10 h) could be seen as the concentration of OligoG CF-5/20 increased. For all four strains, OligoG CF-5/20, when used alone (6%) and in combination, significantly reduced fungal growth. Other research has shown that OligoG CF-5/20 treatment significantly reduces the growth of *Candida*, as well as *Aspergillus* species, at concentrations ≥2% (Tøndervik et al. 2014). This positive effect seen against the growth of a range of fungal species, including *A. fumigatus*, a pathogen listed as a pathogen of 'critical' priority, and which was ranked as number one most important public health pathogen with azole resistant strains responsible for ~20% of cases, and which were responsible for 50% of subsequent mortality (Vermeulen et al. 2013; Osherov and Kontoyiannis 2016; Nguyen et al. 2022; WHO 2022b).

Nystatin has poor solubility in water, poor gastric absorbance when taken orally and is too toxic to be delivered intravenously (Semis et al. 2013; Garcia-Cuesta et al. 2014). For oral candidiasis, treatment using liquid nystatin is, therefore, often administered via a dropper, allowing it to be applied topically, before being expectorated. OligoG CF-5/20 is safe for oral administration, so could therefore, be used in combination with conventional antifungal therapies to overcome resistance, while enhancing the antimicrobial activity of currently employed antifungals (Spitzer et al. 2011).

As well as looking at the effect of OligoG CF-5/20 on planktonic cells, its effect on biofilm formation and disruption with/without nystatin was also investigated. Previous studies have shown that OligoG CF-5/20 has anti-biofilm effects, when combined with fluconazole against *C. tropicalis*, producing a more porous biofilm structure (Tøndervik et al. 2014). Results suggested that OligoG CF-5/20 when used alone as well as in combination with nystatin was effective at disrupting established biofilms, compared to the untreated controls when measuring cell viability. Compared to nystatin treatment, OligoG CF-5/20 showed significant effects in all but one of the *Candida* strains tested and in all but two, when treated with combination therapy. This apparent synergy may be due to the ability of OligoG CF-5/20 to break down the biofilm EPS network that acts as a barrier to prevent antimicrobial penetration, thereby allowing nystatin to penetrate more deeply into the biofilm than when used alone. Interestingly, it has been shown that the morphology of *C. parapsilosis* biofilms varies greatly from those of *C. albicans* strains, being thinner and less complex due to the lack of hyphae or extracellular matrix material, perhaps explaining why OligoG CF-5/20 may be unable to disrupt these biofilms as effectively (Kuhn et al. 2002).

CLSM imaging and COMSTAT analysis showed how different treatments affected the *Candida* biofilms. For all *Candida* strains, biofilm formation in the presence of OligoG CF-5/20 alone or both antimicrobials in combination, had a significant effect. This was less evident for the biofilm disruption assay, where the greatest effect was noted with *C. albicans* GBJ 13/4A, which was isolated from a failed tracheoesophageal prosthesis. The fact that OligoG CF-5/20 treatment alone was efficient at reducing the biofilm biovolume of *C. albicans* GBJ 13/4A means it could potentially treat other biofilm-related candidal infections on silicone-based indwelling medical devices, such as voice prosthesis, and in turn extend their lifespan. Previous

research has similarly shown that 2% OligoG CF-5/20 treatment resulted in *C. tropicalis* 519468 biofilms having increased cell and hyphal death, as well as a matrix that was less dense and with a more open structure (Tøndervik et al. 2014). This could allow treatments to penetrate further into the biofilm architecture reaching regions of the biofilm that are depleted of nutrients and oxygen, exposing cells which have reduced metabolic activity and greater tolerance to antimicrobial treatment (Dufour et al. 2010; Høiby et al. 2010a).

Sorbitol stabilises the fungal protoplast, acting as a cell wall osmotic protective agent (Turecka et al. 2018). Its presence therefore maintains normal biosynthesis of the cell wall in the presence of antifungal agents that target the cell wall. Ergosterol, like cholesterol in mammalian cells, provides cell membrane structure and integrity. As there was no significant difference seen in MICs obtained in the presence or absence of sorbitol and minimal increases (maximum 2-fold) in the presence of ergosterol, the antifungal mode of action of OligoG CF-5/20 does not appear to be directly against the fungal cell wall unlike current anti-candidal therapies, such as Amphotericin B, used as a control showing significant increase in MIC values (MIC increase for ¾ strains).

Transmission electron microscopy showed that the *Candida* cell membrane detached from the cell wall, when treated with nystatin in both the presence and absence of OligoG CF-5/20 treatment. This was reflected by increasing cell permabilisation compared to the untreated control. However, with OligoG CF-5/20 alone no significant increases in cell permeability or any major structural changes were observed. Other studies have shown that the cell membrane has been disrupted after exposure to antifungal drugs, such as fluconazole and Amphotericin B deoxycholate

(AmB and more recently antifungal peptides with damage to essential organelles, “wrinkling” of the cell wall and the nucleus becoming smaller and more condensed (a marker of cell death) being observed (Jia et al. 2019; Ma et al. 2020; Seyedjavadi et al. 2020; Silva et al. 2020; Hifney et al. 2022).

It has been hypothesized that the mechanism of action that OligoG CF-5/20 uses to modify biofilms is through its ability to chelate calcium ions (Ermund et al. 2017). Research using ethylenediaminetetraacetic acid (EDTA), a calcium chelating agent, has shown to influence *C. albicans* morphogenesis and growth resulting in cell wall collapse (Sen et al. 2000; Ates et al. 2005). EDTA has been shown to display an inhibitory effect against biofilm formation with the biofilms formed being composed mainly of yeast and pseudohyphae and killing high quantities of *C. albicans* and *C. tropicalis* biofilm cells (Ramage et al. 2006; Harrison et al. 2007). Furthermore, it has been shown to be effective at clearing *C. albicans* embedded in a biofilm on a catheter surface, as well as *Staphylococcal* species, when used with AmB (Raad et al. 2003; 2008). When EDTA was used in combination with nystatin and with AmB, synergistic effects were evident against numerous *Aspergillus* species and when in combination with fluconazole, was shown to reduce the metabolic activity of cells within a disrupted biofilm (Ruhil et al. 2014; Casalinuovo et al. 2017).

Previous studies have shown that OligoG CF-5/20 can affect hyphal formation and invasion. *C. albicans* ATCC 90028 exhibited significantly reduced hyphae production when treated with 6% and 10% OligoG CF-5/20, while *C. tropicalis* showed significant results with a 0.5% OligoG CF-5/20 treatment (Tøndervik et al. 2014). In this study, horse serum was used to stimulate hyphal growth in the germ tube assay, a small non-significant decrease in cells with germ tubes was seen when

treated with nystatin and OligoG CF-5/20 combination therapy. The strains selected for the germ tube assay included *C. albicans* GBJ 13/4A, which only a minority of the population formed germ tubes, compared to the majority of *C. albicans* ATCC 90028 forming germ tubes.

C. glabrata is the second most common cause of candidiasis after *C. albicans* and has become associated with high mortality rate (Seneviratne et al. 2010). *C. glabrata* is not dimorphic and is only able to form blastoconidia (1-4 μm), compared to the much bigger (4-6 μm) of *C. albicans* and the other NCAC blastoconidia, leads to a biofilm structure that varies greatly from those of the other NCAC species and *C. albicans*, whose biofilms are composed of high levels of hyphal cells (Silva et al. 2012). These features perhaps give the hyphal-free *C. glabrata*, a significant advantage over the dimorphic *Candida* strains (including *C. tropicalis*, *C. albicans* and *C. dubliniensis*), which form true hyphae while *C. parapsilosis* exist as yeast or pseudohyphae and *C. auris*, which rarely form pseudohyphae and do not form germ tubes (Tøndervik et al. 2014; Pritchard et al. 2017a). Invasion is a key phenotype that contributes to the virulence of *Candida.* The ability of *Candida* to cause infection is mediated through enzymes or through hyphae, research has shown that hyphal production, as well as invasion being reduced suggesting that OligoG CF-5/20 could contribute to limiting IFIs (Pritchard et al. 2017a). Furthermore, this study showed that the production of SAPs 4-6, which are hyphal specific and important for invasion, was also reduced, a possible reason for the reduction in hyphal infiltration that was observed.

2.5 Conclusion

These results have shown that OligoG CF-5/20, when used in combination with nystatin, display potentiation against both planktonic and biofilm cells. In addition to potentiating the activity of nystatin, OligoG CF-5/20 when used alone also displayed considerable antifungal activity. The combination therapy was very successful at disrupting established biofilms as confirmed by the ATP viability assay, as well as by the CLSM imaging and COMSTAT analysis. Disruption of the biofilm architecture may facilitate and improve penetration of antifungal agents into the matrix. The combined use of OligoG CF-5/20 and nystatin demonstrated considerable potential as an alternative to single drug treatments, allowing the dosage of nystatin to be decreased, and enabling increases in the longevity of treatment via reduced toxicity.

Chapter 3

Comparison and characterisation of the antimicrobial effects of OligoG CF-5/20 and tailored alginate, OligoM

3.1 Introduction

3.1.1 *Pseudomonas aeruginosa*

The Gram-negative bacterium, *Pseudomonas aeruginosa*, is an opportunistic pathogen found ubiquitously in the environment, which can grow and survive in many different environmental conditions, growing between 25-42°C, causing disease in animals, plants, and humans particularly in immunosuppressed patients (Santajit and Indrawattana 2016). *P. aeruginosa* can cause life-threatening chronic infections, notably in those with chronic obstructive pulmonary disease and cystic fibrosis (CF). The importance of *P. aeruginosa* has been highlighted recently in the WHO list of ESKAPE pathogens (*Enterococcus faecium*, *Staphylococcus aureus*, *Klebsiella pneumoniae*, *Acinetobacter baumannii*, *P. aeruginosa*, and *Enterobacter* species); designated as top "priority" antibiotic resistant strains (Shrivastava et al. 2018). The ESKAPE pathogens are responsible for almost all nosocomial infections worldwide (with *P. aeruginosa* being responsible for 10%), and pose a significant threat due to their resistance to antimicrobial treatment and ability to exacerbate the morbidity, and mortality of disease (Rice 2010; Oliveira et al. 2020).

3.1.2 Quorum sensing

In *P. aeruginosa*, the quorum sensing (QS) network consists of four separate hierarchical systems; Las, Rhl, PQS, and IQS. Two of the systems are based on synthesis and recognition of acyl homoserine lactone (AHLs); LasI/LasR and RhlI/RhlR, which work in tandem, controlling virulence factors (**Figure 3.1**). The *lasI* gene product produces the autoinducer *N*-(3-oxododecanoyl)-AHL (3-oxo-C12-AHL) and the *rhlI* gene product produces *N*-butyryl-AHL (C4-AHL). Once the autoinducer has reached a threshold level, it binds to its respective receptor protein (i.e., LasR or RhlR

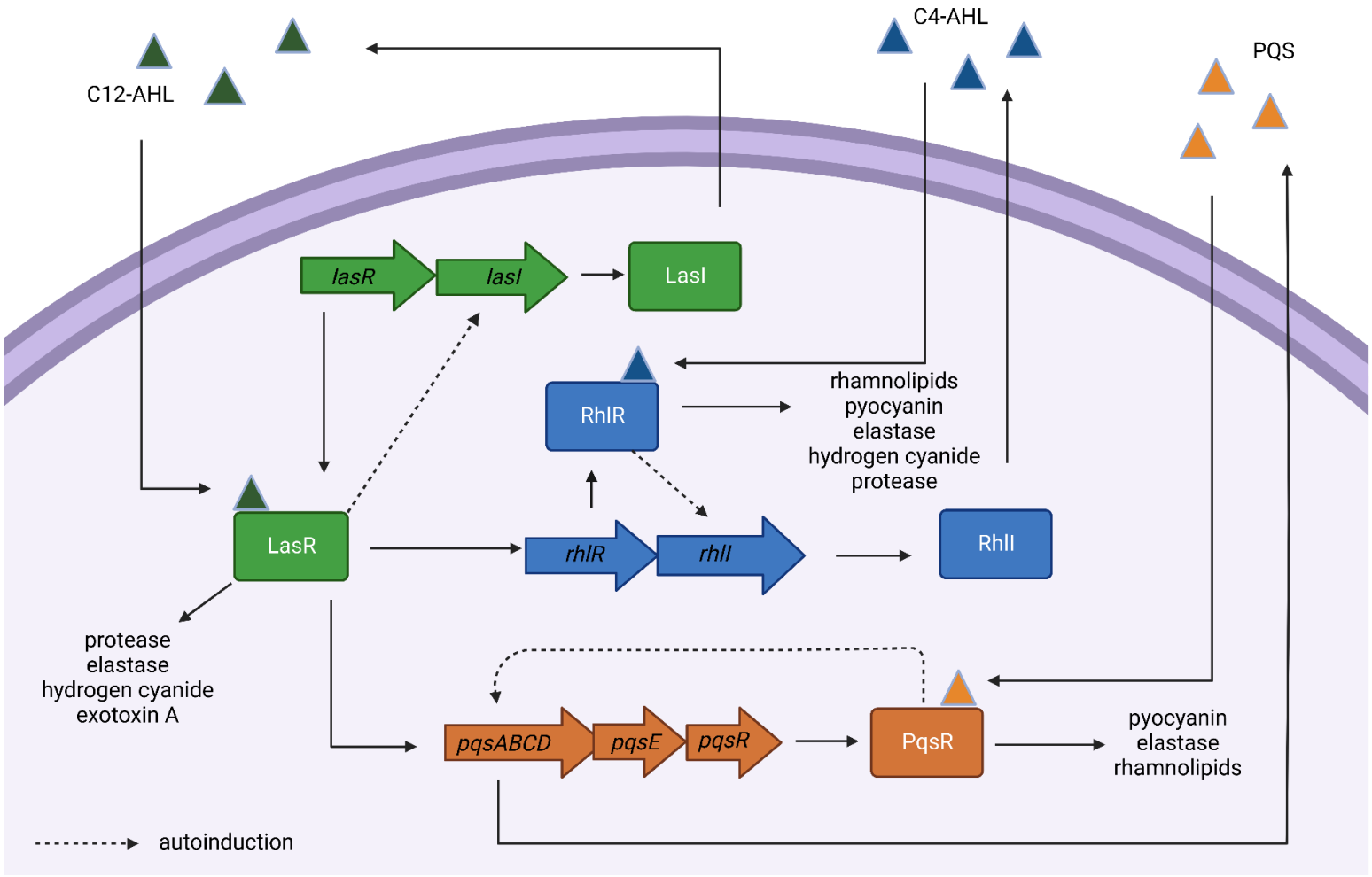

Figure 3.1. Schematic of the *LasI/LasR, RhlI/RhlR* and PQS QS circuits in *P. aeruginosa.*

respectively). This binding causes the activation of virulence factors, such as *LasA* and *LasB* elastase, as well as proteases, exotoxin A and pyocyanin (Whitehead et al. 2001). QS has roles in biofilm development, with mutants which are unable to produce autoinducers producing "thinner" biofilms, which lack characteristic 3-dimensional (3D) microcolonies (Kievit and Iglewski 2000). The LasR-autoinducer complex acts as an autoinduction feedback loop, leading to further activation, while also activating expression of the RhlI/RhlR QS circuit (Miller and Bassler 2001; Smith and Iglewski 2003; Waters and Bassler 2005).

An additional connected "third" QS system, called the *Pseudomonas* quinolone signal (PQS) system, uses alkyl-4-quinolones (AQs) as signalling molecules, mainly a anthranilic acid derivative, 2-heptyl-3-hydroxy-4-quinolone (PQS) and its precursor, 2-heptyl-4-quinolone (HHQ) (Pesci et al. 1999; McKnight et al. 2000). PQS was discovered in a *lasl rhll* mutant that did not produce 3-oxo-C12-AHL or C4-AHL, but was still able to express the LasR protein. The latter is linked to *lasB* transcription, suggesting the involvement of a third molecule closely interconnected with LasI/LasR and RhlI/RhlR (Pesci et al. 1999; Holden et al. 2000). In the PQS system, five genes in the *pqsABCDE* operon are responsible for production of HHQ, which is converted to PQS by PqsH and PqsL. Notably, autoinduction can occur when AQs bind to the transcription regulator, PqsR (also known as MvfR), amplifying operon expression (García-Reyes et al. 2020; Soh et al. 2021). The importance of the PQS system is seen in its involvement in the positive regulation of *rhll*, which is essential for the production of virulence factors, such as pyocyanin and elastase, as well as biofilm formation, while RhlR is seen to negatively regulate *pqsR* (Jack et al. 2018; Li et al. 2022).

Finally, the integrated QS (IQS) system, which was discovered more recently, where 2-(2-hydroxylphenyl)-thiazole-4-carbaldehyde is secreted (Lee and Zhang 2015). It was believed that IQS was affected by the LasI/LasR system, so any disruption downregulates the activation of *ambBCDE* and IQS production (Lee et al. 2013). However, it has been shown recently that *ambBCD* genes are not involved in IQS synthesis (Cornelis 2020). Disruption of IQS causes the PQS and Rhl systems to be halted, stopping the production of virulence factors (Rather et al. 2022).

3.1.3 Bacterial virulence factors

Virulence factors are expressed in both acute- and chronic infections, making them popular targets for antimicrobial treatments. There are many phenotypic and genotypic changes that occur in *P. aeruginosa* over the course of an infection as it develops from acute to chronic. The virulence factors possessed by bacteria contribute to the likelihood of them causing infection, and along with host factors and environmental conditions, play a significant role in disease outcomes. QS has been shown to regulate the production of *P. aeruginosa* virulence factors that are required for invasion of the host, including proteases, elastases, pyocyanin, along with swarming motility (Strateva and Mitov 2011).

3.1.3.1 Bacterial motility

Three forms of motility have been described in *P. aeruginosa*, namely: swimming, twitching, and swarming (**Figure 3.2**). The presence of functional flagella allows bacteria to be motile, helping them to: locate nutrients, find favourable niches for colonisation, as well as initiating infection through adherence, all showing that motility is closely associated with successful biofilm formation (Josenhans and Suerbaum 2002).

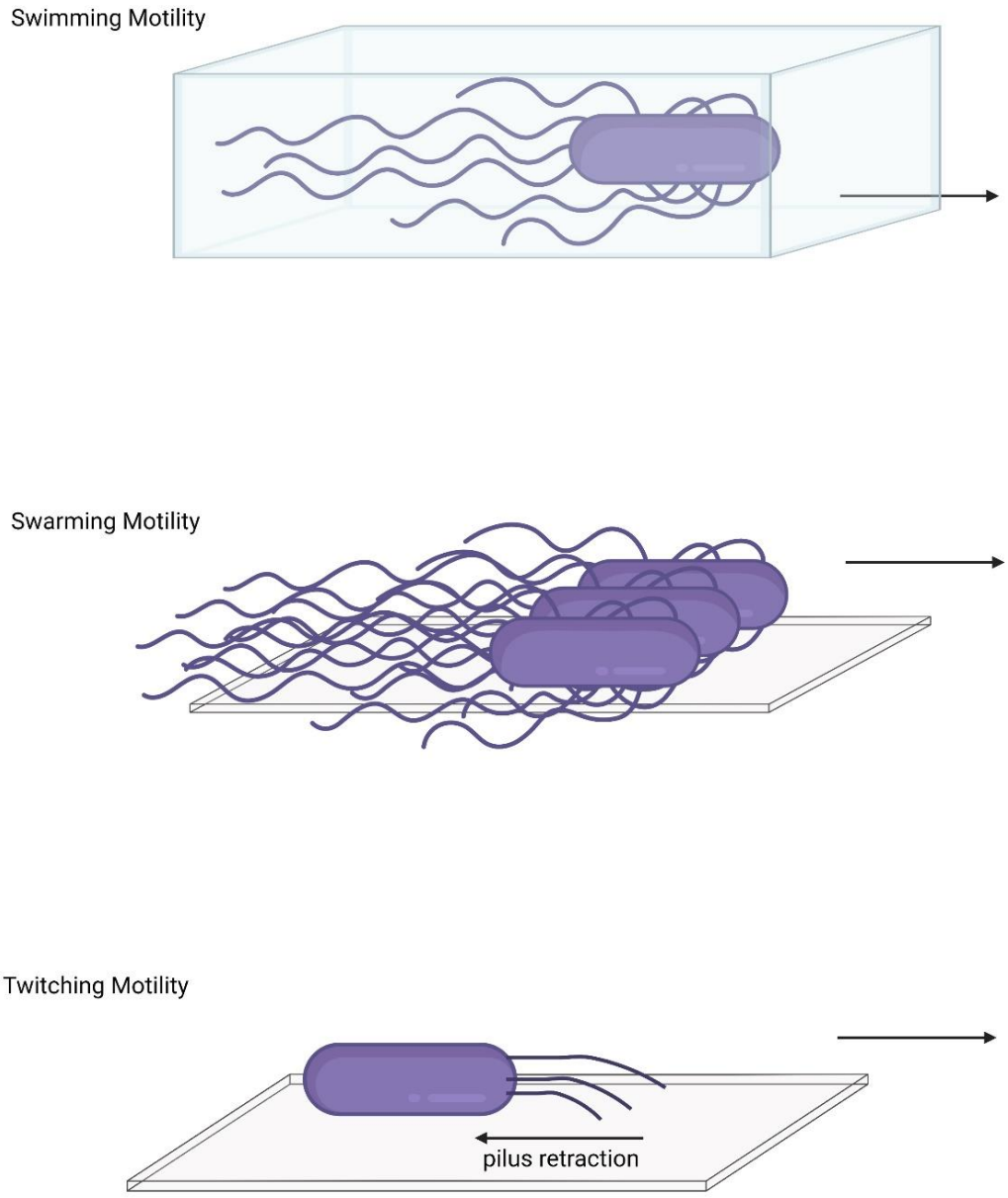

Figure 3.2. Schematic diagram showing the three types of bacterial motility in *P. aeruginosa:* swimming, swarming and twitching motility.

Swimming motility is the movement of an individual bacterium through a liquid with low viscosity propelled by rotating flagella. In contrast, twitching motility uses type IV pili retraction and extension for propulsion in a jerky, "twitching" manner (Kearns 2010). Swarming motility is the coordinated multicellular movement of bacteria using flagella to move across a semi-solid surface, instead of existing in a sessile aggregation. Motility has been reported to be present to only three bacterial families; Firmicutes, Alphaproteobacteria, and Gammaproteobacteria which include many Gram-negative pathogens of *Proteus*, *Escherichia*, *Salmonella*, *Vibrio* genus as well as Gram-positive species, including *Clostridium* and *Bacillus* genus (Lai et al. 2009).

Swarming motility requires "hyper-flagellation" i.e. multiple flagella randomly distributed on the cell surface (known as peritrichous flagellation), and a surfactant (a surface-active agent) or polysaccharide secretion to reduce surface tension between the bacteria and the substrate (Fraser and Hughes 1999). The peritrichous flagellum bundle together when the flagella motor rotates, pushing the cell forward. When the motor changes direction, the body of the cell "tumbles" in a random direction, with the flagella becoming pushed apart and redirecting the cell, before they reform into a polar bundle (Hintsche et al. 2017). Cell-cell communication and external environmental signals can trigger this translocation, with surface contact and the physiological status of the cell both contributing to differentiation (Fraser and Hughes 1999). Swarming motility shows complex and differing motility patterns for different species, with *P. aeruginosa* producing tendrils which spread out from the point of inoculation, whilst *Proteus mirabilis* creates a "bullseye" pattern made up of concentric 'swarm' rings (Caiazza et al. 2005).

3.1.3.2 Additional bacterial factors

One way of identifying *P. aeruginosa* is through the many pigments that are secreted including pyoverdine (fluorescent yellow green), pyorubrin (red brown), pyomelanin (pale brown) and pyocyanin (green blue) (Reyes et al. 1981). Pyocyanin is a water-soluble secondary metabolite belonging to the phenazine family, which are heterocyclic compounds containing nitrogen (Jayaseelan et al. 2014). Synthesis of pyocyanin is a complex process involving gene products from two *phzABCDEFG* operons and ***phzH***, with *phzM* and *phzS*, being important in the final conversion of phenazine-1-carboxyclic acid (PCA) to pyocyanin (1-hydroxy-g-methyl phenazine) (Mavrodi et al. 2001; Lau et al. 2004). Pyocyanin production is regulated via QS, with all three Las, Rhl and PQS QS systems involved in its transcriptional control. RhlR and PqsR have both been shown to be involved in upregulating pyocyanin synthesis (García-Reyes et al. 2020).

Due to high levels of colonisation and infection with *Pseudomonas* spp., levels of pyocyanin production are much higher in people with CF than in non-CF controls, displaying antimicrobial effects against both bacteria and fungi (Wilson et al. 1988; Fothergill et al. 2007; Kaleli et al. 2007). Studies have also shown that pyocyanin interferes with biofilm formation, with eDNA release (a principal component of biofilm extracellular polymeric substances [EPS]), being promoted, and other modifications of the immune system being apparent includincludeding, neutrophil apoptosis and increased interleukin production (Allen et al. 2005; Das and Manefield 2012). The antimicrobial effect of pyocyanin reflect its redox-active nature, in that it can accept or donate electrons to the production of reactive oxygen species (ROS) affecting calcium homeostasis and leading to oxidative stress or even death (Hassan and Fridovich 1980; Denning et al. 1998).

P. aeruginosa produces several extracellular proteases; LasA (encoded by *lasA*), LasB (encoded by *lasB*), as well as alkaline proteases (encoded by *aprA*) (Stehling et al. 2008). Proteases aid in the breakdown of host tissues and the lysis of cells. *LasB* encodes for elastase, which has the ability to degrade extracellular matrix and disrupt tight junctions, promoting pathogen invasion and establishment. Elastase can also degrade components of the immune system, facilitating maintenance of infection (Cowell et al. 2003; Kuang et al. 2011; Strateva and Mitov 2011). The regulation of proteases is mediated through all three QS systems: Las, Rhl, and PQS (Jack et al. 2018).

Rhamnolipids are glycolipid biosurfactants made from two components: a hydrophilic rhamnose and a hydrophobic lipid. The rhamnose moity can either be mono- or di-(L) rhamnose molecule joined by an α-1,2-glycosidic bond, while the lipid moiety is made up of β-hydroxy fatty acid chains joined by an ester bond (Abdel-Mawgoud et al. 2010). The production of rhamnolipids by *Pseudomonas* is associated with virulence, a reduction in surface tension, stimulation of cytokine release, as well as promotion of biofilm formation (Déziel et al. 2003). *rhlA* and *rhlB* genes are linked with *rhlR* and *rhlI* as a single operon, while *rhlC* (also needed for rhamnolipid synthesis) makes up a second operon (Soberón-Chávez et al. 2005). Rhamnolipids are involved in biofilm development and their architecture; rhamnolipid-deficient mutants typically forming much "flatter" biofilms than the wild-type (Davey et al. 2003). Studies have shown that rhamnolipids are involved in the creation and maintenance of open water channels and the formation of microcolonies within biofilm structures, aiding cell-cell interactions and attachment of cells through increasing surface hydrophobicity (Davey et al. 2003; Pamp and Tolker-Nielsen 2007; Abdel-Mawgoud et al. 2010). Rhamnolipids also facilitate the detachment and dispersal of cells in a biofilm state. This occurs through a "central hollowing pattern", with the detachment process

commencing inside the biofilm itself, and in parallel with new cells being prevented from irreversibly attaching (Schooling et al. 2004; Boles et al. 2005).

3.1.4 Fourier Transform Infrared Spectroscopy (FTIR)

Infrared spectroscopy is a technique that creates a unique infrared "molecular fingerprint". A spectrum is created from the infrared radiation that is absorbed by a sample, and the radiation that is transmitted through it. This is typically between 600-4000 cm^{-1} (Dutta 2017). Using the attenuated total reflection (ATR), infrared light is passed through a diamond crystal and internally reflected, before being partially absorbed by the sample (Kazarian and Chan 2006). An advantage of using FTIR is that the data of all wavelengths is collected in one pass, as opposed to samples being irradiated by individual wavelengths. This means that data can be collected much faster than is the case with dispersive techniques (Bruker 2022). The spectrum provides information about which molecules are present, as well as quantitative analysis of their concentrations. FTIR can be used to analyse biological samples detecting changes in the functional groups, allowing a comparison between a treatment group and untreated controls and between healthy- and diseased samples (Lewis et al. 2010; Su and Lee 2020). However, FTIR only shows which functional groups are present, not the exact structure of the compounds which are present. Additionally, FTIR is limited as some vibrations are assigned to multiple chemical groups.

3.1.5 Properties of alginates

The conformation of the mannuronic residues in homopolymeric mannuronic alginates (polyM) is dependent on β-1,4-glycosidic bonds that give a $^4C_1$ conformation, which is more extended in comparison to homopolymeric guluronic (polyG) guluronic alginates, which are linked by α-1,4-glycosidic bonds in a helical $^1C_4$ conformation

(Xing et al. 2020). PolyG residues show an “egg box” structure due to the selectivity for divalent cations, which increases with the concentration of guluronate acid residues. PolyM lacks this selectivity and instead form “belt chains” connected with hydrogen bonds. This composition of polyG compared to polyM (100% M residues) affects the mechanical properties, as the G units contribute to chains which are more brittle and rigid, while M units chains are more flexible and soft (Ashikin et al. 2010). Alginates, however, can vary in in length (degree of polymerization, DPn), composition (G- or M-residues), and secondary structure (alternating G:M residues or homogenous block structures), (Lee and Mooney 2012).

Low molecular weight alginate oligosaccharides still have many of the properties of the high molecular weight polymer alginates, such as exhibiting affinity for mono- and divalent-ions, but do not form a gel in the presence of divalent cations (Xing et al. 2020). Advantages of having a low molecular weight is that the viscosity of solutions, when containing high concentrations, remains without much significant increase (Rye et al. 2018). Alginate oligosaccharides have shown antioxidant, immune regulation, anti-bacterial and anti-inflammatory activities. For example, polyG oligosaccharides (DPn ranging from 3 to 6) induce increased bacterial phagocytosis by macrophages, suggesting that alginates could be used to improve host immunity against infection (Xu et al. 2014). Mannuronate oligosaccharides have a diverse bioactivity with a wide range of clinical application. Mannuronate oligosaccharides made by alginate lyases have shown to inhibit anchorage-independent colony formation of melanoma cells, suggesting that they could have anti-cancer roles (Belik et al. 2020). Further applications of mannuronate oligosaccharides have been proposed in the treatment of Alzheimer’s disease and obesity (Kim 2018; Bi et al. 2021).

P. aeruginosa biofilms contain M-rich high Mw alginate polymers and Ca^{2+} cross-linking is known to play an important role in biofilm stability and antibiotic resistance. Therefore, the ability of guluronate oligosaccharides to scavenge calcium has been proposed as mechanism of action in their demonstrated antimicrobial and antibiofilm activity (Aslam et al. 2008). This study investigates the implication of monomer composition and distribution (M:G ratio) in these activities.

3.1.6 Effect of alginate oligosaccharide composition on Pseudomonal cell membrane binding

Molecular dynamics (MD) simulations have recently shown that the hydrogen bonding between M-block oligomers (DP 6) and Gram-negative lipopolysaccharide (LPS-DPPE) lipid layer do not extend as far into the Gram-negative bacterial membrane as those observed with G-block (α-L-guluronic acid) structures. Instead, the G-block alginates showed a strong interaction (within nanoseconds) with the LPS bilayer via hydrogen bonding and aided by attractive forces between the G residues and Ca^{2+} ions, allowing the large negative charge of both the oligomer and LPS to be overcome (Pritchard et al. 2023)

To compare structure activity relationship (SAR) of the antimicrobial properties of alginate oligomers *in vitro*, OligoM, made up of homopolymeric regions of M (β-D-mannuronic acid) blocks synthesised with a similar degree of polymerization (DPn) to that of OligoG CF-5/20 (DPn = average 19), was prepared (**Figure 3.3**). Isothermal titration calorimetry (ITC) was conducted to measure the amount of heat released or absorbed by OligoG CF-5/20 and OligoM dilutions in the presence of Ca^{2+}, as well as their interactions with pseudomonas LPS (Saboury 2006; Wang et al. 2020c). ITC

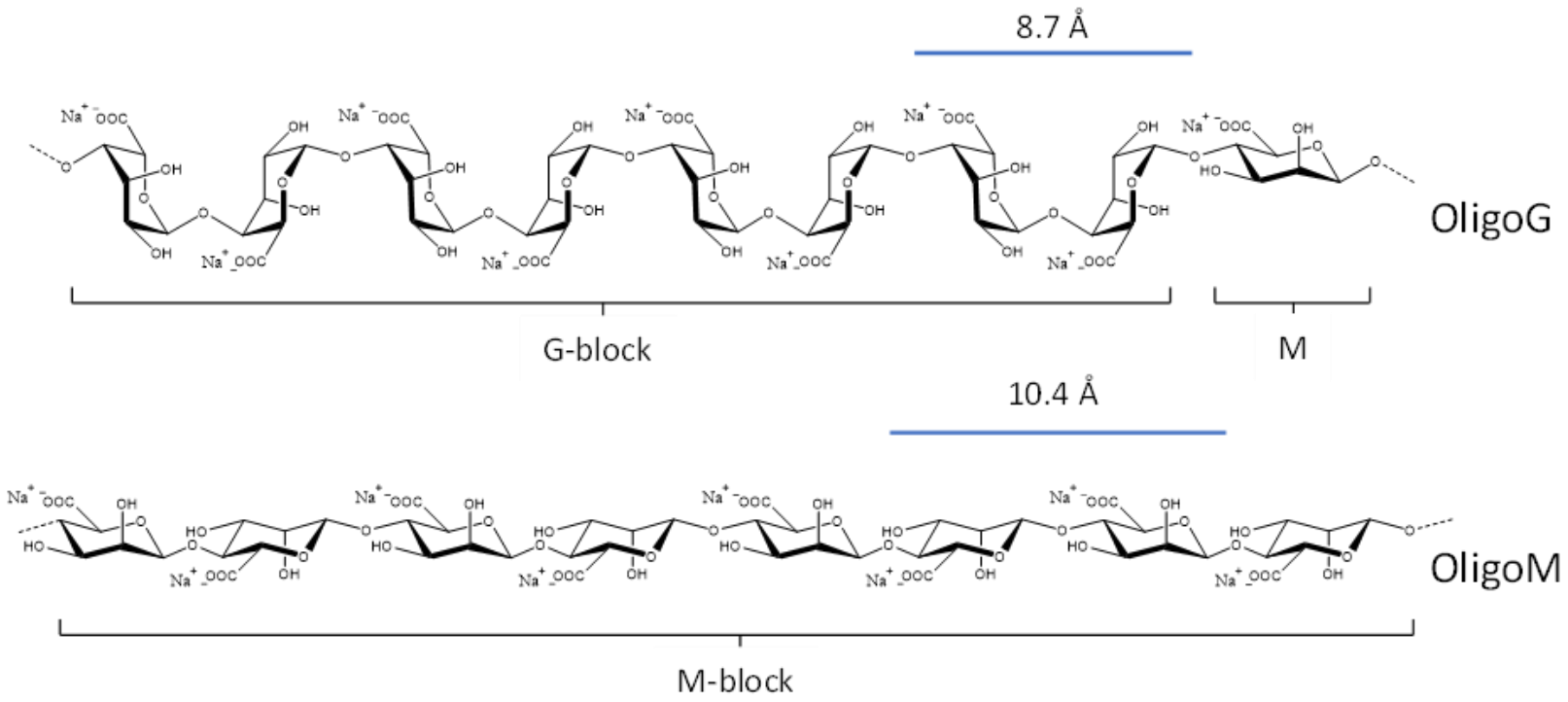

Figure 3.3. Structure of OligoG CF-5/20 and OligoM.

established that that no binding occurred between M-block oligomers and LPS at low calcium concentrations (1 mM) and only weakly at higher concentrations (2.5 mM). While interactions with Ca^{2+} between OligoG CF-5/20 and LPS were shown to occur in a dose-dependent manner (Pritchard et al. 2017c).

3.1.7 Aims and objectives

The objective of this study was to investigate the SAR of alginate oligosaccharide (of comparable DPn and molecular weight distribution), to determine the role of calcium binding in their previously reported antimicrobial and antibiofilm effects.

The specific aims of this study were:

- To investigate the effect of OligoG CF-5/20 and OligoM on planktonic growth of *P. aeruginosa* using growth curves and determine their effects on biofilm formation.
- To investigate the effect of both alginate oligomers on *P. aeruginosa* virulence factor production, swarming motility, and QS signalling.
- To characterise changes in cell-binding between *P. aeruginosa* treated with OligoG CF-5/20 or OligoM, after exposure to hydrodynamic shear using Fourier Transform Infrared (FTIR) spectroscopy.

3.2 Materials and methods

3.2.1 Microbial strains and materials

Pseudomonas aeruginosa strains (mucoid NH57388A isolated from a CF patient and non-mucoid PAO1, ATCC 15692), were grown on 5% horse blood agar (BA) plates (blood agar base No.2; horse blood, TCS Biosciences Ltd). Unless stated, all liquid cultures of *P. aeruginosa* NH57388A and PAO1 were set up in Mueller-Hinton (MH; Sigma Aldrich) broth or Tryptone Soy Broth (TSB) respectively, at 37 °C with 120 rpm shaking overnight before being adjusted to an optical density OD_{600} of 0.08-0.1 (0.5 McFarland standard; ~10^8 CFU/mL). *Chromobacterium violaceum* (Bergonzini ATCC 31532) and *C. violaceum* CV026 (NCTC 13278, mini-*Tn5* mutant of *C. violaceum* ATCC 31532), were grown on Luria-Bertani (LB) agar (10 g/L tryptone, 5 g/L yeast extract, 5 g/L NaCl, 15 g/L agar, Sigma Aldrich), supplemented with 50 μg/mL kanamycin for *C. violaceum* CV026 and liquid overnight cultures were set up in TSB broth at 30 °C, with 200 rpm shaking. All growth media was obtained from LabM, unless otherwise stated.

OligoG CF-5/20 (DPn 19) was produced, as previously described (**Section 1.8**). OligoM was derived from *Pseudomonas fluorescence AlgG* mutant, which lacks the alginate modifying enzyme, mannuronan C-5-epimerase (Gimmestad et al. 2003; Aarstad et al. 2012). Alginates were deacetylated using a mild alkaline treatment and depolymerized using a two-step acid hydrolysis (Holtan et al. 2006). The alginate fractions were analysed by High-Performance Anion-Exchange Chromatography, with pulsed amperometric detection (HPAEC-PAD; Dionex ICS-5000, Sunnyvale, CA; **Figure 3.4**) (Ballance et al. 2005). Metal ion concentrations were determined by ICP

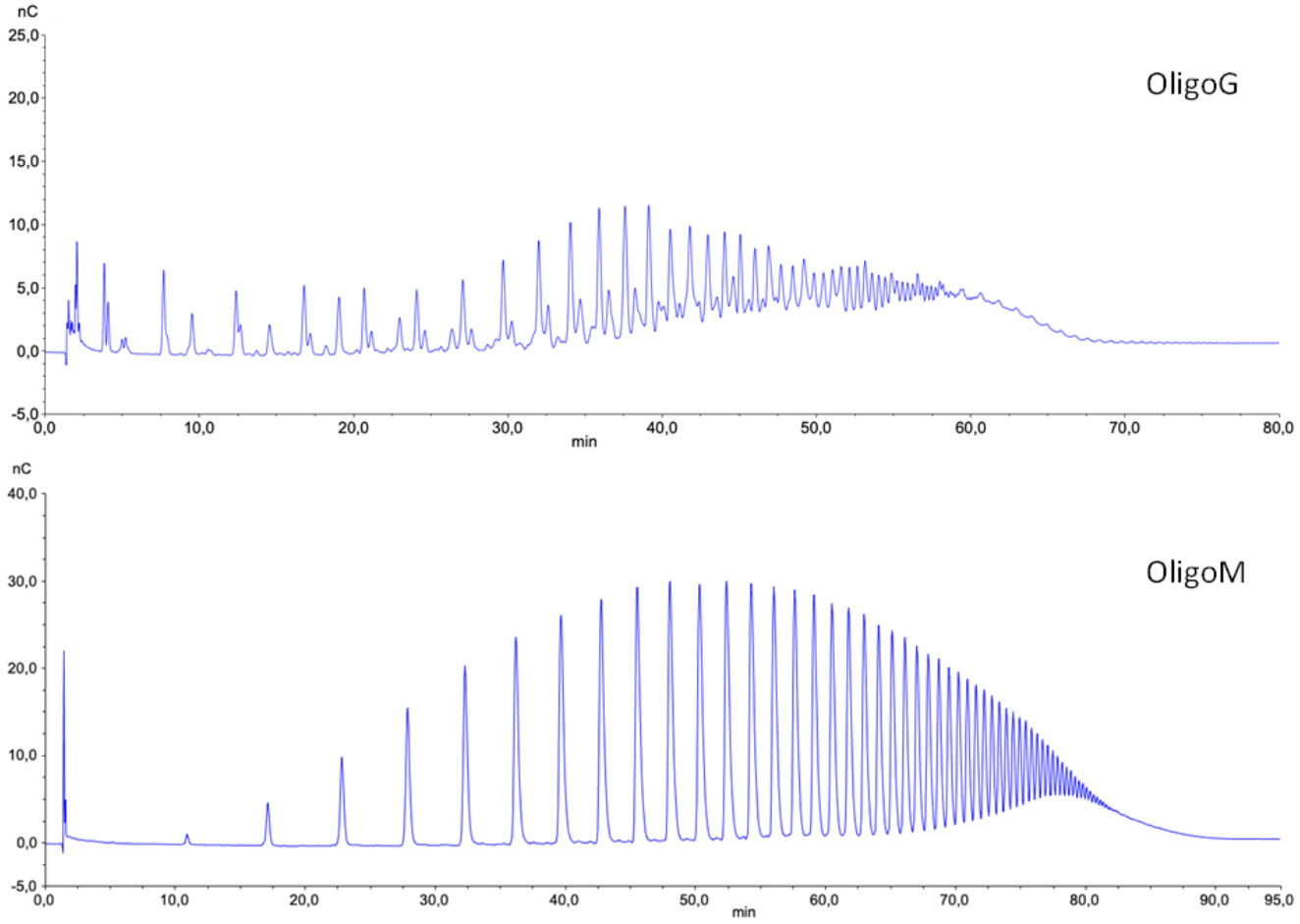

Figure 3.4 Characterization of OligoG CF-5/20 and OligoM with High Performance Anion-Exchange Chromatography with pulsed amperometric detection (HPAEC-PAD).

analysis (Inductively Coupled Plasma Atomic Emission Spectroscopy, ICP-AES), to determine concentrations of trace elements in the various preparations.

3.2.2 Bacterial growth curve analysis

Adjusted overnight cultures of *P. aeruginosa* NH57388A were diluted in a ratio of 1 to 10 in MH broth ± OligoG CF-5/20 (0.5, 2, 6%) or OligoM (0.5, 2, 6%). Growth curves were performed in triplicate in sterile, flat-bottomed 96-well microtiter plates (100 µl/well) and the results presented as mean values. Absorbance measurements were measured hourly at OD_{600} over 48 h at 37 °C using a FLUOstar Omega plate reader. The minimum significant difference (MSD) was calculated using the Tukey-Kramer, method using Minitab 17.2.1 (Minitab Inc, State College, PA, USA).

3.2.3 Small-scale swarming motility assay

Due to limited availability of OligoM, a small-scale assay was adapted from Jack *et al*, 2018. Swarming motility was assessed on 0.5% Basal Medium 2 (BM2) agar (62 mM potassium phosphate buffer [pH 7], 2 mM $MgSO_4$, 10 µM $FeSO_4$, 0.4% [w/v] glucose, 0.5% [w/v] casamino acids and 0.5% [w/v] agar) ± 0.5, 2, and 6% OligoG CF-5/20 or OligoM (Marr et al. 2007). Agar was freshly prepared before use and cooled to 50 °C before addition of the alginate oligomer. Then, 3 mL of BM2 agar (± oligomer) was measured into the wells of a sterile flat-bottomed 6-well microtiter plate and left to dry in a laminar flow cabinet for 30 mins prior to use. After adjusting *P. aeruginosa* PAO1 overnight cultures, the inoculum was diluted 1 to 10 in MH broth and 0.5 µL inoculum was pipetted onto the surface of the dried agar (n=3). Plates were sealed in parafilm and then incubated for 16 h at 37 °C. Bacterial swarming in each well was then photographed and the length of dendritic arms, surface area, perimeter, and shape were analysed, using ImageJ software.

3.2.4 Confocal laser scanning microscopy (CLSM)

3.2.4.1 Biofilm formation assay

Biofilm imaging was performed with the kind assistance of Dr Lydia Powell. Overnight *P. aeruginosa* NH57388A cultures (adjusted to 10^6 cfu/mL) were incubated in a sterile glass-bottomed 96-well plate (Whatman) and grown for 24 h (37 °C; 120 rpm) ,with MH broth ± 0.5, 2, or 6% OligoG CF-5/20 or OligoM. Following incubation, the supernatant was removed and the biofilm stained with 6% (v/v in PBS) LIVE/DEAD® (BacLight™ Bacterial Viability Kit, Invitrogen) for 10 min and Z-stack CLSM images taken (Leica TCS SP5). CLSM images were analysed using COMSTAT image analysis (Heydorn et al. 2000).

3.2.5 Small-scale quorum sensing assay

3.2.5.1 Effect of the alginate oligomers on quorum sensing inhibition

A small-scale QS assay measuring violacein pigment production using *C. violaceum* ATCC 31532 and *C. violaceum* CV026 (unable to produce AHLs and therefore cannot produce violacein pigment without an external AHL source), was adapted from Manner and Fallarero (2018). *Chromobacterium* spp. cultures (ATCC 31532 and CV026) were adjusted in LB broth to OD_{600} 0.7 (~$1x10^9$ cfu/mL). In a sterile flat-bottomed 96-well microtiter plate (200 µL/well) adjusted culture ± oligomer (0.5, 2, and 6%) was added with 0.5 µM *N*-(β-ketocaproyl)-L-homoserine lactone (Sigma Aldrich; C6-AHL dissolved in dimethyl sulfoxide, DMSO), to induce pigment production and incubated at 30 °C, 200 rpm shaking for 48 h in the dark. Furanone (Sigma-Aldrich; dissolved in DMSO), a QS inhibitor (inhibiting the production of violacein) was used as a positive control (prepared to a final concentration of 1 mg/mL). A DMSO equivalent was also included as a control.

To quantify violacein pigment, plates were centrifuged (Heraeus Labofuge 400R centrifuge; ThermoFisher Scientific) at 2,000 *g* for 10 mins. The supernatant was then removed before adding 200 µL 96% ethanol (v/v) to dissolve the violacein before recentrifugation as above. The purple pigmented supernatant (100 µL/well) was transferred to a new sterile flat-bottomed 96-well microtiter plate and the absorbance (OD_{595}) was read using a FLUOstar Omega plate reader. The percentage inhibition of violacein production was calculated as follows:

$$\text{Percentage Inhibition (\%)} = \frac{(\text{untreated control } OD_{595} - \text{sample } OD_{595})}{(\text{untreated control } OD_{595} - \text{media control } OD_{595})} \times 100\%$$

Treatments were classified as highly active QS inhibitors, if the inhibition percentage was ≥90%, moderately active if inhibited by 40-89%, with <40% being classed as inactive (Manner and Fallarero 2018).

3.2.5.2 Effect of the alginate oligomers on cell viability (resazurin control assay)

In parallel with the QS assay, identical duplicate *C. violaceum* ATCC 31532 and CV026 plates were set up, with equivalent DMSO concentrations replacing C6-AHL (described in **Section 3.2.4.1)**, to measure the effect of oligomer on cell viability. After 48 h incubation, the 96-well microtiter plates were centrifuged (Heraeus Labofuge 400R centrifuge; Thermo Fisher Scientific) at 2,000 *g* for 10 mins and all the supernatant removed. Resazurin (Sigma Aldrich; 20 µM prepared in PBS) was added and the plates (200 µL/well) were incubated in the dark for 30 mins at room temperature, before the fluorescence (λex 560 and λem 590) was read using a FLUOstar Omega plate reader. Bactericidal activity of the oligomers was calculated as inhibition percentage of viability as follows:

$$\text{Inhibition percentage (\%)} = \frac{\text{(untreated control – sample)}}{\text{(untreated control – media control)}} \times 100\%$$

Compounds with inhibition percentages >40% were classified as bactericidal and excluded as possible QS inhibitors in line with the previous study (Manner and Fallarero 2018).

3.2.6 Virulence factor assays

3.2.6.1 Effect of the alginate oligomers on pyocyanin production

Overnight cultures of *P. aeruginosa* PAO1 were adjusted to OD_{600} 1.0 with MH broth. Cultures (n=3) were diluted in a ratio of 1 to 100 in 1 mL MH broth ± 0.5, 2, 6% OligoG CF-5/20 or OligoM, and incubated for 24 h (37 °C, 125 rpm) in sterile universals with the lids left loose to allow for maximum oxygenation. The cells were centrifuged (Heraeus Fresco 21; ThermoFisher Scientific; 10,000 *g*, 4 °C, 10 mins) and pyocyanin extracted from the supernatant using chloroform (Sigma Aldrich; 3:2; volume per volume [v/v]). Samples were vortexed for 1 min and then centrifuged (10,000 *g*, 4 °C, 10 mins), before being re-extracted with 0.2 M hydrochloric acid (HCl; Sigma Aldrich; 2:1; v/v). The top aqueous (pink) layer was then transferred to sterile Eppendorfs and the absorbance read at 520 nm, using a Beckman Coulter DU 800 Spectrophotometer. 0.2 M HCl was used as the blank and MH broth as a negative control.

3.2.6.2 Effect of the alginate oligomers on protease production

Cultures were adjusted and prepared as described **(Section 3.2.6.1)**. Cell-free supernatant (200 μL) was incubated in a 1:1 ratio with 2% azocasein solution (Sigma Aldrich; prepared in 100 mM sodium phosphate [pH 7]) at 37 °C for 1 h. To stop the reaction, 10% trichloroacetic acid (ThermoFisher Scientific) was added, and the mixture

was centrifuged (8,000 *g*, 5 mins) to remove the azocasein. The absorbance (OD_{400}) was measured using a Shimadzu UV-1900i Spectrophotometer.

3.2.6.3 Effect of the alginate oligomers on elastase production

Cultures were adjusted and prepared, as described **(Section 3.2.6.1)**. Elastin-congo red solution (Sigma Aldrich; 5 mg/mL prepared in 0.1 M Tris-HCl, pH 8; 1 mM $CaCl_2$) was incubated with cell-free supernatant (in a 1:3 ratio) and incubated for 16 h (37 °C, 200 rpm). After incubation, the mixture was centrifuged (3,000 *g*, 10 mins) and the absorbance (OD_{490}) measured using a Shimadzu UV-1900i Spectrophotometer.

3.2.6.4 Effect of the alginate oligomers on rhamnolipid production

Cultures were adjusted and prepared, as described in **(Section 3.2.6.1)**. Cell-free supernatant was mixed with ethyl acetate in a 1:1 ratio and vortexed for 10 s, before centrifugation (10,000 *g*, 4 °C, 5 mins). The top layer of ethyl acetate was transferred to a new tube and this process was repeated three times. The upper layer was then left to evaporate overnight, and the precipitate reconstituted in 100 µL deionized water (dH_2O). To this precipitate, 900 µL of orcinol reagent (0.19% orcinol in 53% sulphuric acid, H_2SO_4) was added and the resulting mixture was incubated at 80 °C for 30 mins. Once cooled to room temperature, the absorbance (OD_{421}) was read using a Shimadzu UV-1900i Spectrophotometer.

3.2.7 FTIR analysis of alginate oligomer interaction with pseudomonal cell surface membrane

Overnight cultures of *P. aeruginosa* (PAO1) (n=6) were centrifuged (Pendragon ALC PK120R) at 3,000 *g* for 20 mins and washed (x2) in dH_2O Cultures were standardised to an optical density OD_{600} of 1, before being recentrifuged at 3,000 *g* for 20 mins and resuspended in 66.6 µL dH_2O ± 0.5% OligoG CF-5/20 or OligoM.

Samples were left at room temperature for 20 mins, before being subjected to hydrodynamic shear, (centrifugation at 5,000 *g* for 6 mins), to remove excess alginate oligomer. The supernatant was removed, and the pellet resuspended in dH_2O prior to centrifugation (5,000 *g*, 6 mins) and resuspended in dH_2O. Then, 15 µL of sample was pipetted onto the attenuated total reflectance (ATR) sampling module of a Nicolet 380 Fourier Transform IR Instrument (ThermoFisher Scientific) and allowed to fully air dry prior to recording the IR spectra. Wavelength scans were taken between 525-4000 cm^{-1} at a resolution of 4 cm^{-1} and 64 scans taken to create a mean. Each sample was run in triplicate.

Data processing and analysis were performed using the R statistical environment. Wavenumbers from 1850 to 950 cm^{-1} were pre-processed using two-point liner subtraction baseline correction methods and then normalized using vector normalization. Wilcox-Rank-Sum was used to determine wavenumbers that were significantly different ($P < 0.05$) between the OligoG and OligoM spectra, to compensate for multiple testing, Bonferroni correction was applied. These selected wavenumbers were put forward into hierarchical cluster analysis (HCA) and a dendrogram produced. With thanks Dr. Georgina Menzies for data analysis.

3.2.8 ATP cell viability assay

Biofilm formation was analysed in the presence of a "dual treatment" of azithromycin and alginate oligomer therapy, using a Beckman Coulter Biomek NXP Robotic System. Overnight cultures of *P. aeruginosa* (PAO1) in TSB were adjusted to an OD_{600} of 0.005 in MH broth (LabM), before adding 30 µL of inoculum to the wells of a sterile black walled flat-bottomed 96-well plate (ThermoFisher Scientific), containing 150 µl MHB with 0, 2 or 6% OligoG or OligoM and a gradient of

azithromycin (Sigma-Aldrich; 10 mg/mL stock in ethanol), ranging from 0-512 µg/mL. Plates were incubated for 19 h at 37 ^{o}C (n=4). The supernatant was removed, and the biofilms washed (x4) with 100 µL PBS. PBS (100 µL) was then added to each well before addition of 100 µl of Bac-Titer-Glo™ Microbial Cell Viability Assay (Promega) reagent. Plates were incubated at room temperature in the dark for 5 min, mixed briefly and luminescence measured on a Molecular Devices SpectraMax Paradigm Multi-Mode Detection Platform. The minimum significant difference (MSD) was calculated using the Tukey-Kramer method using Minitab 17.2.1 (Minitab Inc, State college, PA, USA). With thanks to Dr Anne Tøndervik for plate set up.

3.2.9 Statistical analysis

GraphPad Prism® was used for all statistical analysis, with one-way analysis of variance (ANOVA) test used to calculate any significant changes between treatments (n >2), followed by a Dunnett's multiple comparison test. P values <0.05 were considered significant. MiniTab was used for calculation of the MSD and ImageJ software was used for analysis of swarming motility.

3.3 Results

3.3.1 Effect of oligomers on viability of mucoid *Pseudomonas aeruginosa*

Growth curves of the mucoid *P. aeruginosa* strain, NH57388A, showed that both OligoG CF-5/20 and OligoM had a comparable dose-dependent effect on planktonic growth (**Figure 3.5**). The MSD showed that at 6%, both alginate oligomers had a significant effect on growth in the exponential phase (16-40 h), compared to the untreated control. These effects were not significant at ≤2%. The effect of oligomers on biofilm formation of the mucoid *Pseudomonas* strain in CLSM imaging mirrored that observed in planktonic systems: OligoG CF-5/20 and OligoM showed a reduction in biofilm formation in a dose-dependent manner (**Figure 3.6**). Furthermore, COMSTAT analysis demonstrated that at 2 and 6%, both oligomers had significant effects on biofilm biovolume, mean thickness and surface roughness, compared to the untreated control (**Figure 3.7**). No significant effect was seen at 0.5% for either oligomer.

3.3.2 Effect of alginate oligomers on *Pseudomonas* swarming motility

Swarming motility plates (after 16 h) and the calculated surface area of the swarm on the surface of the agar are seen in **Figure 3.8.** The small scale of the assay (3 mL vs 20 mL of agar) made reproducibility between replicates a problem, as can be seen in **Figures 3.8A and B** and the resultant large standard deviation in **Figure 3.8C**. No significant differences were seen in motility in the presence of 0.5 and 2% oligomers, reflecting the poor reproducibility between replicates (**Figure 3.8C**). Both oligomers were shown to affect the swarm surface area of *P. aeruginosa*, with 6% showing the greatest effect (inhibiting growth and swarming motility) although this was not significant ($p > 0.05$; **Figure 3.8C**).

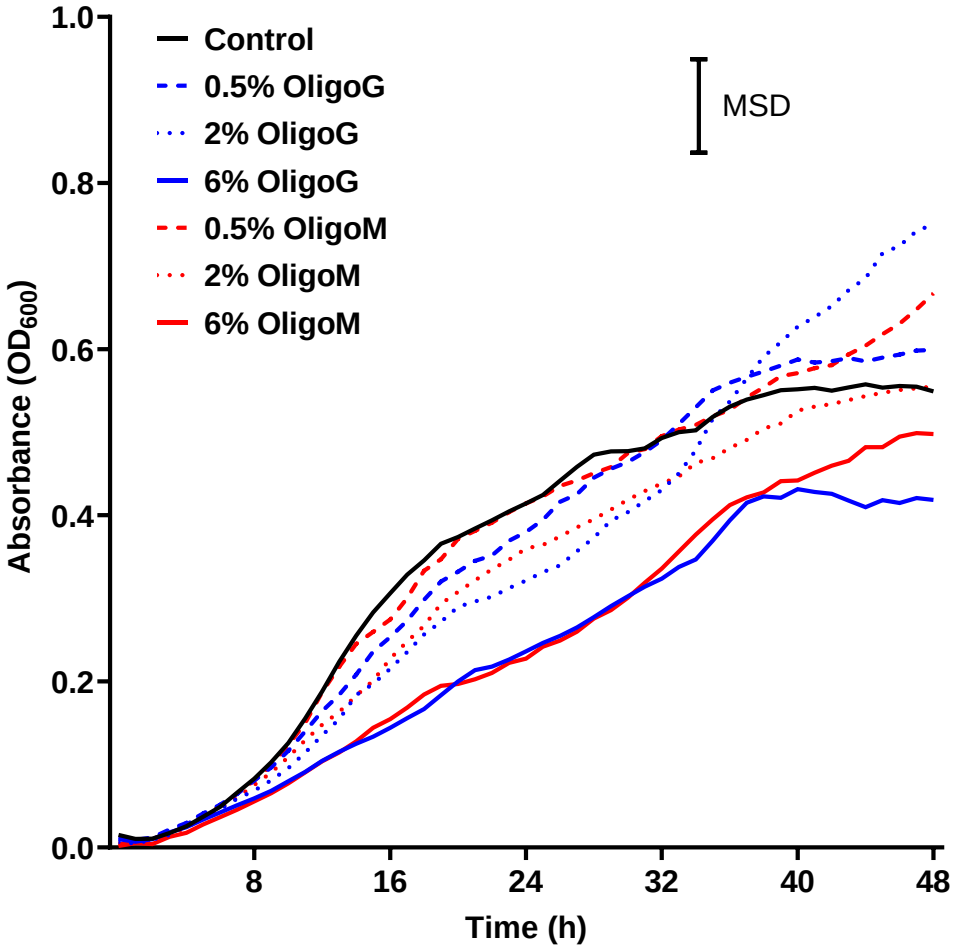

Figure 3.5. Growth curves of *P. aeruginosa* NH57388A, treated with OligoG CF-5/20 or OligoM (0, 0.5, 2, 6%) for 48 h. Minimum significant difference (MSD) for absorbance was calculated in MiniTab, using the Tukey-Kramer method (MSD=0.11; n=3).

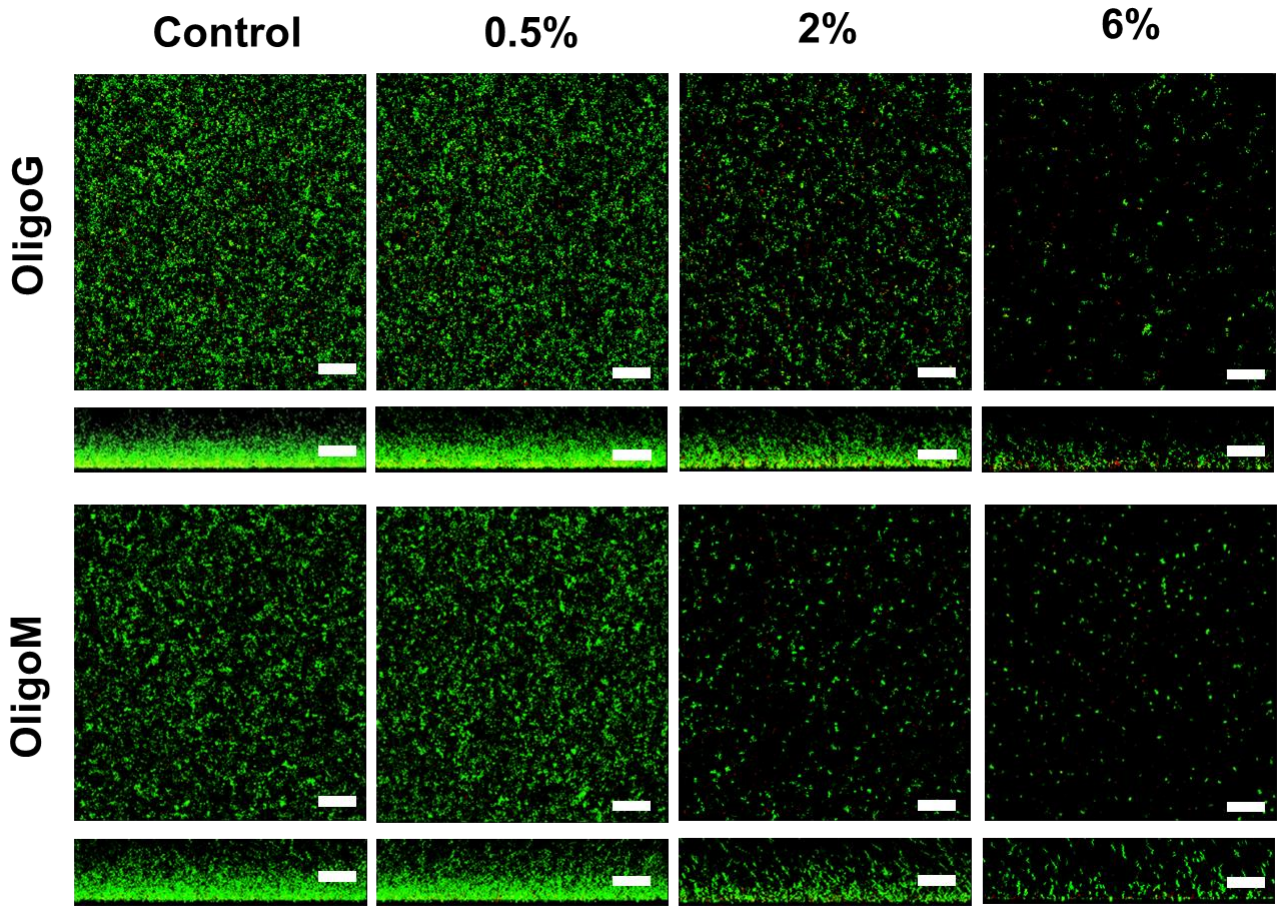

Figure 3.6. Biofilm formation assay showing CLSM Z-stack imaging of *P. aeruginosa* NH57388A biofilms with LIVE/DEAD® staining. For the assay, biofilms were grown for 24 h ± OligoG CF-5/20 or OligoM (0.5, 2, 6%); scale bar = 30 μm.

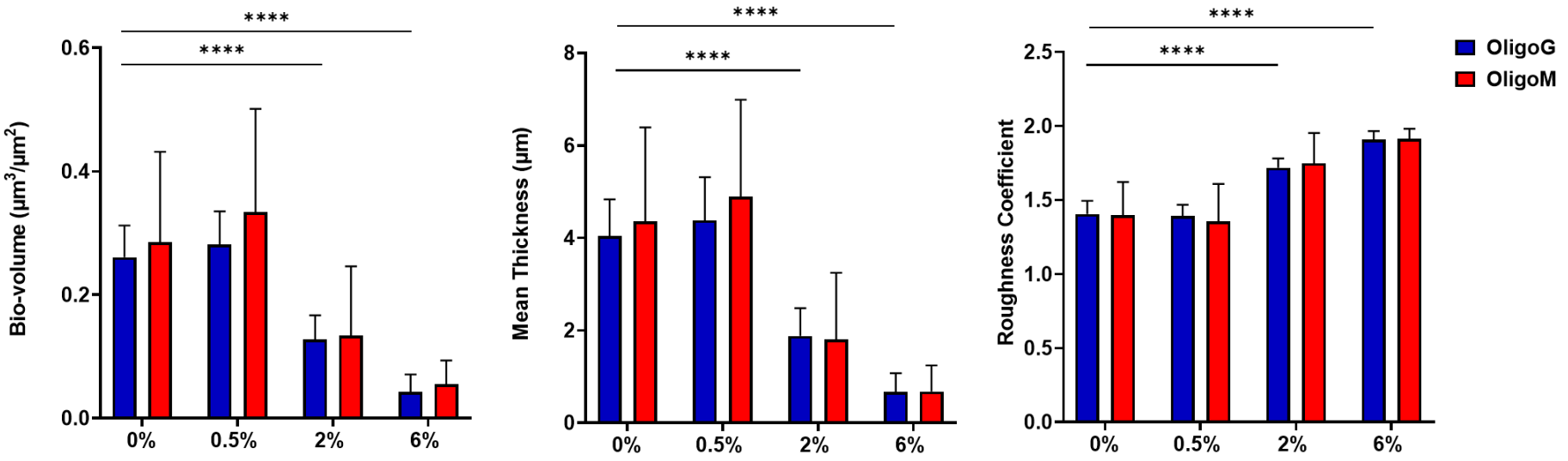

Figure 3.7. COMSTAT image analysis of *P. aeruginosa* NH57388A formation assay, treated with OligoG CF-5/20 or OligoM (0.5, 2 or 6%) (**Figure 3.6**), showing bio-volume ($\mu m^3/\mu m^2$), mean thickness (µm) and roughness coefficient ± S.D; n=3 biologicals; n=5 technicals, Group wise comparisons were analysed using one-way ANOVA, followed by Dunnett's post hoc tests; *P <0.05; **P <0.01; ***P <0.001; ****P <0.0001 denotes significance.

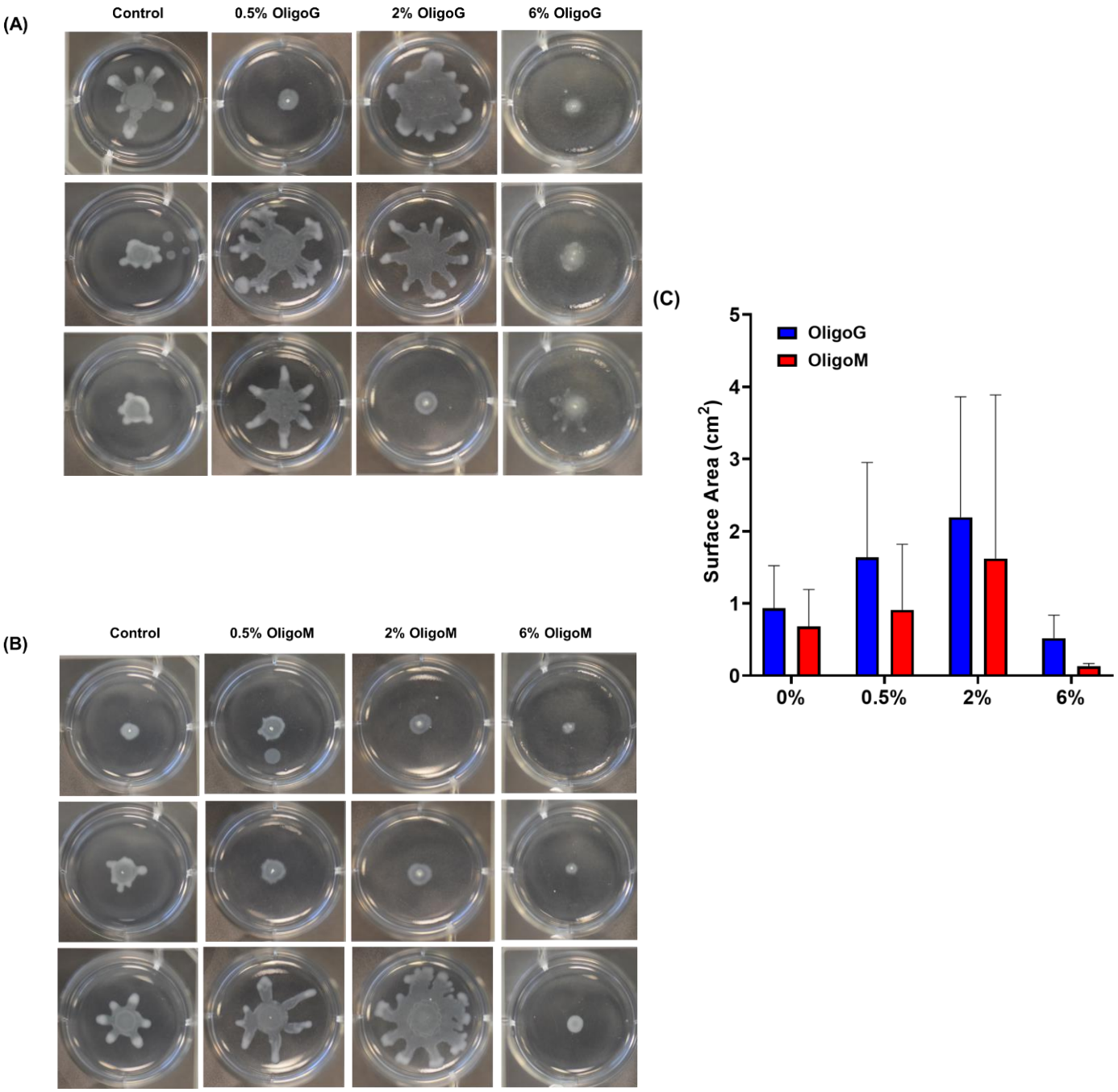

Figure 3.8. Effect of the alginate oligomers on *P. aeruginosa* PAO1 swarming motility on BM2 agar **(A)** ± OligoG CF-5/20 (0.5, 2 or 6%); **(B)** ± OligoM (0.5, 2 or 6%), after 16 h incubation and; **(C)** surface area (cm^2) of swarm ± SD (n=3). Group-wise comparisons were analysed using one-way ANOVA, followed by Dunnett's post hoc tests; *P <0.05; **P <0.01; ***P <0.001; ****P <0.0001 denotes significance.

3.3.3 Effect of alginate oligomers on *P. aeruginosa* quorum sensing inhibition

Violacein pigment production by *C. violaceum* ATCC 31532 in the QS assays was shown to be reduced by both OligoG CF-5/20 and OligoM in a dose-dependent manner, with ≥2% oligomer showing a significant reduction in pigment; with a non-significant reduction observed when treated with 0.5% OligoM (**Figure 3.9**). *C. violaceum* CV026 behaved similarly when treated with the oligomers and in the presence of exogenous C6-AHL, which is required for the strain to produce the pigment violacein (**Figure 3.10**). Similarly with this strain, a significant dose-dependent reduction in pigment production was also seen when treated with OligoG CF-5/20 and OligoM for 48 h. Neither of the oligomers showed highly active QS inhibition against both strains, although 6% OligoG CF-5/20 was close demonstrating high percentage inhibition against *C. violaceum* CV026 (93.6%) and moderate activity against *C. violaceum* ATCC 31532 (88%). Moderate inhibition against both strains was observed for 2 and 6% OligoM and 2% OligoG CF-5/20 (**Figure 3.11**), whilst both oligomers at 0.5% failed to display any activity (≤ 40% against both strains).

Furanone (a QS inhibitor) was used as a positive control in the QS assay. A cut-off for QS inhibition was set at ≥ 90% inhibition for both *C. violaceum* strains in the QSI assay and ≤ 40% inhibition in the cell viability assa,y as previously defined (Manner and Fallarero 2018). Furanone at 1 mg/mL displayed strong QS inhibition, with ≥ 90% inhibition against *C. violaceum* ATCC 31532 (99.2%) and against *C. violaceum* CV026 (94.3%). The viability inhibition assay showed that, at 1 mg/mL, cell viability was unaffected with inhibition ≤ 40% against both *Chromobacterium* strains (12.3% inhibition against *C. violaceum* CV026 and 23.8% against ATCC 31532).

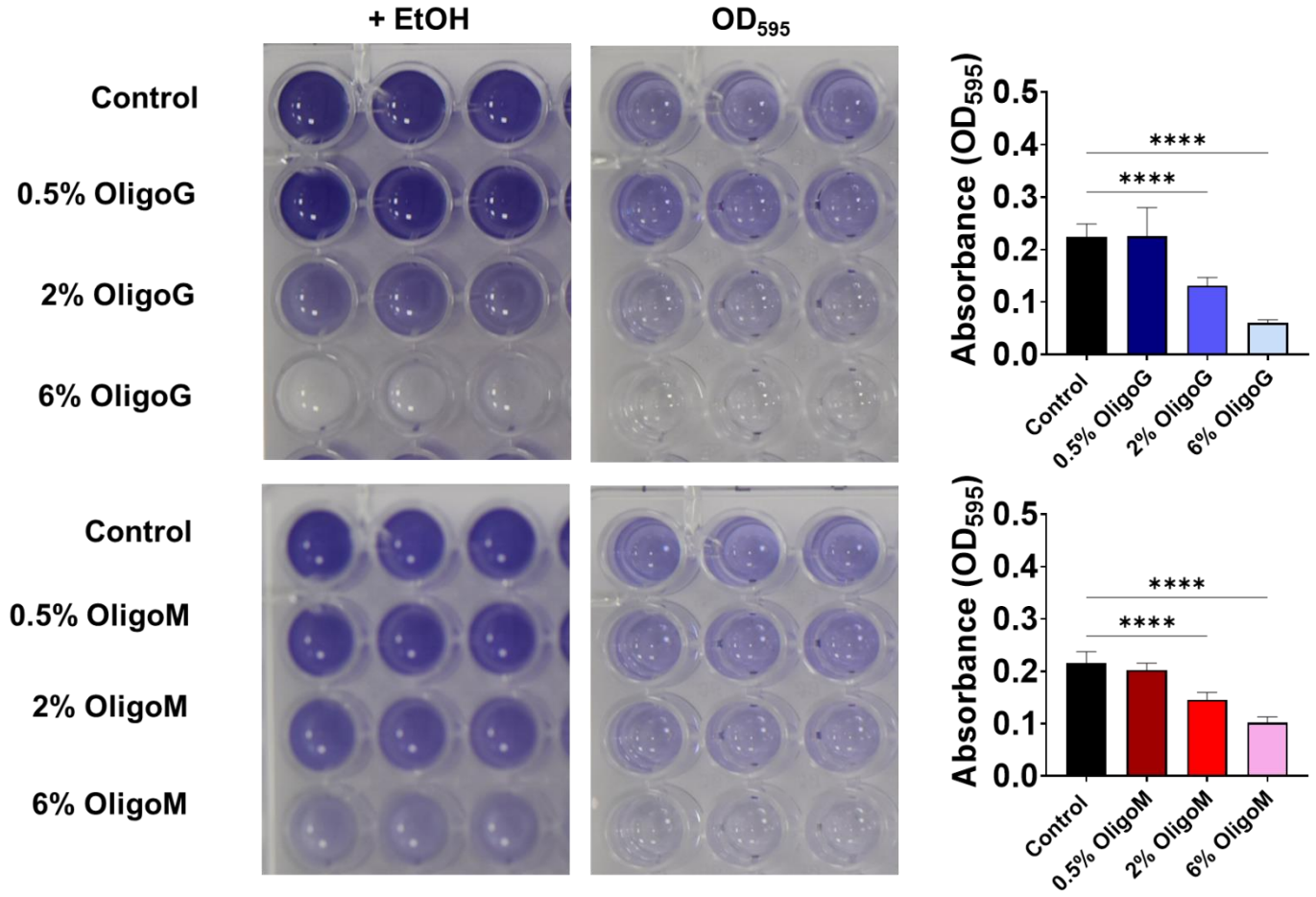

Figure 3.9. Effect of alginate oligomers on violacein pigment production by *C. violaceum* ATCC 31532 after 48 h treatment with OligoG CF-5/20 or OligoM (0.5, 2 and 6%). After 48 h incubation, the violacein pigment was dissolved in 96% (v/v) ethanol (EtOH), before absorbance was measured at OD_{595}; n=3; Group wise comparisons were analysed using one-way ANOVA, followed by Dunnett's post hoc tests; *P <0.05; **P <0.01; ***P <0.001; ****P <0.0001 denotes significance.

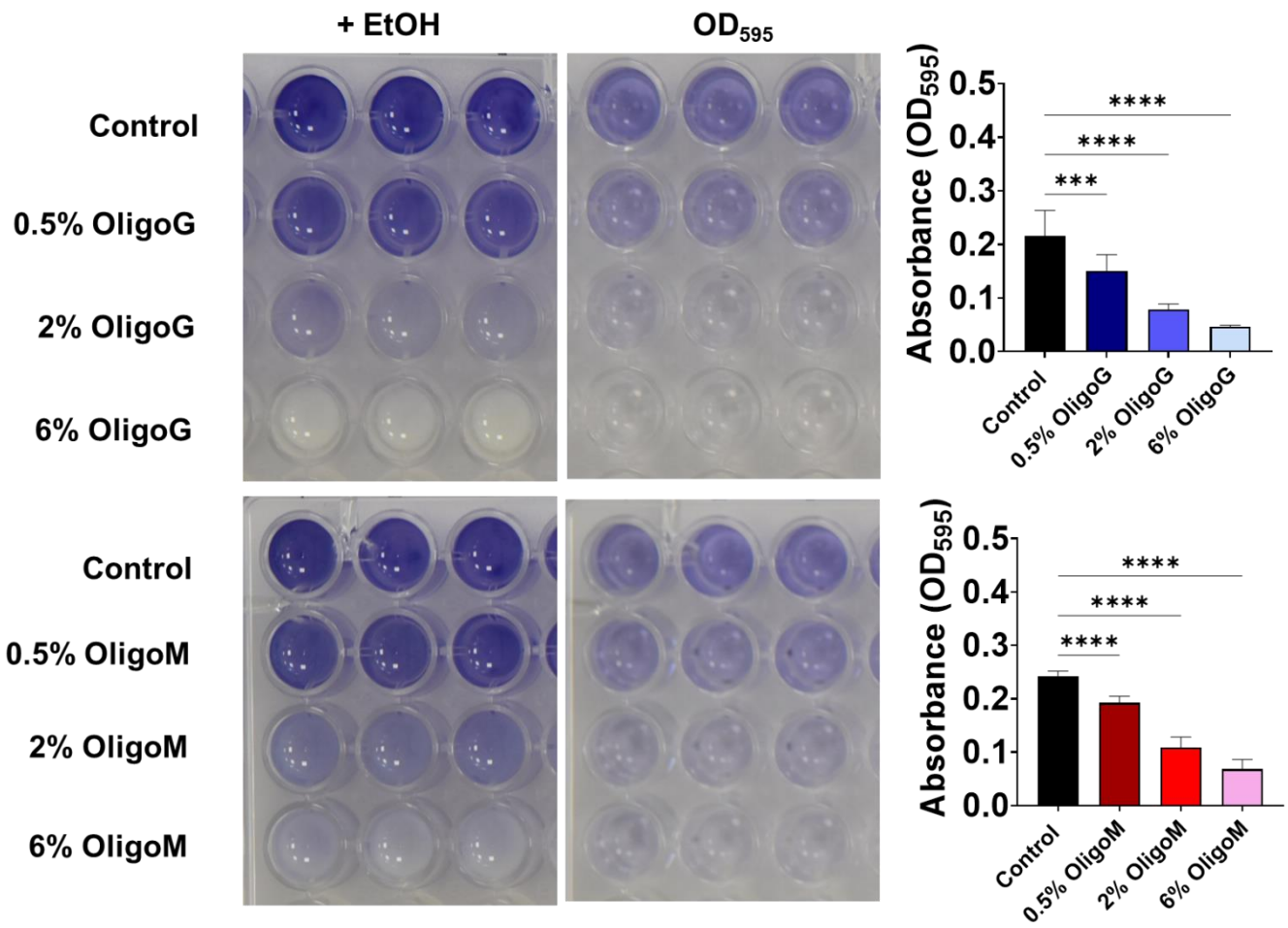

Figure 3.10. Effect of alginate oligomers on violacein pigment production by *C. violaceum* CV026 in the presence of exogenous C6-AHL, after 48 h treatment with OligoG CF-5/20 or OligoM (0.5, 2 and 6%). After 48 h incubation, the violacein pigment was dissolved in 96% (v/v) ethanol (EtOH), before absorbance was measured at OD_{595}; n=3; Group wise comparisons were analysed using one-way ANOVA, followed by Dunnett's post hoc tests; *P <0.05; **P <0.01; ***P <0.001; ****P <0.0001 denotes significance.

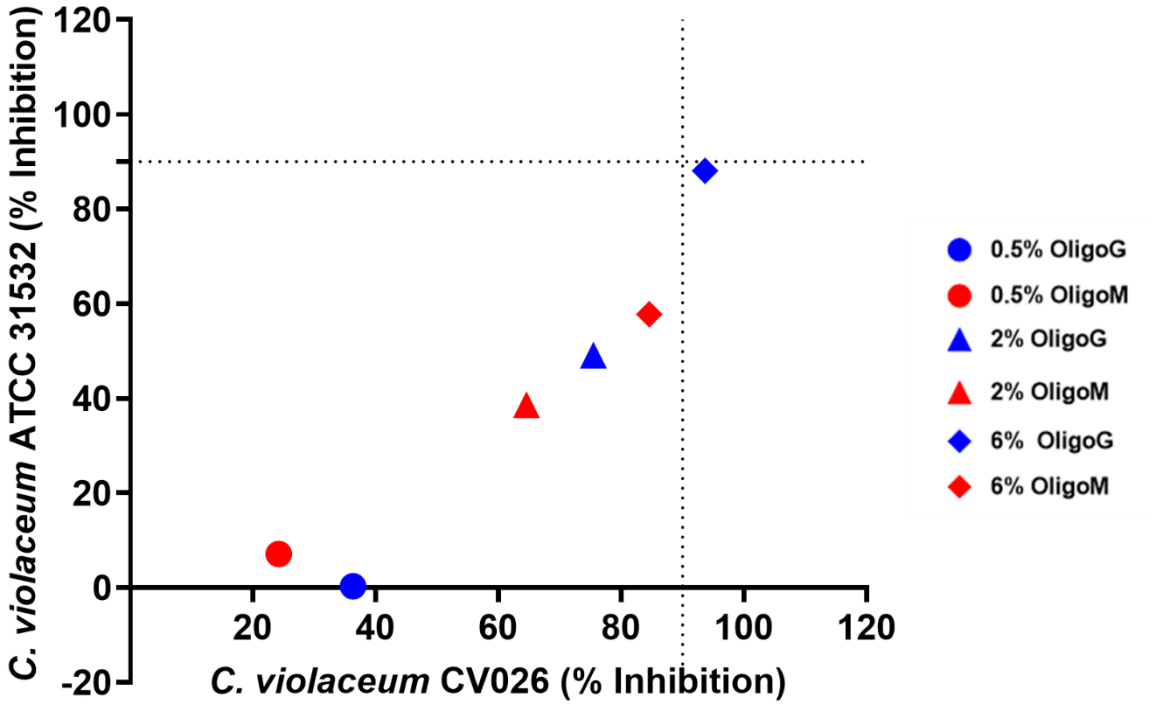

Figure 3.11. Inhibition of violacein production in *C. violaceum* ATCC 31532 and CV026, after 48 h incubation with OligoG CF-5/20 or OligoM (0.5, 2 or 6%). The threshold for highly active QS inhibitors (QSIs) was set at ≥ 90% inhibition of violacein production (*dotted line*).

3.3.4 Effect of alginate oligomers on cellular viability of *Chromobacterium* strains

The QS cell viability assay was run in parallel to the QSI assay, to determine if reduced pigment production was due to a reduction in cell viability (i.e., reduced cell numbers), rather than the effect of the compounds actively inhibiting QS. The addition of resazurin was used to enable visual assessment of cell viability after 48 h (without addition of C6-AHL). Only 6% OligoG CF-5/20 showed a significant change in viability for both *C. violaceum* ATCC 31532 and *C. violaceum* CV026 strains, suggesting that growth was promoted, compared to the untreated control (**Figure 3.12 and 3.13**).

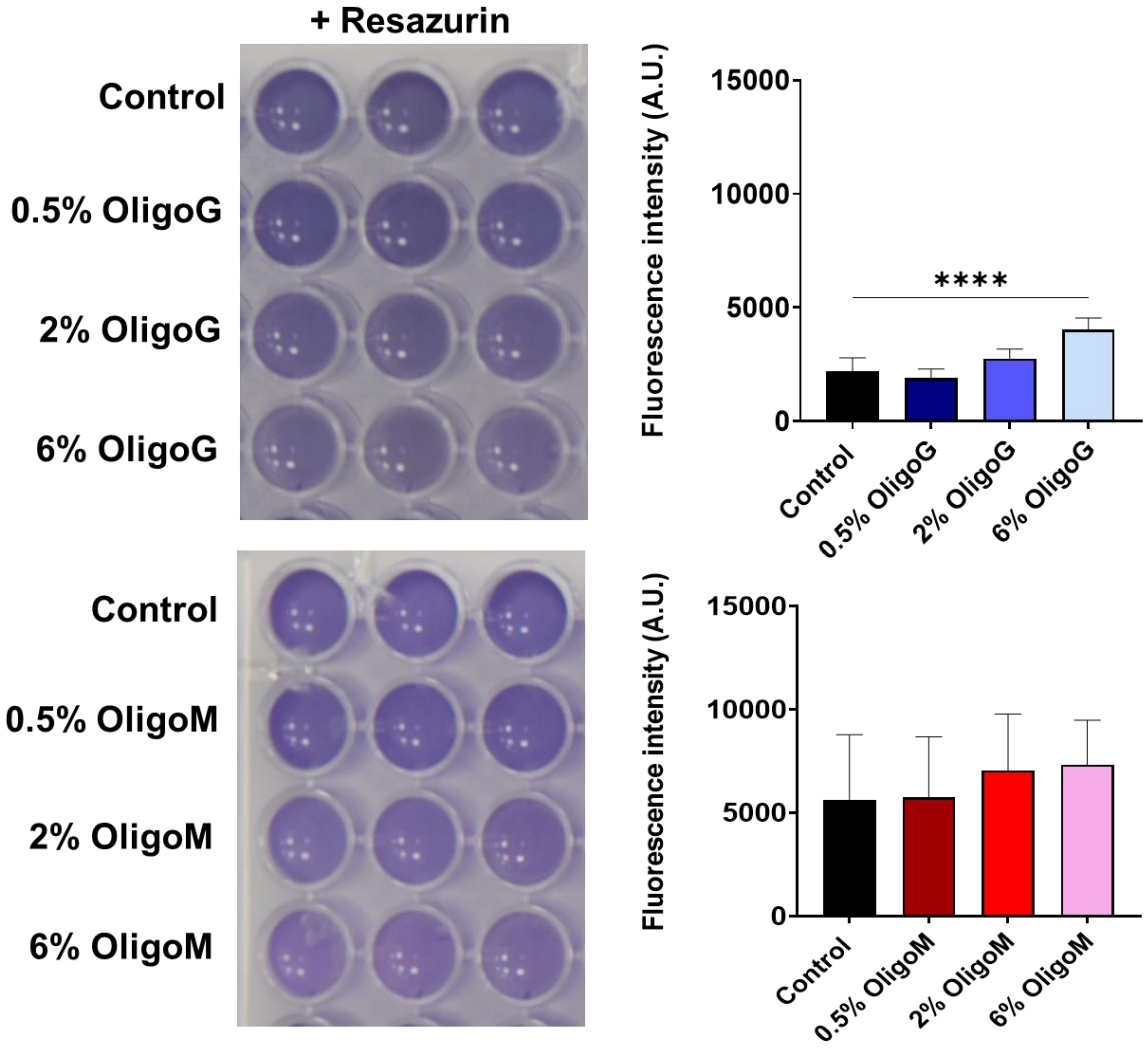

Figure 3.12. Effect of OligoG CF-5/20 and OligoM on *C. violaceum* ATCC 31532 cell viability. Cell viability was measured by colour change, after staining with resazurin (20 μM in PBS). Fluorescence intensity measured at λex = 560 nm, λem = 590 nm. n=3; Group wise comparisons were analysed using one-way ANOVA, followed by Dunnett's post hoc tests; *P <0.05; **P <0.01; ***P <0.001; ****P <0.0001 denotes significance.

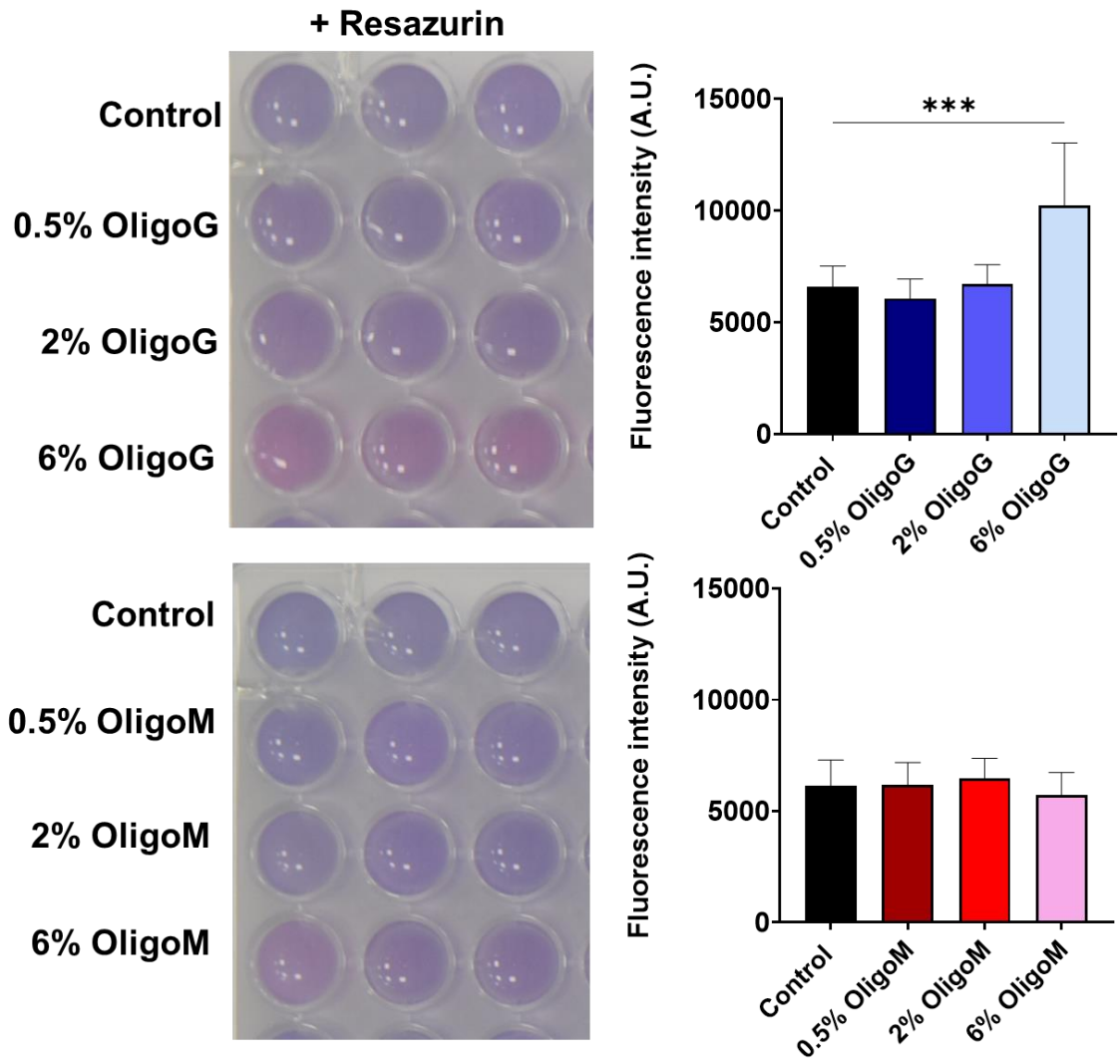

Figure 3.13. Effect of OligoG CF-5/20 and OligoM on *C. violaceum* CV026 cell viability. Cell viability was measured by colour change after staining with resazurin (20 μM in PBS). Fluorescence intensity measured at λex = 560 nm, λem = 590 nm. n=3; Group wise comparisons were analysed using one-way ANOVA, followed by Dunnett's post hoc tests; *P <0.05; **P <0.01; ***P <0.001; ****P <0.0001 denotes significance.

Figure 3.14 shows that none of the concentrations of OligoG or OligoM tested showed bactericidal effects, (i.e., all showed ≤ 40% inhibition in viability against both strains), indicating that any QSI seen was not due to a reduced cell count.

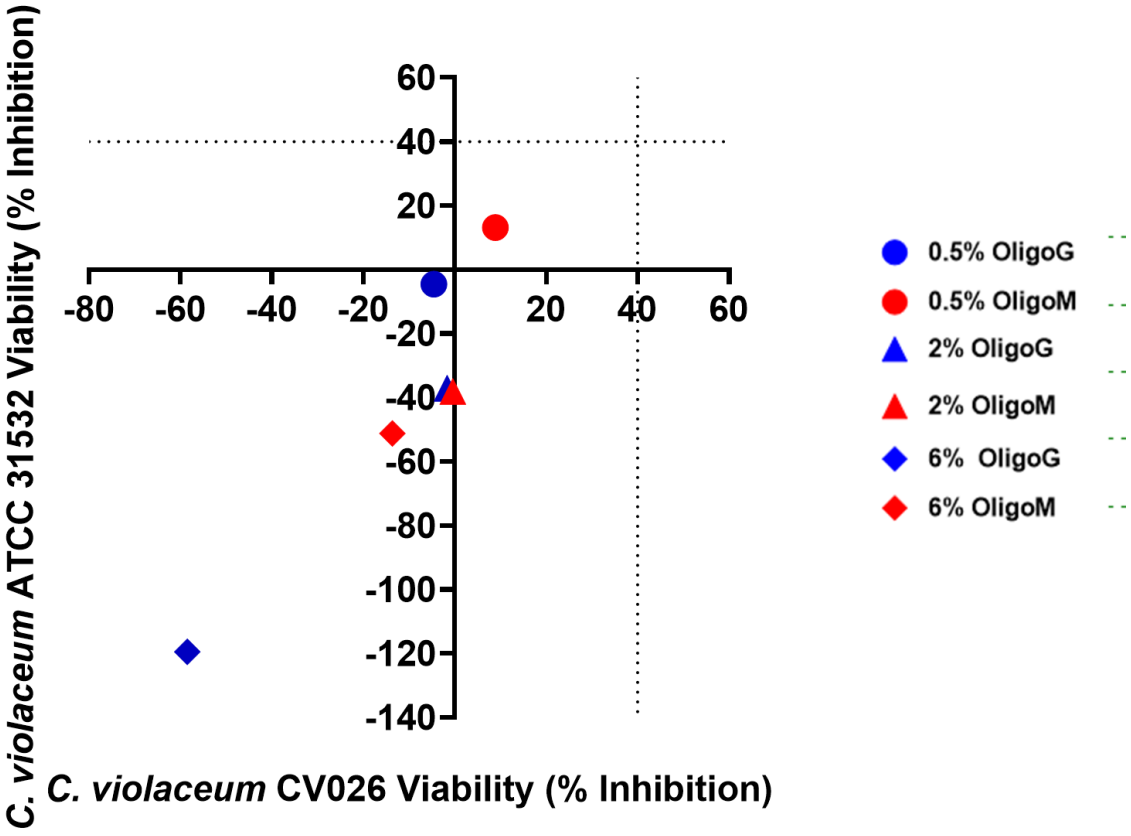

Figure 3.14. Percentage inhibition of *C. violaceum* ATCC 31532 and *C. violaceum* CV026 cell viability, when treated with OligoG CF-5/20 or OligoM (0.5, 2 and 6%). Compounds at ≤ 40% (dotted line) showed no bactericidal activity.

3.3.5 Effect of alginate oligomers on *P. aeruginosa* virulence factor production

Interestingly, both oligomers at low concentrations (0.5% and 2%) appeared to show a significant stimulation of pyocyanin production after 24 h treatment, with OligoG CF-5/20 and OligoM only demonstrating significant inhibition at 6% (**Figures 3.15 A and B**). The effect of both oligomers on protease (**Figure 3.16 A and B**) and elastase (**Figure 3.17 A and B**) production was also investigated, with concentrations of ≥ 2% significantly reducing the amount of both produced by *P. aeruginosa*. Reduction in elastase production was also significant at 0.5% OligoM. Rhamnolipid production showed unclear results, with 0.5% OligoG CF-5/20 and OligoM showing a significant reduction in rhamnolipid production, which was unexpectedly not evident at the higher concentrations tested (≥ 2%) (**Figures 3.18A and B**). Furthermore, the optical density measurements did not reflect the visual changes in pigmentation seen in the cell-free supernatants in **Figure 3.18A.**

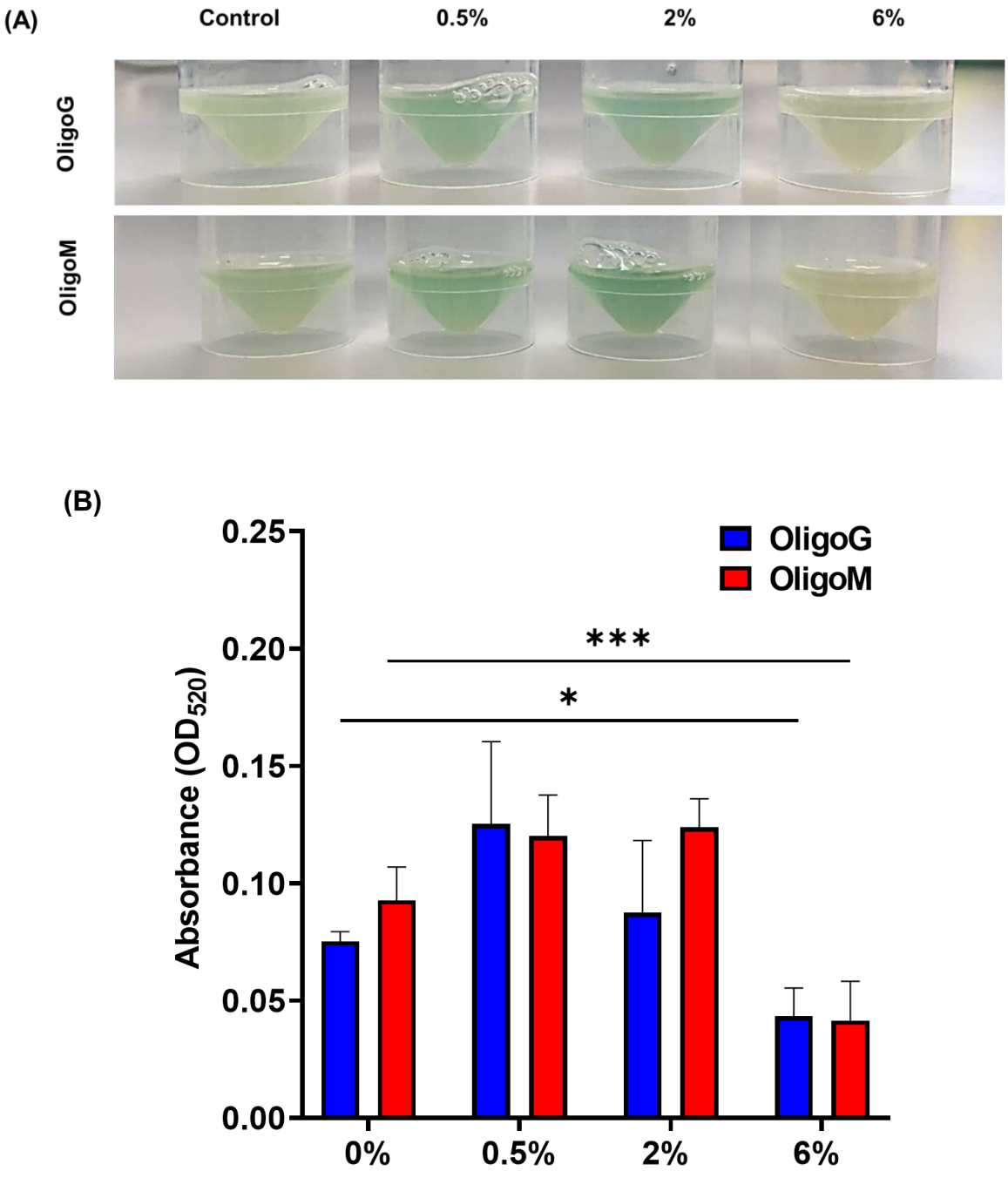

Figure 3.15. Pyocyanin production by *P. aeruginosa* PAO1 after 24 h treatment with OligoG CF-5/20 or OligoM (0.5, 2 and 6%) (**A)** Overnight cell-free culture supernatants showing differing extents of pyocyanin production (green pigmentation) after treatment; (**B)** optical density measurements at OD_{520} (mean ± SD; n=3; *P <0.05; **P <0.01; ***P <0.001; ****P <0.0001 denotes significance.).

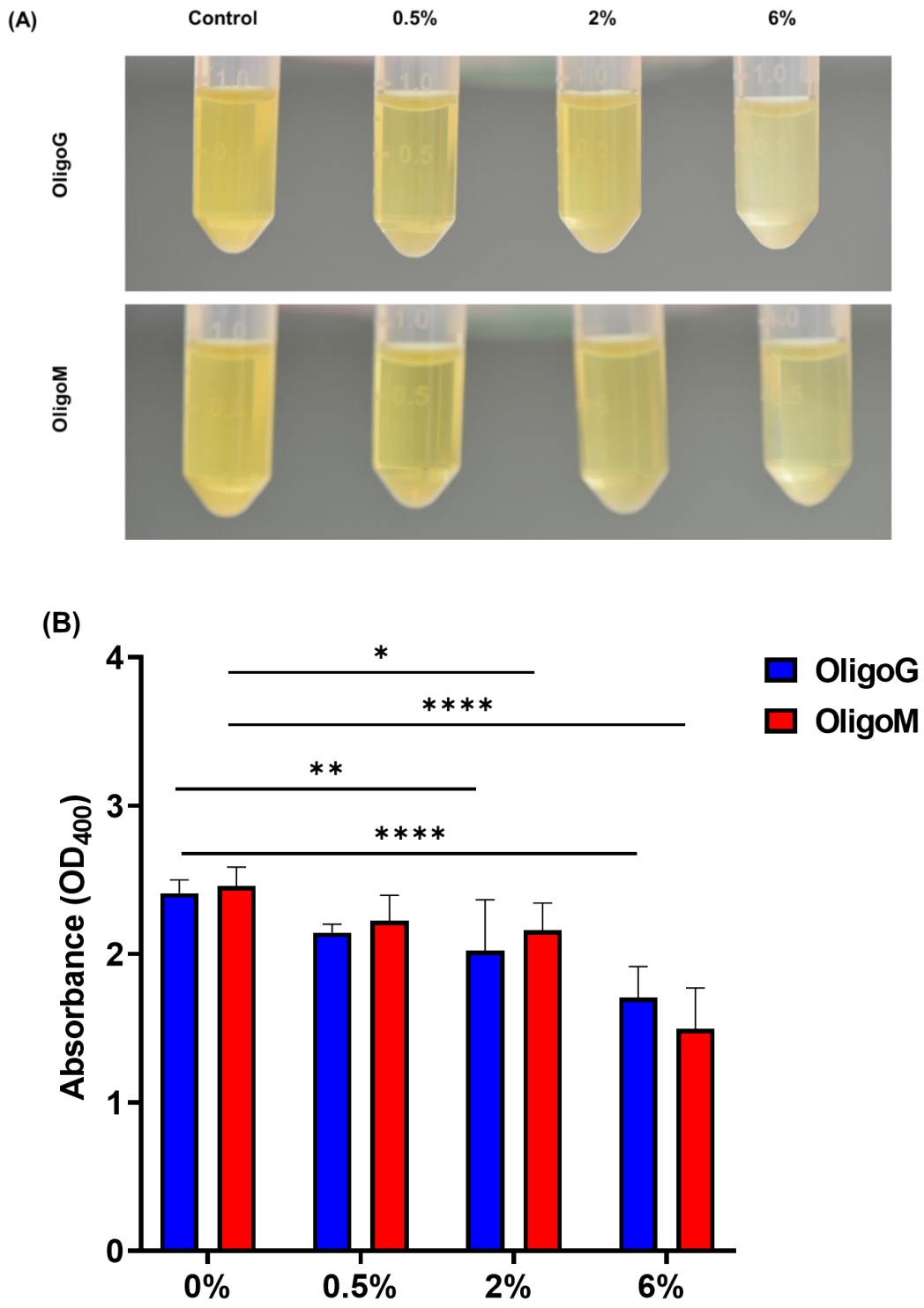

Figure 3.16. Protease production by *P. aeruginosa* PAO1, after 24 h treatment with OligoG CF-5/20 or OligoM (0.5, 2 and 6%). (**A)** Overnight cell-free culture supernatants showing differing extents of pigmentation after treatment; (**B)** optical density measurements at OD_{400} (mean ± SD; n=3; *P <0.05; **P <0.01; ***P <0.001; ****P <0.0001 denotes significance.).

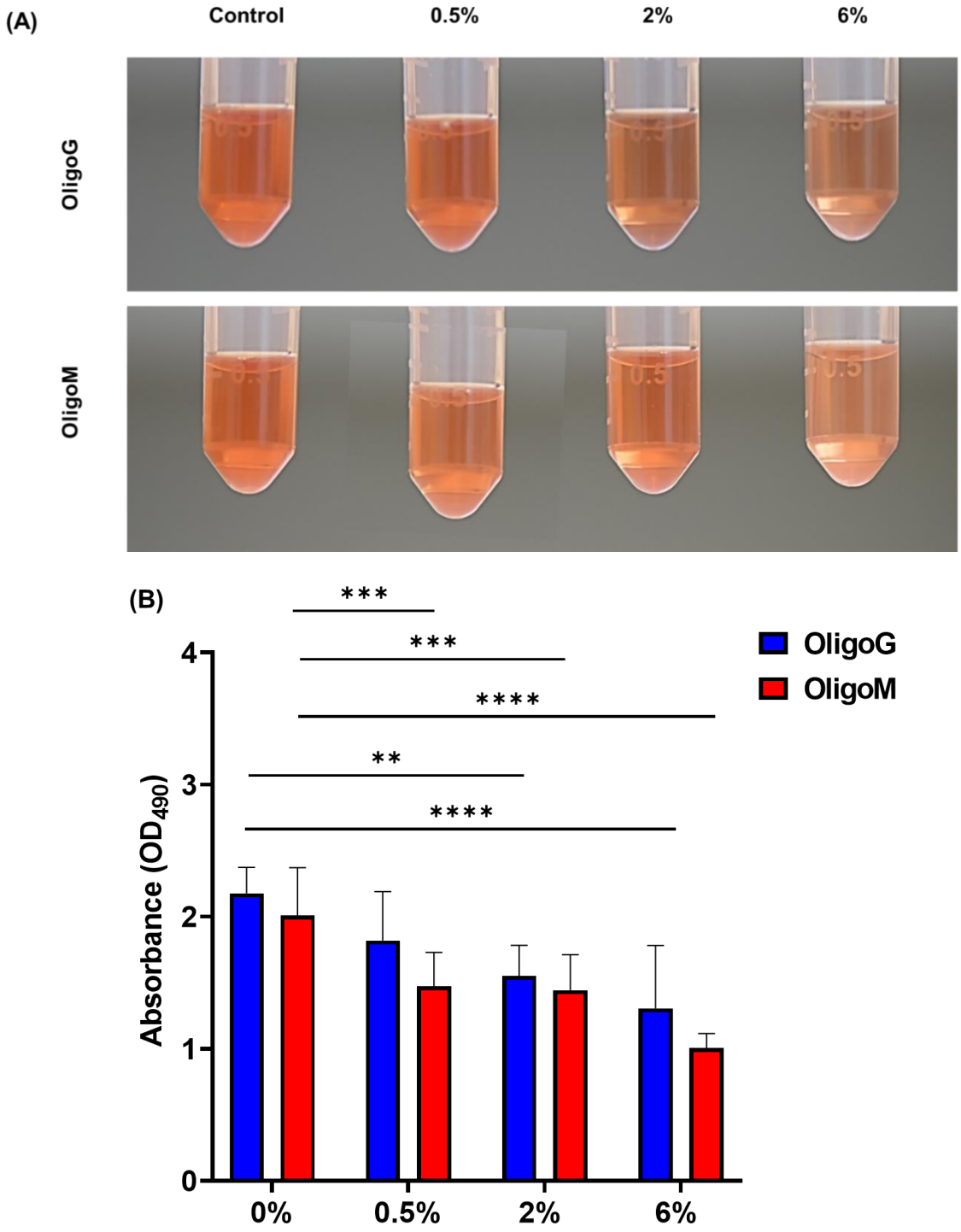

Figure 3.17. Elastase production by *P. aeruginosa* PAO1, after 24 h treatment with OligoG CF-5/20 or OligoM (0.5, 2 and 6%). (**A)** Overnight cell-free culture supernatants showing differing extents of pigmentation after treatment; (**B)** optical density measurements at OD_{400} (mean ± SD; n=3; *P <0.05; **P <0.01; ***P <0.001; ****P <0.0001 denotes significance.).

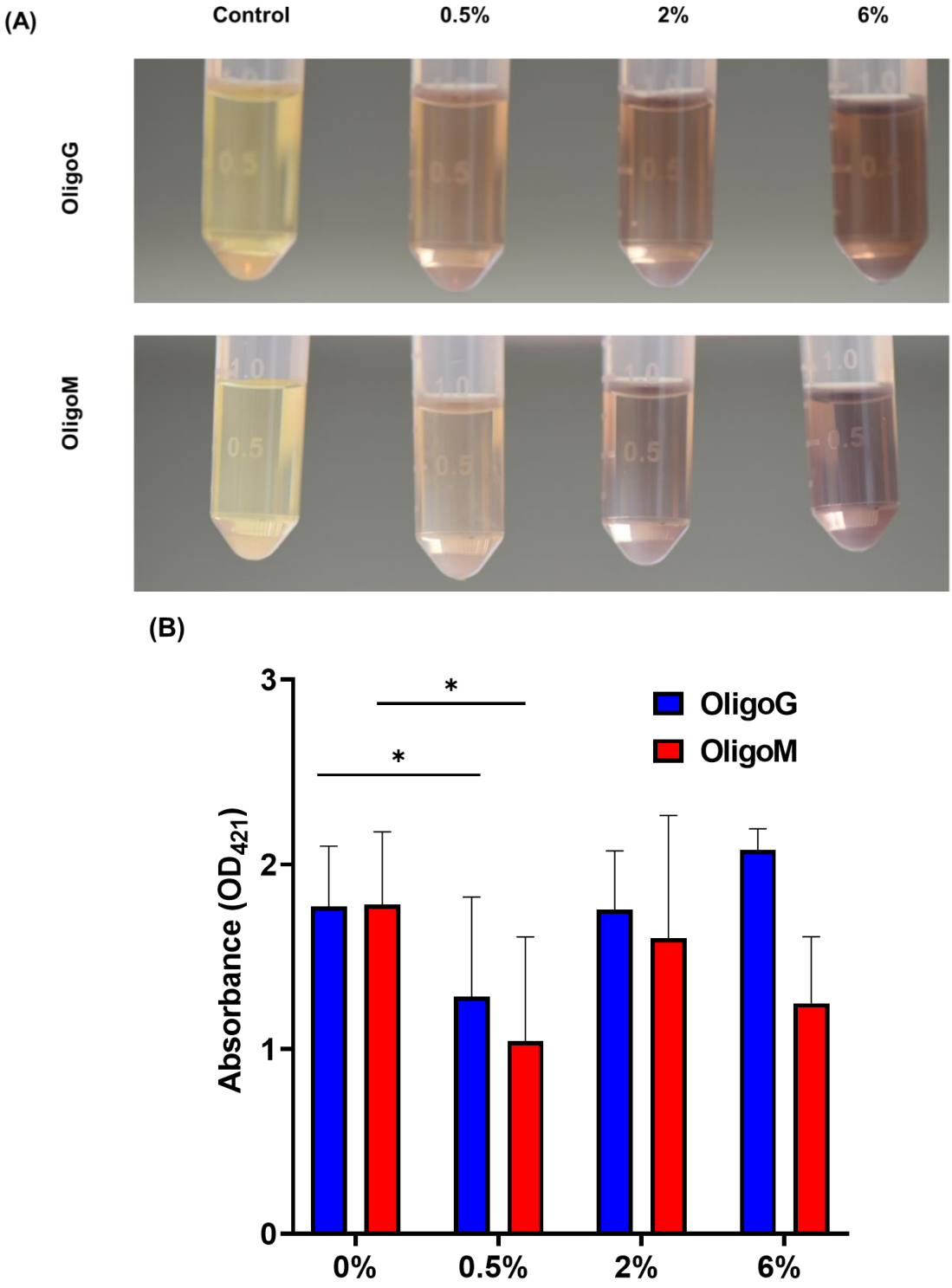

Figure 3.18. Rhamnolipid production by *P. aeruginosa* PAO1, after 24 h treatment with OligoG CF-5/20 or OligoM (0.5, 2 and 6%). (**A)** Overnight cell-free culture supernatants showing differing extents of pigmentation after treatment; (**B)** optical density measurements at OD_{421} (mean ± SD; n=3; *P <0.05; **P <0.01; ***P <0.001; ****P <0.0001 denotes significance.).

3.3.6 Effect of oligomers on cell surface binding

FTIR analysis showed the presence of both 0.5% OligoG and OligoM on *P. aeruginosa* cell surface after being exposed to hydrodynamic shear (**Figure 3.19 A**). Hierarchical cluster analysis (HCA) showed distinct clustering of control samples, compared to alginate-treated groups (**Figure 3.19 B**). Exceptions to this clustered grouping were two biological repeats, one OligoG and one OligoM treatment (sample G5 and M4 respectively), which seem to have lost any oligosaccharide from the cell surface. 184 wavelengths were identified from Wilcox rank sum analysis that showed statistically different wavenumbers between OligoG and OligoM treatments.

3.3.7 Potentiation effect of azithromycin with oligomers on cell viability

ATP viability assays showed that the combined treatment of 2% OligoM with azithromycin showed no significant effect, while 6% was shown to significantly reduce cellular viability (MSD= 85393 A.U.), compared to control samples (**Figure 3.20**). However, the combination of OligoG CF-5/20 at both 2% and 6% was shown to potentiate azithromycin in a dose-dependent manner. It was shown that 2% OligoG with 256 μg/mL azithromycin and 6% OligoG with 128 μg/mL azithromycin was sufficient to fully eradicate *P. aeruginosa* PAO1 biofilms. However, for ≥2% OligoM a concentration of 512 g/mL azithromycin was required to eradicate the biofilm.

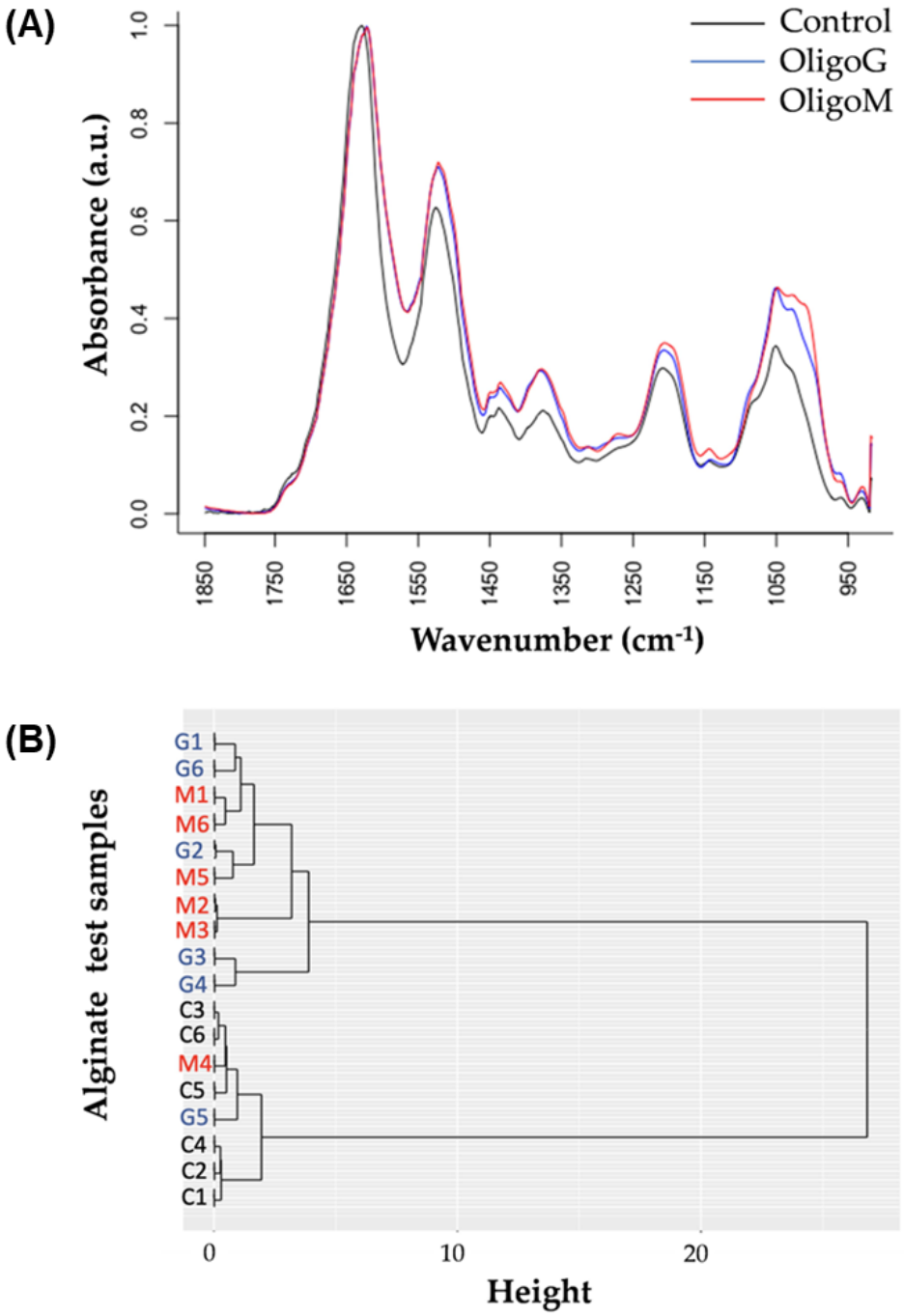

Figure 3.19. Fourier transform infrared spectroscopy (FTIR) of *P. aeruginosa* PAO1 cells. **(A)** FTIR absorbance spectra showing differential peak positions between control, 0.5% OligoG, and 0.5% OligoM treated cells, following hydrodynamic shear. **(B)** Hierarchical cluster analysis (HCA) grouping of the 18 spectra; Control C1-C6, OligoG G1-G6, OligoM M1-M6, n=6 biological repeats, n=3 technical repeats.

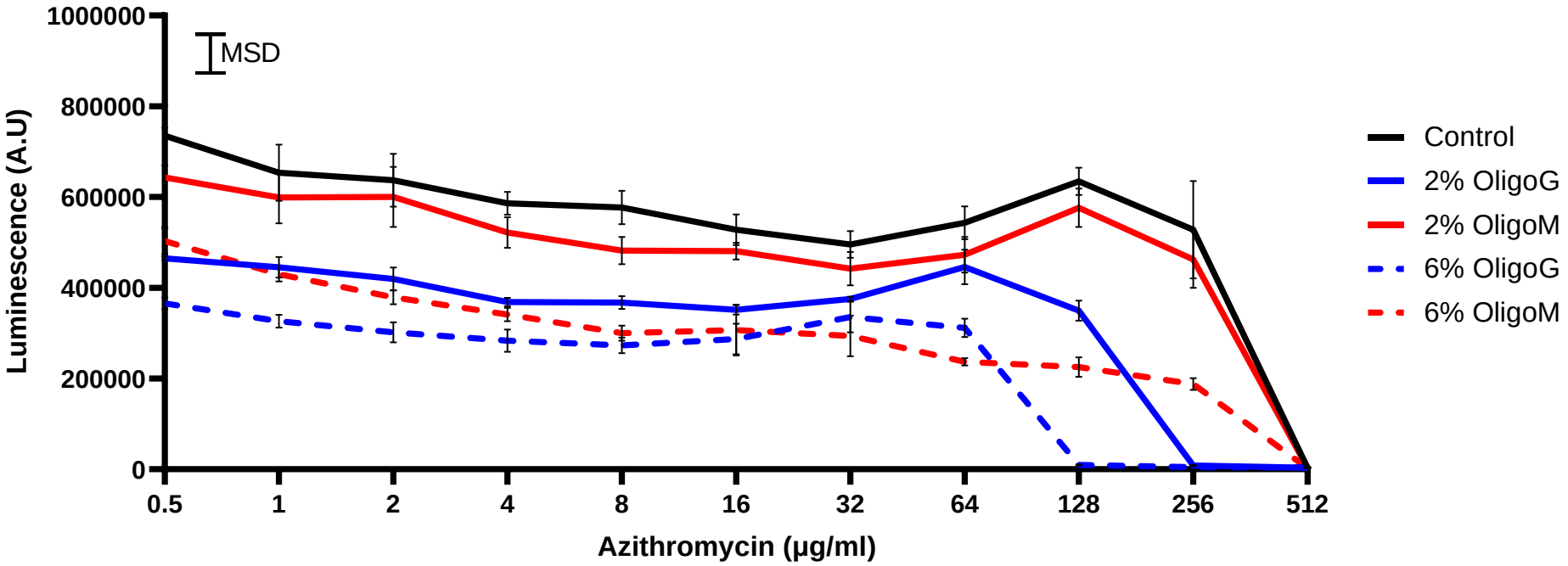

Figure 3.20. ATP cell viability for *P. aeruginosa* PAO1 biofilms grown for 19 h with OligoG CF-5/20 or OligoM (2 or 6%) in the presence of azithromycin (0.5-512 µg/mL). Minimum significant difference (MSD) for luminescence was calculated in MiniTab, using the Tukey-Kramer method (n=4): MSD= 85393 A.U.

3.4 Discussion

OligoG CF-5/20 (>85% G residues) has shown activity against multiple Gram-negative pathogens, which are responsible for chronic infections along with potentiation of multiple antibiotics (Khan et al. 2012; Powell et al. 2013b; Powell et al. 2023). Previous studies on OligoM and OligoMG (composed of 46% G blocks) of similar molecular weights to OligoG CF-5/20, have shown to have a slight potentiation effect, reducing the MIC of several antibiotics against *P. aeruginosa* and *A. baumannii*, though this was not as notable compared to the potentiation effect of OligoG, which showed to potentiate the effect of antimicrobials against many MDR pathogens (Khan et al. 2012). Similarly, it was found that M-block fractions (M1-M5) of varying molecular weights showed antimicrobial activity, showing a wider spectrum and greater inhibition than G-block fractions (G1-5). The study hypothesised that the M-blocks were more soluble, therefore, allowing easier passage through bacterial envelopes (Hu et al. 2005).

Persistent chronic infections due to *P. aeruginosa* colonisation, particularly those linked to a mucoid phenotype, are associated with greater patient morbidity and mortality (Hogardt and Heesemann 2010). Previous studies have shown that OligoG CF-5/20 is effective at reducing planktonic growth in a dose-dependent manner against a wide range of bacteria, including the ESKAPE pathogens (Khan et al. 2012; Jack et al. 2018). The growth curves performed with NH57388A (a mucoid strain of *P. aeruginosa* isolated from a CF patient), showed that 6% OligoM and OligoG CF-5/20 behaving similarly. This indicates that the antimicrobial effect is not purely dependent upon the stronger Ca^{2+} binding capabilities of OligoG, compared to OligoM.

Swarming bacteria can produce a myriad of different colony morphotypes, which in *P. aeruginosa* are typified by a dendritic appearance. Although bacterial

species and the environmental conditions, are known to influence the form of the morphological colony patterns obtained, the specific factors involved remain largely unknown (Kearns 2010; Fauvart et al. 2012; Ke et al. 2015; Yang et al. 2017a). Due to the limited quantities of alginate material available in this study, the effects of OligoG CF-5/20 and OligoM on swarming motility were tested in small-scale (3 mL agar) assays. Previous studies using stab assays, tested at 6% OligoG CF-5/20, demonstrated inhibited swarming motility in *P. aeruginosa, Escherichia coli* and *Proteus mirabilis* (Khan et al. 2012). Subsequently, large scale plate (20 mL) assays with OligoG CF-5/20 (0-6%) incorporated in BM2 agar demonstrated a dose-dependent reduction in *P. aeruginosa* swarming (Powell et al. 2013a). Unfortunately, in contrast to these studies, the results obtained here showed a high degree of variability in the swarming patterns obtained between biological replicates for both alginates. The size of the plates used here (35 mm cf. 90 mm diameter), will have limited the distance the bacteria were able to swarm in the 20 h of the experiment, having a significant impact on the results obtained. Ideally, given access to more alginate materials, this assay would have been repeated in the larger plates, matching those of the previous research.

Preliminary expression profiling of PAO1 suggested that *pilE* is down-regulated upon OligoG treatment (Powell et al. 2013a). Furthermore, atomic force microscopy (AFM) imaging has previously demonstrated strong binding-induced cellular aggregation between OligoG CF-5/20 and pseudomonal cells, in which bacterial flagella were encased in alginate, perhaps creating a physical restraint on motility (Khan et al. 2012; Powell et al. 2013a). The ability of these oligomers to inhibit swarming motility by targeting QS, as well as by physical means, demonstrates how they can inhibit colonisation and biofilm formation and cells that have reverted to their planktonic state. Powell *et al* (2013) also

showed that OligoG can resist hydrodynamic shear when bound the cell surface of *Pseudomonas*, which is also seen in the FTIR studies when using OligoM.

I, therefore, sought to compare the biofilm forming ability of *P. aeruginosa* in the presence of OligoG CF-5/20 or OligoM. COMSTAT analysis revealed that both alginate oligomers inhibited the ability of mucoid *P. aeruginosa* NH57388A biofilm, to decrease bio-volume, mean thickness, and an increase in roughness. Previous studies have also shown that OligoG CF-5/20 is effective *in vivo* against mucoid *P. aeruginosa* NH57388A in a biofilm state in a mouse model; 1 and 5% OligoG CF-5/20 reducing the microbial burden in a dose-dependent manner (Hengzhuang et al. 2016). Previous studies have shown that OligoG CF-5/20 is efficient at reducing biofilm formation, as well as disrupting established biofilms, compared to untreated biofilms (Jack et al. 2018). OligoG CF-5/20 treated biofilms have altered structures with significantly lower Young's moduli, meaning that they are less robust, more inclined to detachment and are more prone to hydrodynamic stress (Powell et al. 2013b; 2018).

Divalent cations, such as Ca^{2+}, provide strength and stability to the outer membrane of bacteria, facilitating cross linkers within the biofilm matrix with an ability to influence biofilm formation; electrostatic interactions affecting attachment, as well as EPS synthesis (Song and Leff 2006). These calcium-dependent processes were thought to be the mechanism of action of OligoG CF-5/20. However, these results comparing OligoM with contrasting Ca^{2+} binding properties indicate other potential mechanisms of action e.g., the modification of QS signalling, which was further investigated.

Regulation of QS in *P. aeruginosa* is complex and is sensitive to growth and environmental conditions, both of which can significantly impact the timing of *lasIR* and *rhlIR* expression (Duan and Surette 2007). The complexity of the QS system in *P. aeruginosa* is believed one of the main factors responsible for its phenotypic elasticity

and versatility (Juhas et al. 2005). QS systems control 10% of the *P. aeruginosa* genome, having been shown to be central to biofilm formation, as well as contributing to the production of virulence factors, making them an ideal target for antibiofilm therapies (Schuster and Greenberg 2006).

Therapeutic targets have tended to focus on LasR, as it "sits" at the top of the QS hierarchal cascade, with QSIs, such as furanone, inhibiting QS through LasR antagonism (Hentzer et al. 2003). QS disruption can occur via several methods including: degradation of the AHL molecule (i.e., quorum quenching); scavenging of AHL by antibodies; inhibition of AHL recognition and/or synthesis (i.e. QS inhibition [QSI]); or mimicking of signal molecules using synthetic analogues that outcompete AHL for receptor binding, as well as alterations to the AHL molecule (Hentzer et al. 2003; Park et al. 2007; Rémy et al. 2018). Alternatively, natural, and synthetic therapies could target RhlR or both LasR and RhlR. QSIs can reduce or even completely inhibit the production of virulence factors before the innate immune system can come into effect; a potentially highly beneficial trait compared to conventional treatments, preventing bacteria from adapting to their environment and developing resistance (Mattmann and Blackwell 2010; Proctor et al. 2020).

A small-scale QS assay was developed in this study, utilising *C. violaceum* ATCC 31532 and the biosensor strain, *C. violaceum* CV026. Addition of AHLs with a carbon chain length of C_4 to C_8, induces violacein production in the biosensor, while inhibition can be induced by the addition of AHLs with a carbon chain length of C_{10} to C_{14} (Jack et al. 2018). CV026 can, therefore, be used to identify compounds with quorum quenching activity (Kalia 2013). When an external AHL is added (to CV026), QSIs can target it before it is able to reach the bacterial cells, so preventing violacein production. This

would be reflected in the marked inhibition (a decrease in purple violacein pigmentation) of the mutant strain (CV026), but not of the control parent strain (ATCC 31532). OligoG CF-5/20 and OligoM were both shown to reduce violacein production by *C. violaceum* strains in a dose-dependent manner (without significantly affecting cellular viability), suggesting that they did both behave as QSIs (≥ 2%), with 6% OligoG CF-5/20 showing the greatest inhibition.

Pyocyanin is a redox-active, virulence factor, which when administered chronically in mice has been shown to induce a CF-like lung phenotype (Hao et al. 2012). Pyocyanin is secreted by stationary phase bacteria, with maximal pyocyanin production reported at 24 h in *P aeruginosa* PAO1 (Rada and Leto 2013; Jack et al. 2018). OligoG CF-5/20 has previously been shown to significantly inhibit 24 h pyocyanin production at concentrations ≥ 0.2% (Jack et al. 2018). In contrast in this study, a significant decrease in pyocyanin was only noted at 6% OligoG CF-5/20.

Regulation of protease and elastase is via the *rhlI-rhlR* QS system (Jack et al. 2018). Similar to Jack *et al.* (2018), protease and elastase production both showed dose-dependent reductions when treated with OligoG CF-5/20 for 24 h, with OligoM also showing similar effects. Proteases and elastase are known for their ability to cause tissue damage mainly during acute infections, LasB degrades elastin resulting in the tight junctions present in the epithelium to become disrupted, also interfering with immune defences and wound healing (Faure et al. 2018).

Rhamnolipids are known to influence swarm morphology through their ability to reduce surface tension. The unusual purple pigmentation produced from the orcinol assay specifically after incubation may be due to a pH change, resulting in the rhamnose head or fatty-acid tail changing the charge of the rhamnolipid, or the heat may cause other

interactions to occur resulting in a colour change. Jack *et al.* (2018) found that as pyocyanin and rhamnolipid production was significantly reduced by OligoG CF-5/20 in both a dose-dependent and time-dependent manner, compared to protease and elastase, it suggested that the oligomer preferentially targeted the *Rhl* and *pqs* QS system that activates the genes for virulence factors, such as pyocyanin rather than the *las* system.

Again, using a smaller scale assay with 1 mL of culture being prepared for these virulence determinations compared to Jack *et al.* (2018), which employed 6 mL volumes, made reproducibility of the previous results difficult. This led to an unexpected increase in production of pyocyanin (at 0.5 and 2%) and rhamnolipids (at 2 and 6%) for both OligoM and OligoG CF-5/20. Furthermore, virulence was only measured at one time point (24 h), instead of four over the course of 30 h incubation, with previous research showing that maximum production of AHLs at 12 h with a decline seen after this time-point (Jack et al. 2018). A time course could not be conducted in this study, due to limited availability of OligoM.

This study confirmed the superior ability of OligoG to potentiate the effect of azithromycin against *P. aeruginosa* PAO1 strain, compared to OligoM. Biofilms grown with azithromycin and ≥ 2% of OligoG showed significant potentiation effects, while research has shown that *P. aeruginosa* grown in the presence of azithromycin reduces resistance to other antibiotics, such as aztreonam (Oakley et al. 2021). This further spotlighting its potential use as a treatment for CF sufferers as a stand-alone treatment, or in combination with the commonly prescribed azithromycin.

3.5 Conclusion

This study focused on the SAR of OligoG CF-5/20 and OligoM with comparable DPn for targeted antimicrobial applications. These results show that both

OligoG CF-5/20 and the tailored OligoM were both effective at reducing the planktonic and biofilm microbial growth of *P. aeruginosa* in a dose-dependent manner. Therefore, the antimicrobial effect is not solely related to their calcium binding ability. OligoG CF-5/20, however, exhibited a far stronger QSI effect than OligoM. Synergistic responses with azithromycin were also shown to be superior for OligoG, when compared to OligoM, in biofilm models. This study confirms the potential clinical utility of OligoG CF-5/20 in treating infections of MDR bacterial pathogens, such as *P. aeruginosa* infections in CF patients.

Chapter 4

Modelling the loss of plasmid mediated colistin resistance genes, *mcr-1* and *mcr-3*, in *E. coli* in a biofilm model

4.1 Introduction

4.1.1 Polymyxins

Polymyxin antibiotics were originally derived from the Gram-positive bacterium, *Paenibacillus polymyxa* (previously known as *Bacillus polymyxa*) in 1947 (Storm et al. 1977). These are comprised of polymyxin A to E, although only polymyxin B (PMB) and polymyxin E (colistin) are now used in a clinical setting, due to toxicity issues (Rigatto et al. 2019). All five polymyxin subtypes have the same molecular structure, namely: a polycationic peptide ring, a linear tripeptide side chain and a long hydrophobic fatty acid tail (Velkov et al. 2010). The hydrophilic peptide end, combined with the hydrophobic fatty acid component, makes the polymyxins amphipathic and therefore, stable when reacting with surfaces that are charged or uncharged (Loho and Dharmayanti 2015). Colistin is composed of two components, colistin A (polymyxin E_1) and colistin B (polymyxin E_2) (**Figure 4.1A**); while the only difference between colistin and PMB is a single amino acid at position 6', with D-Leu (D-leucine) in colistin being replaced by D-Phe (D-phenylalanine) in polymyxin B (**Figure 4.2B**), (Falagas et al. 2005).

4.1.2 Mechanism of action

The mode of action of colistin results in permeabilisation of the bacterial outer membrane (OM, Anandan et al. 2017). The positive charge of the colistin molecule is electrostatically attracted to the negatively charged OM, causing divalent cations e.g., Mg^{2+} and Ca^{2+} that are associated with stabilisation of the lipopolysaccharide (LPS) molecule to be displaced from their phosphate groups by binding of the polycationic peptide ring. This leads to increased permeability of the cell, resulting in

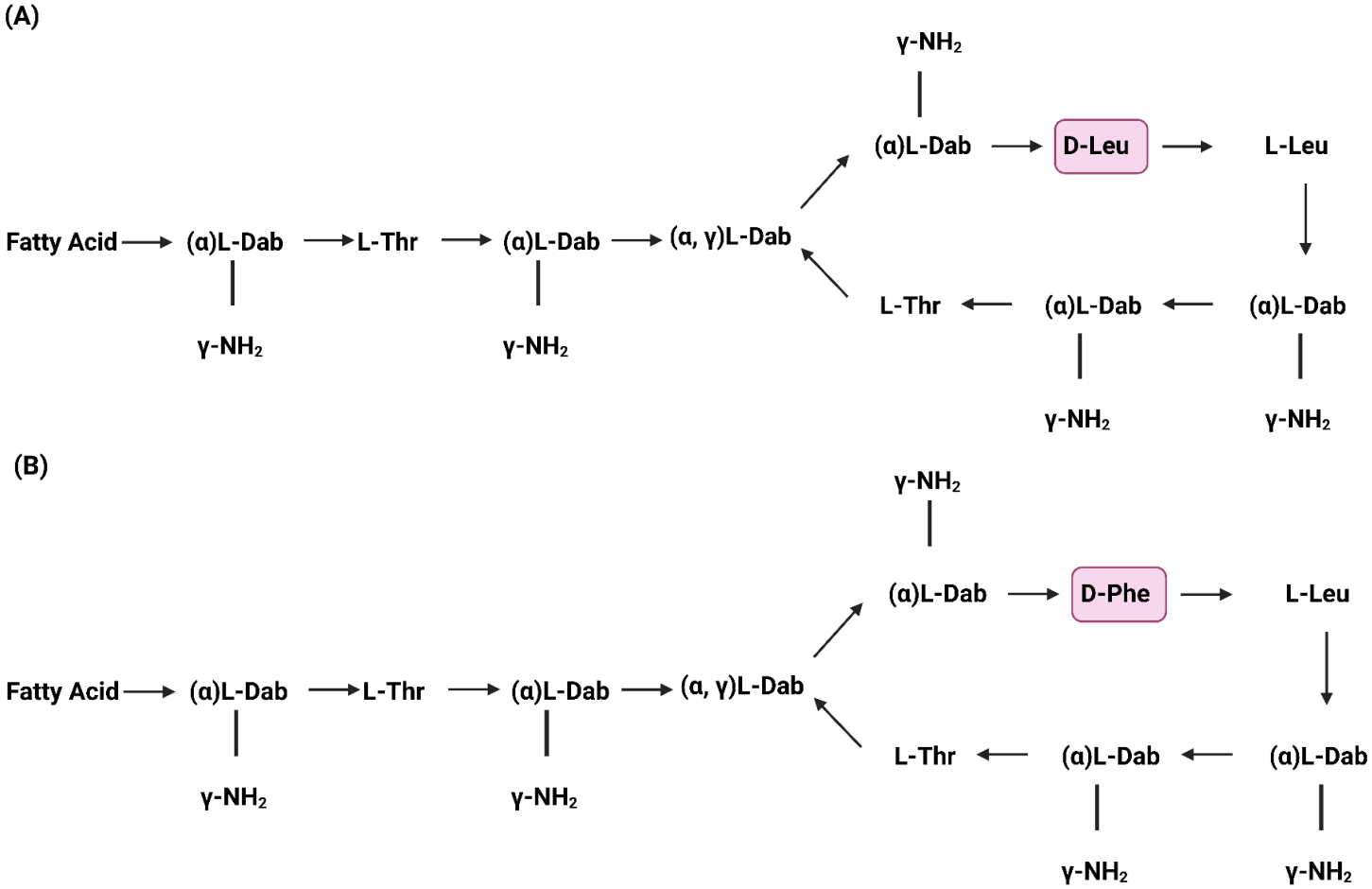

Figure 4.1 (A) Structure of colistin A and B. Fatty acid; 6-methyloctanoic acid for colistin A and 6-methylheptanoic acid for colistin B. (**B)** Structure of polymyxin B. Thr, threonine; Dab, diaminobutyric acid; Leu, leucine; Phe, phenylalanine.

leakage of cellular contents and ultimately cell death (Falagas et al. 2005; Nation and Li 2009). Furthermore, any damage sustained affecting membrane integrity will likely make bacteria more susceptible to further treatment (Landman et al. 2008).

A potential alternative mechanism of action through the formation of vesicle-vesicle contacts (Clausell et al. 2007). Once it has traversed the OM, colistin can interact with anionic phospholipid vesicles, specifically those found in the periplasmic region facing the inner membrane (IM) and OM, allowing for the exchange of phospholipids (Elias et al. 2021). This can result in phospholipid loss, osmotic imbalance, and results in the leakage of intracellular contents and eventually cell lysis (Yu et al. 2015). An additional third pathway that bactericidal agents possess is via the production of high levels of reactive oxygen species (ROS) in an oxidative burst causing rapid cell death (Kohanski et al. 2007). When colistin crosses the OM, ROS, such as hydrogen peroxide (H_2O_2), superoxide (O_2^-), and hydroxyl radical (•OH), are produced and all contribute to oxidative damage of cellular components such as DNA, proteins, and lipids (Imlay 2015).

4.1.3 Toxicity issues with colistin

Despite the initial widespread use of colistin following its discovery and its introduction into clinical use, its usage was stopped during the 1970's due to issues surrounding nephro- and neurotoxicity (Avedissian et al. 2019). Neurotoxicity arises as colistin causes impaired release of acetylcholine into the synaptic gap, causing depolarisation and loss of Ca^{2+} from neurons resulting in the build-up of ROS contributing to oxidative stress, lysis, and nerve damage (Falagas and Kasiakou 2006; Camargo et al. 2021). Signs of neurotoxicity caused by colistin can manifest as dysphagia, paraesthesia, deafness, seizures, and ataxia, with neurological side-effects

in 7-27% of patients, with onset often occurring within a week of treatment (Landman et al. 2008; Ordooei Javan et al. 2015; Poirel et al. 2017).

Nephrotoxicity (the decline in renal function) is a common side-effect of treatment with colistin. However, recent reports suggest that rates may not be as severe as perceived, although acuter tubular necrosis will result from overuse (Bialvaei and Samadi Kafil 2015). It is thought that oxidative stress, apoptosis, and inflammation all contribute to kidney damage, with preventative methods generally focusing on antioxidant and antiapoptotic agents (Jafari and Elyasi 2021). It has also been found that if other nephrotoxic agents, such as vancomycin or aminoglycosides, are co-administered, the risk of nephrotoxicity is increased (Michalopoulos and Karatza 2010). It is clear that the effects of nephrotoxicity and neurotoxicity are dose-dependent, and with a reduction or discontinuation of treatment, the symptoms become reversible (Ordooei Javan et al. 2015).

4.1.4 Clinical formulations

While polymyxin B is only available in one form as a sulphate salt, there are two forms of colistin available for commercial use. Colistin sulfate which is applied topically (for skin infections), orally (for bowel decontamination) or inhaled (for cystic fibrosis) and colistimethate sodium (also known as colistin methanesulfonate; CMS), a less toxic and potent prodrug given via inhalation or parenterally, which is administered intramuscularly, intravenously, or via nebulisation (Dhariwal and Tullu 2013). Research has shown that when the prodrug form is administered intravenously, the efficacy of colistin is maximised while toxicity is kept to a minimum (Beringer 2001). The inactive prodrug CMS is formed by a sulfomethylation reaction, where colistin is treated with formaldehyde followed by sodium bisulfite, resulting in the

addition of sulfomethyl groups (-CH_2SO_3)- onto the five primary amines on the 2,4-diaminobutyric acid (Dab) residues (**Figure 4.2**) (Wallace et al. 2010; Bialvaei and Samadi Kafil 2015). These five sulfomethyl groups need to be cleaved for active colistin to be released through hydrolysis, which can occur *in vivo,* although this process is often incomplete and often occurs slowly (Bergen et al. 2006).

4.1.5 Application of colistin

4.1.5.1 Animal use

Although the use of colistin for human infection was discontinued for a period, colistin has been continually used as a growth-promoting additive in animal husbandry across the globe, predominantly in Asian countries where it is administered in food, milk or water for poultry, cattle, and swine (Kempf et al. 2016). Colistin as a stand-alone therapy (as well as a combination therapy), is also used to treat and prevent Enterobacteriaceae infections, for which it can be administered orally, as well as intravenously (Nguyen Nhung et al. 2016). However, due to poor absorption in the GI tract, subinhibitory concentrations of colistin may inadvertently result in a selective pressure, and the emergence of resistance. The discovery and inexorable global spread of *mcr-1* led to China in 2016 banning the use of colistin as an animal food-additive, with other countries including Brazil, India, and Thailand following suit (Walsh and Wu 2016; Wang et al. 2020d). This ban means that more than 8000 tonnes of colistin per annum are no longer being used in China. Following this ban, a significant reduction in the incidence of *mcr-1* in animals and humans has been noted in China and across Europe (Fournier et al. 2020; Liu et al. 2020; Shen et al. 2020).

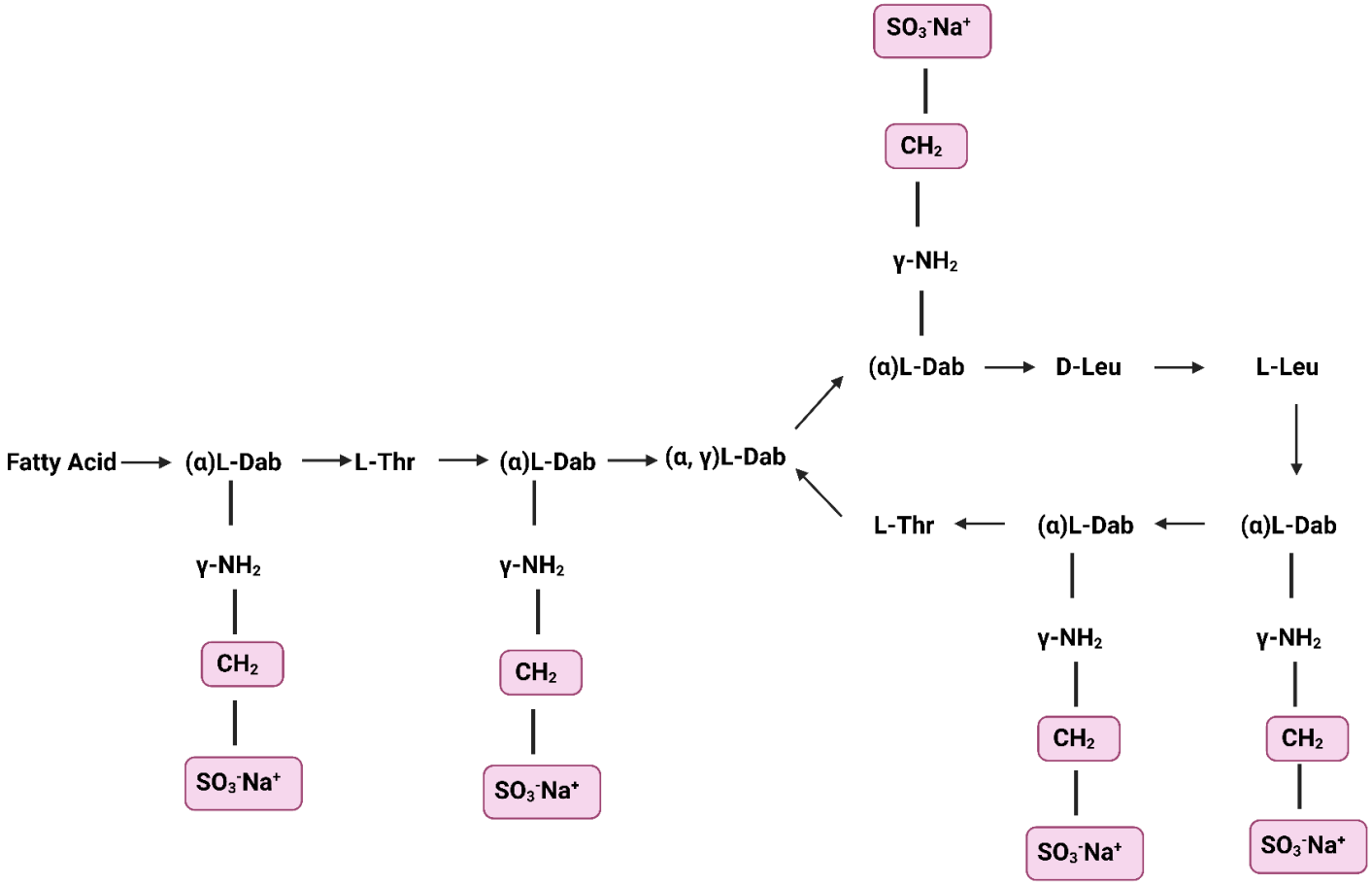

Figure 4.2. Structure of colistimethate sodium (CMS). Fatty acid; 6-methyloctanoic acid for colistin A and 6-methylheptanoic acid for colistin B. Dab; diaminobutyric acid, Thr; threonine, Leu; leucine, Phe; phenylalanine. Sulfomethyl groups are highlighted.

4.1.5.2 Clinical use

In recent years, the use of colistin for humans has been resumed, with it now being considered a 'last resort' antibiotic treatment for multi drug resistant (MDR) infections caused by Gram-negative bacteria, such as *Pseudomonas aeruginosa, Klebsiella pneumoniae and Acinetobacter baumannii,* that are associated with high morbidity and mortality due to limited availability of other effective treatments (**Section 1.3**). Favourable properties of colistin include rapid bacterial killing, a narrow spectrum of activity with activity against most aerobic Gram-negative bacilli that include MDR pathogens, and an associated slow development of resistance (Yahav et al. 2012).

The WHO has reclassified polymyxins as "highest priority critically important antimicrobials", with colistin often now used for cases of ventilator associated pneumonia, sepsis, and for urinary and gastrointestinal tract infections (Loho and Dharmayanti 2015; WHO 2018). The rising incidence of infections involving MDR pathogens means that increasing numbers of patients require colistin treatment. Additionally, the European Medicines Agency (EMA) has classified colistin as a Category B antibiotic to "restrict", and only be considered for treatment when no other antibiotic from a lower risk category "caution" or "prudence" could be used as an alternative (EMA 2019).

4.1.6 Emerging polymyxin resistance

4.1.6.1 Chromosomally mediated resistance

4.1.6.1.1 Efflux pumps

There are five classes of efflux pumps that are associated with antibiotic resistance; ATP-binding cassette (ABC) that uses energy from ATP hydrolysis to

transport ions, and multidrug and toxin extrusion (MATE), small multidrug resistance (SMR), resistance-nodulation-division (RND) and major facilitator superfamily (MFS), that gets energy from proton motive force (Sun et al. 2014).

The presence of efflux pumps, such as AcrAB-TolC in *K. pneumoniae* and *E. coli*, contributes to polymyxin resistance (as well as simultaneously, resistance to other antibiotics), with e.g., MexAB-OprM in *P. aeruginosa* facilitating resistance to β-lactams, chloramphenicol, and tetracycline (Dreier and Ruggerone 2015; Pesingi et al. 2019). Evidence for the influence of efflux is demonstrated in research which has shown that mutations in the multidrug efflux pump subunit, *acrB* gene, results in greater polymyxin susceptibility, compared to the wild type (Padilla et al. 2010). As well as extruding harmful compounds such as antibiotics from the cell, the presence of efflux pumps is also increasingly being associated with biofilm formation, pathogenicity, and virulence which, in turn, involve efflux of quorum sensing (QS) molecules to allow matrix formation, QS regulation and stimulation of aggregation through promotion of cell adhesion (Alav et al. 2018).

4.1.6.1.2 Loss of Lipopolysaccharides (LPS)

A particular phenomenon of polymyxin resistance in *A. baumannii* is the complete loss of lipopolysaccharides (LP) production, including the Lipid A moiety in resistant isolates. Mutations in the *lpxA, C* or *D* genes in the Lipid A biosynthesis pathway resulting in the loss of Lipid A and therefore LPS, (the key initial binding target of colistin), result in high levels of resistance (MIC >128 μg/mL) and showing the importance of colistin-LPS binding for effective treatment (Moffatt et al. 2010; 2011).

4.1.6.1.3 LPS modification

An increasing number of cases of polymyxin resistance in clinical isolates are being identified, arising either via over-expression of efflux pumps or (predominantly), due to LPS-modifications in the OM which is the main target of colistin. The modification of LPS occurs via the PhoP/Q and PmrA/B two-component regulatory system, encoded by the *pmrCAB* and *pmrHFIJKLM* operons **(Figure 4.3;** Chen and Groisman 2013). The *pmrCAB* operon encodes three genes; the sensor kinase *PmrB,* which responds to changes in the environment, such as decreases in concentration of Mg^{2+} and Ca^{2+} and pH; and the response regulators PmrA and PmrC, phosphoethanolamine proteins which transfer phosphoethanolamine (pEtN) to the LPS (Olaitan et al. 2014; Poirel et al. 2017). The *pmrHFIJKLM* operon encodes seven different genes, including *pmrE,* which is involved in LPS modification through 4-amino-4-deoxy-L-arabinose (L-Ara4N) addition causing increased resistance to colistin and resulting in reduced virulence; and *pmrD,* which stabilises phosphorylated PmrA (McPhee et al. 2006; El-Sayed Ahmed et al. 2020).

4.1.6.2.1 Discovery and spread of plasmid-mediated colistin resistance

Antimicrobial resistance genes can be carried on circular extrachromosomal DNA termed plasmids, that can replicate independently within a bacterial cell. Since the 1970's, plasmids have been categorized and grouped according to their incompatibility. Incompatibility (Inc) refers to the inability of plasmids with similar replication and partition systems to be stably propagated within the same host cell line (Thomas 2021). Inc groups have been separately classified in three distinct genera, based on the amino acid sequence of the replication initiation protein. In Enterobacteriaceae, there are 27 Inc groups, while *Pseudomonas* spp. has 14 Inc

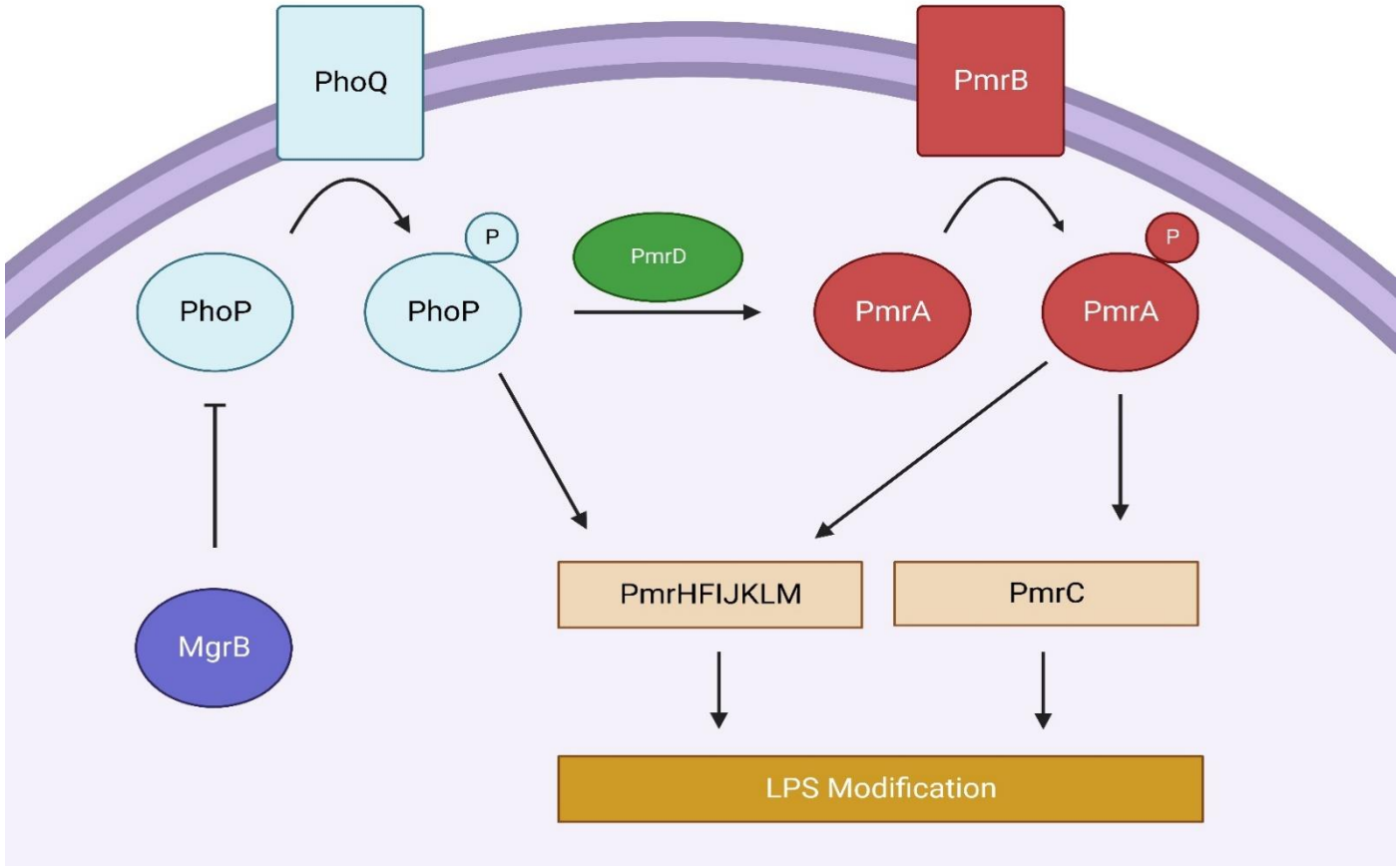

Figure 4.3. LPS modification through the PhoP/Q and PmrA/B two-component system.

groups, and *Staphylococcus* spp. has approximately 18 Inc groups (Shintani et al. 2015).

4.1.6.2 Plasmid-mediated resistance

The first plasmid-mediated colistin resistance gene, *mcr-1*, was isolated in 2015 from *E. coli* strain SHP45, during routine surveillance of AMR isolates in pigs in China (Liu et al. 2016). This *mcr-1* was first isolated on an IncI2-type plasmid and conferred an MIC of 8 μg/mL to colistin and 4 μg/mL to polymyxin. Plasmids from IncI2 groups are often medium sized (~55-80 kb), low copy number and have been shown to carry multiple antibiotic resistance genes, including various β-lactamase genes such as bla_{CTX-M} and is a common carrier of *mcr-1* (Wang et al. 2018; Meinersmann 2019). IncI plasmids are found predominantly in Europe in *E. coli* found in poultry (Rozwandowicz et al. 2018).

The global spread of *mcr-1* since then has been rapid, having now been isolated in Africa, Europe, South and North America and across Asia (Fernandes et al. 2016; El Garch et al. 2017; Meinersmann et al. 2017; Bachiri et al. 2018; Dadashi et al. 2022). Furthermore, *mcr-1* is not limited to *E. coli*, but has been found in other Enterobacteriaceae, such as *Klebsiella pneumoniae* and *Salmonella enterica*, and on multiple plasmid types, with its carriage on IncI2, IncX4 and IncHI2 plasmids accounting for more than 90% of cases, although its carriage on others, such as IncP1, IncY and IncN, are less common (Matamoros et al. 2017; Boueroy et al. 2022). The *mcr-1* plasmid can be transferred by conjugation, with rates of transfer varying between 10^{-1} to 10^{-10}, but with some isolates showing transfer rates as high as 10^{-1} to 10^{-3} (Wang et al. 2017). The conjugation frequency can vary due to multiple factors, such as the incompatibility group, host range, growth phase, cell density,

donor:recipient ratio, temperature, pH, and mating time (Alderliesten et al. 2020). To date, a further ten *mcr* genes (*mcr-1* through *mcr-10*) have been identified (Wang et al. 2020a).

Within two years of *mcr-1* being first described, the third mobile colistin resistance gene, *mcr-3,* was discovered, showing 45.0% and 47.0% nucleotide sequence homology to *mcr-1* and *mcr-2* (Yin et al. 2017). Phylogenetics has suggested MCR-3 is distinct from the MCR-1/-2 family, instead being clustered to MCR-like proteins (phosphoethanolamine transferases), predominantly found in *Aeromonas* spp and has been found to coexist with other *mcr* genes, such as *mcr-1* in MDR pathogens (Hernández et al. 2017; Xu et al. 2018).

The development of pan drug-resistant strains remains a continuing and growing concern, with the coexistence of *mcr-1* and carbapenemase genes (carbapenem degrading enzymes), such as *bla*KPC (*K. pneumoniae* carbapenemase) and *bla*NDM (New Delhi metallo-β-lactamase), being particularly worrying and further compromising the treatment of patients (Du et al. 2016; Yao et al. 2016). Plasmid pWJ1 (~250 kb in size) carrying *mcr-3* has been shown to possess 12 resistance genes in common with plasmid pHNSHP45 (the original isolate *E. coli* SHP45 in which *mcr-1* was first identified), but also resistance to drugs, such as ciprofloxacin (*aac(6')-Ib-cr*), chloramphenicol (*floR*, *cmlA1*, *catB3*), streptomycin (*strA*, *strB*, *aadA1*, *aadA2*), gentamicin (*aac(3)-Iva*), rifampicin (*arr3*), amoxicillin ($bla_{\text{OXA-1}}$), trimethoprim-sulfamethoxazole (*sul1*, *sul2*, *sul3*) and tetracycline (*tetA*) (Yin et al. 2017).

4.1.6.2.2 Mechanism of resistance

The MCR-1 protein is made up of two folded domains, with a transmembrane region at the N-terminal, and a catalytic domain at the C-terminus (Stojanoski et al. 2016). The *mcr-1* gene encodes for a phosphoethanolamine (pEtN) transferase, as do all MCR proteins (Sun et al. 2018). The pEtN moiety is added to the 1' or 4' position phosphate groups of Lipid A present in the bacterial cell membrane, resulting in its modification, conferring resistance to colistin as the overall negative charge of the membrane is reduced (Samantha and Vrielink 2020). This modification of Lipid A results in a lowering of its affinity for polymyxins, reducing its ability to induce the innate immune response, thereby making colistin less effective (Samantha and Vrielink 2020).

4.1.6.2.3 Fitness cost

It has been shown that the presence of *mcr-1* and the modification of lipid A has a fitness cost on the host cell, which results in a lower growth rate of the bacteria carrying the plasmid, as well as reduced cell viability and competitive ability (Yang et al. 2017b). Previous research has shown that the presence of *mcr-1* reduced cell survival when the cells were exposed to high osmotic pressure (compared to *E. coli* without *mcr-1*), due to the *mcr*-induced alteration of membrane permeability. Interestingly, deletion of *mcr-1* was shown to lead to increased resistance to hydrophobic antibiotics, such as gentamicin, kanamycin, and rifampicin, while no change was seen for hydrophilic antibiotics (Li et al. 2020a).

4.1.7 Aims and objectives

The objectives of this study were to firstly characterise and compare the *mcr-1* and *mcr-3* plasmid-carrying colistin resistant *E. coli* strains and then secondly, to investigate treatment of biofilms of these *E. coli* strains with OligoG CF-5/20 by itself, as well as in combination with colistin.

The specific aims for this project were:

- To characterise *mcr* carrying *E. coli* strains by susceptibility testing and growth curves.
- To assess the stability and fitness of *E. coli mcr* strains in a bead biofilm model over time.
- To examine the effect of OligoG CF-5/20 on biofilm disruption of colistin resistant *E. coli*, using selective staining of key biofilm matrix components, using confocal laser scanning microscopy (CLSM) and COMSTAT image analysis.
- To investigate the effect of OligoG CF-5/20 in combination with colistin on biofilm disruption in colistin resistant *E. coli*, using CLSM and COMSTAT analysis.

4.2 Materials and methods

4.2.1 Microbial strains and media used in this study

Laboratory strain, *E. coli* J53, was selected as the recipient host strain for the *mcr* plasmids as it is colistin-sensitive (COL^{sens}) and plasmid-free (**Table 4.1**). Transconjugants of *E. coli* J53 carrying either an *mcr-1* (pE30) plasmid or an *mcr-3* (pWJ1) plasmid had previously been generated from E30 (*mcr-1.1*) and WJ1 (*mcr-3.1*), respectively (Yang et al. 2020). Both plasmids were designated IncHI2 (**Table 4.2**). All strains were provided courtesy of Dr. Brad Spiller from the Division of Infection and Immunity, Cardiff University.

J53 was maintained on LB agar and grown in LB broth for liquid culture. All *E. coli mcr* strains were cultured on LB agar or broth containing 1 μg/mL colistin to ensure maintenance of the plasmid. Overnight cell suspensions were adjusted with MH broth to an optical density (OD_{600}) ranging between 0.08 to 0.1, unless otherwise stated. Colistin sulphate (Sigma-Aldrich) was prepared in sterile distilled water (dH_2O) to a stock concentration of 1 mg/mL. Stocks were filter-sterilised using a 0.2 μm hydrophilic polyethersulfone membrane filter (Sigma-Aldrich), before use.

4.2.2 Minimum inhibitory concentration (MIC) assay

Two-fold serial dilutions of colistin were prepared in MH broth in a sterile flat-bottomed 96-well microtiter plate (100 μL/well) ± colistin, with a starting concentration of 64 μg/mL. Overnight broth cultures of *E. coli* were adjusted in sterile phosphate buffered saline (PBS) to an optical density (OD_{600}) between 0.08-0.1 before being further diluted 1:10 in MH broth. A 5 μL inoculum of the adjusted cultures was then added to each well, resulting in a final bacterial cell concentration of ~$5x10^5$ cfu/mL. Plates were wrapped in parafilm and incubated statically for 16-20 h at 37 °C

Table 4.1. *E. coli* strains described in this study, their source, country of origin and information related to their *mcr* plasmids.

Name	Country of Origin	Source	MLST group	Phylogenetic Type	*mcr* Plasmid	Reference
J53*	USA	Laboratory Strain	10	A		Jacoby and Han 1996
E30	China	Swine	48	A	IncHI2/IncHIA [ST3]/(252 729 bp)	Li 2023
WJ1	China	Swine Faeces	1642	B1	IncHI2/IncHIA [ST3]/(247 821 bp)	Yin et al. 2017

MLST, Multilocus sequence type; ST; sequence type.
*Laboratory mutant of *E. coli* K-12 resistant to sodium azide

Table 4.2. *E. coli* J53 transconjugant strains used in this study with information about donors, recipients and plasmid carrying *mcr* genes.

Transconjugant Strain	Donor	Recipient	Gene Transferred	Plasmid Size	Reference
J53(pE30)	E30	J53	*mcr-1.1*	252,729 bp	Yang et al. 2020
J53(pWJ1)	WJ1	J53	*mcr-3.1*	247,821 bp	Yang et al. 2020

Bp; base pairs.

(n=3). The MIC values were determined as the modal value of the lowest concentration at which there was no visible growth. When reading the plate, 30 μL of resazurin (prepared at 0.01% in sterile dH_2O), was added to each well to confirm the MIC value read by eye. A blue colour indicated no bacterial growth, while a pink colouration was indicative of growth. A significant difference between two MIC values was accepted, if they differed by at least a two-fold change.

4.2.3 Minimum biofilm eradication concentration (MBEC) assay

Adjusted culture inoculum as described above (100 μL/well) was added to the wells of a sterile, flat-bottomed 96-well microtiter plate, and biofilms were grown for 24 h at 37 °C with 30 rpm rocking. In a fresh 96-well plate, two-fold serial dilutions of colistin were prepared in MH broth ± colistin with a starting concentration of 4096 μg/mL. Following incubation, biofilms were washed once gently with PBS and then colistin from the serial dilution plate (100 μL/well) was transferred into the plate containing biofilms, which was then incubated for a further 24 h (37 °C, 30 rpm). After incubation, the supernatant was removed from the wells and replaced with MH broth before reincubation for 24 h (37 °C, 30 rpm) to study biofilm regrowth. To assess the MBEC value, 30 μL of resazurin (0.01% in dH_2O) was added to each well, before visually reading the result in the same manner as the MIC assay (**Section 4.2.2**).

4.2.4 Bacterial growth curve analysis

The growth curves of all *E. coli* strains were performed in a sterile, flat-bottomed 96-well microtiter plate. Overnight broth cultures of the five *E. coli* strains were adjusted to OD_{600} 0.08-0.1 in LB broth. Then, 5 μL of adjusted overnight culture was added to each well, which contained 200 μL LB broth ± 1 μg/mL colistin. Plates were wrapped in parafilm, and absorbance read hourly at OD_{600} over 96 h at 37 °C

using a FLUOstar Omega plate reader (BMG Labtech). Experiments were conducted in triplicate and results presented as mean values (n=3). The minimum significant difference (MSD) was calculated using the Tukey-Kramer method, using Minitab 17.2.1 (Minitab Inc, State College, PA, USA).

4.2.5 Evolutionary bead biofilm model

A bead model adapted from a previous study (Oakley et al. 2021), was used to study the stability of colistin resistance (with and without selection) encoded by *mcr-1* and *mcr-3* genes over time, following serial passage of bacterial biofilms grown on the beads, as seen in **Figure 4.4**. Biofilms were grown on beads (7 mm diameter glass beads without holes; John F Allen & Sons Inc.) with blue or red beads (used for alternate transfer days) placed in each well of a sterile flat bottomed 24-well microtiter plate with 1.5 mL broth. Plates were incubated continuously at 37 °C (20 rpm rocking), allowing biofilms to grow on the bead surface. Plates were sampled every 48 h, before transferring a single "biofilm coated" bead into fresh medium in a new plate.

On day 1, two beads (one red, one blue) were placed in each well. To this, 1.5 mL of overnight inoculum of *E. coli* J53, J53(pE30), or J53(pWJ1) which had been adjusted to an optical density (OD_{600}) of 5 x 10^4 cfu/mL using LB broth ± 0.125 or 1 μg/mL colistin (n=4 for each condition) was also added. After 48 h incubation, one bead (red) was transferred using sterile tweezers into the same corresponding well of a fresh 24-well microtiter plate, which contained a sterile bead (blue) and 1.5 mL sterile LB broth ± colistin. On transfer days, the remaining supernatant was removed, and "old" bead was extracted and vortexed for 2 mins in 1.5 mL of fresh LB broth

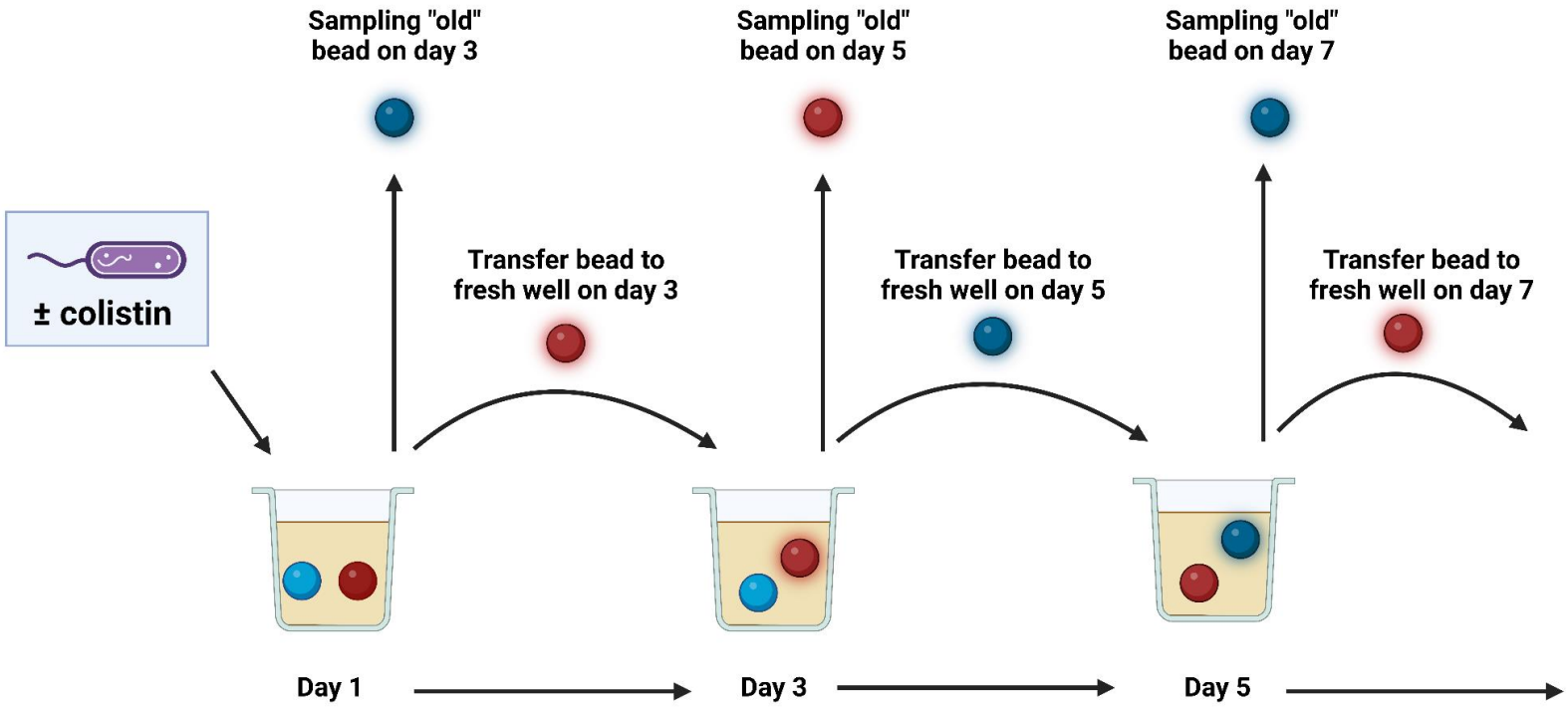

Figure 4.4. Schematic of the evolutionary bead biofilm model. On day 1, a 24-well plate with two sterile glass beads (one red, one blue) was inoculated with *E. coli* J53, J53(pE30) or J53(pWJ1) in 1.5 mL LB broth ± 0.125 or 1 μg/mL colistin per well (n=4). Every 48 h, one of the 'biofilm coated' beads was transferred into a fresh 24-well plate containing a new sterile bead and fresh LB broth ± colistin. The remaining biofilm on the 'old' bead and the supernatant were 'sampled' and frozen until required.

to remove bacteria (Poltak and Cooper 2011). All samples were stored in a 2 mL screw-cap microcentrifuge tubes at -80 °C for future use. Each plate contained sterility control wells containing LB broth alone. This sampling process continued every 2 days for 31 days. The bead culture model was completed with Jingxiang Wu, who assisted in maintaining and sampling the model.

4.2.6 Real-time quantitative polymerase chain reaction (RT-qPCR)

Absolute quantification of *mcr-1* and *mcr-3* in the bead biofilm and supernatant samples was assessed using RT-qPCR. The RT-qPCR mastermix was made up of 1 mL SsoAdvanced Universal Probe Supermix (Bio-Rad), 40 µL of *mcr-1, mcr-3* and *rpoB* probes (10 pmol/µL stock concentration prepared in 1X TE buffer and diluted in MilliQ water), with FAM, ROX, and HEX fluorophores attached, respectively, (Sigma Aldrich); and 40 µL of both forward and reverse *mcr-1, mcr-3* and *rpoB* primers (10 pmol/µL stock concentration prepared in MilliQ water, ThermoFisher Scientific, **Table 4.3**). In a white hard shell 96-well plate (Bio-Rad), the final RT-qPCR reaction (20 µL/well) consisting of 5 µL of mastermix and 5 µL bead biofilm model sample (from -80 °C stocks), were made up to volume with Milli-Q water. RT-qPCR was performed on a CFX96 PCR system (Bio-Rad), with the following conditions: an initial denaturing step at 95 °C for 5 mins, then denaturing for 44 cycles at 95 °C for 15 s, annealing/extension at 60 °C for 15 s (when using dual labelled probes [DLP], extension at 60 °C is acceptable, due to sufficient activity of the DNA polymerase at this temperature).

GenScript Custom Gene Synthesis (GenScript Biotech, New Jersey, USA) was used to construct a copy number standard for the standard curve (Dr. Qiu E Yang,

Table 4.3. Primers and probe sequences used to identify *rpoB, mcr-1* and *mcr-3* genes in RT-qPCR.

Gene		Sequence (5'-3')	Reference
rpoB	Forward Primer	AAGCTGCTTTCCGTTCCGTA	B. Spiller, personal communication
	Reverse Primer	CGCCACGGATTTGACATTCC	
	Probe	**HEX**- ATACGTCAGCTACCGCCTTG -**BHQ1**	
mcr-1	Forward Primer	TGGCGTTCAGCAGTCATTAT	Irrgang et al. 2016
	Reverse Primer	AGCTTACCCACCGAGTAGAT	Irrgang et al. 2016
	Probe	**FAM**[a] -AGTTTCTTTCGCGTGCATAAGCCG-**BHQ1**[a]	Adapted from Irrgang et al. 2016
mcr-3	Forward Primer	CGTGTTCCTATGCAGGTGTG	Yang et al. 2020
	Reverse Primer	CGAGTATCAGCGGCTTTCTG	
	Probe	**ROX**[a] -TGCAAACACGCCATATCAACGCCT-**BHQ2**[a]	Adapted from Yang et al. 2020

[a]The indicated fluorophores on the original probes have been adapted as shown for this study.

personal communication). For this, a 695 bp insertion carrying *mcr-1* (120 bp), *mcr-3* (150 bp), *rpoB* (200 bp) and bla_{NDM} (125 bp) targets (derived from qPCR products), separated by 25 bp adaptor sequences (GenScript Biotech), was cloned into the cloning vector pUC57 plasmid (2710 bp). The resulting DNA amount was determined to be 36.8 pg, (~10^7 copies, as calculated using the website: http://cels.uri.edu/gsc/cndna.html). The housekeeping *rpoB* gene (encoding the β subunit of RNA polymerase), was used as a positive control for levels of expression. The abundance of each *mcr* gene was determined by comparing their absolute copy numbers to that of *rpoB*, and the results were expressed as the copy number per cell.

4.2.7 Confocal laser scanning microscopy (CLSM)

4.2.7.1 Biofilm disruption assay

Broth cultures of *E. coli* J53, J53(pE30) and J53(pWJ1) were adjusted using MH broth to an optical density of OD_{600} 0.05, before being added to a sterile glass-bottomed 96-well plate with MH broth, in a 1:10 ratio (100 µL/well) and incubated for 24 h (37 ^{o}C, 30 rpm), allowing biofilms to form. The biofilms were then disrupted as described below, (**Sections 4.2.7.2** and **4.2.7.3**).

4.2.7.2 Selective staining of matrix EPS components

4.2.7.2.1 Effect of OligoG CF-5/20 treatment

After incubation of *E. coli* J53, J53(pE30) and J53(pWJ1) biofilms, half of the well supernatant volume was removed and replaced with fresh MH broth ± OligoG (0.5, 2, or 6%) and the plate was re-incubated for a further 24 h (37^{o}C, 30 rpm). After incubation, all the supernatant was gently removed from wells, and biofilms were stained firstly with 50 µL of 1 mg/mL stock concentration calcofluor white M2R

(fluorescent brightener 28 disodium salt solution, prepared in PBS; Sigma Aldrich) for 30 mins. The stain was then removed, before film tracer SYPRO ruby protein stain (50 µL of 1X concentration; ThermoFisher Scientific) was added for 1 h. The plate was washed once with PBS, before adding SYTO-9 stain (4 µL of 10 µM concentration prepared in PBS; ThermoFisher Scientific), dropwise and staining for 10 mins. The plate was washed once with PBS and a final 50 µL of PBS was added to prevent the biofilms from drying out, before imaging by CLSM.

4.2.7.2.2 Effect of OligoG CF-5/20 and colistin treatments

After incubation of *E. coli* J53, half of the supernatant volume was removed and replaced with fresh MH broth ± OligoG (0.5%) ± colistin (32 µg/mL) and the plate was re-incubated for a further 24 h (37 °C, 30 rpm). After incubation, the supernatant was carefully removed from wells, and biofilms were stained with calcofluor white, SYPRO ruby and SYTO-9, as described above in **4.2.7.2.1**. The plate was washed once with PBS and a final 50 µL PBS was added to prevent the biofilms from drying out, before imaging by CLSM.

4.2.7.3 LIVE/DEAD® staining

After incubation of *E. coli* J53, J53(pE30) and J53(pWJ1) biofilms, half of the well supernatant volume was removed and replaced with fresh MH broth ± OligoG (0.5%) ± colistin (32 µg/mL), and the plate was re-incubated for a further 24 h (37 ^{o}C, 30 rpm). After incubation, all the supernatant was gently removed from wells, and biofilms were stained with 4 µL of LIVE/DEAD® stain (2 µL of component A SYTO-9 and 2 µL of component B propidium iodide, in 1 mL PBS) for 10 mins covered in foil to prevent exposure to light. A further 46 µL of PBS was added to prevent the biofilms desiccation, prior to CLSM imaging.

4.2.7.4 COMSTAT image analysis

CSLM experiments were performed in triplicate with five Z-stack images taken of each sample (n=3 samples), using a Leica SP5 CLSM on x63 magnification oil lens with a resolution of 512 x 512, zoom x1 (**Section 4.2.7.2.1**) or x2 (**Section 4.2.7.2.2 and 4.2.7.3). A** line average of 1, step size of 0.69 µm and step number 90 was taken. Las-X software was used for exporting images, as well as processing data. CLSM z-stack images were analysed using COMSTAT software for quantification of the 3D biofilm structure (biomass volume, thickness, surface roughness and LIVE/DEAD® biomass ratio) (Heydorn et al. 2000AMR).

4.2.8 Statistical analysis

GraphPad Prism® was used for all data analysis. Any outliers were identified and removed by the robust regression and outlier removal (ROUT) method, with the Q coefficient set to between 1-10%. One-way analysis of variance (ANOVA) test was used to calculate any significant changes between treatments (n>2), followed by the Dunnett's multiple comparisons test.

4.3 Results

4.3.1 Antibacterial effect of colistin against *E. coli* strains

After incubation, the MIC values were read visually and then confirmed with the addition of resazurin (**Table 4.4**). The MIC value for the colistin sensitive strain *E. coli* J53 was 0.25 μg/mL, while the MICs for all the other strains tested were 8 μg/mL regardless of which *mcr* gene was carried. The MBEC values measuring antimicrobial treatment of cells in a biofilm mode of growth (as opposed to the MIC in which the bacteria are in a planktonic state), demonstrated slightly higher values for the *mcr-1.1* carrying strains (128 μg/mL), a two-fold increase compared to the wild-type (WJ1) and a three-fold increase compared to the *mcr-3.1* transconjugant J53(pWJ1).

Table 4.4. Minimum inhibitory concentration (MIC) and minimum biofilm eradication concentration (MBEC) determinations of colistin against the *E. coli* strains used in this study (μg/mL).

	***E. coli* strains**				
		mcr-1.1		*mcr-3.1*	
	J53	**E30**	**J53(pE30)**	**WJ1**	**J53(pWJ1)**
MIC	0.25	8	8	8	8
MBEC	32	128	128	64	32

4.3.2 Effect of colistin on planktonic growth of *E. coli* strains

The growth kinetics of the wild-type and transconjugant *mcr*-carrying strains were compared using bacterial growth curves. When *E. coli* J53 transconjugant strains were grown in the presence and absence of 1 µg/mL colistin for 96 h, it was apparent that the *mcr-1* and *mcr-3* carrying strains displayed consistently lower fitness/growth rates (between 8-96 h), compared to that of the plasmid-free J53 (**Figure 4.5**). However, only the wild-type *mcr-1* strain E30 (with and without colistin treatment), showed a significant decrease in growth compared to the J53 control (MSD=0.268). There was also a difference between carriage of *mcr-1* or *mcr-3*, with strains carrying *mcr-1* (E30 and J53[pE30]), generally also showing significantly lower growth rates than those carrying *mcr-3* (WJ1 and J53[pWJ1]), both in the presence and absence of colistin. This suggests that there was a fitness cost to carriage of *mcr* affecting both cell viability and growth, with *mcr-1* having a greater cost than *mcr-3*.

4.3.3 Evolutionary pressures of *mcr* carrying *E. coli* strains

Supernatant and biofilm samples from *E. coli* J53(pE30) and J53(pWJ1) grown in the evolutionary bead biofilm model were analysed by RT-qPCR to measure the relative levels of the house-keeping gene *rpoB*, and the colistin resistance genes *mcr-1* and *mcr-3* present. Levels of all three genes were measured in both biofilm samples (taken from the "spent bead") (**Figure 4.6**), as well as in planktonic samples from the supernatant (**Figure 4.7**) from the same experiment with the absolute copy number/cell calculated from the standard curve.

The *mcr-1* gene was seen to be lost at day 23, when grown in the absence of colistin in both supernatant and biofilm samples, while in the presence of colistin

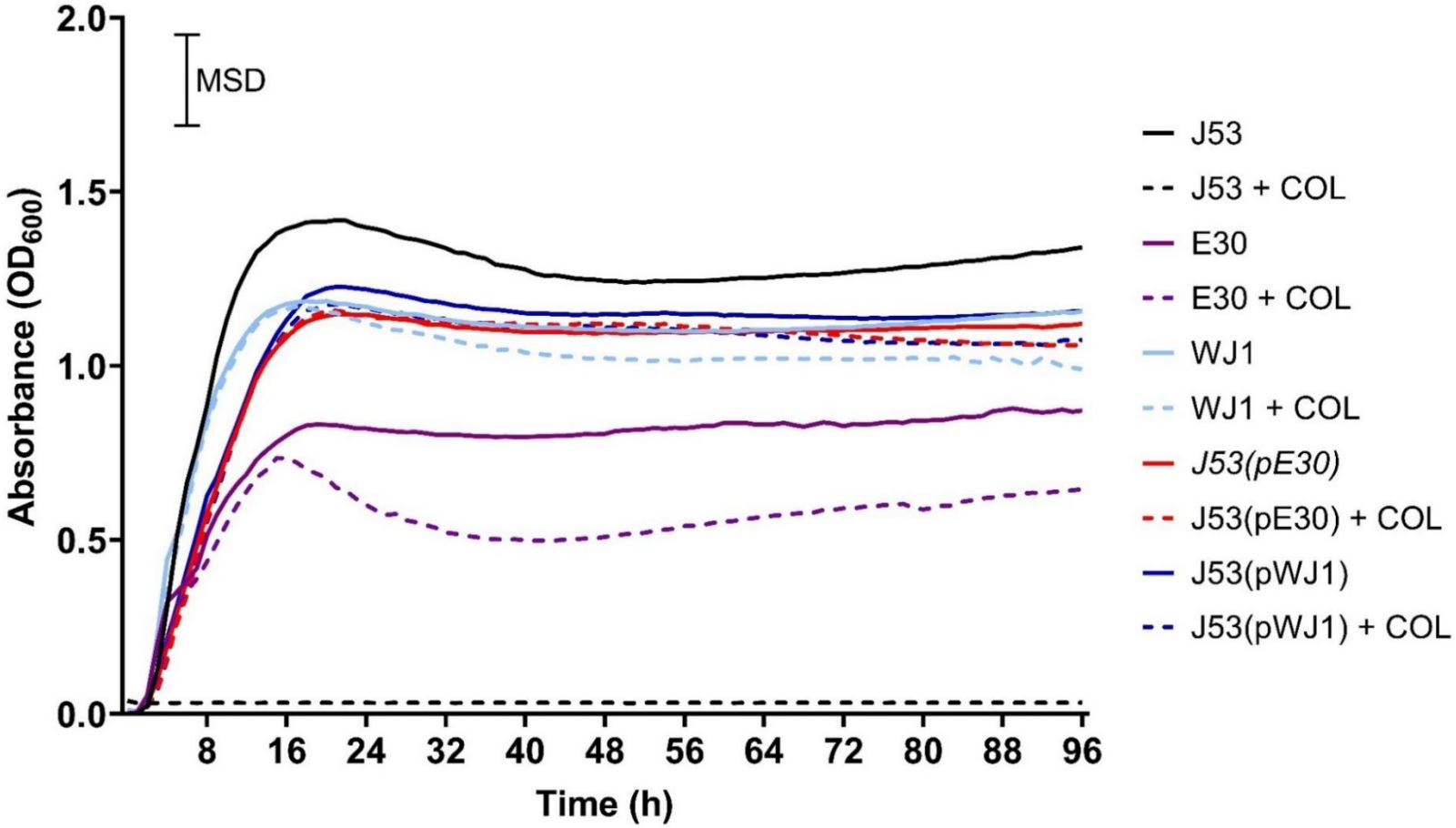

Figure 4.5. Growth curves of *E. coli* J53, E30, WJ1, J53(pE30) and J53(pWJ1) ± 1 µg/mL colistin (COL) for 96 h (n=3). Minimum significant difference (MSD) for absorbance was calculated in MiniTab, using the Tukey-Kramer method: 0.268.

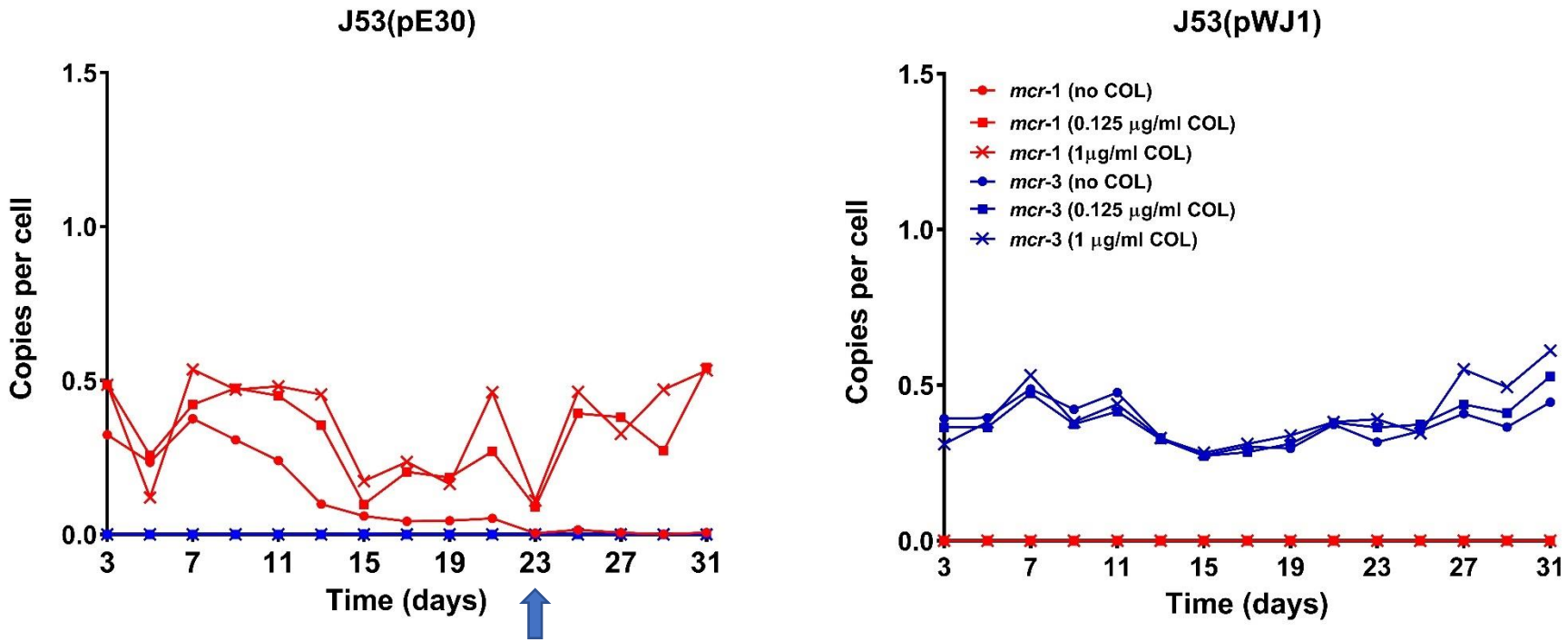

Figure 4.6. Biofilm samples: Copies per cell of *mcr*-1 and *mcr*-3 genes in *E. coli* J53(pE30) *mcr-1.1* and J53(pWJ1) *mcr-3.1* biofilms, taken from the evolutionary bead biofilm model sampled every 48 h over 31 days ± 0.125 or 1 μg/mL colistin. Blue arrow indicates apparent loss of plasmid/colistin resistance.

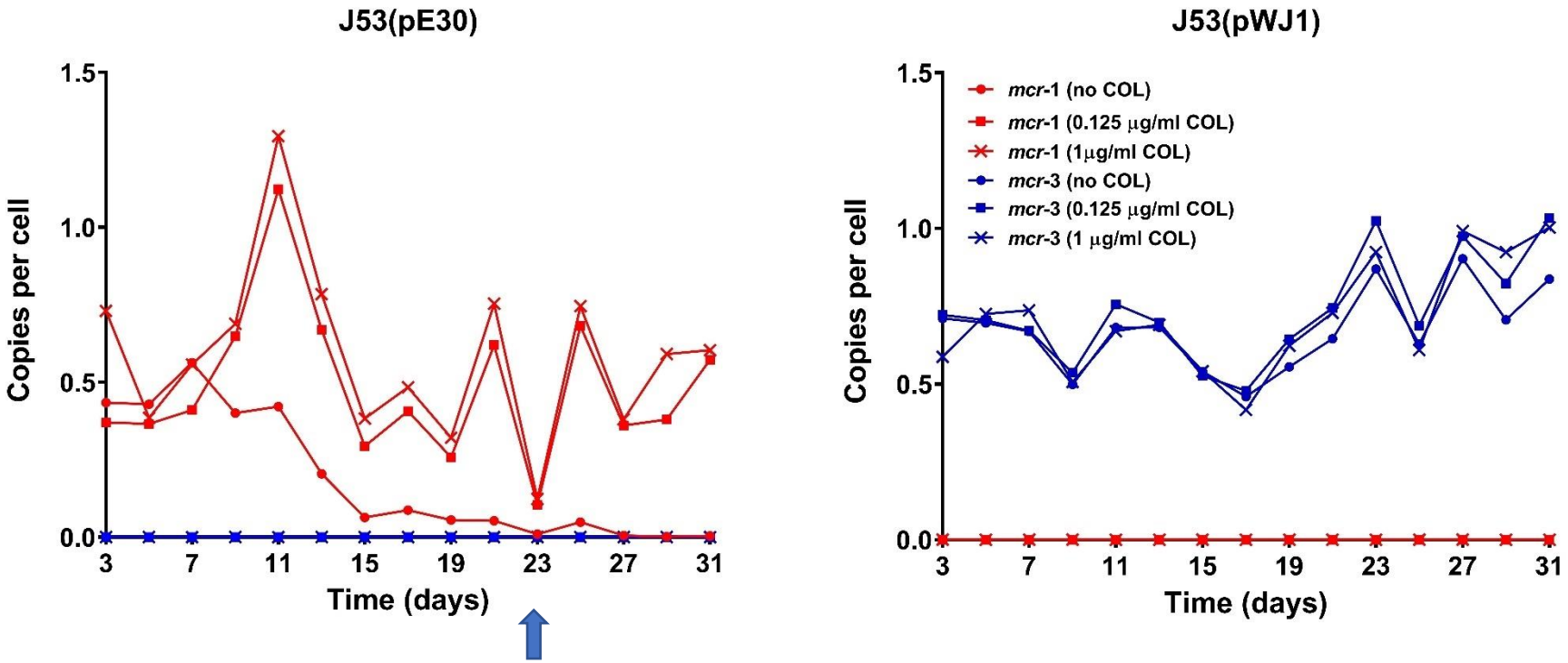

Figure 4.7. Supernatant samples: Copies per cell of *mcr*-1 and *mcr*-3 gene in *E. coli* J53(pE30) *mcr-1.1* and J53(pWJ1) *mcr-3.1* taken from the evolutionary bead model supernatant sampled every 48 h over 31 days ± 0.125 or 1 μg/mL colistin. Blue arrow indicates apparent loss of plasmid/colistin resistance.

(0.125 and 1 µg/mL) *mcr-1* carriage was maintained. In contrast, *mcr-3* remained present after day 31 of the study, in both the presence and absence of colistin selection. The supernatant sample results generally mimicked those of the biofilm samples, although counts were slightly higher overall (≤1.3 copies per cell, compared to ≤0.6 respectively).

4.3.4 EPS matrix composition of *mcr* carrying *E. coli* strains

To visualise key components of bacterial biofilms, a number of staining protocols were developed using a triple-stain cocktail. The staining of untreated *E. coli* J53, J53(pE30) and J53(pWJ1) biofilms using calcofluor white (to stain β-polysaccharides), SYPRO ruby (to stain proteins) and SYTO-9 (to stain nucleic acids) are shown in **Figure 4.8A**. The CLSM images showed much brighter levels of staining on *E. coli* J53 strain for all three stains, the COMSTAT analysis (**Figure 4.8B to D**) showed that for both *mcr* carrying *E. coli* (J53(pE30) and J53(pWJ1), biofilm biovolume was significantly less in comparison to *E. coli* J53, with the biofilm thickness of J53(pWJ1) also lower and biofilm roughness significantly higher than controls. Although there were slight differences between J53(pE30) and J53(pWJ1) for all 3 parameters tested, these were not significant ($P > 0.05$).

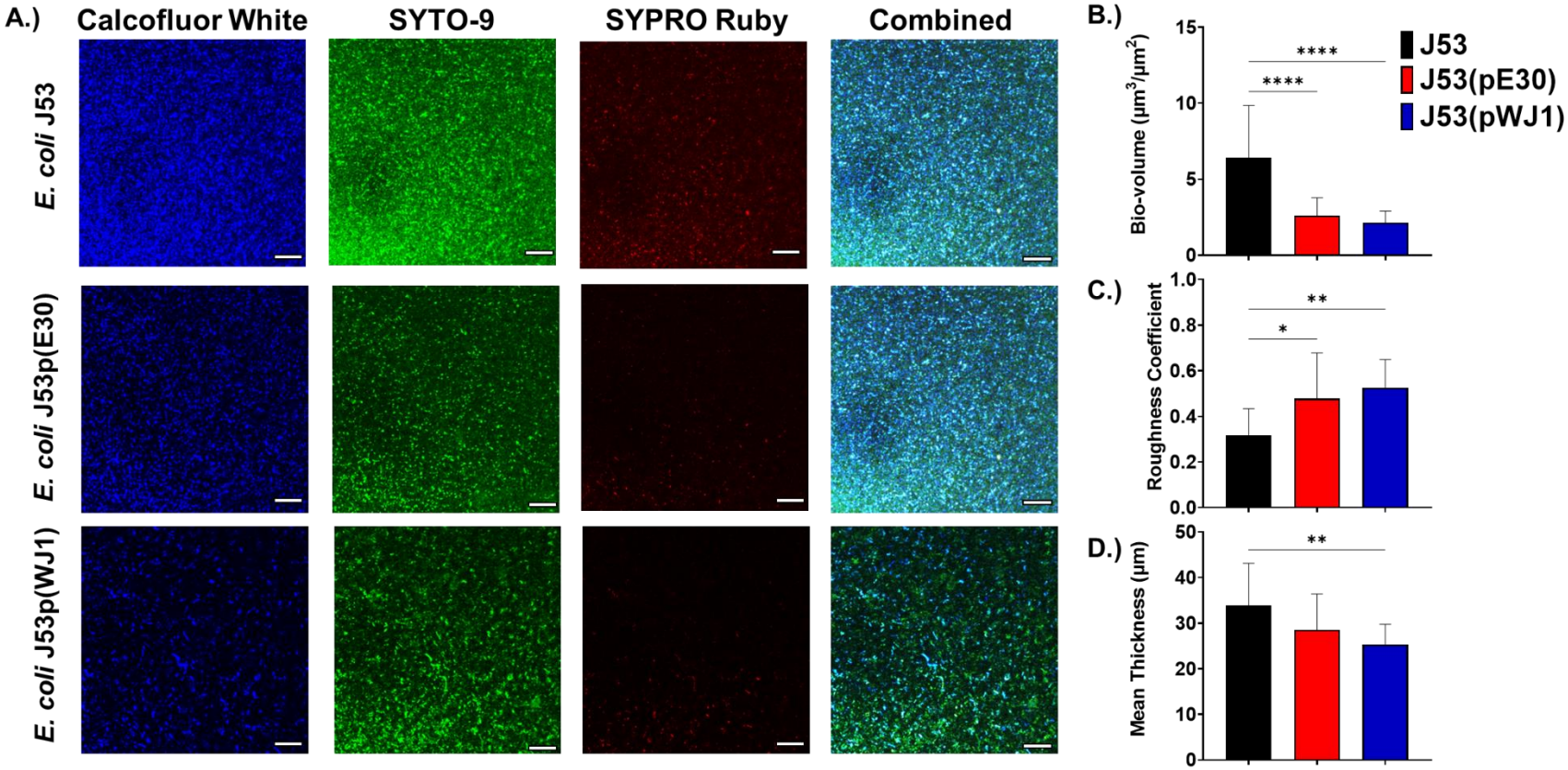

Figure 4.8. (A) CLSM Z-stack imaging of untreated 48 h *E. coli* J53*,* J53(pE30*)* and J53(pWJ1) biofilms, stained with calcofluor white (targeting polysaccharides), SYTO-9 (targeting nucleic acids) and SYPRO ruby (targeting proteins). Biofilms were grown for 24 h, before replacing the growth medium and growing the biofilms for a further 24 h. Scale bar = 30 µm. COMSTAT image analysis showing **(B)** biofilm bio-volume ($\mu m^3/\mu m^2$), **(C)** roughness coefficient, and **(D)** mean thickness (µm) ± S.D; n=3 biological repeats; n=5 technical repeats. Group wise comparisons were analysed using one-way ANOVA, followed by Dunnett's post hoc tests; *P<0.05; **P<0.01; ***P<0.001; ****P<0.0001 denotes significance.

4.3.5 Effect of OligoG CF-5/20 treatment on *E. coli* biofilm disruption

Further CLSM imaging of *E. coli* J53, J53(pE30) and J53(pWJ1) biofilms treated with OligoG CF-5/20 (0.5, 2 and 6%), was performed in a biofilm disruption assay. Staining with calcofluor white is seen in **Figure 4.9** with respective COMSTAT analysis (**Figure 4.10**). Biofilms treated with 0.5% OligoG were shown to significantly reduce the mean thickness of *E. coli* J53 and J53(pE30), while significantly increasing the roughness of the biofilms. In *E. coli* J53, this 0.5% OligoG treatment also significantly reduced the biovolume. In contrast, biofilms treated with 6% OligoG showed significantly higher biovolume for all three strains, and with significantly increased biofilm thickness and reduced roughness coefficient for both *E. coli* J53(pE30) and J53(pWJ1). However, this is likely to be due to non-specific staining of calcofluor white with OligoG, so only 0.5 and 2% OligoG treatment concentrations were utilised in subsequent experiments.

Staining with SYTO-9 is seen in **Figure 4.11** and its respective COMSTAT analysis in **Figure 4.12**. Biofilms treated with 0.5% OligoG were shown to significantly reduce the biovolume of *E. coli* J53, while also increasing the roughness coefficient. Furthermore, 2% OligoG also showed similar effects, namely reduced biofilm biovolume, mean thickness and increased surface roughness, although the results here were not significant. In contrast, *E. coli* J53(pE30) and J53(pWJ1) when treated with either 0.5% or 2% OligoG showed no significant effects, compared to the untreated control. Similarly, SYPRO ruby staining (**Figure 4.13**) and associated COMSTAT analysis (**Figure 4.14**) showed similar findings. However again, only 0.5% treatment showed significant reductions in the biovolume and mean thickness of *E. coli* J53 biofilms, and a significant increase in surface roughness. Although *E. coli*

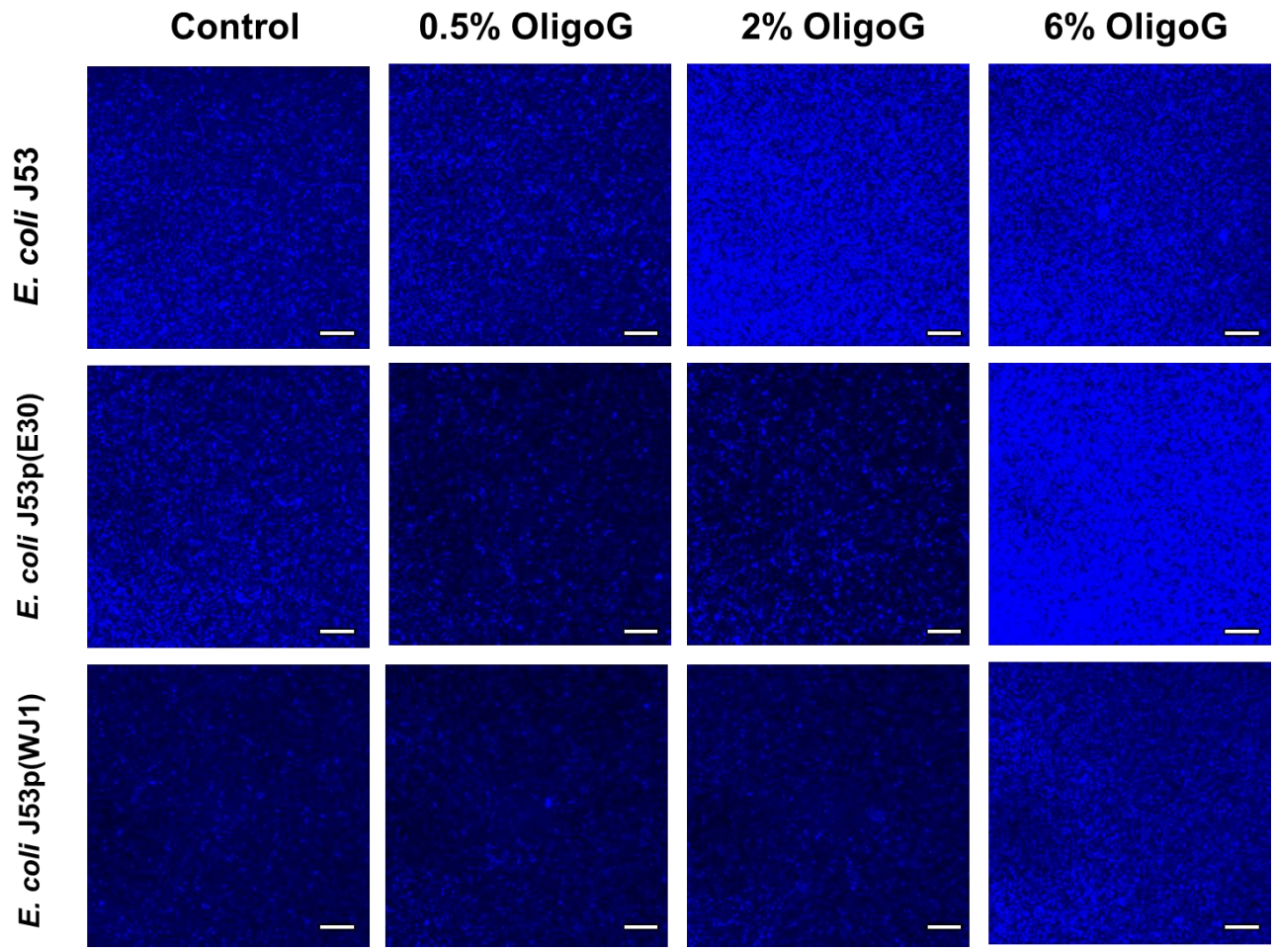

Figure 4.9. Biofilm disruption assay showing CLSM Z-stack imaging of OligoG CF-5/20 treated *E. coli* J53, J53(pE30), and J53(pWJ1) biofilms, with calcofluor white (targeting polysaccharides) staining. Biofilms were grown for 24 h, before a 24 h treatment ± OligoG CF-5/20 (0.5, 2 and 6%); Scale bar = 30 μm.

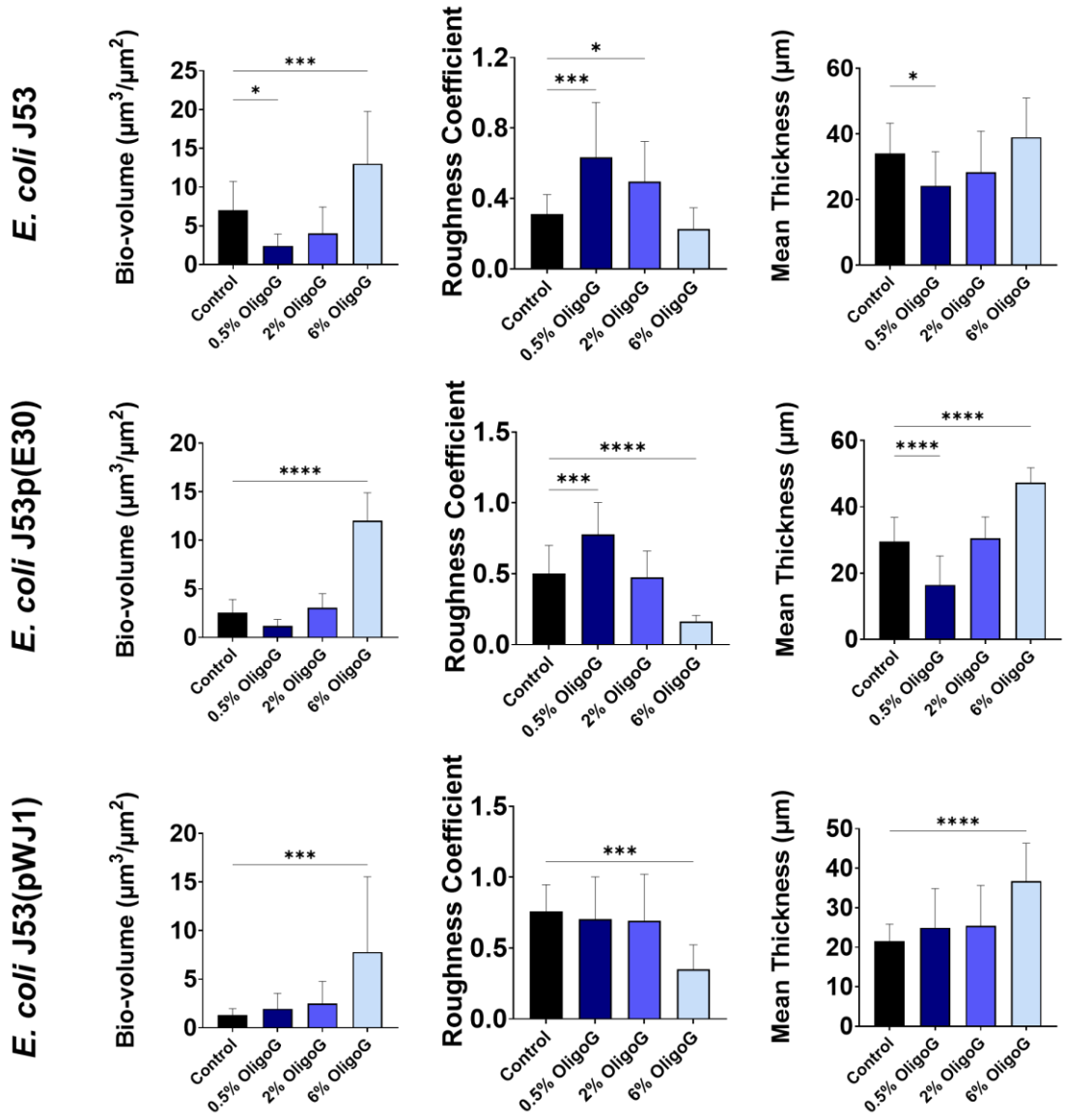

Figure 4.10. COMSTAT image analysis of *E. coli* J53, J53(E30) and J53(pWJ1), treated with OligoG (0.5, 2, or 6%) and stained with calcofluor white (as seen in **Figure 4.9**), showing biofilm bio-volume ($\mu m^3/\mu m^2$), roughness coefficient, and mean thickness (µm) ± S.D; n=3 biological repeats; n=5 technical repeats. Group wise comparisons were analysed using one-way ANOVA, followed by Dunnett's post hoc tests; *P<0.05; **P<0.01; ***P<0.001; ****P<0.0001 denotes significance.

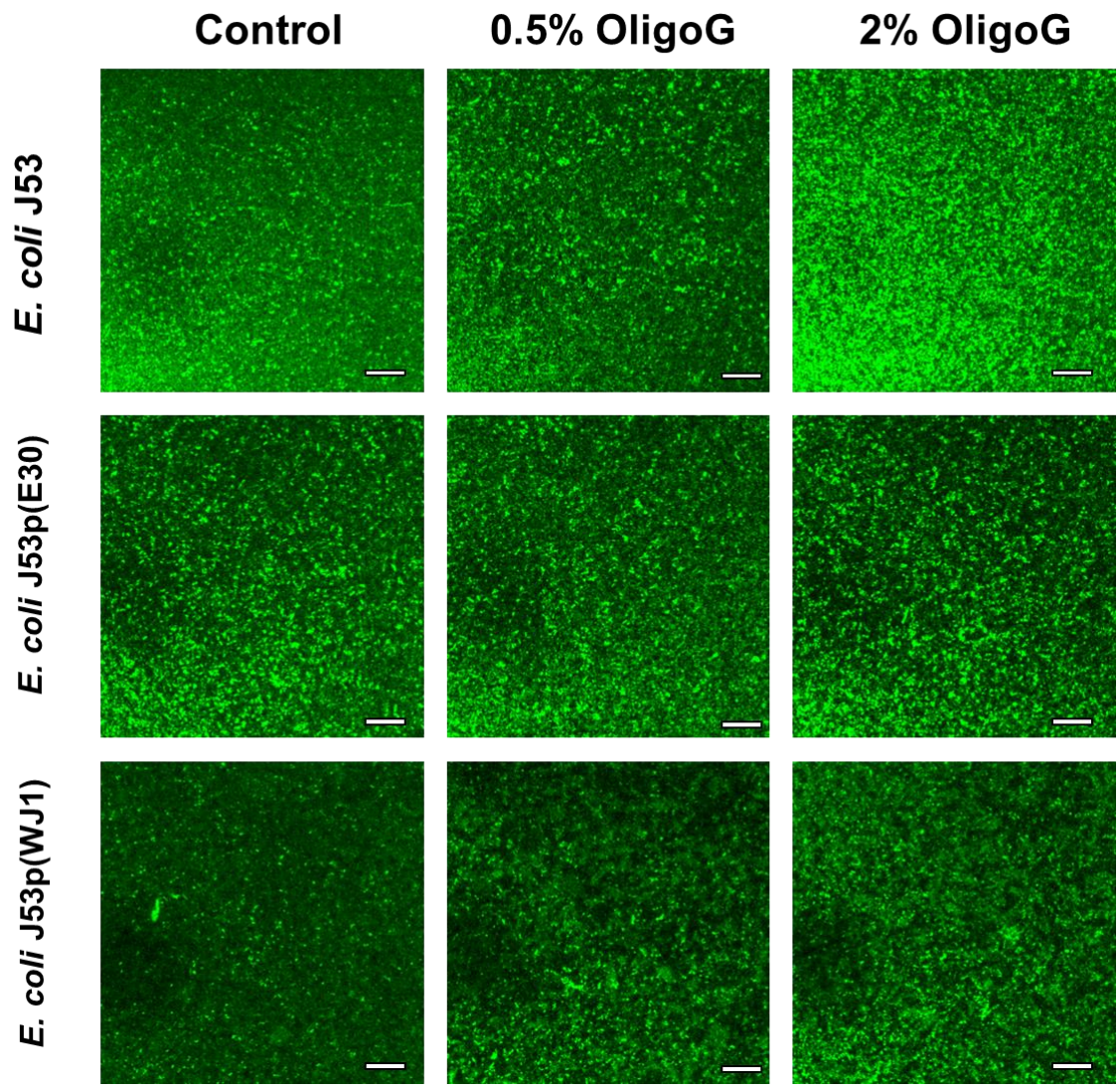

Figure 4.11. Biofilm disruption assay showing CLSM Z-stack imaging of OligoG CF-5/20 treated *E. coli* J53, J53(pE30), and J53(pWJ1) biofilms, with SYTO-9 staining (targeting nucleic acids). Biofilms were grown for 24 h, before a 24 h treatment ± OligoG CF-5/20 (0.5 or 2%); Scale bar = 30 μm.

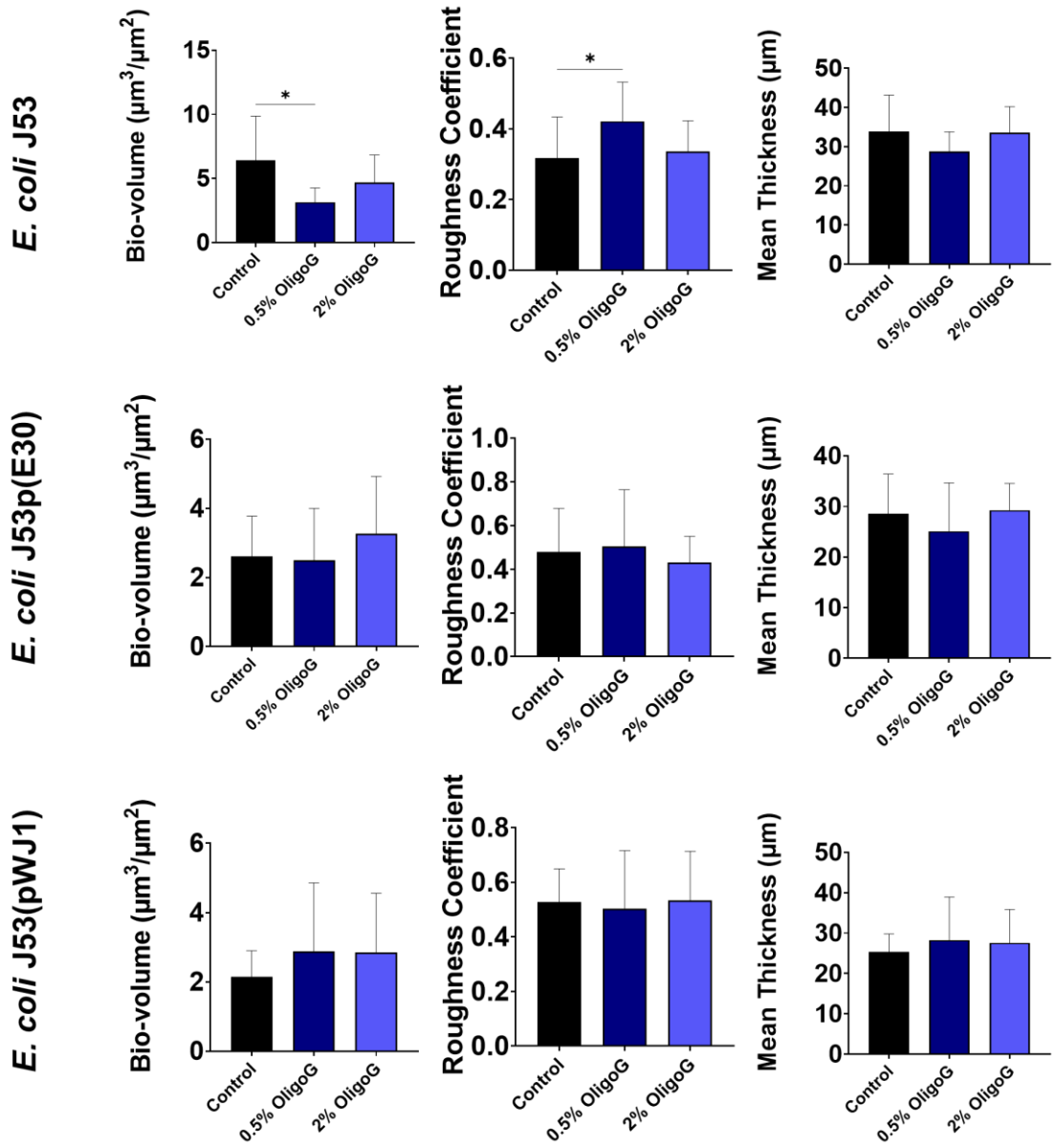

Figure 4.12. COMSTAT image analysis of *E. coli* J53, J53(E30) and J53(pWJ1) treated with OligoG (0.5 or 2%) and stained with SYTO-9 (as seen in **Figure 4.11**), showing biofilm bio-volume ($\mu m^3/\mu m^2$), roughness coefficient, and mean thickness (µm) ± S.D; n=3 biological repeats; n=5 technical repeats. Group wise comparisons were analysed using one-way ANOVA followed by Dunnett's post hoc tests; *P<0.05; **P<0.01; ***P<0.001; ****P<0.0001 denotes significance.

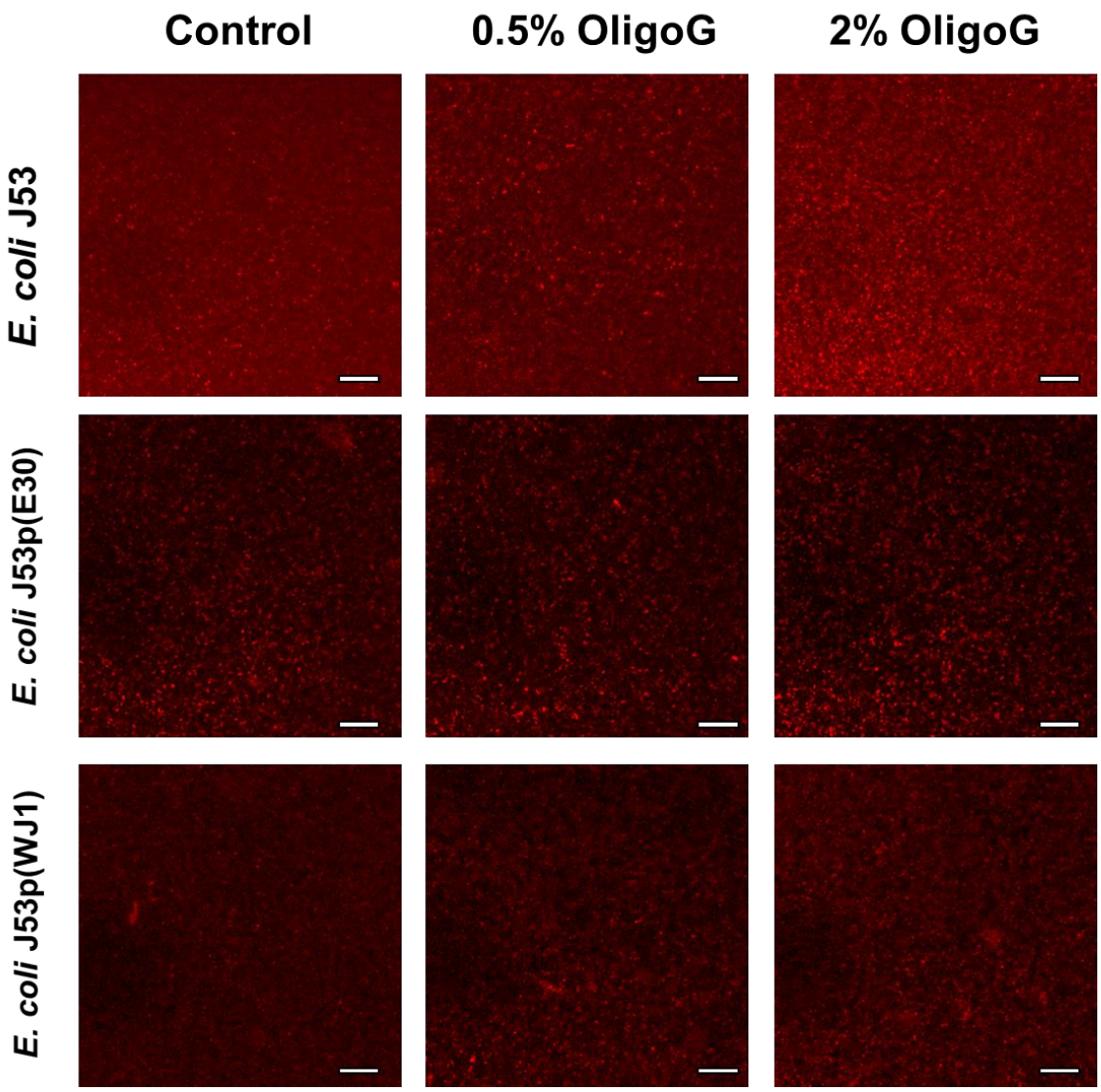

Figure 4.13. Biofilm disruption assay showing CLSM Z-stack imaging of OligoG CF-5/20 treated *E. coli* J53, J53(pE30), and J53(pWJ1) biofilms, with SYPRO ruby (targeting proteins) staining. Biofilms were grown for 24 h, before a 24 h treatment ± OligoG CF-5/20 (0.5 or 2%); Scale bar = 30 μm.

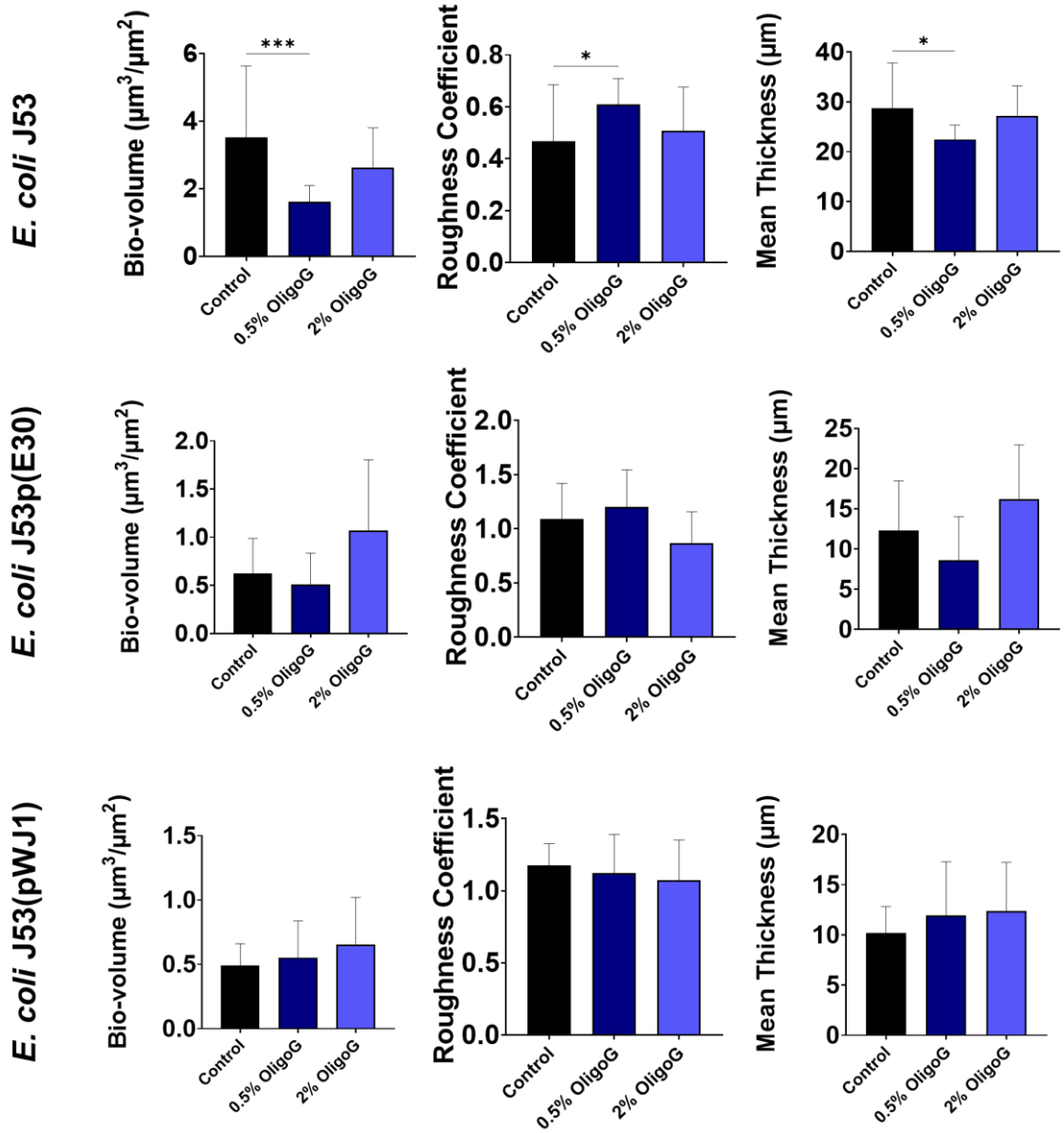

Figure 4.14. COMSTAT image analysis of *E. coli* J53, J53(E30) and J53(pWJ1) treated with OligoG (0.5 or 2%) and stained with SYPRO ruby (as seen in **Figure 4.13**) showing biofilm bio-volume ($\mu m^3/\mu m^2$), roughness coefficient, and mean thickness (µm) ± S.D; n=3 biological repeats; n=5 technical repeats. Group wise comparisons were analysed using one-way ANOVA, followed by Dunnett's post hoc tests; *P<0.05; **P<0.01; ***P<0.001; ****P<0.0001 denotes significance.

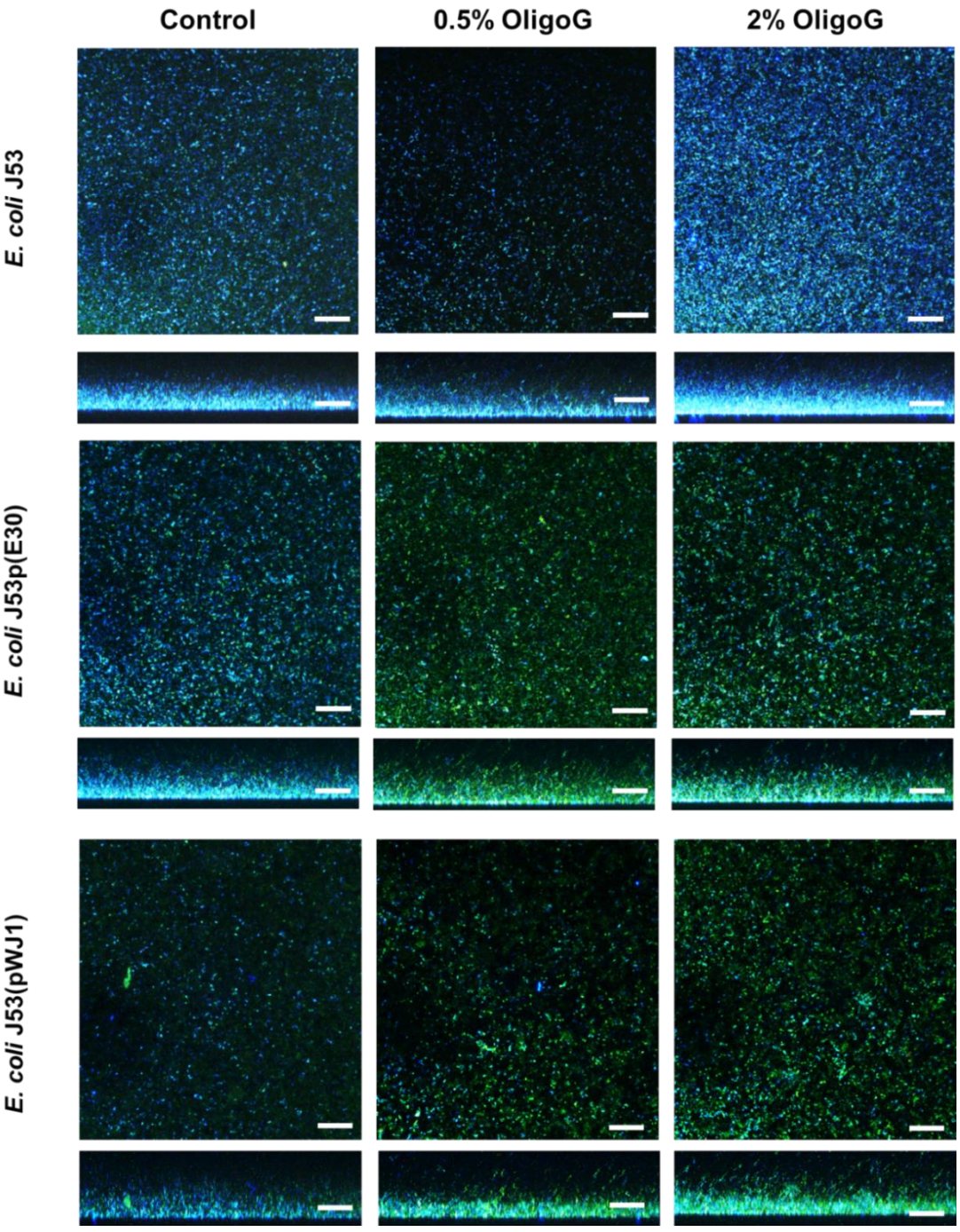

Figure 4.15. Overview of biofilm disruption assays showing CLSM Z-stack imaging of OligoG CF-5/20 treated *E. coli* J53, J53(pE30), and J53(pWJ1) biofilms, with calcofluor white M2R (targeting polysaccharides), SYTO-9 (targeting nucleic acids) and SYPRO ruby (targeting proteins) staining. Biofilms were grown for 24 h, before a 24 h treatment ± OligoG CF-5/20 (0.5 or 2%); Scale bar = 30 μm.

J53(pE30) biofilms treated with 0.5% OligoG showed a reduction in both biofilm thickness and biovolume, the results were not significant. **Figure 4.15** shows an overlay of all three stains calcofluor white, SYTO-9 and SYPRO ruby with matching side on images of the Z-stack.

4.3.6 Effect of OligoG CF-5/20 and colistin treatment on *E. coli* biofilm disruption

The effects of the combination treatment (0.5% OligoG CF-5/20 and 32 µg/mL colistin) on COL^{sens} *E. coli* J53, using the triple EPS staining protocol comprised of calcofluor white, SYTO-9 and SYPRO ruby, are shown in **Figure 4.16**. COMSTAT analysis showed unsurprisingly that the colistin treatment alone (at MBEC value) was highly effective, significantly reducing both the biovolume and mean thickness of the biofilm, while also significantly increasing the biofilm surface roughness (**Figure 4.17**).

Further analysis was performed using LIVE/DEAD® staining (**Figure 4.18**). Here, *E. coli* J53 showed that all three treatment combinations reduced the biovolume of the biofilm significantly. The colistin therapy alone showed a significant increase in biofilm roughness, while the OligoG alone treatment also showed a slight increase in roughness and DEAD/LIVE ratio, although these were not found to be significant. *E. coli* J53(pE30) when treated with either colistin or the dual colistin/OligoG therapies showed no significant changes in biovolume, while colistin treatment produced a reduced roughness coefficient and DEAD/LIVE ratio (**Figure 4.19**). Similarly, when treated with combination therapy, the roughness and DEAD/LIVE ratio was reduced. *E. coli* J53(pWJ1) with all treatments showed a significant reduction

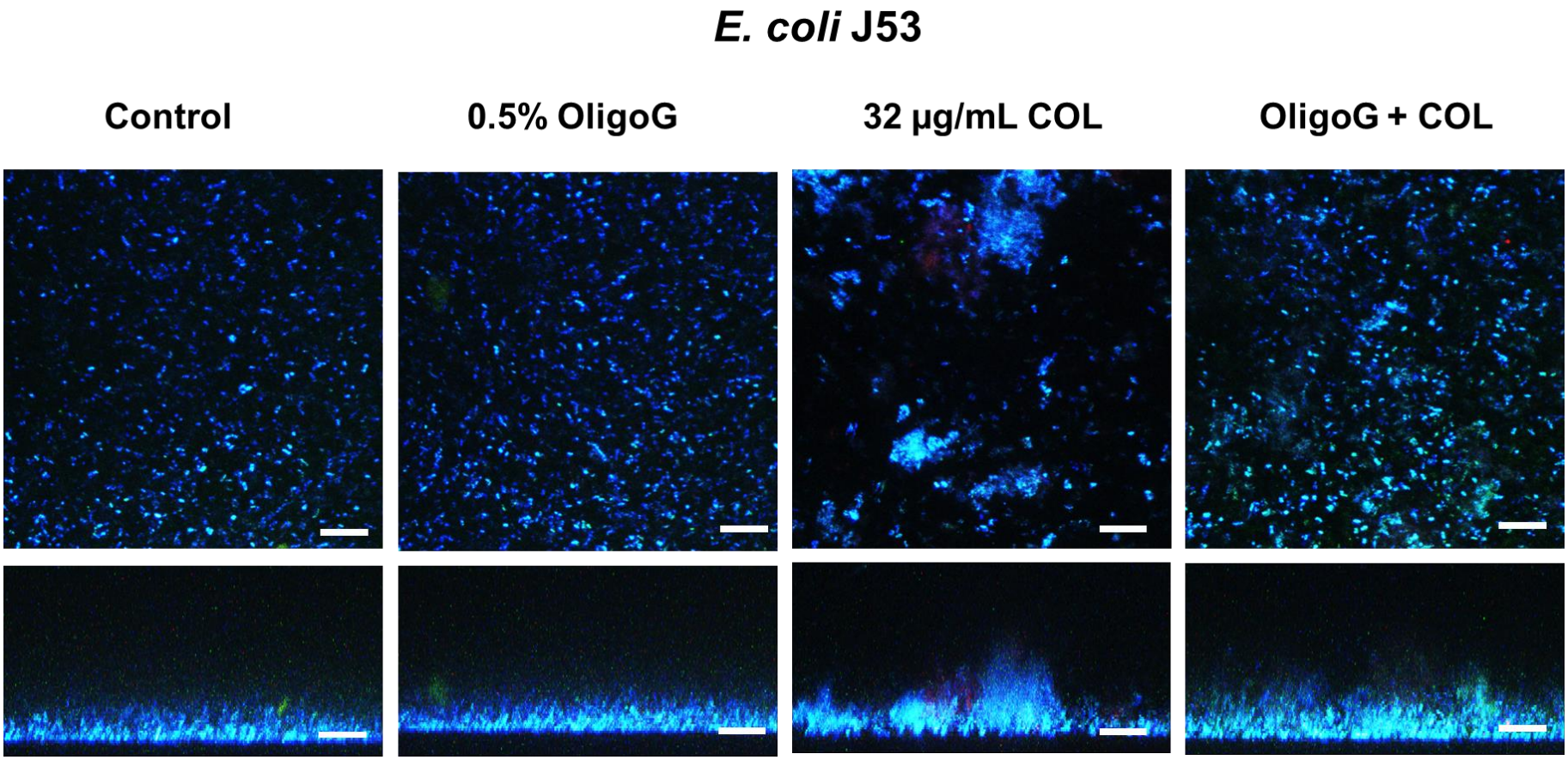

Figure 4.16. Biofilm disruption assay showing CLSM Z-stack imaging of *E. coli* J53 biofilms, with calcofluor white (polysaccharides), SYTO-9 (nucleic acids) and SYPRO ruby (proteins) staining. Biofilms were grown for 24 h, before a 24 h treatment ± 0.5% OligoG CF-5/20 ± 32 µg/mL colistin (COL); Scale bar, 30 µm.

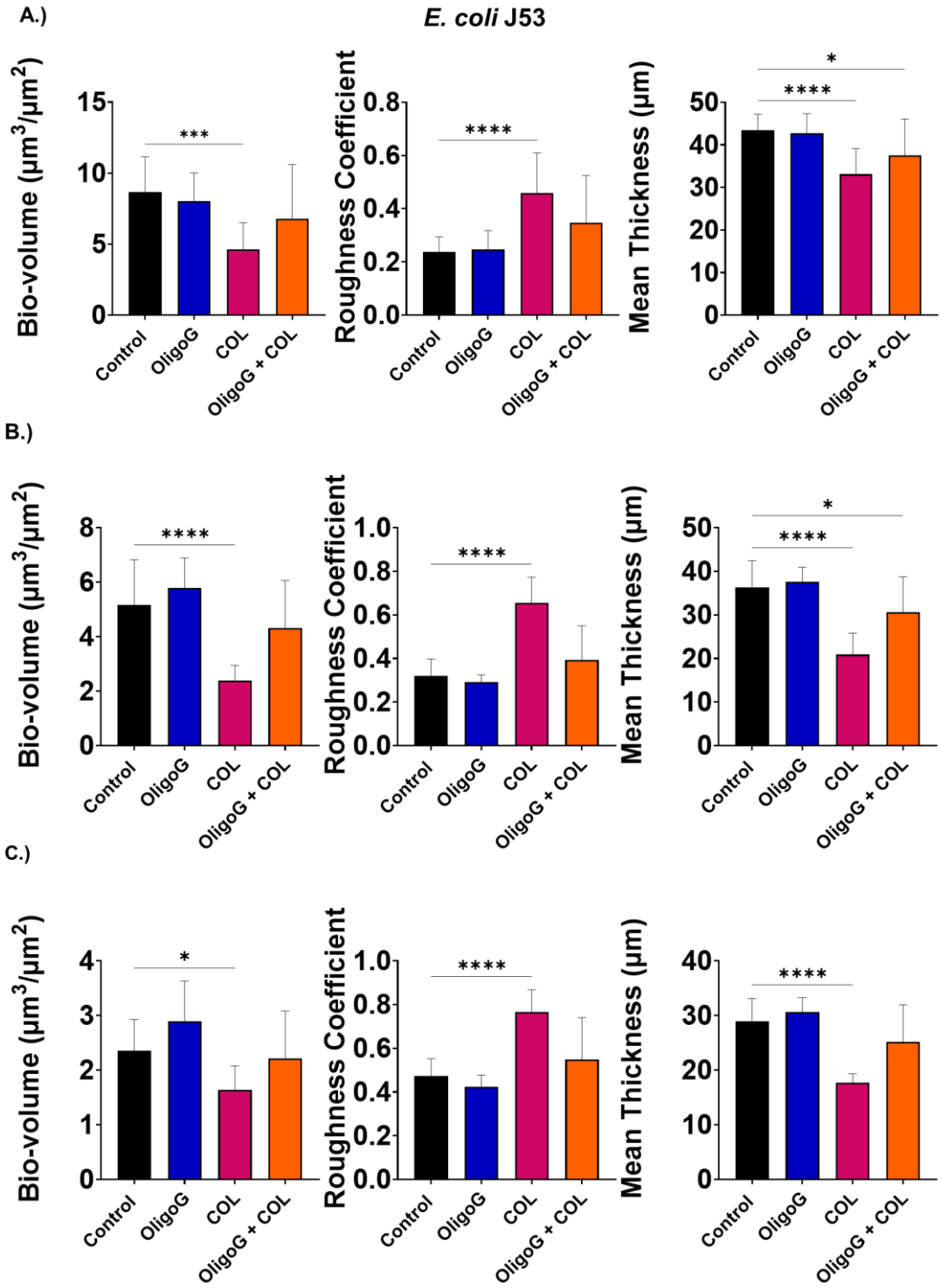

Figure 4.17. COMSTAT image analysis of the *E. coli* J53 disruption assay (**Figure 4.16**), showing bio-volume ($\mu m^3/\mu m^2$), roughness coefficient, and mean thickness (µm) ± S.D; n=3 biologicals; n=5 technicals of (**A)** Calcofluor white M2R (polysaccharides); (**B)** SYTO-9 (nucleic acids) and (**C)** SYPRO ruby (proteins). Group wise comparisons were analysed using one-way ANOVA, followed by Dunnett's post hoc tests *P<0.05 **P<0.01 ***P<0.001 ****P<0.0001 denotes significance.

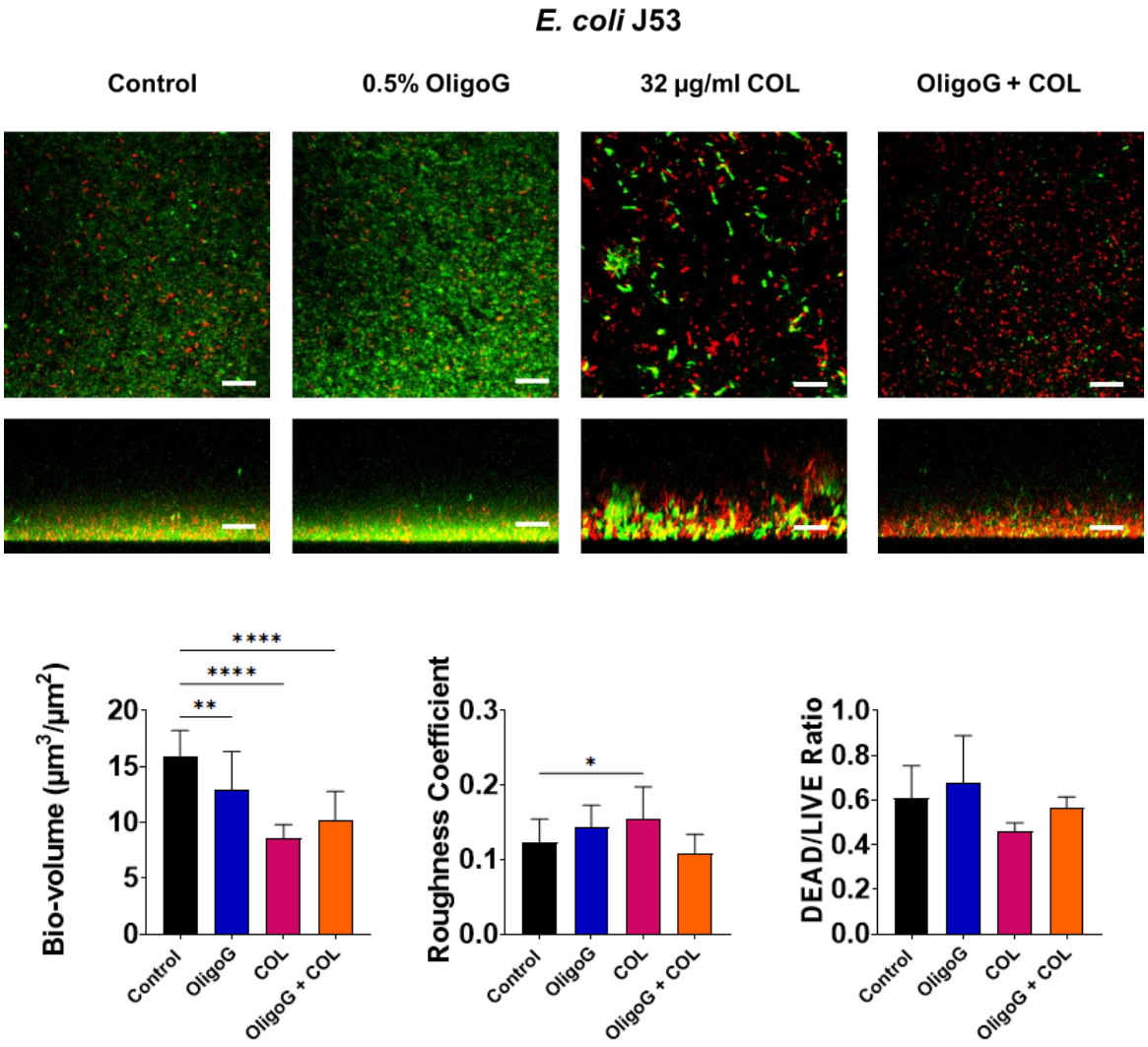

Figure 4.18. Biofilm disruption assay, showing CLSM Z-stack imaging of *E. coli* J53 biofilms with LIVE/DEAD® staining. Biofilms were grown for 24 h, before a 24 h treatment ± 0.5% OligoG CF-5/20 ± 32 µg/mL colistin (COL); Scale bar, 30 µm COMSTAT image analysis of *E. coli* J53 disruption assay shows bio-volume ($\mu m^3/\mu m^2$), surface roughness coefficient and DEAD/LIVE cell ratio ± S.D; n=3 biological repeats; n=5 technical repeats. Group wise comparisons were analysed using one-way ANOVA, followed by Dunnett's post hoc tests *P<0.05 **P<0.01 ***P<0.001 ****P<0.0001 denotes significance.

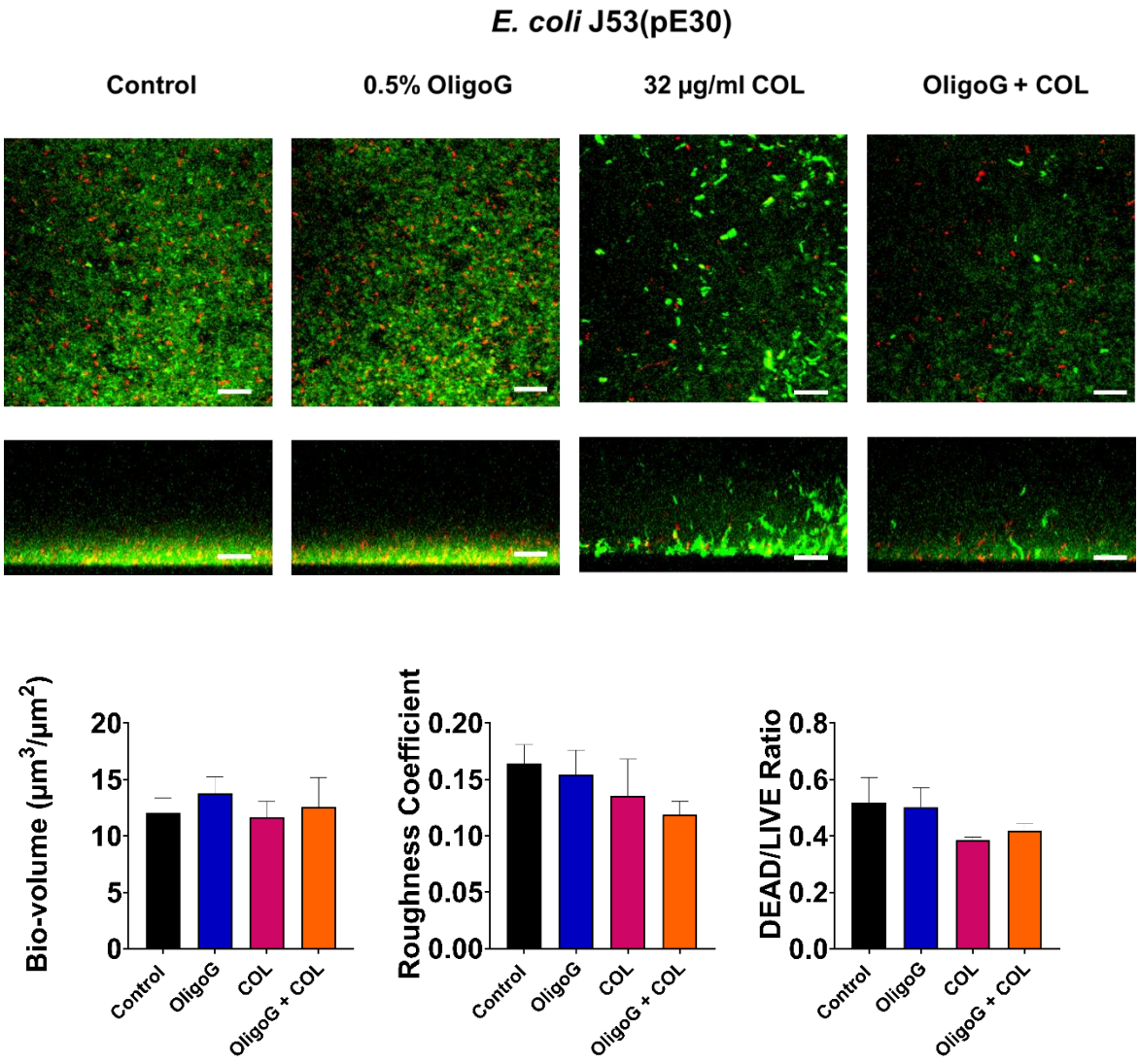

Figure 4.19. Biofilm disruption assay showing CLSM Z-stack imaging of *E. coli* J53(pE30) biofilms with LIVE/DEAD® staining. Biofilms were grown for 24 h, before a 24 h treatment ± 0.5% OligoG CF-5/20 ± 32 µg/mL colistin (COL); Scale bar, 30 µm. COMSTAT image analysis of *E. coli* J53(pE30) disruption assay shows bio-volume ($\mu m^3/\mu m^2$), surface roughness coefficient and DEAD/LIVE cell ratio ± S.D; n=3 biological repeats; n=5 technical repeats. Group wise comparisons were analysed using one-way ANOVA, followed by Dunnett's post hoc tests *P<0.05 **P<0.01 ***P<0.001 ****P<0.0001 denotes significance.

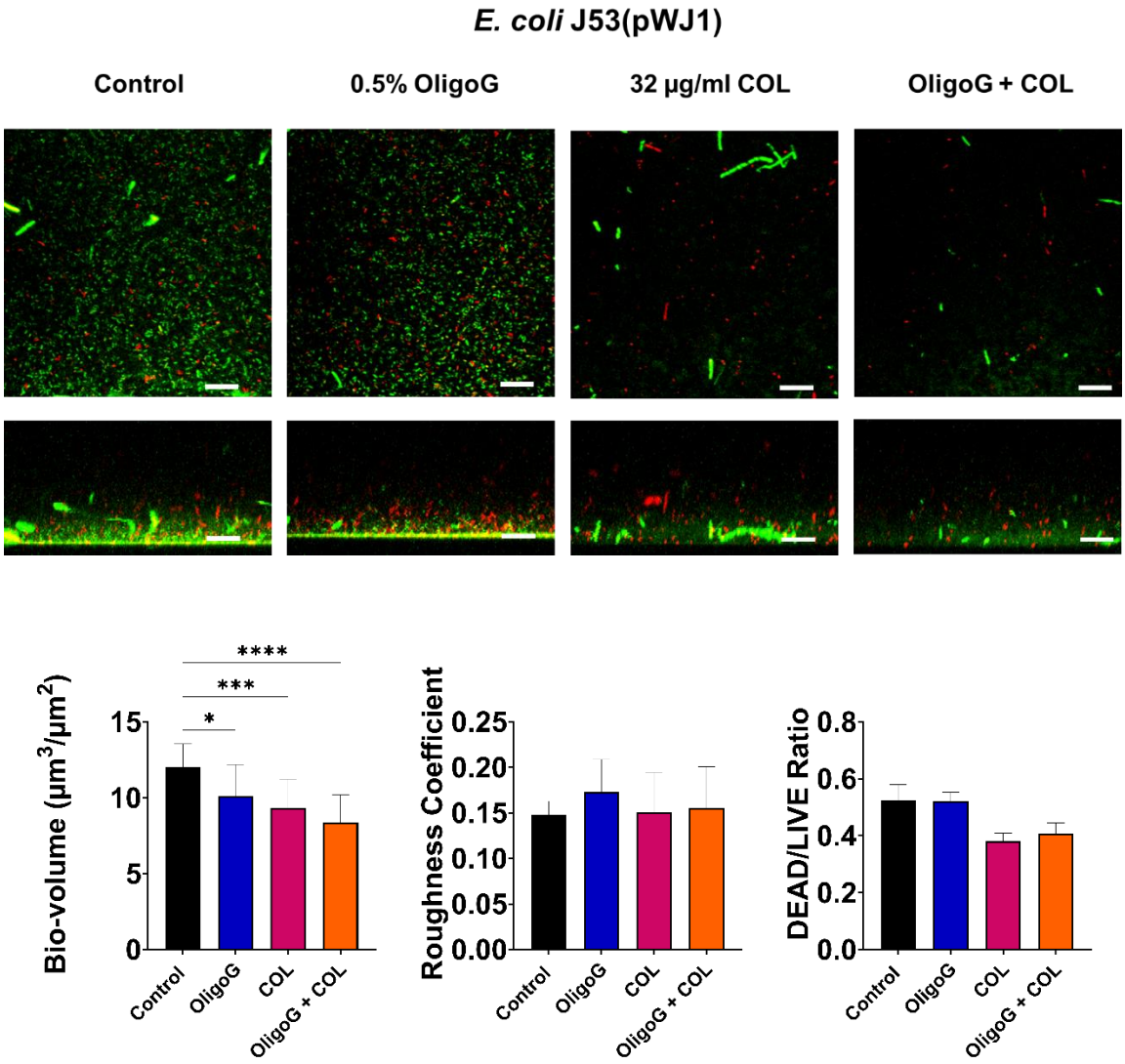

Figure 4.20. Biofilm disruption assay showing CLSM Z-stack imaging of *E. coli* J53(pWJ1) biofilms with LIVE/DEAD® staining. Biofilms were grown for 24 h, before a 24 h treatment ± 0.5% OligoG CF-5/20 ± 32 µg/mL colistin (COL); Scale bar, 30 µm. COMSTAT image analysis of *E. coli* J53(pWJ1) disruption assay shows bio-volume ($\mu m^3/\mu m^2$), surface roughness coefficient and DEAD/LIVE cell ratio (µm) ± S.D; n=3 biological repeats; n=5 technical repeats. Group wise comparisons were analysed using one-way ANOVA, followed by Dunnett's post hoc tests *P<0.05 **P<0.01 ***P<0.001 ****P<0.0001 denotes significance.

In biovolume (**Figures 4.20**). A slight increase in roughness was seen for OligoG alone, however, it was not significant. Whilst J53 and J53(pWJ1) were treated at their MBEC values for colistin (32 µg/mL), the MBEC for COL^R, *E. coli* J53(pE30) was considerably higher (at 128 µg/mL). Therefore the colistin does not have as great an effect. This was evident in the weak antimicrobial activity noted for either individual or combination OligoG/colistin treatments.

4.4 Discussion

The use of colistin as a last-resort antibiotic treatment for MDR pathogens is crucial. However, the rapid discovery and global spread of colistin-resistant strains are concerning. This widespread dissemination of *mcr* genes significantly diminishes the available treatment options for patients, intensifying the challenge of combating MDR infections. This study and previous authors have shown that in *E. coli mcr-1* usually confers low level colistin resistance (with MICs between 2-8 µg/mL), although some ESKAPE pathogens, such as *A. baumannii* and *K. pneumoniae,* have been shown to display far higher levels (>128 µg/mL; (Liu et al. 2016; Yin et al. 2017). The different resistance mechanisms between *Klebsiella* spp. and *E. coli* explain the different MIC values, as colistin resistance in *K. pneumoniae* is due to chromosomal mutations affecting the PmrA/B and PhoP/Q two-component system or through alteration in the *mgrB* gene (Yap et al. 2022). As expected, the MBEC values for the *E. coli* strains were 2-7-fold higher than the MICs, being highest for J53. Similar levels of resistance have been found in other *E. coli* from diverse sources, including isolates from poultry in the food chain in Pakistan which demonstrated MICs to colistin of 2 µg/mL and MBEC values at 28-64 µg/mL (Noreen et al. 2022). These findings highlight the increasing threat that the *mcr* genes could have should they become disseminated into other hosts, e.g. *A. baumannii* and *K. pneumoniae,* in a clinical setting (Liu et al. 2017b). With *mcr* also now found on conjugative (self-transferable) and broad-host range plasmids, such as those of the IncP incompatibility group, this scenario seems increasingly likely.

The characterisation of 10 distinct *mcr* genes may suggest that they contribute different evolutionary advantages to their hosts. Recent growth and competition assays in *E. coli* have previously revealed that carriage of *mcr-1* has a greater fitness

cost than *mcr-3* (demonstrated by decreased cell viability), with *mcr*-3 plasmids shown to be more stable, even in the absence of colistin selection (Yang et al. 2020). Furthermore, other researchers have shown that *mcr-1* cloned into a TOPO expression vector significantly decreased the growth rates of both *E. coli* and *K. pneumoniae, w*hen compared to vector-free parental strains, showing that carriage of *mcr-1* was a metabolic burden. This contrasted with carriage of the wildtype plasmid (a 217 kb IncHI2-type plasmid pKP2442), when transferred into the same hosts, which showed no impact in *E. coli* J53, but a significant decrease in fitness (reduced growth rates compared to the parental strain) in *K. pneumoniae* (Tietgen et al. 2018). More extensive studies on the different *mcr* groups have been performed by Li et al. (2021), examining the effects of *mcr-1-5* on growth kinetics, LIVE/DEAD® staining, and virulence in a *Galleria mellonella* model in the presence and absence of colistin. In this case, the *mcr* genes were separately cloned into the same genetic background namely, *E. coli* TOP10 (*mcr-1-5*/pBAD). Here, *mcr-1* and *mcr-2* were found to show improved growth kinetics, viability, and lower virulence levels than *mcr-3, 4* and *5,* which had significant effects on all three test parameters. The authors go on to suggest that *mcr-1* and *2* may be better adapted to the host compared to the other *mcr* genes, which inferred a greater fitness cost for *mcr-3, 4* and *5*. While Li et al. (2021) contradicts findings from this study, some reasons for differences in fitness cost could be due to the host bacteria and the plasmids carrying the *mcr* genes, as well as the study using an inducible arabinose model that may affect the levels of *mcr* genes expressed. In *E. coli* wild type strains, PN4, PN24 and PN42, co-existence of both *mcr-1* and *mcr-3.1* in the same host was followed over 14 days in a planktonic model (Yang et al. 2020). *mcr-1* plasmids were found to be slowly lost, while *mcr-3.1* plasmids although initially in decline (within the first fifty generations) were able to

fully recover. In *E. coli* J53 transconjugants, both *mcr-1* and *3.1* also declined in monoculture and in direct competition with each other, showing that both confer a fitness cost, but with *mcr-1* carriage being the more costly of the two. Similarly, following a 14-day passage assay performed with *mcr-1* carried on plasmids belonging to several different incompatibility groups, results showed that InCI2, IncHI2, IncX4 and IncY plasmids were maintained over the 14 days, but that IncFII was lost from day 5 onwards. It was also shown that IncHI2, IncY and IncFII inferred a fitness cost, while strains carrying IncI2 and IncX4 showed an increase in fitness after 96 h (Wu et al. 2018). The apparent competitive advantage displayed by IncI2 and IncX4 plasmids may help to provide an explanation for why (along with IncHI2 plasmids), they are the predominant (>90%) most disseminated *mcr-1* gene carrying plasmid type around the world (Matamoros et al. 2017). While this study only focused on *mcr* genes carried on IncHI2 plasmids, it would be interesting to see the behaviour of other *mcr* carrying plasmids in an evolutionary biofilm model.

In another planktonic 14-day passage experiment with an *E. coli* J53 transconjugant carrying a 265 kb IncHI2 plasmid conferring *mcr-1* gene, the plasmid was shown to be stable in nutrient-rich (LB) and nutrient-limited (M9) media, and that any fitness cost could be "compensated" for after numerous passages via mutations in the chromosome, plasmid, or both (Ma et al. 2018; Yang et al. 2020).

Research looking at colistin-resistant *E. coli, A. baumannii, P. aeruginosa* and *K. pneumoniae,* showed that after 32-day passage in the absence of colistin, 75% of *P. aeruginosa* and 25% of *E. coli* strains reverted back to being sensitive to colistin, although for *A. baumannii,* only 1/5 strains became colistin sensitive over the 64-day passage, with all four *K. pneumoniae* strains maintaining their colistin resistance (Lee

et al. 2015). The stability of *A. baumannii* has been previously noted, with nosocomial transmission from a patient treated with colistin into patients not receiving treatment, showing that the strain was readily able to acquire resistance, and that its carriage was not costly enough to allow it to be outcompeted by sensitive strains (Snitkin et al. 2013).

Much of the previous research suggesting that *mcr-1* possession has a greater effect on bacterial fitness than *mcr*-3, has looked at the fitness costs of *mcr* in planktonic cells (growth curves/competition models). However, few studies have looked at these effects in 3-D biofilms. Hence, an evolutionary bead biofilm model was used to examine the effect of transmission of *mcr-1* and *mcr-3* in biofilms grown on glass beads, following serial passage over 31 days. Both genes were found to be stably maintained over the entirety of the experiment in the presence of colistin selection (at 0.125 and 1 µg/mL). In contrast, in the absence of colistin, *mcr-1* was lost after 23 days while *mcr*-3 gene was maintained, further supporting the hypothesis that *mcr-1* has a greater fitness cost in *E. coli* than *mcr-3*.

The formation of 72 h biofilms by *E. coli* J53 has been previously investigated using LIVE/DEAD® staining, where it was shown to form thick and healthy biofilms in batch and in continuous flow chamber assays (Chiang et al. 2009). In contrast, *mcr-1* positive *E. coli* strains have been shown to produce medium to low level thickness biofilms (Ćwiek et al. 2021). Distinct differences between COL^R and COL^{sens} isolates in other bacterial genera have also previously been noted. For example, in COL^R *P. aeruginosa* clinical isolates, the majority of strains (84%) formed weak biofilms with 16% forming moderate biofilms, in contrast to colistin-susceptible strains of which 52% formed strong biofilms, with 32% forming moderate ones (Azimi and Lari 2019).

Similarly, in clinical isolates of COL^R *A. baumannii*, biofilm-forming ability was also found to be significantly reduced compared to COL^{sens} strains, due to mutations in biofilm formation genes, *ppk* and *modA,* linked to chromosomal colistin resistance (Dafopoulou et al. 2016). In this case, colistin resistance arose due to mutations in *pmrAB* which reduced growth and biofilm formation in static and dynamic conditions, compared to the COL^{sens} control strain. This suggests that the reduced growth might be responsible for lower levels of biofilm formation, as well as affecting infectivity and virulence (López-Rojas et al. 2013; Beceiro et al. 2014).

OligoG CF-5/20 has previously been shown to disrupt the EPS matrix of mucoid (CF isolate) *P. aeruginosa* NH57388A biofilms, as well as potentiate the action of certain antibiotics such as macrolides (Khan et al. 2012; Powell et al. 2018). In established biofilms, 2% and 6% of OligoG CF-5/20 treatment was shown to specifically target polysaccharides (ConcavalinA staining) and eDNA (TOTO-1 staining) in the biofilm matrix, resulting in significant reductions in fluorescent intensity compared to the untreated control, although the same effects were not observed in biofilm formation assays. Recently, using molecular dynamics and density-functional theory, researchers in Manchester showed that OligoG does not appear to disrupt established biofilms through breakage of the cross links between divalent cations and biofilm EPS, but rather through prevention of Ca^{2+}-EPS binding by sequestration of free calcium ions (Hills et al. 2022). Furthermore, *P. aeruginosa* NH57388A was shown to be significantly disrupted by OligoG and colistin, when used individually and as a combined treatment with OligoG treated biofilms showing microcolony disruption (Pritchard et al. 2017b).

The calcofluor white staining used in this study, which binds non-specifically to all β-polysaccharides, was clearly also found to bind to OligoG CF-5/20, explaining

why the biofilms treated at 6% concentrations appeared to be significantly thicker than the untreated controls, with the biovolume also significantly affected in all three strains tested. As a result, lower concentrations (0.5% and 2%) of OligoG CF-5/20 were used for further CLSM imaging and COMSTAT analysis, using SYTO-9 and SYPRO ruby. While SYTO-9 staining was used for labelling nucleic acids, SYPRO ruby labelled proteins with the CLSM (the images being very dark despite prolonged staining protocols). The images could, therefore, be further improved for staining for even longer periods of time (up to 4 h), as previously done in other studies (Powell et al. 2018).

The combined therapy of 0.5% OligoG CF-5/20 and colistin (32 µg/mL; tested at MBEC [4xMIC]), significantly reduced biovolume, compared to OligoG and colistin alone treatments in *E. coli* J53(pWJ1) and equally as effective in *E. coli* J53, although this efficacy was not also translated to DEAD to LIVE cell ratio results. Previous research has shown that the SYTO-9 stain can be used to stain for nucleic acids, as well as eDNA, the eDNA may be released due to the colistin treatment disrupting the membrane (Sena-Vélez et al. 2016). In a clinical setting when treating CF, 1-2 million international units (IU) of inhaled colistin is given to adults 2-3 times daily, in comparison to this study a dose of ~52.63-105.26 mg (based on colistin potency ≥19,000 IU/mg) would be administered up to three times a day, which is much greater than the amounts administered in the biofilm formation studies (BNF 2023). Given more time, these *in vitro* assays could be repeated using the higher doses of colistin.

Combined therapies have many benefits including increasing the effectiveness of treatment, reducing the development of resistance and, reducing possible negative side effects in patients, all of which are beneficial to treat MDR pathogens. Most

current combination therapies using colistin are combined with carbapenems or rifampicin. With the emergence of MDR pathogens innovative strategies such as the use of triple combination therapies may be the only way forward. Bulman Zackery *et al.* (2017) used a triple cocktail, comprised of polymyxin B, aztreonam, and amikacin to completely kill *E. coli* harbouring both *mcr-1* and $bla_{\text{NDM-5,}}$ which also prevented the formation of persister cells. As colistin has been classified by the WHO as a last resort treatment for "critical" level pathogens, the use of a combined therapy can subvert many of the issues that are associated with using it in a clinical setting.

4.5 Conclusion

This chapter has confirmed the fitness costs that carriage of *mcr* genes can have on the growth of planktonic bacteria, with *mcr*-1 shown to have a greater fitness cost compared to *mcr-3*. These findings were confirmed by the evolutionary bead biofilm model, with loss of *mcr*-1 (but not *mcr-3*) after multiple passages over the course of thirty-one days, showing the greater stability of the *mcr-3* plasmid over time, even in the absence of colistin selection. CLSM and COMSTAT analysis showed significant disruption of EPS matrix of *E. coli* J53 strain, but with limited effects seen on *mcr-1* and *3* carrying strains. Previous research has shown that OligoG CF-5/20 has the ability to potentiate the effects of various antifungals and antibacterial agents. However, effective OligoG-colistin combination treatments were limited or not observed here.

Chapter 5

General Discussion

5.1 General discussion

The UK government has implemented a 5-year action plan, as part of their 20-year vision, to contain and control AMR by 2040 (GOV.UK 2022). In this policy, the three main methods of preventing AMR focuses on the reduction and unintentional use of antimicrobials, optimising antimicrobial use, and investing in the innovation, supply, and access of antimicrobials.

The drying pipeline of antibiotics combined with the waning interest of pharmaceutical companies, along with the high costs of developments has led to need for novel treatments and looking at the natural world to reduce AMR, hence the development of OligoG. Furthermore, alginate oligomers can be harvested from two sources (species of certain seaweed and bacteria) and optimised via a greater understanding of epimerase and lyase enzymology in alginate production for clinical application via structure-activity relationships (SARs).

The main aims of this project were to investigate the use and effectiveness of the alginate oligosaccharide, OligoG CF-5/20, as an antibiofilm treatment, and to look at synergistic responses when used in combination with therapies which are currently limited by the development of multidrug resistance (MDR) and toxicity issues. The SAR of alginate oligomers was also investigated to determine the role of calcium binding in the mechanism of action. The rise in resistance to antifungal therapy, alongside toxicity has led to the need for novel therapies (Fisher et al. 2022). Previous research has shown that 5% OligoG can potentiate nystatin up to 16-fold dilutions for *Candida* spp. and 4-fold dilutions for *Aspergillus* spp., with both strains noted in the WHO fungal priority pathogens list as a ‘critical’ pathogen, which needs to be addressed as an urgent concern (Tøndervik et al. 2014). This Thesis expanded the

work on a further thirteen *Candida* spp. (**Chapter 2**), including eight *C. albicans* strains selected based on their contribution to serious invasive fungal infections (IFI's), high concern of public health and the 'critical' need for novel treatment options (WHO 2022b). Moreover, five non-*Candida albicans Candida* (NCAC) were also screened as these are becoming an increasing clinical burden, with in recent years, a shift being seen from *C. albicans* as the major cause of infection to other non-*Candida* species (WHO 2022b). The results from minimum inhibitory concentration (MIC) assays showed potentiation of OligoG CF-5/20 with the antifungal nystatin, with an MIC decrease of up to five-fold dilutions observed in the presence of 6% OligoG CF-5/20, suggesting that OligoG when combined with nystatin may be used to overcome candidal biofilms that have a tolerance to current antifungal therapies (Taff et al. 2013).

In addition to potentiating the effect of nystatin in planktonic assays, OligoG has shown antibiofilm effects, inhibiting bacterial viability, reducing the formation of biofilms, and disrupting established *Candida* biofilms. ATP viability studies showed that 4% OligoG was able to significantly reduce viability of all thirteen strains of *Candida,* suggesting that as a "stand-alone" treatment, it is also a potential treatment option. LIVE/DEAD® confocal laser scanning microscopy (CLSM) imaging showed that the combination therapy was highly efficient at reducing the formation of biofilms, with scanning electron microscopy (SEM) imaging confirming reduction of biofilms grown on a silicone prothesis materials. Previous research using CLSM and SEM imaging showed similar potentiation effects with azoles, a different class of antifungal, although OligoG at the lower concentration of 2% proved to be effective in that study with the ability to alter the biofilm structure causing cell and hyphal death, and in combination with fluconazole was more efficient at reducing the biofilm biovolume

than the antifungal treatment alone (Tøndervik et al. 2014). Both this and the previous study, show that OligoG could have a clinical application for biofilm-related infections affecting catheters and voice box prosthesis caused by *Candida* spp.

Pritchard et al. (2017) showed that OligoG could alter the production of virulence factors, such as secreted aspartyl proteinases (SAPs) and phospholipases, as well as reducing hyphal invasion of *C. albicans*. Further studies were conducted to investigate the potential mechanism of action of OligoG (CF-5/20) on the cell membrane through ergosterol and sorbitol assays. This work suggests a secondary mechanism of action (other than ergosterol binding), being responsible for the antifungal results. While the permeability assay showed a significant increase in cell permeabilisation on the combination of OligoG and nystatin, compared to the untreated control, no significant differences were evident compared to the OligoG administered alone. These findings were in-line with the transmission electron microscopy (TEM) imaging, which showed some structural reorganization of the cell membrane when *Candida* was treated with the combination therapy, which was not seen with control or OligoG alone treatment groups. Further research could investigate this secondary mechanism of action of OligoG CF-5/20, such as divalent ion chelation which has been suggested as a possible mode of action (Tøndervik et al. 2014).

Molecular weight and G:M composition of alginates has previously been shown to affect biological activity, suggesting that treatments could potentially be personalised for specific clinical applications (Şen 2011). A number of tailored oligomers are currently in clinical trials with different potential clinical applications, due to their antitumour and anti-inflammatory effects (Wang et al. 2019b; Xing et al. 2020). G-block oligomers have a high affinity for divalent cations, such as calcium

and magnesium, compared to both homopolymeric M-block and copolymeric MG-blocks, with four guluronate units binding to calcium forming a classic 'tilted egg box' structure (Smidsrød 1974; Borgogna et al. 2013). Previous OligoG CF-5/20 studies have suggested this chelation of Ca^{2+} ions, and the associated disruption of Ca^{2+} binding in pseudomonal biofilms, could be directly responsible for its antimicrobial and antibiofilm effects (Powell et al. 2018). *P. aeruginosa* is known for its biofilm forming abilities, which are commonly associated with chronic infections, especially in immunocompromised patients or patients with high antibiotic use, such as CF patients. Furthermore, *P. aeruginosa* is commonly found to infect chronic wounds, such as burns or leg ulcers, findings which are linked to increased morbidity levels and high associated healthcare costs (Serra et al. 2015). This study compared on the structure-function relationships of M- and G-block alginate oligosaccharides for targeted antimicrobial applications against *P. aeruginosa*.

OligoM with a comparable DPn and molecular weight, but with contrasting Ca^{2+} binding selectivity, was compared with the prototype OligoG CF-5/20 (Smidsrød and Haug 1968). The experiments demonstrated OligoG and OligoM showed similar antimicrobial properties, with treatment leading to a reduction in bacterial growth and a disruption of biofilm formation. The activity was not solely related to Ca^{2+} binding ability. FTIR studies demonstrated that both alginate oligomers remained bound to the pseudomonal cell surface, following hydrodynamic shear. Interestingly, the G-block oligosaccharides interacted most strongly with the LPS of Gram-negative bacteria and exhibited a stronger QSI effect than OligoM (Pritchard et al. 2023). Identification of natural strategies that interfere with bacterial cell-cell communication is promising and could provide novel mechanism of action to overcome AMR (Huang et al. 2020).

Azithromycin is commonly prescribed to CF patients, due it's anti-inflammatory effects (Nichols et al. 2020; Acosta et al. 2021). Synergistic responses with azithromycin were also shown to be superior for OligoG, compared to OligoM, in biofilm models (Pritchard et al. 2023). Previous studies demonstrated that OligoG has no effect on acquisition of azithromycin resistance, and potentially reducing cross resistance (Oakley et al. 2021). This study confirms the potential clinical utility of G-block alginate oligosaccharides in treating infections of MDR bacterial pathogens and supports its potential use as an inhaled therapy. The therapeutic potential of OligoG CF-5/20 is evident in the completed clinical trials in healthy and CF patients (outlined in **Chapter 1**), which along with the results of this study demonstrate further applications of OligoG in the treatment of CF.

Prior to the discovery of *mcr* genes in 2015, the isolates that showed increased MIC values to colistin all had chromosomal mutations, which was the most common mutation leading to LPS modification (Olaitan et al. 2014). In this study, we focus on two of the most prevalent genes; *mcr-1* and *mcr-3*, which have different fitness costs as seen in growth curve which showed that the carriage of *mcr-1* lowered the growth rates more than those carrying *mcr-3* (**Chapter 4**). To expand the planktonic model performed by Yang *et al*. (2020), a bead model was set up to determine the effect of *mcr* carriage on fitness in biofilm systems. The *mcr-1* carried on the IncHI2 plasmid pE30 is on a composite transposon, Tn*6330*, which is flanked on both sides by an IS*Apl1* insertion sequence (Li et al. 2017). The loss of a single IS*Apl1* or both insertion sequences results in the *mcr-1* gene being incapable of transfer and therefore, trapped on its host vector (Snesrud et al. 2018). This explained why some *mcr-1* have high levels of stability and are maintained for long period in the biofilm bead model (>30 days in the absence of colistin selection). *mcr-3* in comparison, in this study was found

on a ΔISK*pn40-mcr-3-dgkA*-ISK*pn40* structure, with ΔTn*As2* located upstream. It is still unknown if the ΔISK*pn40-mcr-3-dgkA*-ISK*pn40* structure has the ability to move through homologous recombination, or if it can form a circular intermediate (Xiang et al. 2018; Sia et al. 2020).

EDTA has shown to influence the activity of MCR-1, causing a reduction in the MIC of colistin (Esposito et al. 2017). In this study, where OligoG has shown an effect on *mcr* positive strains, this may also be the case as OligoG is known to bind divalent cations and the mechanism of colistin is through displacing calcium and magnesium from the outer cell membrane, causing permeability changes and leakage of cell contents. The EPS layer is an important target for antimicrobials, as it is involved in multiple stages of biofilm formation and development, with its chemical composition that can be targeted with proteases, DNases and hydrolases, as well as EPS synthesis and secretion also being a therapeutic target (Jiang et al. 2020). OligoG has previously been shown to disrupt EPS, reducing the quantify of polysaccharides and eDNA (Powell et al. 2018). Previous *in vitro* and *in vivo* studies demonstrated the potentiation of colistin in the presence of OligoG in artificial sputum and mouse models, respectively (Hengzhuang et al. 2016; Stokniene et al. 2022). Therefore, selective staining was used for CLSM imaging to provide some insights into how OligoG affected bacterial biofilms and the EPS matrix (**Chapter 5**). However, the combined effect of OligoG and colistin was not as effective and this may be due to the concentration of colistin used (32 μg/mL), which is sub-MBEC value for most strains.

5.2 Limitations and future research

Experiments in this study focused mainly on single species biofilms. However, in clinical settings, this is rarely the case for chronic infections, which have been shown

to have a diverse microflora, as well as being highly dynamic. While previous work has shown the effect of OligoG CF-5/20 on several different bacterial and fungal species, using both planktonic and biofilm models, there has been limited research on its effects on mixed-species biofilms. The increasing importance of invasive fungal infections (IFIs) has been of note in recent years due to their severity, with *Candida* sp. in CF patients found to coexist with pathogenic bacteria, such as *P. aeruginosa* in ~40% of individuals (Haiko et al. 2019). Although the findings here have shown that OligoG could be used as a therapeutic treatment for both *Candida* and *P. aeruginosa*, more research on mixed microbial populations is still required. Furthermore, in **Chapter 2**, not all experiments were performed on all thirteen strains, due to time constraints.

Comparison of OligoG with OligoM in **Chapter 3** was limited by the amount of OligoM alginate available (from Algipharma AS) for the study. This resulted in multiple "small scale" assays being developed and performed. A problem here was that the results obtained e.g., motility assays, did not always reflect those that had been previously universally obtained for OligoG in standard larger scale assays; findings which may reflect nutrient availability limiting growth and motility. If more oligomer had been available, an analysis of changes to cell surface charge (zeta-potential), following OligoM treatment would have been useful. Pritchard et al. (2017). have already shown that OligoG treatment resulted in a decrease in the surface charge of the *P. aeruginosa* PAO1 bacterial cell membrane, making it more negatively charged, contributing to altered bacterial adhesion that could reduce adherence and biofilm formation. Additional QS experiments could also have been performed, with measurements taken at varying time points to provide insight into the quorum sensing

processes affected by the alginate oligosaccharides, giving a wider picture than that available from the single observation at 24 h. It has been shown that virulence factor production varies at different time points (Jack et al. 2018). The use of RT-qPCR to look at these effects at the molecular level would also have been possible.

Colistin-resistant *E. coli* strains used in this study carried IncHI2 *mcr* plasmids, commonly associated with the carriage of all *mcr* genes (Mmatli et al. 2022). The use of *mcr* plasmids of differing incompatibility groups could give a much deeper insights into the results obtained from **Chapter 4,** especially as the Chinese colistin ban in 2017 has resulted in a shift in predominance of *mcr-1* carriage to IncI2 plasmids (Shen et al. 2020). Use of the bead-biofilm model or biofilm flow-cells to compare growth and maintenance of IncI2 *mcr* plasmids with the (IncH12 plasmid carrying) strains used here might give insights into why this might be occurring. Furthermore, these models could also be used to look at plasmid transfer events since most of the recent research on *mcr* plasmid transfer appears to be performed on planktonic cells. Analysis of transfer in biofilms and mixed species populations may help to describe and mimic more closely events occurring in the natural environment, including the use of IncP plasmids which have an extremely broad host-range and high transfer frequencies.

Future work with the evolutionary bead biofilm model could be performed to examine direct competition between *mcr-1* and *mcr-3* genes using co-inoculation of both *mcr* strains. Previous research using biofilm experiments in flow cells (which provides a continuous supply of nutrients), has shown this may be a more realistic model for such experiments as it more closely mimics real-life biofilm conditions, compared to the bead biofilm model which undergoes consecutive cycles of "feast and famine"; growth conditions more akin to the oral plaque environment (Steenackers et

al. 2016). Also, given further time, it would be of great interest to run the bead model until depletion of *mcr-3* from the cultures and perform genetic sequence analysis to provide an insight into what is happening at a molecular level. Further in depth phenotypic and genotypic testing could be performed on the *mcr* strains at the end of the bead model experiment, once their *mcr* genes are lost. It is particularly important to know it this is a reversible or irreversible effect. This could help determine what happens to *mcr* over time, once antibiotic selection is no longer present. Additional CLSM imaging could also be performed on the original wild-type strains E30 (*mcr-1.1*) and WJ1 (*mcr-3.1*), which may behave differently to the transconjugants (J53[pE30] and J53[pWJ1]) used in this study, with the same J53 host background or a greater panel of both clinical and farm isolates could be used to give greater understanding. This could involve staining of other EPS matrix components than those targeted in this study, such as eDNA or lipids.

5.3 Conclusion

This study demonstrates that OligoG CF-5/20 is an effective antimicrobial and anti-biofilm agent against numerous *Candida* spp, and *P. aeruginosa*. However, it was not that effective against *mcr* positive *E. coli* strains, in comparison. With increasing growing concerns about AMR set to increase the demand for novel antimicrobials the potential of alginate oligomers to treat MDR pathogens is shown in this study.

Supplementary

Supplementary Table 1. P values of Tukey's post-hoc comparison testing of ATP cellular viability assay for the data shown in **Figure 2.3**. Significant reductions in ATP values are highlighted in grey.

Comparison	**Candidal Strain**												
	C. albicans								***C. parapsilosis***	***C. auris***	***C. tropicalis***	***C. glabrata***	***C. dubliniensis***
	ATCC 90028	**GBJ 13/4A**	**SC5314**	**CCUG 39342**	***4*80/00**	**PB1/93**	**LR1/93**	**PTR/94**	**W23**	**NCPF 8971**	**519468**	**ATCC 2001**	**40/01**
Control v OligoG	<0.0001	<0.0001	<0.0001	<0.0001	<0.0001	<0.0001	<0.0001	0.0001	0.0002	<0.0001	<0.0001	<0.0001	0.0394
Control v NYS	0.0442	<0.0001	<0.0001	<0.0001	<0.0001	<0.0001	0.0366	0.5431	0.3739	0.4618	0.0054	0.0421	0.0431
Control v OligoG + NYS	<0.0001	<0.0001	<0.0001	<0.0001	<0.0001	<0.0001	<0.0001	<0.0001	0.0056	<0.0001	<0.0001	<0.0001	0.1916
OligoG v NYS	<0.0001	<0.0001	<0.0001	<0.0001	<0.0001	<0.0001	<0.0001	0.0060	<0.0001	<0.0001	<0.0001	0.0001	<0.0001
OligoG v OligoG + NYS	0.1567	0.0006	0.2334	<0.0001	0.0286	0.0043	0.6671	0.8348	0.5907	0.0720	0.5956	<0.0001	0.8697
NYS v OligoG + NYS	<0.0001	<0.0001	<0.0001	<0.0001	<0.0001	<0.0001	<0.0001	0.0006	<0.0001	<0.0001	<0.0001	<0.0001	0.0002

References

Aarstad, OA., Tondervik, A., Sletta, H. and Skjak-Braek, G. (2012) Alginate Sequencing: An Analysis of Block Distribution in Alginates Using Specific Alginate Degrading Enzymes. *Biomacromolecules* 13(1), pp. 106-116. doi: 10.1021/bm2013026

Abdel-Mawgoud, AM., Lépine, F. and Déziel, E. (2010) Rhamnolipids: diversity of structures, microbial origins, and roles. *Applied Microbiology and Biotechnology* 86(5), pp. 1323-1336. doi: 10.1007/s00253-010-2498-2

Acharya, Y., Dhanda, G., Sarkar, P. and Haldar, J. (2022) Pursuit of next-generation glycopeptides: a journey with vancomycin. *Chemical Communications* 58(12), pp. 1881-1897. https://doi.org/10.1039/D1CC06635H

Achkar, JM. and Fries, BC. (2010) *Candida* Infections of the Genitourinary Tract. *Clinical Microbiology Reviews* 23(2), pp. 253-273. doi: 10.1128/CMR.00076-09

Acosta, N., Thornton, CS., Surette, MG., Somayaji, R., Rossi, L., Rabin, HR. and Parkins, MD. (2021) Azithromycin and the microbiota of cystic fibrosis sputum. *BMC microbiology* 21(1), p. 96. doi: 10.1186/s12866-021-02159-5

Alav, I., Sutton, JM. and Rahman, KM. (2018) Role of bacterial efflux pumps in biofilm formation. *Journal of Antimicrobial Chemotherapy* 73(8), pp. 2003-2020. doi: 10.1093/jac/dky042

Alderliesten, JB., Duxbury, SJN., Zwart, MP., de Visser, JAGM., Stegeman, A. and Fischer, EAJ. (2020) Effect of donor-recipient relatedness on the plasmid conjugation frequency: a meta-analysis. *BMC microbiology* 20(1), p. 135. doi: 10.1186/s12866-020-01825-4

AlgiPharma. (2020) https://algipharma.com/clinical-trials. AlgiPharma - Clinical Trials,

Allen, L., Dockrell, DH., Pattery, T., Lee, DG., Cornelis, P., Hellewell, PG. and Whyte, MK. (2005) Pyocyanin production by *Pseudomonas aeruginosa* induces

neutrophil apoptosis and impairs neutrophil-mediated host defenses in vivo. *The Journal of Immunology* 174(6), pp. 3643-3649. doi: 10.4049/jimmunol.174.6.3643.

Alvarez-Ortega, C., Wiegand, I., Olivares, J., Hancock, RE. and Martínez, JL. (2011) The intrinsic resistome of *Pseudomonas aeruginosa* to β-lactams. *Virulence* 2(2), pp. 144-146. doi: 10.4161/viru.2.2.15014

Álvarez, R., Cortés, LEL., Molina, J., Cisneros, JM. and Pachón, J. (2016) Optimizing the Clinical Use of Vancomycin. *Antimicrobial Agents and Chemotherapy* 60(5), pp. 2601-2609. doi:10.1128/AAC.03147-14

Aly, R. and Berger, T. (1996) Common Superficial Fungal Infections in Patients with AIDS. *Clinical Infectious Diseases* 22(Supplement_2), pp. S128-S132. doi: 10.1093/clinids/22.Supplement_2.S128

Ameye, D., Honraet, K., Loose, D., Vermeersch, H., Nelis, H. and Paul Remon, J. (2005) Effect of a buccal bioadhesive nystatin tablet on the lifetime of a Provox™ silicone tracheoesophageal voice prosthesis. *Acta oto-laryngologica* 125(3), pp. 304-306. doi: 10.1080/00016480410022778

Ami, RB., Lewis, RE. and Kontoyiannis, DP. (2008) Immunopharmacology of Modern Antifungals. *Clinical Infectious Diseases* 47(2), pp. 226-235. doi: 10.1086/589290

Aminov, R. (2017) History of antimicrobial drug discovery: Major classes and health impact. *Biochemical Pharmacology* 133, pp. 4-19. https://doi.org/10.1016/j.bcp.2016.10.001

AMR-review.org (2015) Securing new drugs for future generations: the pipeline of antibiotics. Review on Antimicrobial Resistance.

Anandan, A., Evans, GL., Condic-Jurkic, K., O'Mara, ML, John, CM, Phillips, NJ., Jarvis, GA., Wills, SS., Stubbs, KA., Moraes, I., Kahler, CM. and Vrielink, A. (2017) Structure of a lipid A phosphoethanolamine transferase suggests how conformational changes govern substrate binding. *Proceedings of the National Academy of Sciences* 114(9), pp. 2218-2223. doi:10.1073/pnas.1612927114

Anderson, TM., Clay, MC., Cioffi, AG., Diaz, KA., Hisao, GS., Tuttle, MD., Nieuwkoop, AJ., Comellas, G., Maryum, N., Wang, S., Uno, BE., Wildeman, EL., Gonen, T., Rienstra, CM., and Burke, MD. (2014) Amphotericin forms an extramembranous and fungicidal sterol sponge. *Nature chemical biology* 10(5), pp. 400-406. https://doi.org/10.1038/nchembio.1496

Andrade, FF., Silva, D., Rodrigues, A. and Pina-Vaz, C. (2020) Colistin Update on Its Mechanism of Action and Resistance, Present and Future Challenges. *Microorganisms* 8(11), p. 1716. doi: 10.3390/microorganisms8111716.

Ann Chai, LY., Denning, DW. and Warn, P. (2010) *Candida tropicalis* in human disease. *Critical Reviews in Microbiology* 36(4), pp. 282-298. doi: 10.3109/1040841X.2010.489506

Antimicrobial Resistance Collaborators (2022) Global burden of bacterial antimicrobial resistance in 2019: a systematic analysis. *The Lancet* 399(10325), pp. 629-655. doi:10.1016/S0140-6736(21)02724-0

Arendrup, MC. and Patterson, TF. (2017) Multidrug-Resistant *Candida*: Epidemiology, Molecular Mechanisms, and Treatment. *The Journal of Infectious Diseases* 216(suppl_3), pp. S445-S451. doi: 10.1093/infdis/jix131

Ashikin, WHNS., Wong, TW. and Law, CL. (2010) Plasticity of hot air-dried mannuronate-and guluronate-rich alginate films. *Carbohydrate Polymers* 81(1), pp. 104-113. https://doi.org/10.1016/j.carbpol.2010.02.002

Aslam, SN., Newman, MA., Erbs, G., Morrissey, KL., Chinchilla, D., Boller, T., Jensen, TT., De Castro, C., Ierano, T., Molinaro, A., Jackson, RW., Knight, MR. and Cooper, RM. (2008) Bacterial polysaccharides suppress induced innate immunity by calcium chelation. *Current Biology* 18(14), pp. 1078-1083. doi: 10.1016/j.cub.2008.06.061

Aspinall, SA., Mackintosh, KA., Hill, DM., Cope, B. and McNarry, MA. (2022) Evaluating the Effect of Kaftrio on Perspectives of Health and Wellbeing in Individuals with Cystic Fibrosis. *Int J Environ Res Public Health* 19(10), doi: 10.3390/ijerph19106114

Ates, M., Akdeniz, BG. and Sen, BH. (2005) The effect of calcium chelating or binding agents on *Candida albicans*. *Oral Surgery, Oral Medicine, Oral Pathology,*

Oral Radiology, and Endodontology 100(5), pp. 626-630. https://doi.org/10.1016/j.tripleo.2005.03.004

Avedissian, SN., Liu, J., Rhodes, NJ., Lee, A., Pais, GM., Hauser, AR. and Scheetz, MH. (2019) A Review of the Clinical Pharmacokinetics of Polymyxin B. *Antibiotics* 8(1), p. 31. doi: 10.3390/antibiotics8010031.

Azimi, L. and Lari, AR. (2019) Colistin-resistant *Pseudomonas aeruginosa* clinical strains with defective biofilm formation. *GMS hygiene and infection control* 14, doi: 10.3205/dgkh000328

Bachiri, T., Lalaoui, R., Bakour, S., Allouache, M., Belkebla, N., Rolain, JM. and Touati, A. (2018) First report of the plasmid-mediated colistin resistance gene *mcr-1* in *Escherichia coli* ST405 isolated from wildlife in Bejaia, Algeria. *Microbial Drug Resistance* 24(7), pp. 890-895. doi: 10.1089/mdr.2017.0026.

Baddley, JW. and Poppas, PG. (2005) Antifungal Combination Therapy. *Drugs* 65(11), pp. 1461-1480. doi: 10.2165/00003495-200565110-00002

Baig, AA., Zulkiflee, NASB., Hassan, M., Rohin, MAKB., Johari, MKBZ., Latif, AZBA., Khan, MU, and Simbak, NB. (2021) Narrative review: Use of competent stimulating peptide in gene transfer via suicide plasmid in *Streptococcus pneumoniae*. *Advancements in Life Sciences* 8(2), pp. 211-216.

Baillie, GS. and Douglas, LJ. (1998) Effect of Growth Rate on Resistance of *Candida albicans* Biofilms to Antifungal Agents. *Antimicrobial Agents and Chemotherapy* 42(8), pp. 1900-1905. doi: 10.1128/AAC.42.8.1900

Ballance, S., Holtan, S., Aarstad, OA., Sikorski, P., Skjak-Braek, G. and Christensen, BE. (2005) Application of high-performance anion-exchange chromatography with pulsed amperometric detection and statistical analysis to study oligosaccharide distributions - a complementary method to investigate the structure and some properties of alginates. *Journal of Chromatography* A 1093(1-2), pp. 59-68. doi: 10.1016/j.chroma.2005.07.051

Bansil, R. and Turner, BS. (2018) The biology of mucus: Composition, synthesis and organization. *Advanced Drug Delivery Reviews* 124, pp. 3-15. doi: https://doi.org/10.1016/j.addr.2017.09.023

Bartie, KL., Williams, DW., Wilson, MJ., Potts, AJC. and Lewis, MAO. (2004) Differential invasion of *Candida albicans* isolates in an in vitro model of oral candidosis. *Oral Microbiology and Immunology* 19(5), pp. 293-296. doi: 10.1111/j.1399-302X.2004.00155.x

Bauters, TGM., Moerman, M., Vermeersch, H. and Nelis, HJ. (2002) Colonization of Voice Prostheses by Albicans and Non-Albicans *Candida* Species. *The Laryngoscope* 112(4), pp. 708-712. https://doi.org/10.1097/00005537-200204000-00021

Beceiro, A., Moreno, A., Fernández, N., Vallejo, JA., Aranda, J., Adler, B., Harper, M., Boyce, JD, and Bou, G. (2014) Biological Cost of Different Mechanisms of Colistin Resistance and Their Impact on Virulence in *Acinetobacter baumannii*. *Antimicrobial Agents and Chemotherapy* 58(1), pp. 518-526. doi: 10.1128/AAC.01597-13

Belik, A., Silchenko, A., Malyarenko, O., Rasin, A., Kiseleva, M., Kusaykin, M. and Ermakova, S. (2020) Two New Alginate Lyases of PL7 and PL6 Families from Polysaccharide-Degrading Bacterium Formosa algae KMM 3553T: Structure, Properties, and Products Analysis. *Marine Drugs* 18(2), p. 130. doi: 10.3390/md18020130

Bell, SC., Mall, MA., Gutierrez, H., Macek, M., Madge, S., Davies, JC., Burgel, PR., Tullis, E., Castaños, C., Castellani, C., Byrnes, CA., Cathcart, F., Chotirmall, SH., Cosgriff, R., Eichler, I., Fajac, I., Goss, CH., Drevinek, P., Farrell, PM., Gravelle, AM., Havermans, T., Mayer-Hamblett, N., Kashirskaya, N., Kerem, E., Mathew, JL., McKone, EF., Naehrlich, L., Nasr, SZ., Oates, GR., O'Neill, C., Pypops, U., Raraigh, KS., Rowe, SM., Southern, KW., Sivam, S., Stephenson, AL., Zampoli, M. and Ratjen F. (2020) The future of cystic fibrosis care: a global perspective. *The Lancet Respiratory Medicine* 8(1), pp. 65-124. doi: https://doi.org/10.1016/S2213-2600(19)30337-6

Bergen, PJ., Li, J., Rayner, CR. and Nation, RL. (2006) Colistin methanesulfonate is an inactive prodrug of colistin against *Pseudomonas aeruginosa*. *Antimicrobial agents and chemotherap*y 50(6), pp. 1953-1958. doi: 10.1128/AAC.00035-06.

Beringer, P. (2001) The clinical use of colistin in patients with cystic fibrosis. *Current Opinion in Pulmonary Medicine* 7(6), pp. 434-440. doi: 10.1097/00063198-200111000-00013.

Beveridge, TJ. (1999) Structures of Gram-Negative Cell Walls and Their Derived Membrane Vesicles. *Journal of Bacteriology* 181(16), pp. 4725-4733. doi: 10.1128/JB.181.16.4725-4733.1999.

Bi, D., Yao, L., Lin, Z., Chi, L., Li, H., Xu, H., Du, X., Liu, Q., Hu, Z., Lu, J. and Xu, X. (2021) Unsaturated mannuronate oligosaccharide ameliorates β-amyloid pathology through autophagy in Alzheimer's disease cell models. *Carbohydrate Polymers* 251, p. 117124. doi: https://doi.org/10.1016/j.carbpol.2020.117124

Bialvaei, AZ. and Samadi Kafil, H. (2015) Colistin, mechanisms and prevalence of resistance. *Current Medical Research and Opinion* 31(4), pp. 707-721. doi: 10.1185/03007995.2015.1018989

Blair, JMA., Webber, MA., Baylay, AJ., Ogbolu, DO. and Piddock, LJV. (2015) Molecular mechanisms of antibiotic resistance. *Nature Reviews Microbiology* 13(1), pp. 42-51. doi: 10.1038/nrmicro3380

BNF. (2023) Colistimethate sodium. https://bnf.nice.org.uk/drugs/colistimethate-sodium/ [Accessed: 01/06/2023]

Boles, BR., Thoendel, M. and Singh, PK. (2005) Rhamnolipids mediate detachment of *Pseudomonas aeruginosa* from biofilms. *Molecular Microbiology* 57(5), pp. 1210-1223. https://doi.org/10.1111/j.1365-2958.2005.04743.x

Bongomin, F., Gago, S., Oladele, RO. and Denning, DW. (2017) Global and Multi-National Prevalence of Fungal Diseases—Estimate Precision. *Journal of Fungi* 3(4), doi: 10.3390/jof3040057

Borgogna, M., Skjåk-Bræk, G., Paoletti, S. and Donati, I. (2013) On the Initial Binding of Alginate by Calcium Ions. The Tilted Egg-Box Hypothesis. *The Journal of Physical Chemistry B* 117(24), pp. 7277-7282. doi: 10.1021/jp4030766

Boueroy, P., Wongsurawat, T., Jenjaroenpun, P., Chopjitt, P., Hatrongjit, R., Jittapalapong, S. and Kerdsin, A. (2022) Plasmidome in *mcr-1* harboring carbapenem-resistant enterobacterales isolates from human in Thailand. *Scientific Reports* 12(1), p. 19051. doi: 10.1038/s41598-022-21836-7

Brown, DG., Wobst, HJ., Kapoor, A., Kenna, LA. and Southall, N. (2022) Clinical development times for innovative drugs. *Nature reviews. Drug discovery* 21(11), pp. 793-794. doi: 10.1038/d41573-021-00190-9

Brown, GD., Denning, DW., Gow, NAR., Levitz, SM., Netea, MG. and White, TC. (2012) Hidden Killers: Human Fungal Infections. *Science Translational Medicine* 4(165), pp. 165rv113-165rv113. doi: 10.1126/scitranslmed.3004404

Bruker. (2022) Guide to Infrared Spectroscopy. https://www.bruker.com/en/products-and-solutions/infrared-and-raman/ft-ir-routine-spectrometer/what-is-ft-ir-spectroscopy.html: [Accessed: 10/11/22].

Bulman, ZP., Chen, L., Walsh, TJ., Satlin, MJ., Qian, Y., Bulitta, JB., Peloquin, CA., Holden, PN., Nation, RL., Li, J., Kreiswirth, BN. and Suji BT. (2017) Polymyxin Combinations Combat *Escherichia coli* Harboring *mcr-1* and blaNDM-5: Preparation for a Postantibiotic Era. *mBio* 8(4), pp. e00540-00517. doi: 10.1128/mBio.00540-17

Bush, K. (2012) Antimicrobial agents targeting bacterial cell walls and cell membranes. *Rev Sci Tech* 31(1), pp. 43-56. doi: 10.20506/rst.31.1.2096

Bush, K. and Bradford, PA. (2016) β-Lactams and β-Lactamase Inhibitors: An Overview. *Cold Spring Harbor Perspectives in Medicine* 6(8), doi: 10.1101/cshperspect.a025247

Caiazza, NC., Shanks, RMQ. and O'Toole, GA. (2005) Rhamnolipids Modulate Swarming Motility Patterns of *Pseudomonas aeruginosa. Journal of Bacteriology* 187(21), pp. 7351-7361. doi:10.1128/JB.187.21.7351-7361.2005

Calderone, RA. and Fonzi, WA. (2001) Virulence factors of *Candida albicans. Trends in Microbiology* 9(7), pp. 327-335. doi: 10.1016/S0966-842X(01)02094-7

Camargo, C., Narula, T., Jackson, DA., Padro, T. and Freeman, WD. (2021) Colistin neurotoxicity mimicking Guillain-Barré syndrome in a patient with cystic fibrosis: case report and review. *Oxford Medical Case Reports* 2021(9), p. omab080. doi: 10.1093/omcr/omab080

Campoy, S. and Adrio, JL. (2017) Antifungals. *Biochemical Pharmacology* 133, pp. 86-96. doi: 10.1016/j.bcp.2016.11.019

Cantin, AM., Hartl, D., Konstan, MW. and Chmiel, JF. (2015) Inflammation in cystic fibrosis lung disease: Pathogenesis and therapy. *Journal of Cystic Fibrosis* 14(4), pp. 419-430. https://doi.org/10.1016/j.jcf.2015.03.003

Canuto, MM. and Rodero, FG. (2002) Antifungal drug resistance to azoles and polyenes. *The Lancet Infectious Diseases* 2(9), pp. 550-563. doi: 10.1016/S1473-3099(02)00371-7

Casalinuovo, IA., Sorge, R., Bonelli, G. and Di Francesco, P. (2017) Evaluation of the antifungal effect of EDTA, a metal chelator agent, on *Candida albicans* biofilm. *European review for medical and pharmacological sciences* 21(6), pp. 1413-1420.

Castellani, C. and Assael, BM. (2017) Cystic fibrosis: a clinical view. *Cellular and Molecular Life Sciences* 74(1), pp. 129-140. doi: 10.1007/s00018-016-2393-9

CDC. (2019) General Information about *Candida auris*.

Chaffin, WL. (2008) *Candida albicans* Cell Wall Proteins. *Microbiology and Molecular Biology Reviews* 72(3), pp. 495-544. doi: 10.1128/MMBR.00032-07

Chahine, EB., Dougherty, JA., Thornby, KA. and Guirguis, EH. (2022) Antibiotic Approvals in the Last Decade: Are We Keeping Up With Resistance? *Annals of Pharmacotherapy* 56(4), pp. 441-462. doi: 10.1177/10600280211031390

Chen, HD. and Groisman, EA. (2013) The biology of the PmrA/PmrB two-component system: the major regulator of lipopolysaccharide modifications. *Annual review of microbiology* 67, pp. 83-112. doi: 10.1146/annurev-micro-092412-155751

Chen, L. and Wen, YM. (2011) The role of bacterial biofilm in persistent infections and control strategies. *International Journal of Oral Science* 3(2), pp. 66-73. doi: 10.4248/IJOS11022

Cheng, SC., Joosten, LAB., Kullberg, BJ. and Netea, MG. (2012) Interplay between *Candida albicans* and the Mammalian Innate Host Defense. *Infection and Immunity* 80(4), pp. 1304-1313. doi: 10.1128/IAI.06146-11

Chiang, WC., Schroll, C., Hilbert, LR., Møller, P. and Tolker-Nielsen, T. (2009) Silver-palladium surfaces inhibit biofilm formation. *Applied and Environmental Microbiology* 75(6), pp. 1674-1678. doi: 10.1128/AEM.02274-08

Chiang, YN., Penadés, JR. and Chen, J. (2019) Genetic transduction by phages and chromosomal islands: The new and noncanonical. *PLoS Pathogens* 15(8), p. e1007878. doi: 10.1371/journal.ppat.1007878

Childers, DS., Avelar, GM., Bain, JM., Pradhan, A., Larcombe, DE., Netea, MG., Erwig, LP., Gow, NAR. and Brown, AJP. (2020) Epitope Shaving Promotes Fungal Immune Evasion. *mBio* 11(4), pp. e00984-00920. doi:10.1128/mBio.00984-20

Cižman, M. and Plankar Srovin, T. (2018) Antibiotic consumption and resistance of gram-negative pathogens (collateral damage). *GMS Infect Dis* 6, p. Doc05. doi: 10.3205/id000040

Clausell, A., Garcia-Subirats, M., Pujol, M., Busquets, M. A., Rabanal, F. and Cajal, Y. (2007) Gram-Negative Outer and Inner Membrane Models: Insertion of Cyclic Cationic Lipopeptides. *The Journal of Physical Chemistry* B 111(3), pp. 551-563. doi: 10.1021/jp064757+

Coates, A. R., Halls, G. and Hu, Y. (2011) Novel classes of antibiotics or more of the same? *Br J Pharmacol* 163(1), pp. 184-194. doi: 10.1111/j.1476-5381.2011.01250.x

Colavecchio, A., Cadieux, B., Lo, A. and Goodridge, LD. (2017) Bacteriophages Contribute to the Spread of Antibiotic Resistance Genes among Foodborne Pathogens of the Enterobacteriaceae Family – A Review. *Frontiers in Microbiology* 8, doi: 10.3389/fmicb.2017.01108

Coleman, DC., Sullivan, DJ., Bennett, DE., Moran, GP., Barry, HJ. and Shanley, DB. (1997) Candidiasis: the emergence of a novel species: *Candida dubliniensis*. *AIDS* 11(5), pp. 557-567. doi: 10.1097/00002030-199705000-00002.

Cook, MA. and Wright, GD. (2022) The past, present, and future of antibiotics. *Science Translational Medicine* 14(657), p. eabo7793. doi:10.1126/scitranslmed.abo7793

Cornelis, P. (2020) Putting an end to the *Pseudomonas aeruginosa* IQS controversy. *Microbiology Open* 9(2), p. e962. https://doi.org/10.1002/mbo3.962

Corriveau, S., Sykes, J. and Stephenson, AL. (2018) Cystic fibrosis survival: the changing epidemiology. *Current Opinion in Pulmonary Medicine* 24(6), doi: 10.1097/MCP.0000000000000520.

Costerton, J. (1999) Introduction to biofilm. *International Journal of Antimicrobial Agents* 11(3-4), pp. 217-221. doi: 10.1016/S0924-8579(99)00018-7

Costerton, JW., Lewandowski, Z., Caldwell, DE., Korber, DR. and Lappin-Scott, HM. (1995) Microbial Biofilms. *Annual Review of Microbiology* 49(1), pp. 711-745. doi: 10.1146/annurev.mi.49.100195.003431

Cowell, BA., Twining, SS., Hobden, JA., Kwong, MSF. and Fleiszig, SMJ. (2003) Mutation of *lasA* and *lasB* reduces *Pseudomonas aeruginosa* invasion of epithelial cells. *Microbiology* 149(8), pp. 2291-2299. https://doi.org/10.1099/mic.0.26280-0

Cox, G. and Wright, GD. (2013) Intrinsic antibiotic resistance: Mechanisms, origins, challenges, and solutions. *International Journal of Medical Microbiology* 303(6), pp. 287-292. doi: 10.1016/j.ijmm.2013.02.009

Cuenca-Estrella, M., Bernal-Martinez, L., Buitrago, MJ., Castelli, MV., Gomez-Lopez, A., Zaragoza, O. and Rodriguez-Tudela, JL. (2008) Update on the epidemiology and diagnosis of invasive fungal infection. *International Journal of Antimicrobial Agents* 32 Suppl 2, pp. S143-147. doi: 10.1016/S0924-8579(08)70016-5

Ćwiek, K., Woźniak-Biel, A., Karwańska, M., Siedlecka, M., Lammens, C., Rebelo, AR., Hendriksen, RS., Kuczkowski, M., Chmielewska-Władyka, M. and Wieliczko, A. (2021) Phenotypic and genotypic characterization of *mcr-1*-positive multidrug-resistant *Escherichia coli* ST93, ST117, ST156, ST10, and ST744 isolated from poultry in Poland. *Brazilian Journal of Microbiology* 52(3), pp. 1597-1609. doi: 10.1007/s42770-021-00538-8

Cystic Fibrosis Foundation. (2022) 2021 Patient Registry Annual Report.

Dadashi, M., Sameni, F., Bostanshirin, N., Yaslianifard, S., Khosravi-Dehaghi, N., Nasiri, MJ., Goudarzi, M., Hashemi, A. and Hajikhani, B. (2022) Global prevalence and molecular epidemiology of *mcr*-mediated colistin resistance in *Escherichia coli* clinical isolates: a systematic review. *Journal of Global Antimicrobial Resistance* 29, pp. 444-461. doi: https://doi.org/10.1016/j.jgar.2021.10.022

Dafopoulou, K., Xavier, BB., Hotterbeekx, A., Janssens, L., Lammens, C., Dé, E., Goossens, H., Tsakris, A., Malhotra-Kumar, S. and Pournaras, S. (2016) Colistin-Resistant *Acinetobacter baumannii* Clinical Strains with Deficient Biofilm Formation. *Antimicrobial Agents and Chemotherapy* 60(3), pp. 1892-1895. doi: 10.1128/AAC.02518-15

Das, T. and Manefield, M. (2012) Pyocyanin promotes extracellular DNA release in *Pseudomonas aeruginosa.* PLoS ONE 7(10): e46718. https://doi.org/10.1371/journal.pone.0046718

Davey, ME., Caiazza, NC. and O'Toole, GA. (2003) Rhamnolipid Surfactant Production Affects Biofilm Architecture in *Pseudomonas aeruginosa* PAO1. *Journal of Bacteriology* 185(3), pp. 1027-1036. doi:10.1128/JB.185.3.1027-1036.2003

Davies, J. (2006) Where have All the Antibiotics Gone? *Can J Infect Dis Med Microbiol* 17(5), pp. 287-290. doi: 10.1155/2006/707296

De Bernardis, F., Arancia, S., Morelli, L., Hube, B., Sanglard, D., Schäfer, W. and Cassone, A. (1999) Evidence that members of the secretory aspartyl proteinase gene family, in particular SAP2, are virulence factors for *Candida vaginitis*. *The Journal of infectious diseases* 179(1), pp. 201-208. doi: 10.1086/314546.

De Boeck, K. and Amaral, MD. (2016) Progress in therapies for cystic fibrosis. *The Lancet Respiratory Medicine* 4(8), pp. 662-674. https://doi.org/10.1016/S2213-2600(16)00023-0

De Boeck, K., Vermeulen, F. and Dupont, L. (2017) The diagnosis of cystic fibrosis. *La Presse Médicale* 46(6, Part 2), pp. e97-e108. https://doi.org/10.1016/j.lpm.2017.04.010

Delaloye, J. and Calandra, T. (2014) Invasive candidiasis as a cause of sepsis in the critically ill patient. *Virulence* 5(1), pp. 161-169. doi: 10.4161/viru.26187

Delhaes, L., Monchy, S., Fréalle, E., Hubans, C., Salleron, J., Leroy, S., Prevotat, A., Wallet, F., Wallaert, B., Dei-Cas, E., Sime-Ngando, T., Chabé, M. and Viscogliosi, E. (2012) The Airway Microbiota in Cystic Fibrosis: A Complex Fungal and Bacterial Community—Implications for Therapeutic Management. *PLOS ONE* 7(4), doi: 10.1371/journal.pone.0036313

Denning, DW. (2003) Echinocandin antifungal drugs. *The Lancet* 362(9390), pp. 1142-1151. doi: 10.1016/S0140-6736(03)14472-8

Denning, GM., Railsback, MA., Rasmussen, GT., Cox, CD. and Britigan, BE. (1998) *Pseudomonas* pyocyanine alters calcium signaling in human airway epithelial cells. *American Journal of Physiology Lung Cellular and Molecular Physiology* 274(6), pp. L893-L900. doi: 10.1152/ajplung.1998.274.6.L893

Deorukhkar, SC., Saini, S. and Mathew, S. (2014a). Non-albicans *Candida* Infection: An Emerging Threat. *Interdisciplinary Perspectives on Infectious Diseases* p. e615958. doi: 10.1155/2014/615958

Deorukhkar, SC., Saini, S. and Mathew, S. (2014b). Virulence Factors Contributing to Pathogenicity of *Candida tropicalis* and Its Antifungal Susceptibility Profile. *International Journal of Microbiology* p. 456878. doi: 10.1155/2014/456878

Déziel, E., Lépine, F., Milot, S. and Villemur, R. (2003) rhlA is required for the production of a novel biosurfactant promoting swarming motility in *Pseudomonas aeruginosa*: 3-(3-hydroxyalkanoyloxy)alkanoic acids (HAAs), the precursors of

rhamnolipids. *Microbiology* 149(8), pp. 2005-2013. https://doi.org/10.1099/mic.0.26154-0

Dhariwal, A. and Tullu, M. (2013) Colistin: re-emergence of the 'forgotten' antimicrobial agent. *Journal of postgraduate medicine* 59(3), p. 208. doi: 10.4103/0022-3859.118040

Dinos, GP., Athanassopoulos, CM., Missiri, DA., Giannopoulou, PC., Vlachogiannis, IA., Papadopoulos, GE., Papaioannou, D. and Kalpaxis, DL. (2016) Chloramphenicol Derivatives as Antibacterial and Anticancer Agents: Historic Problems and Current Solutions. *Antibiotics* 5(2), p. 20. doi: 10.3390/antibiotics5020020.

Dominguez, E., Zarnowskim R., Sanchezm H., Covelli, AS., Westler, WM., Azadi, P., Nett, J., Mitchell, AP. and Andes, DR. (2018) Conservation and Divergence in the *Candida* Species Biofilm Matrix Mannan-Glucan Complex Structure, Function, and Genetic Control. *mBio* 9(2), pp. e00451-00418. doi: doi:10.1128/mBio.00451-18

Donati, I. and Paoletti, S. (2009) Material Properties of Alginates. In: Rehm, B. (eds) *Alginates: Biology and Applications*. Microbiology Monographs, vol 13. Springer, Berlin, Heidelberg. https://doi.org/10.1007/978-3-540-92679-5_1

Donlan, RM. (2001) Biofilm Formation: A Clinically Relevant Microbiological Process. *Clinical Infectious Diseases* 33(8), pp. 1387-1392. doi: 10.1086/322972

Douglas, LJ. (2003) *Candida* biofilms and their role in infection. *Trends in Microbiology* 11(1), pp. 30-36. doi: 10.1016/S0966-842X(02)00002-1

Dreier, J. and Ruggerone, P. (2015) Interaction of antibacterial compounds with RND efflux pumps in *Pseudomonas aeruginosa*. Frontiers in Microbiology 6, doi: 10.3389/fmicb.2015.00660

Du, H., Bing, J., Hu, T., Ennis, CL., Nobile, CJ. and Huang, G. (2020) *Candida auris:* Epidemiology, biology, antifungal resistance, and virulence. *PLoS Pathogens* 16(10), p. e1008921. doi: 10.1371/journal.ppat.1008921

Du, H., Chen, L., Tang, YW. and Kreiswirth, BN. (2016) Emergence of the *mcr-1* colistin resistance gene in carbapenem-resistant *Enterobacteriaceae*. *The Lancet Infectious Diseases* 16(3), pp. 287-288. doi: 10.1016/S1473-3099(16)00056-6.

Duan, K. and Surette, MG. (2007) Environmental regulation of *Pseudomonas aeruginosa* PAO1 Las and Rhl quorum-sensing systems. *Journal of bacteriology* 189(13), pp. 4827-4836. doi: 10.1128/JB.00043-07.

Dufour, D., Leung, V. and Lévesque, CM. (2010) Bacterial biofilm: structure, function, and antimicrobial resistance. *Endodontic Topics* 22(1), pp. 2-16. https://doi.org/10.1111/j.1601-1546.2012.00277.x

Dunne, WM. (2002) Bacterial adhesion: seen any good biofilms lately? *Clinical Microbiology Reviews* 15(2), pp. 155-166. doi: 10.1128/cmr.15.2.155-166.2002

Dutta, A. (2017). Chapter 4 - Fourier Transform Infrared Spectroscopy. In: Thomas, S., Thomas, R., Zachariah, A.K. and Mishra, R.K. eds. *Spectroscopic Methods for Nanomaterials Characterization*. Elsevier, pp. 73-93.

Egan, AJF., Cleverley, RM., Peters, K., Lewis, RJ. and Vollmer, W. (2017) Regulation of bacterial cell wall growth. *The FEBS Journal* 284(6), pp. 851-867. https://doi.org/10.1111/febs.13959

Eggimann, P., Garbino, J. and Pittet, D. (2003) Epidemiology of *Candida* species infections in critically ill non-immunosuppressed patients. *The Lancet Infectious Diseases* 3(11), pp. 685-702. doi: 10.1016/S1473-3099(03)00801-6

El-Sayed Ahmed, M. AEG., Zhong, LL., Shen, C., Yang, Y., Doi, Y. and Tian, GB. (2020) Colistin and its role in the Era of antibiotic resistance: an extended review (2000–2019). *Emerging Microbes & Infections* 9(1), pp. 868-885. doi: 10.1080/22221751.2020.1754133

El Garch, F., Sauget, M., Hocquet, D., LeChaudee, D., Woehrle, F. and Bertrand, X. (2017) *mcr-1* is borne by highly diverse *Escherichia coli* isolates since 2004 in food-producing animals in Europe. *Clinical Microbiology and Infection* 23(1), pp. 51. e51-51. e54. doi: 10.1016/j.cmi.2016.08.033.

Elias, R., Duarte, A. and Perdigão, J. (2021) A Molecular Perspective on Colistin and *Klebsiella pneumoniae*: Mode of Action, Resistance Genetics, and Phenotypic Susceptibility. *Diagnostics (Basel)* 11(7), doi: 10.3390/diagnostics11071165

Eliopoulos, GM., Perea, S. and Patterson, TF. (2002) Antifungal Resistance in Pathogenic Fungi. *Clinical Infectious Diseases* 35(9), pp. 1073-1080. doi: 10.1086/344058

Elving, GJ., van der Mei, HC., Busscher, HJ., Amerongen, AVN., Veerman, ECI., van Weissenbruch, R. and Albers, FWJ. (2000) Antimicrobial Activity of Synthetic Salivary Peptides Against Voice Prosthetic Microorganisms. *The Laryngoscope* 110(2), pp. 321-321. https://doi.org/10.1097/00005537-200002010-00027

EMA. (2019) Categorisation of Antibiotics in the European Union. Answer to the Request from the European Commission for Updating the Scientific Advice on the Impact on Public Health and Animal Health of the Use of Antibiotics in Animals. https://www.ema.europa.eu/en/documents/report/categorisation-antibiotics-european-union-answer-request-european-commission-updating-scientific_en.pdf:

Enoch, DA., Ludlam, HA. and Brown, NM. (2006) Invasive fungal infections: a review of epidemiology and management options. *Journal of Medical Microbiology* 55(7), pp. 809-818. doi: 10.1099/jmm.0.46548-0

Ermund, A., Recktenwald, CV., Skjåk-Braek, G., Meiss, LN., Onsøyen, E., Rye, PD., Dessen, A., Myrset, AH. and Hansson, GC. (2017) OligoG CF-5/20 normalizes cystic fibrosis mucus by chelating calcium. *Clinical and Experimental Pharmacology and Physiology* 44(6), pp. 639-647. doi: 10.1111/1440-1681.12744

Ertesvåg, H., Sletta, H., Senneset, M., Sun, YQ., Klinkenberg, G., Konradsen, TA., Ellingsen, TE. and Valla, S. (2017) Identification of genes affecting alginate biosynthesis in *Pseudomonas fluorescens* by screening a transposon insertion library. *BMC Genomics* 18(1), p.11. doi: 10.1186/s12864-016-3467-7

Escalante, A., Gattuso, M., Pérez, P. and Zacchino, S. (2008) Evidence for the mechanism of action of the antifungal phytolaccoside B isolated from Phytolacca tetramera Hauman. *Journal of Natural Products* 71(10), pp. 1720-1725. doi: 10.1021/np070660i.

Esposito, F., Fernandes, MR., Lopes, R., Muñoz, M., Sabino, CP., Cunha, MP., Silva, KC., Cayô, R., Martins, WMBS., Moreno, AM., Knöbl, T., Gales, AC. and Lincopan, N. (2017) Detection of Colistin-Resistant MCR-1-Positive *Escherichia coli* by Use of Assays Based on Inhibition by EDTA and Zeta Potential. *Journal of Clinical Microbiology* 55(12), pp. 3454-3465. doi:10.1128/jcm.00835-17

Falagas, ME. and Kasiakou, SK. (2006) Toxicity of polymyxins: a systematic review of the evidence from old and recent studies. *Critical Care* 10(1), p. R27. doi: 10.1186/cc3995

Falagas, ME., Kasiakou, SK. and Saravolatz, LD. (2005) Colistin: The Revival of Polymyxins for the Management of Multidrug-Resistant Gram-Negative Bacterial Infections. *Clinical Infectious Diseases* 40(9), pp. 1333-1341. doi: 10.1086/429323

Faria, SI., Teixeira-Santos, R., Romeu, MJ., Morais, J., Vasconcelos, V. and Mergulhão, FJ. (2020) The relative importance of shear forces and surface hydrophobicity on biofilm formation by coccoid cyanobacteria. *Polymers* 12(3), p. 653. https://doi.org/10.3390/polym12030653

Faure, E., Kwong, K. and Nguyen, D. (2018) *Pseudomonas aeruginosa* in Chronic Lung Infections: How to Adapt Within the Host? *Frontiers in Immunology* 9, doi: 10.3389/fimmu.2018.02416

Faustino, C. and Pinheiro, L. (2020) Lipid Systems for the Delivery of Amphotericin B in Antifungal Therapy. *Pharmaceutics* 12(1), p. 29. doi: 10.3390/pharmaceutics12010029.

Fauvart, M., Phillips, P., Bachaspatimayum, D., Verstraeten, N., Fransaer, J., Michiels, J. and Vermant, J. (2012) Surface tension gradient control of bacterial swarming in colonies of *Pseudomonas aeruginosa*. *Soft Matter* 8(1), pp. 70-76. doi: 10.1039/C1SM06002C

Fazli, M., Almblad, H., Rybtke, ML., Givskov, M., Eberl, L. and Tolker-Nielsen, T. (2014) Regulation of biofilm formation in *Pseudomonas* and *Burkholderia* species. *Environmental Microbiology* 16(7), pp. 1961-1981. https://doi.org/10.1111/1462-2920.12448

Fazli, M., Bjarnsholt, T., Kirketerp-Møller, K., Jørgensen, B., Andersen, AS., Krogfelt, KA., Givskov, M. and Tolker-Nielsen, T. (2009) Nonrandom Distribution of *Pseudomonas aeruginosa* and *Staphylococcus aureus* in Chronic Wounds. *Journal of Clinical Microbiology* 47(12), pp. 4084-4089. doi: 10.1128/JCM.01395-09

Fernandes, MR., Moura, Q., Sartori, L., Silva, KC., Cunha, MP., Esposito, F., Lopes, R., Otutumi, LK., Gonçalves, DD., Dropa, M., Matté, MH., Monte, DF., Landgraf, M., Francisco, GR., Bueno, MF., de Oliveira Garcia, D., Knöbl, T., Moreno, AM. and Lincopan, N. (2016) Silent dissemination of colistin-resistant *Escherichia coli* in South America could contribute to the global spread of the *mcr-1* gene. *Eurosurveillance* 21(17), p. 30214. doi: 10.2807/1560-7917.ES.2016.21.17.30214.

Fertah, M. (2017) Chapter 2 - Isolation and Characterization of Alginate from Seaweed. In: Venkatesan, J., Anil, S. and Kim, SK. eds. Seaweed Polysaccharides. *Elsevier*, pp. 11-26.

Fidel, PL., Vazquez, JA. and Sobel, JD. (1999) *Candida glabrata*: Review of Epidemiology, Pathogenesis, and Clinical Disease with Comparison to *C. albicans. Clinical Microbiology* Reviews 12(1), pp. 80-96. doi: 10.1128/CMR.12.1.80

Fischer, R., Schwarz, C., Weiser, R., Mahenthiralingam, E., Smerud, K., Meland, N., Flaten, H. and Rye, PD. (2022) Evaluating the alginate oligosaccharide (OligoG) as a therapy for *Burkholderia cepacia* complex cystic fibrosis lung infection. *J Cyst Fibros* 21(5), pp. 821-829. doi: 10.1016/j.jcf.2022.01.003

Fisher, MC., Alastruey-Izquierdo, A., Berman, J., Bicanic, T., Bignell, EM., Bowyer, P., Bromley, M., Brüggemann, R., Garber, G., Cornely, OA., Gurr, SJ., Harrison, TS., Kuijper, E., Rhodes, J., Sheppard, DC., Warris, A., White, PL., Xu, J., Zwaan, B. and Verweij, PE. (2022) Tackling the emerging threat of antifungal resistance to human health. *Nature Reviews Microbiology* 20(9), pp. 557-571. doi: 10.1038/s41579-022-00720-1

Fleming, A. (1929) On the Antibacterial Action of Cultures of a Penicillium, with Special Reference to their Use in the Isolation of *B. influenzæ*. *Br J Exp Pathol.* 1929 Jun;10(3):226-36.

Flemming, HC. and Wingender, J. (2010) The biofilm matrix. *Nature Reviews Microbiology* 8(9), pp. 623-633. doi: 10.1038/nrmicro2415

Flemming, HC., Neu, TR. and Wozniak, DJ. (2007) The EPS matrix: the "house of biofilm cells". *Journal of Bacteriology* 189(22), pp. 7945-7947. doi: 10.1128/jb.00858-07

Fothergill, JL., Panagea, S., Hart, CA., Walshaw, MJ., Pitt, TL. and Winstanley, C. (2007) Widespread pyocyanin over-production among isolates of a cystic fibrosis epidemic strain. *BMC microbiology* 7(1), p. 45. doi: 10.1186/1471-2180-7-45

Foti, C., Piperno, A., Scala, A. and Giuffrè, O. (2021) Oxazolidinone antibiotics: chemical, biological and analytical aspects. *Molecules* 26(14), p. 4280. doi: 10.3390/molecules26144280.

Fournier, C., Aires-de-Sousa, M., Nordmann, P. and Poirel, L. (2020) Occurrence of CTX-M-15-and MCR-1-producing Enterobacterales in pigs in Portugal: Evidence of direct links with antibiotic selective pressure. *International Journal of Antimicrobial Agents* 55(2), p. 105802. doi: 10.1016/j.ijantimicag.2019.09.006.

Fraser, GM. and Hughes, C. (1999) Swarming motility. *Current Opinion in Microbiology* 2(6), pp. 630-635. doi: 10.1016/S1369-5274(99)00033-8

Frost, DJ., Brandt, KD., Cugier, D. and Goldman, R. (1995) A whole-cell *Candida albicans* assay for the detection of inhibitors towards fungal cell wall synthesis and assembly. *The Journal of Antibiotics* 48(4), pp. 306-310. doi: 10.7164/antibiotics.48.306.

Galdiero, S., Falanga, A., Cantisani, M., Tarallo, R., Pepa, MED., D'Oriano, V. and Galdiero, M. (2012) Microbe-Host Interactions: Structure and Role of Gram-Negative Bacterial Porins. *Current Protein & Peptide Science* 13(8), pp. 843-854. doi: 10.2174/138920312804871120

Garcia-Cuesta, C., Sarrion-Pérez, MG. and Bagán, JV. (2014) Current treatment of oral candidiasis: A literature review. *Journal of Clinical and Experimental Dentistry* 6(5), pp. e576-e582. doi: 10.4317/jced.51798

García-Reyes, S., Soberón-Chávez, G. and Cocotl-Yanez, M. (2020) The third quorum-sensing system of *Pseudomonas aeruginosa*: Pseudomonas quinolone signal

and the enigmatic PqsE protein. *Journal of Medical Microbiology* 69(1), pp. 25-34. https://doi.org/10.1099/jmm.0.001116

Garrett, TR., Bhakoo, M. and Zhang, Z. (2008) Bacterial adhesion and biofilms on surfaces. *Progress in Natural Science* 18(9), pp. 1049-1056. doi: 10.1016/j.pnsc.2008.04.001

Gattlen, J., Amberg, C., Zinn, M. and Mauclaire, L. (2010) Biofilms isolated from washing machines from three continents and their tolerance to a standard detergent. *Biofouling* 26(8), pp. 873-882. doi: 10.1080/08927014.2010.524297

Ghannoum, MA. and Rice, LB. (1999) Antifungal Agents: Mode of Action, Mechanisms of Resistance, and Correlation of These Mechanisms with Bacterial Resistance. *Clinical Microbiology Reviews* 12(4), pp. 501-517. doi: 10.1128/CMR.12.4.501.

Gimmestad, M., Sletta, H., Ertesvåg, H., Bakkevig, K., Jain, S., Suh, SJ., Skjåk-Braek, G., Ellingsen, TE., Ohman, DE. and Valla, S. (2003) The *Pseudomonas fluorescens* AlgG protein, but not its mannuronan C-5-epimerase activity, is needed for alginate polymer formation. *J Bacteriol.* 2003 Jun;185(12):3515-23. doi: 10.1128/JB.185.12.3515-3523.2003.

Goltermann, L. and Tolker-Nielsen, T. (2017) Importance of the Exopolysaccharide Matrix in Antimicrobial Tolerance of *Pseudomonas aeruginosa* Aggregates. *Antimicrobial Agents and Chemotherapy* 61(4), pp. e02696-02616. doi: 10.1128/AAC.02696-16

Goss, CH. and Burns, JL. (2007) Exacerbations in cystic fibrosis. 1: Epidemiology and pathogenesis. *Thorax* 62(4), pp. 360-367. doi: 10.1136/thx.2006.060889

Goss, CH. and Muhlebach, MS. (2011) Review: *Staphylococcus aureus* and MRSA in cystic fibrosis. *Journal of Cystic Fibrosis* 10(5), pp. 298-306. https://doi.org/10.1016/j.jcf.2011.06.002

GOV.UK. (2022) Tackling antimicrobial resistance 2019 to 2024: addendum to the UK's 5-year national action plan. https://www.gov.uk/government/publications/addendum-to-the-uk-5-year-action-

plan-for-antimicrobial-resistance-2019-to-2024/tackling-antimicrobial-resistance-2019-to-2024-addendum-to-the-uks-5-year-national-action-plan#optimising-use-of-antimicrobials.

Gow, NAR., Latge, JP. and Munro, CA. (2017) The Fungal Cell Wall: Structure, Biosynthesis, and Function. *Microbiology Spectrum* 5(3), doi: 10.1128/microbiolspec.FUNK-0035-2016

Gow, NAR., van de Veerdonk, FL., Brown, AJP. and Netea, MG. (2012) *Candida albicans* morphogenesis and host defence: discriminating invasion from colonization. *Nature Reviews Microbiology* 10(2), pp. 112-122. doi: 10.1038/nrmicro2711

Grada, A. and Bunick, CG. (2021) Spectrum of Antibiotic Activity and Its Relevance to the Microbiome. *JAMA Network Open* 4(4), pp. e215357-e215357. doi: 10.1001/jamanetworkopen.2021.5357

Graf, FE., Palm, M., Warringer, J. and Farewell, A. (2019) Inhibiting conjugation as a tool in the fight against antibiotic resistance. *Drug Development Research* 80(1), pp. 19-23. https://doi.org/10.1002/ddr.21457

Grover, ND. (2010) Echinocandins: A ray of hope in antifungal drug therapy. *Indian J Pharmacol* 42(1), pp. 9-11. doi: 10.4103/0253-7613.62396

Guilhen, C., Forestier, C. and Balestrino, D. (2017) Biofilm dispersal: multiple elaborate strategies for dissemination of bacteria with unique properties. *Molecular Microbiology* 105(2), pp. 188-210. https://doi.org/10.1111/mmi.13698

Hahn-Ast, C., Glasmacher, A., Mückter, S., Schmitz, A., Kraemer, A., Marklein, G., Brossart, P. and von Lilienfeld-Toal, M. (2010) Overall survival and fungal infection-related mortality in patients with invasive fungal infection and neutropenia after myelosuppressive chemotherapy in a tertiary care centre from 1995 to 2006. *Journal of Antimicrobial Chemotherapy* 65(4), pp. 761-768. doi: 10.1093/jac/dkp507

Haiko, J., Saeedi, B., Bagger, G., Karpati, F. and Özenci, V. (2019) Coexistence of *Candida* species and bacteria in patients with cystic fibrosis. *European Journal of Clinical Microbiology & Infectious Diseases* 38(6), pp. 1071-1077. doi: 10.1007/s10096-019-03493-3

Hajjeh, RA., Sofair, AN., Harrison, LH., Lyon, GM., Arthington-Skaggs, BA., Mirza, SA., Phelan, M., Morgan, J., Lee-Yang, W., Ciblak, MA., Benjamin, LE., Sanza, LT., Huie, S., Yeo, SF., Brandt, ME. and Warnock, DW. (2004) Incidence of Bloodstream Infections Due to *Candida* Species and In Vitro Susceptibilities of Isolates Collected from 1998 to 2000 in a Population-Based Active Surveillance Program. *Journal of Clinical Microbiology* 42(4), pp. 1519-1527. doi: 10.1128/JCM.42.4.1519-1527.2004

Hall, RA. and Gow, NAR. (2013) Mannosylation in *Candida albicans*: role in cell wall function and immune recognition. *Molecular Microbiology* 90(6), pp. 1147-1161. doi: 10.1111/mmi.12426

Hao, Y., Kuang, Z., Walling, BE., Bhatia, S., Sivaguru, M., Chen, Y., Gaskins, HR. and Lau, GW. (2012) *Pseudomonas aeruginosa* pyocyanin causes airway goblet cell hyperplasia and metaplasia and mucus hypersecretion by inactivating the transcriptional factor FoxA2. *Cell Microbiol* 14(3), pp. 401-415. doi: 10.1111/j.1462-5822.2011.01727.x

Harriott, MM. and Noverr, MC. (2009) *Candida albicans* and *Staphylococcus aureus* Form Polymicrobial Biofilms: Effects on Antimicrobial Resistance. *Antimicrobial Agents and Chemotherapy* 53(9), pp. 3914-3922. doi:10.1128/AAC.00657-09

Harriott, MM. and Noverr, MC. (2011) Importance of *Candida*–bacterial polymicrobial biofilms in disease. *Trends in Microbiology* 19(11), pp. 557-563. https://doi.org/10.1016/j.tim.2011.07.004

Harrison, JJ., Turner, RJ. and Ceri, H. (2007) A subpopulation of *Candida albicans* and *Candida tropicalis* biofilm cells are highly tolerant to chelating agents. *FEMS Microbiol Lett* 272(2), pp. 172-181. doi: 10.1111/j.1574-6968.2007.00745.x

Hassan, HM. and Fridovich, I. (1980) Mechanism of the antibiotic action pyocyanine. *Journal of Bacteriology* 141(1), pp. 156-163. doi:10.1128/jb.141.1.156-163.1980

Havlickova, B., Czaika, VA. and Friedrich, M. (2008) Epidemiological trends in skin mycoses worldwide. *Mycoses* 51(s4), pp. 2-15. doi: 10.1111/j.1439-0507.2008.01606.x

Hengzhuang, W., Song, Z., Ciofu, O., Onsøyen, E., Rye, PD. and Høiby, N. (2016) OligoG CF-5/20 Disruption of Mucoid *Pseudomonas aeruginosa* Biofilm in a Murine Lung Infection Model. *Antimicrobial Agents and Chemotherapy* 60(5), pp. 2620-2626. doi: 10.1128/AAC.01721-15

Hengzhuang, W., Wu, H., Ciofu, O., Song, Z. and Høiby, N. (2011) Pharmacokinetics/pharmacodynamics of colistin and imipenem on mucoid and nonmucoid *Pseudomonas aeruginosa* biofilms. *Antimicrobial Agents and Chemotherapy* 55(9), pp. 4469-4474. doi: 10.1128/aac.00126-11

Hentzer, M., Eberl, L., Nielsen, J. and Givskov, M. (2003) Quorum Sensing. *BioDrugs* 17(4), pp. 241-250. doi: 10.2165/00063030-200317040-00003

Hernández, M., Iglesias, MR., Rodríguez-Lázaro, D., Gallardo, A., Quijada, N., Miguela-Villoldo, P., Campos, MJ., Píriz, S., López-Orozco, G., de Frutos, C., Sáez, JL., Ugarte-Ruiz, M., Domínguez, L. and Quesada, A. (2017) Co-occurrence of colistin-resistance genes mcr-1 and mcr-3 among multidrug-resistant *Escherichia coli* isolated from cattle, Spain, September 2015. *Euro Surveill.* 2017 Aug 3;22(31):30586. doi: 10.2807/1560-7917.ES.2017.22.31.30586.

Heydorn, A., Nielsen, AT., Hentzer, M., Sternberg, C., Givskov, M., Ersbøll, BK. and Molin, S. (2000) Quantification of biofilm structures by the novel computer program COMSTAT. *Microbiology,* 146 (Pt 10), pp. 2395-2407. doi: 10.1099/00221287-146-10-2395

Hifney, AF., Soliman, Z., Ali, EF. and Hussein, NA. (2022) Microbial and microscopic investigations to assess the susceptibility of *Candida parapsilosis* and *Prototheca ciferrii* to phyco-synthesized titanium dioxide nanoparticles and antimicrobial drugs. *South African Journal of Botany* 151, pp. 791-799. https://doi.org/10.1016/j.sajb.2022.11.004

Hills, OJ., Yong, CW., Scott, AJ., Smith, J. and Chappell, HF. (2022) Polyguluronate simulations shed light onto the therapeutic action of OligoG CF-5/20. *Bioorganic & Medicinal Chemistry* 72, p. 116945. https://doi.org/10.1016/j.bmc.2022.116945

Hintsche, M., Waljor, V., Großmann, R., Kühn, MJ., Thormann, KM., Peruani, F. and Beta, C. (2017) A polar bundle of flagella can drive bacterial swimming by pushing, pulling, or coiling around the cell body. *Scientific Reports* 7(1), p. 16771. doi: 10.1038/s41598-017-16428-9

Hogardt, M. and Heesemann, J. (2010) Adaptation of *Pseudomonas aeruginosa* during persistence in the cystic fibrosis lung. *International Journal of Medical Microbiology* 300(8), pp. 557-562. https://doi.org/10.1016/j.ijmm.2010.08.008

Høiby, N., Bjarnsholt, T., Givskov, M., Molin, S. and Ciofu, O. (2010a) Antibiotic resistance of bacterial biofilms. *International Journal of Antimicrobial Agents* 35(4), pp. 322-332. doi: 10.1016/j.ijantimicag.2009.12.011

Høiby, N., Bjarnsholt, T., Moser, C., Jensen, PØ., Kolpen, M., Qvist, T., Aanaes, K., Pressler, T., Skov, M. and Ciofu, O. (2017) Diagnosis of biofilm infections in cystic fibrosis patients. *APMIS* 125(4), pp. 339-343. https://doi.org/10.1111/apm.12689

Høiby, N., Ciofu, O. and Bjarnsholt, T. (2010b) *Pseudomonas aeruginosa* biofilms in cystic fibrosis. *Future Microbiology* 5(11), pp. 1663-1674. doi: 10.2217/fmb.10.125

Holden, M., Swift, S. and Williams, P. (2000) New signal molecules on the quorum-sensing block. *Trends in Microbiology* 8(3), pp. 101-103. doi: 10.1016/S0966-842X(00)01718-2

Holtan, S., Zhang, QJ., Strand, WI. and Skjak-Braek, G. (2006) Characterization of the hydrolysis mechanism of polyalternating alginate in weak acid and assignment of the resulting MG-oligosaccharides by NMR spectroscopy and ESI-mass spectrometry. *Biomacromolecules* 7(7), pp. 2108-2121. doi: 10.1021/bm050984q

Hoyer, LL. and Cota, E. (2016) *Candida albicans* Agglutinin-Like Sequence (Als) Family Vignettes: A Review of Als Protein Structure and Function. *Frontiers in Microbiology* 7, doi: 10.3389/fmicb.2016.00280

Hoyer, LL., Green, CB., Oh, SH. and Zhao, X. (2008) Discovering the secrets of the *Candida albicans* agglutinin-like sequence (ALS) gene family — a sticky pursuit. *Medical Mycology* 46(1), pp. 1-15. doi: 10.1080/13693780701435317

Hu, X., Jiang, X., Gong, J., Hwang, H., Liu, Y. and Guan, H. (2005) Antibacterial activity of lyase-depolymerized products of alginate. *Journal of Applied Phycology* 17(1), pp. 57-60. doi: 10.1007/s10811-005-5524-5

Huang, Y., Chen, Y. and Zhang, LH. (2020) The Roles of Microbial Cell-Cell Chemical Communication Systems in the Modulation of Antimicrobial Resistance. *Antibiotics (Basel)* 9(11), doi: 10.3390/antibiotics9110779

Hussein, NH., Al-Kadmy, IMS., Taha, BM. and Hussein, JD. (2021) Mobilized colistin resistance (*mcr*) genes from 1 to 10: a comprehensive review. *Mol Biol Rep* 48(3), pp. 2897-2907. doi: 10.1007/s11033-021-06307-y

Hutchings, MI., Truman, AW. and Wilkinson, B. (2019) Antibiotics: past, present, and future. *Current Opinion in Microbiology* 51, pp. 72-80. https://doi.org/10.1016/j.mib.2019.10.008

Imlay, JA. (2015) Diagnosing oxidative stress in bacteria: not as easy as you might think. *Current Opinion in Microbiology* 24, pp. 124-131. https://doi.org/10.1016/j.mib.2015.01.004

Iram, JH., Michael, AG., James, PG., Christopher, W. and Malcolm, B. (2016) Airway surface liquid homeostasis in cystic fibrosis: pathophysiology and therapeutic targets. *Thorax* 71(3), p. 284. doi: 10.1136/thoraxjnl-2015-207588

Irrgang, A., Roschanski, N., Tenhagen, BA., Grobbel, M., Skladnikiewicz-Ziemer, T., Thomas, K., Roesler, U. and Käsbohrer, A. (2016) Prevalence of *mcr-1* in *E. coli* from Livestock and Food in Germany, 2010–2015. *PLOS ONE* 11(7), p. e0159863. doi: 10.1371/journal.pone.0159863

Jack, AA., Khan, S., Powell, LC., Pritchard, MF., Beck, K., Sadh, H., Sutton, L., Cavaliere, A., Florance, H., Rye, PD., Thomas, DW. and Hill, KE. (2018) Alginate Oligosaccharide-Induced Modification of the lasI-lasR and rhlI-rhlR Quorum-Sensing Systems in *Pseudomonas aeruginosa*. *Antimicrobial Agents and Chemotherapy* 62(5), doi: 10.1128/AAC.02318-17

Jacoby, GA. and Han, P. (1996) Detection of extended-spectrum beta-lactamases in clinical isolates of *Klebsiella pneumoniae* and *Escherichia coli. J Clin Microbiol* 34(4), pp. 908-911. doi: 10.1128/jcm.34.4.908-911.1996

Jafari, F. and Elyasi, S. (2021) Prevention of colistin induced nephrotoxicity: a review of preclinical and clinical data. *Expert Review of Clinical Pharmacology* 14(9), pp. 1113-1131. doi: 10.1080/17512433.2021.1933436

Jayaseelan, S., Ramaswamy, D. and Dharmaraj, S. (2014) Pyocyanin: production, applications, challenges, and new insights. *World Journal of Microbiology and Biotechnology* 30(4), pp. 1159-1168. doi: 10.1007/s11274-013-1552-5

Jeffery-Smith, A., Taori, SK., Schelenz, S., Jeffery, K., Johnson, EM. and Borman, A. (2018) *Candida auris*: a Review of the Literature. *Clinical Microbiology Reviews 31*(1), doi: 10.1128/CMR.00029-17

Jia, C., Zhang, J., Zhuge, Y., Xu, K., Liu, J., Wang, J., Li, L. and Chu, M. (2019) Synergistic effects of geldanamycin with fluconazole are associated with reactive oxygen species in *Candida tropicalis* resistant to azoles and amphotericin B. *Free Radical Research* 53(6), pp. 618-628. doi: 10.1080/10715762.2019.1610563

Jiang, Y., Geng, M. and Bai, L. (2020) Targeting Biofilms Therapy: Current Research Strategies and Development Hurdles. *Microorganisms* 8(8), doi: 10.3390/microorganisms8081222

Josenhans, C. and Suerbaum, S. (2002) The role of motility as a virulence factor in bacteria. *International Journal of Medical Microbiology* 291(8), pp. 605-614. doi: 10.1078/1438-4221-00173

Jovetic, S., Zhu, Y., Marcone, GL., Marinelli, F. and Tramper, J. (2010) β-Lactam and glycopeptide antibiotics: first and last line of defense? *Trends in Biotechnology* 28(12), pp. 596-604. https://doi.org/10.1016/j.tibtech.2010.09.004

Juhas, M., Eberl, L. and Tümmler, B. (2005) Quorum sensing: the power of cooperation in the world of *Pseudomonas*. *Environmental Microbiology* 7(4), pp. 459-471. doi: 10.1111/j.1462-2920.2005.00769.x.

Kaleli, I., Cevahir, N., Demir, M., Yildirim, U. and Sahin, R. (2007) Anticandidal activity of *Pseudomonas aeruginosa* strains isolated from clinical specimens. *Mycoses* 50(1), pp. 74-78. doi: 10.1111/j.1439-0507.2006.01322.x.

Kalia, VC. (2013) Quorum sensing inhibitors: An overview. *Biotechnology Advances* 31(2), pp. 224-245. https://doi.org/10.1016/j.biotechadv.2012.10.004

Kaplan, JB. (2010) Biofilm dispersal: mechanisms, clinical implications, and potential therapeutic uses. *J Dent Res* 89(3), pp. 205-218. doi: 10.1177/0022034509359403

Kapoor, G., Saigal, S. and Elongavan, A. (2017) Action and resistance mechanisms of antibiotics: A guide for clinicians. *J Anaesthesiol Clin Pharmacol* 33(3), pp. 300-305. doi: 10.4103/joacp.JOACP_349_15

Kaur, SP., Rao, R. and Nanda, S. (2011) Amoxicillin: a broad-spectrum antibiotic. *Int J Pharm Pharm Sci* 3(3), pp. 30-37.

Kazarian, SG. and Chan, KLA. (2006) Applications of ATR-FTIR spectroscopic imaging to biomedical samples. *Biochimica et Biophysica Acta (BBA) - Biomembranes* 1758(7), pp. 858-867. https://doi.org/10.1016/j.bbamem.2006.02.011

Ke, WJ., Hsueh, YH., Cheng, YC., Wu, CC. and Liu, ST. (2015) Water surface tension modulates the swarming mechanics of *Bacillus subtilis. Frontiers in Microbiology* 6, doi: 10.3389/fmicb.2015.01017

Kearns, DB. (2010) A field guide to bacterial swarming motility. *Nature Reviews Microbiology* 8(9), pp. 634-644. doi: 10.1038/nrmicro2405

Kempf, I., Jouy, E. and Chauvin, C. (2016) Colistin use and colistin resistance in bacteria from animals. *International Journal of Antimicrobial Agents* 48(6), pp. 598-606. https://doi.org/10.1016/j.ijantimicag.2016.09.016

Kerem, BS., Rommens, JM., Buchanan, JA., Markiewicz, D., Cox, TK., Chakravarti, A., Buchwald, M. and Tsui, LC. (1989) Identification of the cystic fibrosis gene: genetic analysis. *Science* 245(4922), pp. 1073-1080.

Kerr, CJ., Osborn, KS., Rickard, AH., Robson, GD. and Handley, PS. (2003) Biofilms in water distribution systems. In: *Mara, D. and Horan, N. eds. Handbook of Water and Wastewater Microbiology. London: Academic Press*, pp. 757-775.

Khan, S., Tøndervik, A., Sletta, H., Klinkenberg, G., Emanuel, C., Onsøyen, E., Myrvold, R., Howe, RA., Walsh, TR., Hill, KE. and Thomas, DW. (2012) Overcoming Drug Resistance with Alginate Oligosaccharides Able To Potentiate the Action of Selected Antibiotics. *Antimicrobial Agents and Chemotherapy 56*(10), pp. 5134-5141. doi: 10.1128/AAC.00525-12

Kievit, TRD. and Iglewski, BH. (2000) Bacterial Quorum Sensing in Pathogenic Relationships. *Infection and Immunity* 68(9), pp. 4839-4849. doi: 10.1128/IAI.68.9.4839-4849.2000

Kim, DW. (2018) Non-reducing end unsaturated mannuronic acid oligosaccharides and compositions containing same as active ingredient. *Google Patents.*

King, J., Brunel, SF. and Warris, A. (2016) *Aspergillus* infections in cystic fibrosis. *Journal of Infection* 72, pp. S50-S55. https://doi.org/10.1016/j.jinf.2016.04.022

Kohanski, MA., Dwyer, DJ., Hayete, B., Lawrence, CA. and Collins, JJ. (2007) A common mechanism of cellular death induced by bactericidal antibiotics. *Cell* 130(5), pp. 797-810. doi: 10.1016/j.cell.2007.06.049.

Krause, KM., Serio, AW., Kane, TR. and Connolly, LE. (2016) Aminoglycosides: An Overview. *Cold Spring Harbor Perspectives in Medicine 6*(6), doi: 10.1101/cshperspect.a027029

Kreutzberger, MA., Pokorny, A. and Almeida, PF. (2017) Daptomycin-Phosphatidylglycerol Domains in Lipid Membranes. *Langmuir: the ACS journal of surfaces and colloids* 33(47), pp. 13669-13679. doi: 10.1021/acs.langmuir.7b01841

Kuang, Z., Hao, Y., Walling, BE., Jeffries, JL., Ohman, DE. and Lau, GW. (2011) *Pseudomonas aeruginosa* Elastase Provides an Escape from Phagocytosis by Degrading the Pulmonary Surfactant Protein-A. *PLOS ONE* 6(11), p. e27091. doi: 10.1371/journal.pone.0027091

Kuhn, DM., Chandra, J., Mukherjee, PK. and Ghannoum, MA. (2002) Comparison of Biofilms Formed by *Candida albicans* and *Candida parapsilosis* on Bioprosthetic

Surfaces. *Infection and Immunity* 70(2), pp. 878-888. doi:10.1128/IAI.70.2.878-888.2002

Lai, S., Tremblay, J. and Déziel, E. (2009) Swarming motility: a multicellular behaviour conferring antimicrobial resistance. *Environmental Microbiology* 11(1), pp. 126-136. https://doi.org/10.1111/j.1462-2920.2008.01747.x

Lambert, PA. (2002) Mechanisms of antibiotic resistance in *Pseudomonas aeruginosa. Journal of the Royal Society of Medicine* 95(Suppl 41), pp. 22-26.

Landman, D., Georgescu, C., Martin, DA. and Quale, J. (2008) Polymyxins revisited. *Clinical microbiology reviews* 21(3), pp. 449-465. doi: 10.1128/CMR.00006-08.

Lau, GW., Hassett, DJ., Ran, H. and Kong, F. (2004) The role of pyocyanin in *Pseudomonas aeruginosa* infection. *Trends in Molecular Medicine* 10(12), pp. 599-606. doi: 10.1016/j.molmed.2004.10.002

Lee, JY., Choi, MJ., Choi Hyeon, J. and Ko Kwan, S. (2015) Preservation of Acquired Colistin Resistance in Gram-Negative Bacteria. *Antimicrobial Agents and Chemotherapy* 60(1), pp. 609-612. doi: 10.1128/AAC.01574-15

Lee, J., Wu, J., Deng, Y., Wang, J., Wang, C., Wang, J., Chang, C., Dong, Y., Williams, P. and Zhang, LH. (2013) A cell-cell communication signal integrates quorum sensing and stress response. *Nature chemical biology* 9(5), pp. 339-343.

Lee, J. and Zhang, L. (2015) The hierarchy quorum sensing network in *Pseudomonas aeruginosa. Protein & Cell* 6(1), pp. 26-41. doi: 10.1007/s13238-014-0100-x

Lee, KY. and Mooney, DJ. (2012) Alginate: properties and biomedical applications. *Progress in polymer science* 37(1), pp. 106-126. doi: 10.1016/j.progpolymsci.2011.06.003

Leite, MCA., de Brito Bezerra, AP., de Sousa, JP. and de Oliveira Lima, E. (2015) Investigating the antifungal activity and mechanism(s) of geraniol against *Candida albicans* strains. *Medical Mycology* 53(3), pp. 275-284. doi: 10.1093/mmy/myu078

Leung, V., Ajdic, D., Koyanagi, S. and Lévesque Céline, M. (2015) The Formation of *Streptococcus mutans* Persisters Induced by the Quorum-Sensing Peptide Pheromone Is Affected by the LexA Regulator. *Journal of Bacteriology* 197(6), pp. 1083-1094. doi: 10.1128/JB.02496-14

Lewis, BW., Patial, S. and Saini, Y. (2019) Immunopathology of Airway Surface Liquid Dehydration Disease. *Journal of Immunology Research* 2019, p. 2180409. doi: 10.1155/2019/2180409

Lewis PD, Lewis KE, Ghosal R, Bayliss S, Lloyd AJ, Wills J, Godfrey R, Kloer P, Mur LA. Evaluation of FTIR spectroscopy as a diagnostic tool for lung cancer using sputum. BMC Cancer. 2010 Nov 23;10:640. doi: 10.1186/1471-2407-10-640.

Li, B., Yin, F., Zhao, X., Guo, Y., Wang, W., Wang, P., Zhu, H., Yin, Y. and Wang, X. (2020a). Colistin Resistance Gene *mcr-1* Mediates Cell Permeability and Resistance to Hydrophobic Antibiotics. *Frontiers in Microbiology* 10, doi: 10.3389/fmicb.2019.03015

Li, M. (2023) Assessment of the global impact of MCR-1/MCR-3 mediated colistin resistance. Thesis. *Cardiff University.*

Li, Q., Mao, S., Wang, H. and Ye, X. (2022) The Molecular Architecture of *Pseudomonas aeruginosa* Quorum-Sensing Inhibitors. *Marine Drugs* 20(8), p. 488. doi: 10.3390/md20080488.

Li, R., Xie, M., Zhang, J., Yang, Z., Liu, L., Liu, X., Zheng, Z., Chan, EW. and Chen, S. (2017) Genetic characterization of *mcr-1*-bearing plasmids to depict molecular mechanisms underlying dissemination of the colistin resistance determinant. *Journal of Antimicrobial Chemotherapy* 72(2), pp. 393-401. doi: 10.1093/jac/dkw411

Li, WR., Zeng, TH., Xie, XB., Shi, QS. and Li, CL. (2020b) Inhibition of the pqsABCDE and pqsH in the pqs quorum sensing system and related virulence factors of the *Pseudomonas aeruginosa* PAO1 strain by farnesol. *International Biodeterioration & Biodegradation* 151, p. 104956. https://doi.org/10.1016/j.ibiod.2020.104956

Lima, LM., Silva, BNMD., Barbosa, G. and Barreiro, EJ. (2020) β-lactam antibiotics: An overview from a medicinal chemistry perspective. *European Journal of Medicinal Chemistry* 208, p. 112829. https://doi.org/10.1016/j.ejmech.2020.112829

Liu, F., Zhang, Z., Csanády, L., Gadsby, DC. and Chen, J. (2017a) Molecular Structure of the Human CFTR Ion Channel. *Cell* 169(1), pp. 85-95.e88. doi: 10.1016/j.cell.2017.02.024

Liu, JC., Modha, DE. and Gaillard, EA. (2013) What is the clinical significance of filamentous fungi positive sputum cultures in patients with cystic fibrosis? *Journal of Cystic Fibrosis* 12(3), pp. 187-193. https://doi.org/10.1016/j.jcf.2013.02.003

Liu, YY., Chandler, CE., Leung, LM., McElheny, CL., Mettus, RT., Shanks, RMQ., Liu, JH., Goodlett, DR., Ernst, RK. and Doi, Y. (2017b) Structural Modification of Lipopolysaccharide Conferred by *mcr-1* in Gram-Negative ESKAPE Pathogens. *Antimicrobial Agents and Chemotherapy* 61(6), pp. e00580-00517. doi: 10.1128/AAC.00580-17

Liu, YY., Wang, Y., Walsh, TR., Yi, LX., Zhang, R., Spencer, J., Doi, Y., Tian, G., Dong, B., Huang, X., Yu, LF., Gu, D., Ren, H., Chen, X., Lv, L., He, D., Zhou, H., Liang, Z., Liu, JH. and Shen, J. (2016) Emergence of plasmid-mediated colistin resistance mechanism MCR-1 in animals and human beings in China: a microbiological and molecular biological study. *The Lancet Infectious Diseases* 16(2), pp. 161-168. doi: 10.1016/S1473-3099(15)00424-7

Liu, YY., Zhou, Q., He, W., Lin, Q., Yang, J. and Liu, JH. (2020) *mcr-1* and plasmid prevalence in *Escherichia coli* from livestock. *The Lancet Infectious Diseases* 20(10), p. 1126. doi: 10.1016/S1473-3099(20)30697-6.

Loho, T. and Dharmayanti, A. (2015) Colistin: an antibiotic and its role in multiresistant Gram-negative infections. *Acta Med Indones* 47(2), pp. 157-168.

López-Rojas, R., McConnell Michael, J., Jiménez-Mejías Manuel, E., Domínguez-Herrera, J., Fernández-Cuenca, F. and Pachón, J. (2013) Colistin Resistance in a Clinical *Acinetobacter baumannii* Strain Appearing after Colistin Treatment: Effect on Virulence and Bacterial Fitness. *Antimicrobial Agents and Chemotherapy* 57(9), pp. 4587-4589. doi: 10.1128/AAC.00543-13

Lorite, GS., Rodrigues, CM., de Souza, AA., Kranz, C., Mizaikoff, B. and Cotta, MA. (2011) The role of conditioning film formation and surface chemical changes on *Xylella fastidiosa* adhesion and biofilm evolution. *Journal of Colloid and Interface Science* 359(1), pp. 289-295. doi: 10.1016/j.jcis.2011.03.066

Luepke, KH., Suda, KJ., Boucher, H., Russo, RL., Bonney, MW., Hunt, TD. and Mohr III, JF. (2017) Past, Present, and Future of Antibacterial Economics: Increasing Bacterial Resistance, Limited Antibiotic Pipeline, and Societal Implications. *Pharmacotherapy: The Journal of Human Pharmacology and Drug Therapy* 37(1), pp. 71-84. https://doi.org/10.1002/phar.1868

Luo, S., Skerka, C., Kurzai, O. and Zipfel, PF. (2013) Complement and innate immune evasion strategies of the human pathogenic fungus *Candida albicans. Molecular Immunology* 56(3), pp. 161-169. https://doi.org/10.1016/j.molimm.2013.05.218

Lupetti, A., Danesi, R., Campa, M., Tacca, MD. and Kelly, S. (2002) Molecular basis of resistance to azole antifungals. *Trends in Molecular Medicine* 8(2), pp. 76-81. doi: 10.1016/S1471-4914(02)02280-3

Ma, H., Zhao, X., Yang, L., Su, P., Fu, P., Peng, J., Yang, N. and Guo, G. (2020) Antimicrobial Peptide AMP-17 Affects *Candida albicans* by Disrupting Its Cell Wall and Cell Membrane Integrity. *Infection and Drug Resistance* 13, pp. 2509-2520. doi: 10.2147/idr.S250278

Ma, K., Feng, Y. and Zong, Z. (2018) Fitness cost of a *mcr-1*-carrying IncHI2 plasmid. *PLOS ONE* 13(12), p. e0209706. doi: 10.1371/journal.pone.0209706

Magiorakos, AP., Srinivasan, A., Carey, RB., Carmeli, Y., Falagas, ME., Giske, CG., Harbarth, S., Hindler, JF., Kahlmeter, G., Olsson-Liljequist, B., Paterson, DL., Rice, LB., Stelling, J., Struelens, MJ., Vatopoulos, A., Weber, JT. and Monnet, DL. (2012) Multidrug-resistant, extensively drug-resistant, and pandrug-resistant bacteria: an international expert proposal for interim standard definitions for acquired resistance. *Clinical Microbiology and Infection* 18(3), pp. 268-281. https://doi.org/10.1111/j.1469-0691.2011.03570.x

Mah, TF. (2012) Biofilm-specific antibiotic resistance. *Future Microbiol* 7(9), pp. 1061-1072. doi: 10.2217/fmb.12.76

Mall, MA. and Galietta, LJV. (2015) Targeting ion channels in cystic fibrosis. *Journal of Cystic Fibrosis* 14(5), pp. 561-570. https://doi.org/10.1016/j.jcf.2015.06.002

Mall, MA. and Hartl, D. (2014) CFTR: cystic fibrosis and beyond. *European Respiratory Journal* 44(4), pp. 1042-1054. doi: 10.1183/09031936.00228013

Malone, JG. (2015) Role of small colony variants in persistence of *Pseudomonas aeruginosa* infections in cystic fibrosis lungs. *Infection and Drug Resistance* 8, pp. 237-247. doi: 10.2147/IDR.S68214

Mann, EE. and Wozniak, DJ. (2012) *Pseudomonas* biofilm matrix composition and niche biology. *FEMS Microbiology Reviews* 36(4), pp. 893-916. doi: 10.1111/j.1574-6976.2011.00322.x

Manner, S. and Fallarero, A. (2018) Screening of Natural Product Derivatives Identifies Two Structurally Related Flavonoids as Potent Quorum Sensing Inhibitors against Gram-Negative Bacteria. *International Journal of Molecular Sciences* 19(5), p. 1346. doi: 10.3390/ijms19051346

Marr, AK., Overhage, J., Bains, M. and Hancock, REWYR. (2007) The Lon protease of *Pseudomonas aeruginosa* is induced by aminoglycosides and is involved in biofilm formation and motility. *Microbiology* 153(2), pp. 474-482. doi: 10.1099/mic.0.2006/002519-0

Marsh, PD., Do, T., Beighton, D. and Devine, DA. (2016) Influence of saliva on the oral microbiota. *Periodontology* 2000 70(1), pp. 80-92. https://doi.org/10.1111/prd.12098

Martin, C. and Burgel, PR. (2020) Carriers of a single CFTR mutation are asymptomatic: an evolving dogma? *European Respiratory Journal* 56(3), p. 2002645. doi: 10.1183/13993003.02645-2020

Martínez, FV., Muñoz Pamplona, MP., García, EC. and Urzaiz, AG. (2007) Delayed hypersensitivity to oral nystatin. *Contact Dermatitis* 57(3), pp. 200-201. doi: 10.1111/j.1600-0536.2007.01110.x

Maschmeyer, G. (2006) The changing epidemiology of invasive fungal infections: new threats. *International Journal of Antimicrobial Agents* 27, pp. 3-6. doi: 10.1016/j.ijantimicag.2006.03.006

Matamoros, S., van Hattem, JM., Arcilla, MS., Willemse, N., Melles, DC., Penders, J., Vinh, TN., Thi Hoa, N., Bootsma, MCJ., van Genderen, PJ., Goorhuis, A., Grobusch, M., Molhoek, N., Oude Lashof, AML., Stobberingh, EE., Verbrugh, HA., de Jong, MD. and Schultsz, C. (2017) Global phylogenetic analysis of *Escherichia coli* and plasmids carrying the *mcr-1* gene indicates bacterial diversity but plasmid restriction. *Scientific Reports* 7(1), p. 15364. doi: 10.1038/s41598-017-15539-7

Matsumoto-Nakano, M. (2018) Role of *Streptococcus mutans* surface proteins for biofilm formation. *Jpn Dent Sci Rev* 54(1), pp. 22-29. doi: 10.1016/j.jdsr.2017.08.002

Mattmann, ME. and Blackwell, HE. (2010) Small Molecules That Modulate Quorum Sensing and Control Virulence in *Pseudomonas aeruginosa. The Journal of Organic Chemistry* 75(20), pp. 6737-6746. doi: 10.1021/jo101237e

Mavrodi, DV., Bonsall, RF., Delaney, SM., Soule, MJ., Phillips, G. and Thomashow, LS. (2001) Functional Analysis of Genes for Biosynthesis of Pyocyanin and Phenazine-1-Carboxamide from *Pseudomonas aeruginosa* PAO1. *Journal of Bacteriology* 183(21), pp. 6454-6465. doi:10.1128/JB.183.21.6454-6465.2001

Mayer, FL., Wilson, D. and Hube, B. (2013) *Candida albicans* pathogenicity mechanisms. *Virulence* 4(2), pp. 119-128. doi: 10.4161/viru.22913

Maza, PK., Bonfim-Melo, A., Padovan, ACB., Mortara, RA., Orikaza, CM., Ramos, LMD., Moura, TR., Soriani, FM., Almeida, RS., Suzuki, E. and Bahia, D. (2017) *Candida albicans:* The Ability to Invade Epithelial Cells and Survive under Oxidative Stress Is Unlinked to Hyphal Length. *Frontiers in Microbiology* 8, doi: 10.3389/fmicb.2017.01235

McBennett, KA., Davis, PB. and Konstan, MW. (2022) Increasing life expectancy in cystic fibrosis: Advances and challenges. *Pediatr Pulmonol* 57 Suppl 1(Suppl 1), pp. S5-s12. doi: 10.1002/ppul.25733

McDougald, D., Rice, SA., Barraud, N., Steinberg, PD. and Kjelleberg, S. (2012) Should we stay or should we go: mechanisms and ecological consequences for biofilm dispersal. *Nature Reviews Microbiology* 10(1), pp. 39-50. doi: 10.1038/nrmicro2695

McKnight, SL., Iglewski, BH. and Pesci, EC. (2000) The Pseudomonas Quinolone Signal Regulates *rhl* Quorum Sensing in *Pseudomonas aeruginosa. Journal of Bacteriology 182*(10), pp. 2702-2708. doi:10.1128/JB.182.10.2702-2708.2000

McPhee, JB., Bains, M., Winsor, G., Lewenza, S., Kwasnicka, A., Brazas, MD., Brinkman, FS. and Hancock, RE. (2006) Contribution of the PhoP-PhoQ and PmrA-PmrB two-component regulatory systems to Mg^{2+} induced gene regulation in *Pseudomonas aeruginosa. Journal of bacteriology* 188(11), pp. 3995-4006. doi: 10.1128/JB.00053-06

Méar, JB., Kipnis, E., Faure, E., Dessein, R., Schurtz, G., Faure, K. and Guery, B. (2013) *Candida albicans* and *Pseudomonas aeruginosa* interactions: More than an opportunistic criminal association? *Médecine et Maladies Infectieuses* 43(4), pp. 146-151. https://doi.org/10.1016/j.medmal.2013.02.005

Meinersmann, RJ. (2019) The biology of IncI2 plasmids shown by whole-plasmid multi-locus sequence typing. *Plasmid* 106, p. 102444. https://doi.org/10.1016/j.plasmid.2019.102444

Meinersmann, RJ., Ladely, SR., Plumblee, JR., Cook, KL. and Thacker, E. (2017) Prevalence of *mcr-1* in the cecal contents of food animals in the United States. *Antimicrobial agents and chemotherapy* 61(2), pp. e02244-02216.

Melander, RJ., Zurawski, DV. and Melander, C. (2018) Narrow-spectrum antibacterial agents. *Medchemcomm* 9(1), pp. 12-21.

Mesa-Arango, AC., Scorzoni, L. and Zaragoza, O. (2012) It only takes one to do many jobs: Amphotericin B as antifungal and immunomodulatory drug. *Frontiers in Microbiology* 3, doi: 10.3389/fmicb.2012.00286

Michalopoulos, AS. and Karatza, DC. (2010) Multidrug-resistant Gram-negative infections: the use of colistin. *Expert Review of Anti-infective Therapy* 8(9), pp. 1009-1017. doi: 10.1586/eri.10.88

Miller, MB. and Bassler, BL. (2001) Quorum Sensing in Bacteria. *Annual Review of Microbiology* 55(1), pp. 165-199. doi: 10.1146/annurev.micro.55.1.165

Miller, WR., Bayer, AS. and Arias, CA. (2016) Mechanism of Action and Resistance to Daptomycin in *Staphylococcus aureus* and *Enterococci*. *Cold Spring Harbor Perspectives in Medicine* 6(11), doi: 10.1101/cshperspect.a026997

Mmatli, M., Mbelle, NM. and Osei Sekyere, J. (2022) Global epidemiology, genetic environment, risk factors and therapeutic prospects of *mcr* genes: A current and emerging update. *Frontiers in Cellular and Infection Microbiology* 12, doi: 10.3389/fcimb.2022.941358

Moffatt, JH., Harper, M., Adler, B., Nation Roger, L., Li, J. and Boyce John, D. (2011) Insertion Sequence ISAba11 Is Involved in Colistin Resistance and Loss of Lipopolysaccharide in *Acinetobacter baumannii*. *Antimicrobial Agents and Chemotherapy* 55(6), pp. 3022-3024. doi: 10.1128/AAC.01732-10

Moffatt, JH., Harper, M., Harrison, P., Hale, JD., Vinogradov, E., Seemann, T., Henry, R., Crane, B., St Michael, F., Cox, AD., Adler, B., Nation, RL., Li, J. and Boyce, JD. (2010) Colistin Resistance in *Acinetobacter baumannii* Is Mediated by Complete Loss of Lipopolysaccharide Production. *Antimicrobial Agents and Chemotherapy* 54(12), pp. 4971-4977. doi: 10.1128/AAC.00834-10

Molero, G., Díez-Orejas, R., Navarro-García, F., Monteoliva, L., Pla, J., Gil, C., Sánchez-Pérez, M. and Nombela, C. (1998) *Candida albicans:* genetics, dimorphism, and pathogenicity. *International Microbiology* 1(2), pp. 95-106.

Morio, F., Pagniez, F., Lacroix, C., Miegeville, M. and Le Pape, P. (2012) Amino acid substitutions in the *Candida albicans* sterol Δ5,6-desaturase (Erg3p) confer azole resistance: characterization of two novel mutants with impaired virulence. *Journal of Antimicrobial Chemotherapy* 67(9), pp. 2131-2138. doi: 10.1093/jac/dks186

Morrison, CB., Markovetz, MR. and Ehre, C. (2019) Mucus, mucins, and cystic fibrosis. *Pediatr Pulmonol* 54 Suppl 3(Suppl 3), pp. S84-s96. doi: 10.1002/ppul.24530

Mulcahy, H., Charron-Mazenod, L. and Lewenza, S. (2008) Extracellular DNA Chelates Cations and Induces Antibiotic Resistance in *Pseudomonas aeruginosa* Biofilms. *PLoS Pathogens* 4(11), doi: 10.1371/journal.ppat.1000213

Muñoz, P., Giannella, M., Fanciulli, C., Guinea, J., Valerio, M., Rojas, L., Rodríguez-Créixems, M. and Bouza, E. (2011) *Candida tropicalis* fungaemia: incidence, risk factors and mortality in a general hospital. *Clinical Microbiology and Infection* 17(10), pp. 1538-1545. doi: 10.1111/j.1469-0691.2010.03338.x

Murciano, C., Moyes, DL., Runglall, M., Tobouti, P., Islam, A., Hoyer, LL. and Naglik, JR. (2012) Evaluation of the Role of *Candida albicans* Agglutinin-Like Sequence (Als) Proteins in Human Oral Epithelial Cell Interactions. *PLOS ONE* 7(3), p. e33362. doi: 10.1371/journal.pone.0033362

Naehrig, S., Chao, CM. and Naehrlich, L. (2017) Cystic Fibrosis. *Dtsch Arztebl Int* 114(33-34), pp. 564-574. doi: 10.3238/arztebl.2017.0564

Naglik, JR., Challacombe, SJ. and Hube, B. (2003) *Candida albicans* Secreted Aspartyl Proteinases in Virulence and Pathogenesis. *Microbiology and Molecular Biology Reviews* 67(3), pp. 400-428. doi: 10.1128/MMBR.67.3.400-428.2003

Naglik, JR., Moyes, DL., Wächtler, B. and Hube, B. (2011) *Candida albicans* interactions with epithelial cells and mucosal immunity. *Microbes and Infection* 13(12), pp. 963-976. doi: 10.1016/j.micinf.2011.06.009

Nation, RL. and Li, J. (2009) Colistin in the 21st century. *Current opinion in infectious diseases* 22(6), p. 535. doi: 10.1097/QCO.0b013e328332e672.

Negri, M., Silva, S., Henriques, M. and Oliveira, R. (2012) Insights into *Candida tropicalis* nosocomial infections and virulence factors. *European Journal of Clinical Microbiology & Infectious Diseases* 31(7), pp. 1399-1412. doi: 10.1007/s10096-011-1455-z

Nelson, R. (2003) Antibiotic development pipeline runs dry. *Lancet (London, England)* 362(9397), pp. 1726-1727. doi: 10.1016/S0140-6736(03)14885-4

Netea, MG., Gow, NAR., Joosten, LAB., Verschueren, I., van der Meer, JWM. and Kullberg, BJ. (2010). Variable recognition of *Candida albicans* strains by TLR4 and lectin recognition receptors. *Medical Mycology* 48(7), pp. 897-903. doi: 10.3109/13693781003621575

Nett, JE., Crawford, K., Marchillo, K. and Andes, R. (2010a) Role of Fks1p and Matrix Glucan in *Candida albicans* Biofilm Resistance to an Echinocandin, Pyrimidine, and Polyene. *Antimicrobial Agents and Chemotherapy* 54(8), pp. 3505-3508. doi:10.1128/AAC.00227-10

Nett, JE., Sanchez, H., Cain, MT. and Andes, DR. (2010b) Genetic Basis of *Candida* Biofilm Resistance Due to Drug-Sequestering Matrix Glucan. *The Journal of Infectious Diseases* 202(1), pp. 171-175. doi: 10.1086/651200

Ng, WL. and Bassler, BL. (2009) Bacterial Quorum-Sensing Network Architectures. *Annual Review of Genetics* 43(1), pp. 197-222. doi: 10.1146/annurev-genet-102108-134304

Nguyen Nhung, T., Nguyen, HM., Nguyen, CV., Nguyen, TV., Nguyen, MT., Thai, HQ., Ho, MH., Thwaites, G., Ngo, HT., Baker, S. and Carrique-Mas, J. (2016) Use of Colistin and Other Critical Antimicrobials on Pig and Chicken Farms in Southern Vietnam and Its Association with Resistance in Commensal *Escherichia coli* Bacteria. *Applied and Environmental Microbiology* 82(13), pp. 3727-3735. doi: 10.1128/AEM.00337-16

Nguyen, PT., Wacker, T., Brown, AJP., da Silva Dantas, A. and Shekhova, E. (2022) Understanding the Role of Nitronate Monooxygenases in Virulence of the Human Fungal Pathogen *Aspergillus fumigatus. Journal of Fungi* 8(7), p. 736. doi: 10.3390/jof8070736

NHS. (2021a) Cystic Fibrosis. Available at: https://www.nhs.uk/conditions/cystic-fibrosis/ [Accessed: 01/03/2023]

NHS. (2021b) Newborn blood spot test. Available at: https://www.nhs.uk/conditions/baby/newborn-screening/blood-spot-test/: [Accessed: 01/03/2023]

Nichols, DP., Odem-Davis, K., Cogen, JD., Goss, CH., Ren, CL., Skalland, M., Somayaji, R. and Heltshe, SL. (2020) Pulmonary outcomes associated with long-term azithromycin therapy in cystic fibrosis. *American journal of respiratory and critical care medicine* 201(4), pp. 430-437. doi: 10.1164/rccm.201906-1206OC.

Noreen, A., Masood, H., Zaib, J., Rafaque, Z., Fatima, A., Shabbir, H., Alam, J., Habib, A., Noor, S., Dil, K. and Dasti, JI. (2022) Investigating the Role of Antibiotics on Induction, Inhibition and Eradication of Biofilms of Poultry Associated *Escherichia coli* Isolated from Retail Chicken Meat. *Antibiotics* 11(11), p. 1663. doi: 10.3390/antibiotics11111663.

O'Neill, J. (2014) Antimicrobial Resistance: Tackling a crisis for the health and wealth of nations. London: Available at: https://amr-review.org/sites/default/files/AMR%20Review%20Paper%20-%20Tackling%20a%20crisis%20for%20the%20health%20and%20wealth%20of%20nations_1.pdf

Oakley, JL., Weiser, R., Powell, LC., Forton, J., Mahenthiralingam, E., Rye, PD., Hill, KE., Thomas, DW. and Pritchard, MF. (2021) Phenotypic and Genotypic Adaptations in *Pseudomonas aeruginosa* Biofilms following Long-Term Exposure to an Alginate Oligomer Therapy. *mSphere* 6(1), pp. e01216-01220. doi: 10.1128/mSphere.01216-20

Odds, FC., Brown, AJP. and Gow, NAR. (2003) Antifungal agents: mechanisms of action. *Trends in Microbiology* 11(6), pp. 272-279. doi: 10.1016/S0966-842X(03)00117-3

Okuda, K., Shaffer, KM. and Ehre, C. (2022) Mucins and CFTR: Their Close Relationship. *International Journal of Molecular Sciences* 23(18), p. 10232. doi: 10.3390/ijms231810232.

Olaitan, AO., Morand, S. and Rolain, JM. (2014) Mechanisms of polymyxin resistance: acquired and intrinsic resistance in bacteria. *Frontiers in Microbiology* 5, doi: 10.3389/fmicb.2014.00643

de Oliveira, DMP., Forde, BM., Kidd, TJ., Harris, PNA., Schembri, MA., Beatson, SA., Paterson, DL. and Walker, MJ. (2020) Antimicrobial Resistance in ESKAPE Pathogens. *Clinical Microbiology Reviews* 33(3), pp. e00181-00119. doi:10.1128/CMR.00181-19

Ordooei Javan, A., Shokouhi, S. and Sahraei, Z. (2015) A review on colistin nephrotoxicity. *European Journal of Clinical Pharmacology* 71(7), pp. 801-810. doi: 10.1007/s00228-015-1865-4

Osherov, N. and Kontoyiannis, DP. (2016) The anti-*Aspergillus* drug pipeline: Is the glass half full or empty? *Medical Mycology* 55(1), pp. 118-124. doi: 10.1093/mmy/myw060

Ovung, A. and Bhattacharyya, J. (2021) Sulfonamide drugs: structure, antibacterial property, toxicity, and biophysical interactions. *Biophys Rev* 13(2), pp. 259-272. doi: 10.1007/s12551-021-00795-9

Padder, SA., Prasad, R. and Shah, AH. (2018) Quorum sensing: A less known mode of communication among fungi. *Microbiological Research* 210, pp. 51-58. https://doi.org/10.1016/j.micres.2018.03.007

Padilla, E., Llobet, E., Doménech-Sánchez, A., Martínez-Martínez, L., Bengoechea, JA. and Albertí, S. (2010) *Klebsiella pneumoniae* AcrAB efflux pump contributes to antimicrobial resistance and virulence. *Antimicrobial agents and chemotherapy* 54(1), pp. 177-183. doi: 10.1128/AAC.00715-09.

Pamp, SJ. and Tolker-Nielsen, T. (2007) Multiple Roles of Biosurfactants in Structural Biofilm Development by *Pseudomonas aeruginosa. Journal of Bacteriology* 189(6), pp. 2531-2539. doi:10.1128/JB.01515-06

Pankhurst, CL. (2009) Candidiasis (oropharyngeal). *BMJ Clin Evid.* 2009 Mar 18;2009:1304.

Park, J., Jagasia, R., Kaufmann, GF., Mathison, JC., Ruiz, DI., Moss, JA., Meijler, MM., Ulevitch, RJ. and Janda, KD. (2007) Infection control by antibody disruption of bacterial quorum sensing signaling. *Chemistry & biology* 14(10), pp. 1119-1127. doi: 10.1016/j.chembiol.2007.08.013.

Percy, MG. and Gründling, A. (2014) Lipoteichoic Acid Synthesis and Function in Gram-Positive Bacteria. *Annual Review of Microbiology* 68(1), pp. 81-100. doi: 10.1146/annurev-micro-091213-112949

Pesci, EC., Milbank, JB., Pearson, JP., McKnight, S., Kende, AS., Greenberg, EP. and Iglewski, BH. (1999) Quinolone signaling in the cell-to-cell communication system of *Pseudomonas aeruginosa. Proceedings of the National Academy of Sciences* 96(20), pp. 11229-11234.

Pesingi, PV., Singh, BR., Pesingi, PK., Bhardwaj, M., Singh, SV., Kumawat, M., Sinha, DK. and Gandham, RK. (2019) MexAB-OprM Efflux Pump of *Pseudomonas aeruginosa* Offers Resistance to Carvacrol: A Herbal Antimicrobial Agent. *Frontiers in Microbiology* 10, doi: 10.3389/fmicb.2019.02664

Pestrak, MJ., Chaney, SB., Eggleston, HC., Dellos-Nolan, S., Dixit S, Mathew-Steiner, SS., Roy, S., Parsek, MR., Sen, CK. and Wozniak, DJ. (2018) *Pseudomonas aeruginosa* rugose small-colony variants evade host clearance, are hyper-inflammatory, and persist in multiple host environments. *PLoS Pathogens* 14(2), p. e1006842. doi: 10.1371/journal.ppat.1006842

Petrova, OE. and Sauer, K. (2016) Escaping the biofilm in more than one way: desorption, detachment or dispersion. *Curr Opin Microbiol* 30, pp. 67-78. doi: 10.1016/j.mib.2016.01.004

Pettit, RK., Repp, KK. and Hazen, KC. (2010) Temperature affects the susceptibility of *Cryptococcus neoformans* biofilms to antifungal agents. *Medical Mycology* 48(2), pp. 421-426.

Phan, QT., Myers, CL., Fu, Y., Sheppard, DC., Yeaman, MR., Welch, WH., Ibrahim, AS., Edwards, JE Jr. and Filler, SG. (2007) Als3 is a *Candida albicans* invasin that binds to cadherins and induces endocytosis by host cells. *PLoS biology* 5(3), p. e64. doi: 10.1371/journal.pbio.0050064

Plackett, B. (2020) Why big pharma has abandoned antibiotics. *Nature* 586(7830), pp. S50-S50. https://doi.org/10.1038/d41586-020-02884-3

Poirel, L., Jayol, A. and Nordmann, P. (2017) Polymyxins: Antibacterial Activity, Susceptibility Testing, and Resistance Mechanisms Encoded by Plasmids or Chromosomes. *Clinical Microbiology Reviews* 30(2), pp. 557-596. doi:10.1128/CMR.00064-16

Poltak, SR. and Cooper, VS. (2011) Ecological succession in long-term experimentally evolved biofilms produces synergistic communities. *The ISME Journal* 5(3), pp. 369-378. doi: 10.1038/ismej.2010.136

Powell, LC., Adams, JYM., Quoraishi, S., Py, C., Oger, A., Gazze, SA., Francis, LW., von Ruhland, C., Owens, D., Rye, PD., Hill, KE., Pritchard, MF. and Thomas, DW. (2023) Alginate oligosaccharides enhance the antifungal activity of nystatin against candidal biofilms. *Front Cell Infect Microbiol.* 2023 Jan 31;13:1122340. doi: 10.3389/fcimb.2023.1122340.

Powell, LC., Pritchard, MF., Emanuel, C., Onsøyen, E., Rye, PD., Wright, CJ., Hill, KE. and Thomas, DW. (2013a) A Nanoscale Characterization of the Interaction of a Novel Alginate Oligomer with the Cell Surface and Motility of *Pseudomonas aeruginosa. American Journal of Respiratory Cell and Molecular Biology* 50(3), pp. 483-492. doi: 10.1165/rcmb.2013-0287OC

Powell, LC., Pritchard, MF., Ferguson, EL., Powell, KA., Patel, SU., Rye, PD., Sakellakou, SM., Buurma, NJ., Brilliant, CD., Copping, JM., Menzies, GE., Lewis, PD., Hill, KE. and Thomas, DW. (2018) Targeted disruption of the extracellular polymeric network of *Pseudomonas aeruginosa* biofilms by alginate oligosaccharides. *NPJ biofilms and microbiomes* 4, p. 13. doi: 10.1038/s41522-018-0056-3

Powell, LC., Sowedan, A., Khan, S., Wright, CJ., Hawkins, K., Onsøyen, E., Myrvold, R., Hill, KE. and Thomas, DW. (2013b) The effect of alginate oligosaccharides on the mechanical properties of Gram-negative biofilms. *Biofouling* 29(4), pp. 413-421. doi: 10.1080/08927014.2013.777954

Pradhan, A., Avelar, GM., Bain, JM., Childers, D., Pelletier, C., Larcombe, DE., Shekhova, E., Netea, MG., Brown, GD., Erwig, L., Gow, NAR. and Brown, AJP. (2019) Non-canonical signalling mediates changes in fungal cell wall PAMPs that drive immune evasion. *Nature Communications* 10(1), p. 5315. doi: 10.1038/s41467-019-13298-9

Price, CE., Brown, DG., Limoli, DH., Phelan, VV. and O'Toole, GA. (2020) Exogenous Alginate Protects *Staphylococcus aureus* from Killing by *Pseudomonas aeruginosa. Journal of Bacteriology* 202(8), pp. e00559-00519. doi:10.1128/JB.00559-19

Pritchard, MF., Jack, AA., Powell, LC., Sadh, H., Rye, PD., Hill, KE. and Thomas, DW. (2017a) Alginate oligosaccharides modify hyphal infiltration of *Candida albicans* in an in vitro model of invasive human candidosis. *Journal of Applied Microbiology* 123(3), pp. 625-636. doi: 10.1111/jam.13516

Pritchard, MF., Powell, LC., Adams, JYM., Menzies, G., Khan, S., Tøndervik, A., Sletta, H., Aarstad, O., Skjåk-Bræk, G., McKenna, S., Buurma, NJ., Farnell, DJJ., Rye, PD., Hill, KE. and Thomas, DW. (2023) Structure-Activity Relationships of Low Molecular Weight Alginate Oligosaccharide Therapy against *Pseudomonas aeruginosa*. *Biomolecules* 13(9), p. 1366. doi: 10.3390/biom13091366.

Pritchard, MF., Powell, LC., Jack, AA., Powell, K., Beck, K., Florance, H., Forton, J., Rye, PD., Dessen, A., Hill, KE. and Thomas, DW. (2017b) A Low-Molecular-Weight Alginate Oligosaccharide Disrupts Pseudomonal Microcolony Formation and Enhances Antibiotic Effectiveness. *Antimicrobial Agents and Chemotherapy* 61(9), pp. 10.1128/aac.00762-00717. doi:10.1128/aac.00762-17

Pritchard, MF., Powell, LC., Khan, S., Griffiths, PC., Mansour, OT., Schweins, R., Beck, K., Buurma, NJ., Dempsey, CE., Wright, CJ., Rye, PD., Hill, KE., Thomas, DW. and Ferguson, EL. (2017c) The antimicrobial effects of the alginate oligomer OligoG CF-5/20 are independent of direct bacterial cell membrane disruption. *Scientific Reports* 7(1), pp. 1-12. doi: 10.1038/srep44731

Pritchard, MF., Powell, LC., Menzies, GE., Lewis, PD., Hawkins, K., Wright, C., Doull, I., Walsh, TR., Onsøyen, E., Dessen, A., Myrvold, R., Rye, PD., Myrset, AH., Stevens, HN., Hodges, LA., MacGregor, G., Neilly, JB., Hill, KE. and Thomas, DW. (2016) A New Class of Safe Oligosaccharide Polymer Therapy To Modify the Mucus Barrier of Chronic Respiratory Disease. *Molecular Pharmaceutics* 13(3), pp. 863-872. doi: 10.1021/acs.molpharmaceut.5b00794

Proctor, CR., McCarron, PA. and Ternan, NG. (2020) Furanone quorum-sensing inhibitors with potential as novel therapeutics against *Pseudomonas aeruginosa*. *Journal of Medical Microbiology* 69(2), pp. 195-206. https://doi.org/10.1099/jmm.0.001144

Qu, Y., Locock, K., Verma-Gaur, J., Hay, ID., Meagher, L. and Traven, A. (2016) Searching for new strategies against polymicrobial biofilm infections: guanylated

polymethacrylates kill mixed fungal/bacterial biofilms. *Journal of Antimicrobial Chemotherapy* 71(2), pp. 413-421. doi: 10.1093/jac/dkv334

Quindós, G., Gil-Alonso, S., Marcos-Arias, C., Sevillano, E., Mateo, E., Jauregizar, N. and Eraso, E. (2019) Therapeutic tools for oral candidiasis: Current and new antifungal drugs. *Med Oral Patol Oral Cir Bucal* 24(2), pp. e172-e180. doi: 10.4317/medoral.22978

Raad, I., Chatzinikolaou, I., Chaiban, G., Hanna, H., Hachem, R., Dvorak, T., Cook, G. and Costerton, W. (2003) In Vitro and Ex Vivo Activities of Minocycline and EDTA against Microorganisms Embedded in Biofilm on Catheter Surfaces. *Antimicrobial Agents and Chemotherapy* 47(11), pp. 3580-3585. doi:10.1128/AAC.47.11.3580-3585.2003

Raad, II., Hachem, RY., Hanna, HA., Fang, X., Jiang, Y., Dvorak, T., Sherertz, RJ. and Kontoyiannis, DP. (2008) Role of ethylene diamine tetra-acetic acid (EDTA) in catheter lock solutions: EDTA enhances the antifungal activity of amphotericin B lipid complex against *Candida* embedded in biofilm. *International Journal of Antimicrobial Agents* 32(6), pp. 515-518. https://doi.org/10.1016/j.ijantimicag.2008.06.020

Rada, B. and Leto, TL. (2013) Pyocyanin effects on respiratory epithelium: relevance in *Pseudomonas aeruginosa* airway infections. *Trends in Microbiology* 21(2), pp. 73-81. https://doi.org/10.1016/j.tim.2012.10.004

Ramage, G., Martínez, JP. and López-Ribot, JL. (2006) *Candida* biofilms on implanted biomaterials: a clinically significant problem. *FEMS Yeast Research* 6(7), pp. 979-986. doi: 10.1111/j.1567-1364.2006.00117.x

Ramage, G., Rajendran, R., Sherry, L. and Williams, C. (2012) Fungal biofilm resistance. *Int J Microbiol* 2012, p. 528521. doi: 10.1155/2012/528521

Ramsey, DM. and Wozniak, DJ. (2005) Understanding the control of *Pseudomonas aeruginosa* alginate synthesis and the prospects for management of chronic infections in cystic fibrosis. *Molecular Microbiology* 56(2), pp. 309-322. https://doi.org/10.1111/j.1365-2958.2005.04552.x

Rashedy, SH., Abd El Hafez, MSM., Dar, MA., Cotas, J. and Pereira, L. (2021) Evaluation and Characterization of Alginate Extracted from Brown Seaweed Collected in the Red Sea. *Applied Sciences* 11(14), p. 6290. doi:10.3390/app11146290

Rather, MA., Saha, D., Bhuyan, S., Jha, AN. and Mandal, M. (2022) Quorum Quenching: A Drug Discovery Approach Against *Pseudomonas aeruginosa*. *Microbiological Research* 264, p. 127173. https://doi.org/10.1016/j.micres.2022.127173

Remminghorst, U. and Rehm, BHA. (2006) Bacterial alginates: from biosynthesis to applications. *Biotechnology Letters* 28(21), pp. 1701-1712. doi: 10.1007/s10529-006-9156-x

Rémy, B., Mion, S., Plener, L., Elias, M., Chabrière, E. and Daudé, D. (2018) Interference in bacterial quorum sensing: a biopharmaceutical perspective. *Frontiers in pharmacology* 9, p. 203. doi: 10.3389/fphar.2018.00203.

Reyes, E., Bale, MJ., Cannon, WH. and Matsen, JM. (1981) Identification of *Pseudomonas aeruginosa* by pyocyanin production on Tech agar. *Journal of Clinical Microbiology* 13(3), pp. 456-458.

Rice, LB. (2010) Progress and Challenges in Implementing the Research on ESKAPE Pathogens. *Infection Control & Hospital Epidemiology* 31(S1), pp. S7-S10. doi: 10.1086/655995

Rigatto, MH., Falci, DR. and Zavascki, AP. (2019) Clinical Use of Polymyxin B. In: Li, J., Nation, R.L. and Kaye, K.S. eds. Polymyxin Antibiotics: From Laboratory Bench to Bedside. Cham: *Springer International Publishing*, pp. 197-218.

Rodrigues, CF., Rodrigues, ME., Silva, S. and Henriques, M. (2017) *Candida glabrata* Biofilms: How Far Have We Come? *Journal of Fungi* 3(1), p. 11. doi: 10.3390/jof3010011

Rosenblatt-Farrell, N. (2009) The landscape of antibiotic resistance. *Environ Health Perspect* 117(6), pp. A244-250. doi: 10.1289/ehp.117-a244

Rozwandowicz, M., Brouwer, MSM., Fischer, J., Wagenaar, JA., Gonzalez-Zorn, B., Guerra, B., Mevius, DJ. and Hordijk, J. (2018) Plasmids carrying antimicrobial resistance genes in Enterobacteriaceae. *Journal of Antimicrobial Chemotherapy* 73(5), pp. 1121-1137. doi: 10.1093/jac/dkx488

Ruhil, S., Kumar, V., Balhara, M., Malik, M., Dhankhar, S., Kumar, M. and Kumar Chhillar, A. (2014) In vitro evaluation of combination of polyenes with EDTA against *Aspergillus* spp. by different methods (FICI and CI Model). *Journal of Applied Microbiology* 117(3), pp. 643-653. https://doi.org/10.1111/jam.12576

Rye, P., Tøndervik, A., Sletta, H., Pritchard, M., Kristiansen, A., Dessen, A. and Thomas, D. (2018) Alginate oligomers and their use as active pharmaceutical drugs. *Alginates and their biomedical applications*, pp. 237-256.

Saboury, AA. (2006) A review on the ligand binding studies by isothermal titration calorimetry. *Journal of the Iranian Chemical Society* 3(1), pp. 1-21. doi: 10.1007/BF03245784

Samantha, A. and Vrielink, A. (2020) Lipid A Phosphoethanolamine Transferase: Regulation, Structure and Immune Response. *J Mol Biol* 432(18), pp. 5184-5196. doi: 10.1016/j.jmb.2020.04.022

Sanguinetti, M., Posteraro, B., Fiori, B., Ranno, S., Torelli, R. and Fadda, G. (2005) Mechanisms of azole resistance in clinical isolates of *Candida glabrata* collected during a hospital survey of antifungal resistance. *Antimicrobial Agents and Chemotherapy* 49(2), pp. 668-679. doi: 10.1128/AAC.49.2.668-679.2005

Santajit, S. and Indrawattana, N. (2016) Mechanisms of Antimicrobial Resistance in ESKAPE Pathogens. *BioMed Research International* 2016, p. 2475067. doi: 10.1155/2016/2475067

Satoh, K., Makimura, K., Hasumi, Y., Nishiyama, Y., Uchida, K. and Yamaguchi, H. (2009) *Candida auris* sp. nov., a novel ascomycetous yeast isolated from the external ear canal of an inpatient in a Japanese hospital. *Microbiology and Immunology* 53(1), pp. 41-44. doi: 10.1111/j.1348-0421.2008.00083.x

Sauvage, E., Kerff, F., Terrak, M., Ayala, J. A. and Charlier, P. (2008) The penicillin-binding proteins: structure and role in peptidoglycan biosynthesis. *FEMS Microbiology Reviews 32*(2), pp. 234-258. doi: 10.1111/j.1574-6976.2008.00105.x

Scheffers, DJ. and Pinho, MG. (2005) Bacterial Cell Wall Synthesis: New Insights from Localization Studies. *Microbiology and Molecular Biology Reviews* 69(4), pp. 585-607. doi: 10.1128/MMBR.69.4.585-607.2005

Scheibler, E., Garcia, MCR., Medina da Silva, R., Figueiredo, MA., Salum, FG. and Cherubini, K. (2017) Use of nystatin and chlorhexidine in oral medicine: Properties, indications and pitfalls with focus on geriatric patients. *Gerodontology* 34(3), pp. 291-298. https://doi.org/10.1111/ger.12278

Schooling, SR., Charaf, UK., Allison, DG. and Gilbert, P. (2004) A role for rhamnolipid in biofilm dispersion. *Biofilms* 1(2), pp. 91-99. doi: 10.1017/S147905050400119X

Schuster, M. and Greenberg, PE. (2006) A network of networks: Quorum-sensing gene regulation in *Pseudomonas aeruginosa. International Journal of Medical Microbiology* 296(2), pp. 73-81. doi: 10.1016/j.ijmm.2006.01.036

Scotet, V., Gutierrez, H. and Farrell, PM. (2020a) Newborn Screening for CF across the Globe—Where Is It Worthwhile? *International Journal of Neonatal Screening* 4;6(1):18. doi: 10.3390/ijns6010018.

Scotet, V., L'Hostis, C. and Férec, C. (2020b) The Changing Epidemiology of Cystic Fibrosis: Incidence, Survival and Impact of the CFTR Gene Discovery. *Genes (Basel)* 11(6), doi: 10.3390/genes11060589

Sears, P., Ichikawa, Y., Ruiz, N. and Gorbach, S. (2013) Advances in the treatment of *Clostridium difficile* with fidaxomicin: a narrow spectrum antibiotic. *Annals of the New York Academy of Sciences* 1291(1), pp. 33-41. https://doi.org/10.1111/nyas.12135

Semis, R., Kagan, S., Berdicevsky, I., Polacheck, I. and Segal, E. (2013) Mechanism of activity and toxicity of Nystatin-Intralipid. *Medical Mycology* 51(4), pp. 422-431. doi: 10.3109/13693786.2012.731712

Sen, BH., Akdeniz, BG. and Denizci, AA. (2000) The effect of ethylenediamine-tetraacetic acid on *Candida albicans. Oral Surgery, Oral Medicine, Oral Pathology, Oral Radiology, and Endodontology* 90(5), pp. 651-655. https://doi.org/10.1067/moe.2000.109640

Şen, M. (2011) Effects of molecular weight and ratio of guluronic acid to mannuronic acid on the antioxidant properties of sodium alginate fractions prepared by radiation-induced degradation. *Applied Radiation and Isotopes* 69(1), pp. 126-129.

Sena-Vélez, M., Redondo, C., Graham, JH. and Cubero, J. (2016) Presence of Extracellular DNA during Biofilm Formation by *Xanthomonas citri* subsp. citri Strains with Different Host Range. *PLOS ONE* 11(6), p. e0156695. doi: 10.1371/journal.pone.0156695

Seneviratne, CJ., Wang, Y., Jin, L., Abiko, Y. and Samaranayake, LP. (2010) Proteomics of drug resistance in *Candida glabrata* biofilms. *PROTEOMICS* 10(7), pp. 1444-1454. doi: 10.1002/pmic.200900611

Serra, R., Grande, R., Butrico, L., Rossi, A., Settimio, UF., Caroleo, B., Amato, B., Gallelli, L. and de Franciscis, S. (2015) Chronic wound infections: the role of *Pseudomonas aeruginosa* and *Staphylococcus aureus. Expert Review of Anti-infective Therapy* 13(5), pp. 605-613. doi: 10.1586/14787210.2015.1023291

Seyedjavadi, SS., Khani, S., Eslamifar, A., Ajdary, S., Goudarzi, M., Halabian, R., Akbari, R., Zare-Zardini, H., Imani Fooladi, AA., Amani, J. and Razzaghi-Abyaneh, M. (2020) The Antifungal Peptide MCh-AMP1 Derived From Matricaria chamomilla Inhibits *Candida albicans* Growth via Inducing ROS Generation and Altering Fungal Cell Membrane Permeability. *Frontiers in Microbiology* 10, doi: 10.3389/fmicb.2019.03150

Sheehan, DJ., Hitchcock, CA. and Sibley, CM. (1999) Current and Emerging Azole Antifungal Agents. *Clinical Microbiology Reviews* 12(1), pp. 40-79. doi: 10.1128/CMR.12.1.40

Shen, C., Zhong, LL., Yang, Y., Doi, Y., Paterson, DL., Stoesser, N., Ma, F., El-Sayed Ahmed, MAE., Feng, S., Huang, S., Li, HY., Huang, X., Wen, X., Zhao, Z., Lin, M., Chen, G., Liang, W., Liang, Y., Xia, Y., Dai, M., Chen, DQ., Zhang, L., Liao, K. and

Tian, GB. (2020) Dynamics of *mcr-1* prevalence and *mcr-1*-positive *Escherichia coli* after the cessation of colistin use as a feed additive for animals in China: a prospective cross-sectional and whole genome sequencing-based molecular epidemiological study. *The Lancet Microbe* 1(1), pp. e34-e43. doi: https://doi.org/10.1016/S2666-5247(20)30005-7

Shintani, M., Sanchez, ZK. and Kimbara, K. (2015) Genomics of microbial plasmids: classification and identification based on replication and transfer systems and host taxonomy. *Frontiers in Microbiology* 6, doi: 10.3389/fmicb.2015.00242

Shrivastava, S., Shrivastava, P. and Ramasamy, J. (2018) World health organization releases global priority list of antibiotic-resistant bacteria to guide research, discovery, and development of new antibiotics. *Journal of Medical Society* 32(1), pp. 76-77. doi: 10.4103/jms.jms_25_17

Shutter, M. C. and Akhondi, H. 2022. Tetracycline. [Updated 2023 Jun 5]. In: StatPearls [Internet]. Treasure Island (FL): *StatPearls Publishing*

Sia, CM., Greig, DR., Day, M., Hartman, H., Painset, A., Doumith, M., Meunier, D., Jenkins, C., Chattaway, MA., Hopkins, KL., Woodford, N., Godbole, G. and Dallman, TJ. (2020) The characterization of mobile colistin resistance (*mcr*) genes among 33 000 *Salmonella enterica* genomes from routine public health surveillance in England. *Microbial Genomics* 6(2):e000331. doi: 10.1099/mgen.0.000331.

Silva, LN., Oliveira, SSC., Magalhães, LB., Andrade Neto, VV., Torres-Santos, EC., Carvalho, MDC., Pereira, MD., Branquinha, MH. and Santos, ALS. (2020) Unmasking the Amphotericin B Resistance Mechanisms in *Candida haemulonii* Species Complex. *ACS Infectious Diseases* 6(5), pp. 1273-1282. doi: 10.1021/acsinfecdis.0c00117

Silva, S., Henriques, M., Martins, A., Oliveira, R., Williams, D. and Azeredo, J. (2009) Biofilms of non-*Candida albicans Candida* species: quantification, structure and matrix composition. *Medical Mycology* 47(7), pp. 681-689. doi: 10.3109/13693780802549594

Silva, S., Negri, M., Henriques, M., Oliveira, R., Williams, DW. and Azeredo, J. (2012) *Candida glabrata, Candida parapsilosis* and *Candida tropicalis*: biology,

epidemiology, pathogenicity, and antifungal resistance. *FEMS Microbiology Reviews* 36(2), pp. 288-305. doi: 10.1111/j.1574-6976.2011.00278.x

Silver, LL. (2011) Challenges of antibacterial discovery. *Clinical Microbiology Reviews* 24(1), pp. 71-109. doi: 10.1128/cmr.00030-10

Smidsrød, O. (1974) Molecular basis for some physical properties of alginates in the gel state. *Faraday discussions of the Chemical Society* 57, pp. 263-274. https://doi.org/10.1039/DC9745700263

Smidsrød, O. and Haug, A. (1968) Dependence upon uronic acid composition of some ion-exchange properties of alginates. *Acta chem. scand* 22(6), pp. 1989-1997. doi:10.3891/acta.chem.scand.22-1989

Smith, DJ., Anderson, GJ., Bell, SC. and Reid, DW. (2014) Elevated metal concentrations in the CF airway correlate with cellular injury and disease severity. *Journal of Cystic Fibrosis* 13(3), pp. 289-295. doi: 10.1016/j.jcf.2013.12.001

Smith, RS. and Iglewski, BH. (2003) *P. aeruginosa* quorum-sensing systems and virulence. *Current Opinion in Microbiology* 6(1), pp. 56-60. doi: 10.1016/S1369-5274(03)00008-0

Snesrud, E., McGann, P. and Chandler, M. (2018) The Birth and Demise of the ISApl1-*mcr-1*-ISApl1 Composite Transposon: the Vehicle for Transferable Colistin Resistance. *mBio* 9(1), pp. 10.1128/mbio.02381-02317. doi:10.1128/mbio.02381-17

Snitkin, ES., Zelazny, AM., Gupta, J., Palmore, TN., Murray, PR., Segre, JA. and Program, NCS. (2013) Genomic insights into the fate of colistin resistance and *Acinetobacter baumannii* during patient treatment. *Genome research* 23(7), pp. 1155-1162. doi: 10.1101/gr.154328.112.

Sobczyńska-Malefora, A. and Harrington, DJ. (2018) Laboratory assessment of folate (vitamin B9) status. *Journal of Clinical Pathology* 71(11), p. 949. doi: 10.1136/jclinpath-2018-205048

Soberón-Chávez, G., Lépine, F. and Déziel, E. (2005) Production of rhamnolipids by *Pseudomonas aeruginosa. Applied Microbiology and Biotechnology* 68(6), pp. 718-725. doi: 10.1007/s00253-005-0150-3

Soh, EYC., Smith, F., Gimenez, MR., Yang, L., Vejborg, RM., Fletcher, M., Halliday, N., Bleves, S., Heeb, S., Cámara, M., Givskov, M., Hardie, KR., Tolker-Nielsen, T., Ize, B. and Williams, P. (2021) Disruption of the *Pseudomonas aeruginosa* Tat system perturbs PQS-dependent quorum sensing and biofilm maturation through lack of the Rieske cytochrome bc1 sub-unit. *PLoS Pathogens* 17(8), p. e1009425. doi: 10.1371/journal.ppat.1009425

Somogyi-Ganss, E., Chambers, MS., Lewin, JS., Tarrand, JJ. and Hutcheson, KA. (2017) Biofilm on the tracheoesophageal voice prosthesis: considerations for oral decontamination. *Eur Arch Otorhinolaryngol*. 2017 Jan;274(1):405-413. doi: 10.1007/s00405-016-4193-0

Song, B. and Leff, LG. (2006) Influence of magnesium ions on biofilm formation by *Pseudomonas fluorescens. Microbiological Research* 161(4), pp. 355-361. https://doi.org/10.1016/j.micres.2006.01.004

Spitzer, M., Griffiths, E., Blakely, KM., Wildenhain, J., Ejim, L., Rossi, L., De Pascale, G., Curak, J., Brown, E., Tyers, M. and Wright, GD. (2011) Cross-species discovery of syncretic drug combinations that potentiate the antifungal fluconazole. *Molecular Systems Biology* 7(1), p. 499. doi: 10.1038/msb.2011.31

Staniszewska, M., Bondaryk, M., Piłat, J., Siennicka, K., Magda, U. and Kurzatkowski, W. (2012) Virulence factors of *Candida albicans. Przeglad epidemiologiczny* 66(4), pp. 629-633.

Steenackers, HP., Parijs, I., Foster, KR. and Vanderleyden, J. (2016) Experimental evolution in biofilm populations. *FEMS Microbiology Reviews* 40(3), pp. 373-397. doi: 10.1093/femsre/fuw002

Steenbergen, JN., Alder, J., Thorne, GM. and Tally, FP. (2005) Daptomycin: a lipopeptide antibiotic for the treatment of serious Gram-positive infections. *Journal of Antimicrobial Chemotherapy* 55(3), pp. 283-288. doi: 10.1093/jac/dkh546

Stehling, EG., Silveira, WDD. and Leite, DDS. (2008) Study of biological characteristics of *Pseudomonas aeruginosa* strains isolated from patients with cystic fibrosis and from patients with extra-pulmonary infections. *Brazilian Journal of Infectious Diseases* 12, pp. 86-88.

Stewart, PS. (2002) Mechanisms of antibiotic resistance in bacterial biofilms. *International Journal of Medical Microbiology* 292(2), pp. 107-113. doi: 10.1078/1438-4221-00196

Stojanoski, V., Sankaran, B., Prasad, B., Poirel, L., Nordmann, P. and Palzkill, T. (2016) Structure of the catalytic domain of the colistin resistance enzyme MCR-1. *BMC biology* 14(1), pp. 1-10.

Stokniene, J., Varache, M., Rye, PD., Hill, KE., Thomas, DW. and Ferguson, EL. (2022) Alginate oligosaccharides enhance diffusion and activity of colistin in a mucin-rich environment. *Scientific Reports* 12(1), p. 4986. doi: 10.1038/s41598-022-08927-1

Stoltz, DA., Meyerholz, DK. and Welsh, MJ. (2015) Origins of Cystic Fibrosis Lung Disease. *New England Journal of Medicine* 372(4), pp. 351-362. doi: 10.1056/NEJMra1300109

Storm, DR., Rosenthal, KS. and Swanson, PE. (1977) Polymyxin and related peptide antibiotics. *Annual review of biochemistry* 46(1), pp. 723-763. doi: 10.1146/annurev.bi.46.070177.003451

Strateva, T. and Mitov, I. (2011) Contribution of an arsenal of virulence factors to pathogenesis of *Pseudomonas aeruginosa* infections. *Annals of Microbiology* 61(4), pp. 717-732. doi: 10.1007/s13213-011-0273-y

Su, KY. and Lee, WL. (2020) Fourier Transform Infrared Spectroscopy as a Cancer Screening and Diagnostic Tool: A Review and Prospects. *Cancers* 12(1), p. 115. https://doi.org/10.3390/cancers12010115

Sudbery, P., Gow, N. and Berman, J. (2004) The distinct morphogenic states of *Candida albicans. Trends in Microbiology* 12(7), pp. 317-324. doi: 10.1016/j.tim.2004.05.008

Sudbery, PE. (2011) Growth of *Candida albicans* hyphae. *Nature Reviews Microbiology* 9(10), pp. 737-748. doi: 10.1038/nrmicro2636

Sullivan, D., Bennett, D., Henman, M., Harwood, P., Flint, S., Mulcahy, F., Shanley, D. and Coleman, D. (1993) Oligonucleotide fingerprinting of isolates of *Candida* species other than *C. albicans* and of atypical *Candida* species from human immunodeficiency virus-positive and AIDS patients. *Journal of Clinical Microbiology* 31(8), pp. 2124-2133. doi:10.1128/jcm.31.8.2124-2133.1993

Sullivan, DJ., Westerneng, TJ., Haynes, KA., Bennett, DSEE. and Coleman, DC. (1995) *Candida dubliniensis* sp. nov.: phenotypic and molecular characterization of a novel species associated with oral candidosis in HIV-infected individuals. *Microbiology* 141(7), pp. 1507-1521. https://doi.org/10.1099/13500872-141-7-1507

Sun, J., Deng, Z. and Yan, A. (2014) Bacterial multidrug efflux pumps: Mechanisms, physiology, and pharmacological exploitations. *Biochemical and Biophysical Research Communications* 453(2), pp. 254-267. https://doi.org/10.1016/j.bbrc.2014.05.090

Sun, J., Zhang, H., Liu, YH. and Feng, Y. (2018) Towards understanding MCR-like colistin resistance. *Trends in Microbiology* 26(9), pp. 794-808. doi: 10.1016/j.tim.2018.02.006.

Taccetti, G., Francalanci, M., Pizzamiglio, G., Messore, B., Carnovale, V., Cimino, G. and Cipolli, M. (2021) Cystic Fibrosis: Recent Insights into Inhaled Antibiotic Treatment and Future Perspectives. *Antibiotics (Basel)* 10(3), doi: 10.3390/antibiotics10030338

Taff, HT., Mitchell, KF., Edward, JA. and Andes, DR. (2013) Mechanisms of *Candida* biofilm drug resistance. *Future Microbiology* 8(10), pp. 1325-1337. doi: 10.2217/fmb.13.101

Tang, L., Fatehi, M. and Linsdell, P. (2009) Mechanism of direct bicarbonate transport by the CFTR anion channel. *Journal of Cystic Fibrosis* 8(2), pp. 115-121. https://doi.org/10.1016/j.jcf.2008.10.004

Tavanti, A., Davidson, AD., Gow, NAR., Maiden, MCJ. and Odds, FC. (2005) *Candida orthopsilosis* and *Candida metapsilosis* spp. nov. To Replace *Candida parapsilosis* Groups II and III. *Journal of Clinical Microbiology* 43(1), pp. 284-292. doi:10.1128/JCM.43.1.284-292.2005

Terreni, M., Taccani, M. and Pregnolato, M. (2021) New Antibiotics for Multidrug-Resistant Bacterial Strains: Latest Research Developments and Future Perspectives. *Molecules* 26(9), doi: 10.3390/molecules26092671

Thomas, CM. (2021) Plasmid Incompatibility, in *Molecular Life Sciences*: An Encyclopedic Reference(ed. E. Bell), Springer, New York, 2021, 1–3. https://doi.org/10.1007/978-1-4614-6436-5_565-2

Thompson, DS., Carlisle, PL. and Kadosh, D. (2011) Coevolution of Morphology and Virulence in *Candida* Species. *Eukaryotic Cell* 10(9), pp. 1173-1182. doi: 10.1128/EC.05085-11

Tietgen, M., Semmler, T., Riedel-Christ, S., Kempf, VAJ., Molinaro, A., Ewers, C. and Göttig, S. (2018) Impact of the colistin resistance gene *mcr-1* on bacterial fitness. *International Journal of Antimicrobial Agents* 51(4), pp. 554-561. https://doi.org/10.1016/j.ijantimicag.2017.11.011

Tøndervik, A., Sletta, H., Klinkenberg, G., Emanuel, C., Powell, LC., Pritchard, MF., Khan, S., Craine, KM., Onsøyen, E., Rye, PD., Wright, C., Thomas, DW. and Hill, KE. (2014) Alginate Oligosaccharides Inhibit Fungal Cell Growth and Potentiate the Activity of Antifungals against *Candida* and *Aspergillus* spp. *PLOS ONE* 9(11), doi: 10.1371/journal.pone.0112518

Tooke, CL., Hinchliffe, P., Bragginton, EC., Colenso, CK., Hirvonen, VHA., Takebayashi, Y. and Spencer, J. (2019) β-Lactamases and β-Lactamase Inhibitors in the 21st Century. *Journal of Molecular Biology* 431(18), pp. 3472-3500. https://doi.org/10.1016/j.jmb.2019.04.002

Tóth, R., Nosek, J., Mora-Montes, HM., Gabaldon, T., Bliss, JM., Nosanchuk, JD., Turner, SA., Butler, G., Vágvölgyi, C. and Gácser, A. (2019) *Candida parapsilosis*: from Genes to the Bedside. *Clinical Microbiology Reviews* 32(2), pp. e00111-00118. doi:10.1128/CMR.00111-18

Trofa, D., Gácser, A. and Nosanchuk, JD. (2008) *Candida parapsilosis*, an Emerging Fungal Pathogen. *Clinical Microbiology Reviews* 21(4), pp. 606-625. doi:10.1128/CMR.00013-08

Turcios, NL. (2020) Cystic Fibrosis Lung Disease: An Overview. *Respiratory Care* 65(2), p. 233. doi: 10.4187/respcare.06697

Turecka, K., Chylewska, A., Kawiak, A. and Waleron, KF. (2018) Antifungal Activity and Mechanism of Action of the Co(III) Coordination Complexes With Diamine Chelate Ligands Against Reference and Clinical Strains of *Candida* spp. *Frontiers in Microbiology* 9, p. 1594. doi: 10.3389/fmicb.2018.01594

Uddin, TM., Chakraborty, AJ., Khusro, A., Zidan, BRM., Mitra, S., Emran, TB., Dhama, K., Ripon, MKH., Gajdács, M., Sahibzada, MUK., Hossain, MJ. and Koirala, N. (2021) Antibiotic resistance in microbes: History, mechanisms, therapeutic strategies and future prospects. *Journal of Infection and Public Health* 14(12), pp. 1750-1766. https://doi.org/10.1016/j.jiph.2021.10.020

Ueno, M. and Oda, T. (2014) Biological Activities of Alginate. In: Kim, SK. ed. *Advances in Food and Nutrition Research*. Vol. 72. Academic Press, pp. 95-112. doi: 10.1016/b978-0-12-800269-8.00006-3

UK Cystic Fibrosis Registry. (2022) 2021 Annual Data Report.

Vale-Silva, LA., Coste, AT., Ischer, F., Parker, JE., Kelly, SL., Pinto, E. and Sanglard, D. (2012) Azole Resistance by Loss of Function of the Sterol Δ5,6-Desaturase Gene (ERG3) in *Candida albicans* Does Not Necessarily Decrease Virulence. *Antimicrobial Agents and Chemotherapy* 56(4), pp. 1960-1968. doi:10.1128/AAC.05720-11

van Hoek, AHAM., Mevius, D., Guerra, B., Mullany, P., Roberts, AP. and Aarts, HJM. (2011) Acquired Antibiotic Resistance Genes: An Overview. *Frontiers in Microbiology* 2, doi: 10.3389/fmicb.2011.00203

van Koningsbruggen-Rietschel, S., Davies, JC., Pressler, T., Fischer, R., MacGregor, G., Donaldson, SH., Smerud, K., Meland, N., Mortensen, J., Fosbøl, MØ., Downey, DG., Myrset, AH., Flaten, H. and Rye, PD. (2020) Inhaled dry powder alginate

oligosaccharide in cystic fibrosis: a randomised, double-blind, placebo-controlled, crossover phase 2b study. *ERJ Open Res* 6(4), doi: 10.1183/23120541.00132-2020

Vandeputte, P., Tronchin, G., Bergès, T., Hennequin, C., Chabasse, D. and Bouchara, JP. (2007) Reduced Susceptibility to Polyenes Associated with a Missense Mutation in the ERG6 Gene in a Clinical Isolate of *Candida glabrata* with Pseudohyphal Growth. *Antimicrobial Agents and Chemotherapy* 51(3), pp. 982-990. doi: 10.1128/AAC.01510-06

Veit, G., Avramescu, RG., Chiang, AN., Houck, SA., Cai, Z., Peters, KW., Hong, JS., Pollard, HB., Guggino, WB., Balch, WE., Skach, WR., Cutting, GR., Frizzell, RA., Sheppard, DN., Cyr, DM., Sorscher, EJ., Brodsky, JL. and Lukacs, GL. (2016) From CFTR biology toward combinatorial pharmacotherapy: expanded classification of cystic fibrosis mutations. *Mol Biol Cell* 27(3), pp. 424-433. doi: 10.1091/mbc.E14-04-0935

Velkov, T., Thompson, PE., Nation, RL. and Li, J. (2010) Structure− activity relationships of polymyxin antibiotics. *Journal of medicinal chemistry* 53(5), pp. 1898-1916. doi: 10.1021/jm900999h

Ventola, CL. (2015) The Antibiotic Resistance Crisis. *Pharmacy and Therapeutics* 40(4), pp. 277-283.

Vermeulen, E., Lagrou, K. and Verweij, PE. (2013) Azole resistance in *Aspergillus fumigatus*: a growing public health concern. *Curr Opin Infect Dis* 26(6), pp. 493-500. doi: 10.1097/qco.0000000000000005

Viscoli, C., Girmenia, C., Marinus, A., Collette, L., Martino, P., Vandercam, B., Doyen, C., Lebeau, B., Spence, D., Krcmery, V., De Pauw, B. and Meunier, F. (1999) Candidemia in Cancer Patients: A Prospective, Multicenter Surveillance Study by the Invasive Fungal Infection Group (IFIG) of the European Organization for Research and Treatment of Cancer (EORTC). *Clinical Infectious Diseases 28*(5), pp. 1071-1079. doi: 10.1086/514731

von Wintersdorff, CJH., Penders, J., van Niekerk, JM., Mills, ND., Majumder, S., van Alphen, LB., Savelkoul, PH. and Wolffs, PF. (2016) Dissemination of Antimicrobial Resistance in Microbial Ecosystems through Horizontal Gene Transfer. *Frontiers in Microbiology* 7, doi: 10.3389/fmicb.2016.00173

Wallace, SJ., Li, J., Nation, RL., Prankerd, RJ., Velkov, T. and Boyd, BJ. (2010) Self-Assembly Behavior of Colistin and Its Prodrug Colistin Methanesulfonate: Implications for Solution Stability and Solubilization. *The Journal of Physical Chemistry B* 114(14), pp. 4836-4840. doi: 10.1021/jp100458x

Walsh, TR. and Wu, Y. (2016) China bans colistin as a feed additive for animals. *The Lancet Infectious Diseases* 16(10), p. 1102. doi: 10.1016/S1473-3099(16)30329-2

Wang, C., Feng, Y., Liu, L., Wei, L., Kang, M. and Zong, Z. (2020a) Identification of novel mobile colistin resistance gene *mcr-10*. *Emerging Microbes & Infections* 9(1), pp. 508-516. doi: 10.1080/22221751.2020.1732231

Wang, R., van Dorp, L., Shaw, LP., Bradley, P., Wang, Q., Wang, X., Jin, L., Zhang, Q., Liu, Y., Rieux, A., Dorai-Schneiders, T., Weinert, LA., Iqbal, Z., Didelot, X., Wang, H. and Balloux, F. (2018) The global distribution and spread of the mobilized colistin resistance gene *mcr-1*. Nature Communications 9(1), p. 1179. https://doi.org/10.1038/s41467-018-03205-z

Wang, T., Flint, S. and Palmer, J. (2019a) Magnesium and calcium ions: roles in bacterial cell attachment and biofilm structure maturation. *Biofouling* 35(9), pp. 959-974. doi: 10.1080/08927014.2019.1674811

Wang, T., Kuang, W., Chen, W., Xu, W., Zhang, L., Li, Y., Li, H., Peng, Y., Chen, Y., Wang, B., Xiao, J., Li, H., Yan, C., Du, Y., Tang, M., He, Z., Chen, H., Li, W., Lin, H., Shi, S., Bi, J., Zhou, H., Cheng, Y., Gao, X., Guan, Y., Huang, Q., Chen, K., Xin, X., Ding, J., Geng, M. and Xiao, S. (2020b) A phase II randomized trial of sodium oligomannate in Alzheimer's dementia. *Alzheimer's Research & Therapy* 12(1), p. 110. doi: 10.1186/s13195-020-00678-3

Wang, X., Sun, G., Feng, T., Zhang, J., Huang, X., Wang, T., Xie, Z., Chu, X., Yang, J., Wang, H., Chang, S., Gong, Y., Ruan, L., Zhang, G., Yan, S., Lian, W., Du, C., Yang, D., Zhang, Q., Lin, F., Liu, J., Zhang, H., Ge, C., Xiao, S., Ding, J. and Geng, M. (2019b) Sodium oligomannate therapeutically remodels gut microbiota and suppresses gut bacterial amino acids-shaped neuroinflammation to inhibit Alzheimer's disease progression. *Cell Research* 29(10), pp. 787-803. doi: 10.1038/s41422-019-0216-x

Wang, Y., Tian, GB., Zhang, R., Shen, Y., Tyrrell, JM., Huang, X., Zhou, H., Lei, L., Li, HY., Doi, Y., Fang, Y., Ren, H., Zhong, LL., Shen, Z., Zeng, KJ., Wang, S., Liu, JH., Wu, C., Walsh, TR. and Shen, J. (2017) Prevalence, risk factors, outcomes, and molecular epidemiology of *mcr-1*-positive Enterobacteriaceae in patients and healthy adults from China: an epidemiological and clinical study. *The Lancet Infectious Diseases* 17(4), pp. 390-399. https://doi.org/10.1016/S1473-3099(16)30527-8

Wang, Y., Wang, G., Moitessier, N. and Mittermaier, AK. (2020c) Enzyme Kinetics by Isothermal Titration Calorimetry: Allostery, Inhibition, and Dynamics. *Frontiers in Molecular Biosciences* 7, doi: 10.3389/fmolb.2020.583826

Wang, Y., Xu, C., Zhang, R., Chen, Y., Shen, Y., Hu, F., Liu, D., Lu, J., Guo, Y., Xia, X., Jiang, J., Wang, X., Fu, Y., Yang, L., Wang, J., Li, J., Cai, C., Yin, D., Che, J., Fan, R., Wang, Y., Qing, Y., Li, Y., Liao, K., Chen, H., Zou, M., Liang, L., Tang, J., Shen, Z., Wang, S., Yang, X., Wu, C., Xu, S., Walsh, TR. and Shen, J. (2020d) Changes in colistin resistance and *mcr-1* abundance in *Escherichia coli* of animal and human origins following the ban of colistin-positive additives in China: an epidemiological comparative study. *The Lancet Infectious Diseases* 20(10), pp. 1161-1171. https://doi.org/10.1016/S1473-3099(20)30149-3

Waters, CM. and Bassler, BL. (2005) QUORUM SENSING: Cell-to-Cell Communication in Bacteria. *Annual Review of Cell and Developmental Biology* 21(1), pp. 319-346. doi: 10.1146/annurev.cellbio.21.012704.131001

Weiser, R., Rye, PD. and Mahenthiralingam, E. (2021) Implementation of microbiota analysis in clinical trials for cystic fibrosis lung infection: Experience from the OligoG phase 2b clinical trials. *Journal of Microbiological Methods* 181, p. 106133. https://doi.org/10.1016/j.mimet.2021.106133

Whitehead, NA., Barnard, AML., Slater, H., Simpson, NJL. and Salmond, GPC. (2001) Quorum-sensing in Gram-negative bacteria. *FEMS Microbiology Reviews* 25(4), pp. 365-404. doi: 10.1111/j.1574-6976.2001.tb00583.x

WHO. (2018) Critically Important Antimicrobials for Human Medicine. Geneva Switzerland: Available at: https://www.who.int/publications/i/item/9789241515528 [Accessed: 25/04/2022].

WHO. (2021) Antibacterial preclinical pipeline review. https://www.who.int/observatories/global-observatory-on-health-research-and-development/monitoring/who-antibacterial-preclinical-pipeline-review:

WHO. (2022a) Antibacterial products in clinical development for priority pathogens. https://www.who.int/observatories/global-observatory-on-health-research-and-development/monitoring/antibacterial-products-in-clinical-development-for-priority-pathogens:

WHO. (2022b) WHO fungal priority pathogens list to guide research, development and public health action. Geneva Licence CC BY-NC-SA 3.0 IGO:

Wilson, R., Sykes, D. A., Watson, D., Rutman, A., Taylor, GW. and Cole, PJ. (1988) Measurement of *Pseudomonas aeruginosa* phenazine pigments in sputum and assessment of their contribution to sputum sol toxicity for respiratory epithelium. *Infection and Immunity* 56(9), pp. 2515-2517. doi:10.1128/iai.56.9.2515-2517.1988

Wolcott, RD. and Ehrlich, GD. (2008) Biofilms and Chronic Infections. *JAMA* 299(22), pp. 2682-2684. doi: 10.1001/jama.299.22.2682

Wongsuk, T., Pumeesat, P. and Luplertlop, N. (2016) Fungal quorum sensing molecules: Role in fungal morphogenesis and pathogenicity. *Journal of Basic Microbiology* 56(5), pp. 440-447. https://doi.org/10.1002/jobm.201500759

Wouters, OJ., McKee, M. and Luyten, J. (2020) Estimated Research and Development Investment Needed to Bring a New Medicine to Market, 2009-2018. *JAMA* 323(9), pp. 844-853. doi: 10.1001/jama.2020.1166

Wu, R., Yi, LX., Yu, LF., Wang, J., Liu, Y., Chen, X., Lv, L., Yang, J. and Liu, JH. (2018) Fitness Advantage of *mcr-1*–Bearing IncI2 and IncX4 Plasmids in Vitro. *Frontiers in Microbiology* 9, doi: 10.3389/fmicb.2018.00331

Xiang, MJ., Liu, JY., Ni, PH., Wang, S., Shi, C., Wei, B., Ni, YX. and Ge, HL. (2013) *Erg11* mutations associated with azole resistance in clinical isolates of *Candida albicans. FEMS Yeast Research 13*(4), pp. 386-393. doi: 10.1111/1567-1364.12042

Xiang, R., Liu, BH., Zhang, AY., Lei, CW., Ye, XL., Yang, YX., Chen, YP. and Wang, HN. (2018) Colocation of the polymyxin resistance gene *mcr-1* and a variant of *mcr-3* on a plasmid in an *Escherichia coli* isolate from a chicken farm. *Antimicrobial agents and chemotherap*y 62(6), pp. 10.1128/aac. 00501-00518.

Xiao, S., Chan, P., Wang, T., Hong, Z., Wang, S., Kuang, W., He, J., Pan, X., Zhou, Y., Ji, Y., Wang, L., Cheng, Y., Peng, Y., Ye, Q., Wang, X., Wu, Y., Qu, Q., Chen, S., Li, S., Chen, W., Xu, J., Peng, D., Zhao, Z., Li, Y., Zhang, J., Du, Y., Chen, W., Fan, D., Yan, Y., Liu, X., Zhang, W., Luo, B., Wu, W., Shen, L., Liu, C., Mao, P., Wang, Q., Zhao, Q., Guo, Q., Zhou, Y., Li, Y., Jiang, L., Ren, W., Ouyang, Y., Wang, Y., Liu, S., Jia, J., Zhang, N., Liu, Z., He, R., Feng, T., Lu, W., Tang, H., Gao, P., Zhang, Y., Chen, L., Wang, L., Yin, Y., Xu, Q., Xiao, J., Cong, L., Cheng, X., Zhang, H., Gao, D., Xia, M., Lian, T., Peng, G., Zhang, X., Jiao, B., Hu, H., Chen, X., Guan, Y., Cui, R., Huang, Q., Xin, X., Chen, H., Ding, Y., Zhang, J., Feng, T., Cantillon, M., Chen, K., Cummings, JL., Ding, J., Geng, M. and Zhang, Z. (2021) A 36-week multicenter, randomized, double-blind, placebo-controlled, parallel-group, phase 3 clinical trial of sodium oligomannate for mild-to-moderate Alzheimer's dementia. *Alzheimer's Research & Therapy* 13(1), p. 62. doi: 10.1186/s13195-021-00795-7

Xing, M., Cao, Q., Wang, Y., Xiao, H., Zhao, J., Zhang, Q., Ji, A. and Song, S. (2020) Advances in Research on the Bioactivity of Alginate Oligosaccharides. *Mar Drugs* 18(3), doi: 10.3390/md18030144

Xu, X., Bi, D., Wu, X., Wang, Q., Wei, G., Chi, L., Jiang, Z., Oda, T. and Wan, M. (2014) Unsaturated guluronate oligosaccharide enhances the antibacterial activities of macrophages. *The FASEB Journal* 28(6), pp. 2645-2654. https://doi.org/10.1096/fj.13-247791

Xu, Y., Zhong, LL., Srinivas, S., Sun, J., Huang, M., Paterson, DL., Lei, S., Lin, J., Li, X., Tang, Z., Feng, S., Shen, C., Tian, GB. and Feng, Y. (2018) Spread of MCR-3 Colistin Resistance in China: An Epidemiological, Genomic and Mechanistic Study. *EBioMedicine* 34, pp. 139-157. https://doi.org/10.1016/j.ebiom.2018.07.027

Yahav, D., Farbman, L., Leibovici, L. and Paul, M. (2012) Colistin: new lessons on an old antibiotic. *Clinical Microbiology and Infection* 18(1), pp. 18-29. https://doi.org/10.1111/j.1469-0691.2011.03734.x

Yang, A., Tang, WS., Si, T. and Tang, JX. (2017a) Influence of Physical Effects on the Swarming Motility of *Pseudomonas aeruginosa*. *Biophysical Journal* 112(7), pp. 1462-1471. https://doi.org/10.1016/j.bpj.2017.02.019

Yang, Q., Li, M., Spiller, OB., Andrey, DO., Hinchliffe, P., Li, H., MacLean, C., Niumsup, P., Powell, L., Pritchard, M., Papkou, A., Shen, Y., Portal, E., Sands, K., Spencer, J., Tansawai, U., Thomas, D., Wang, S., Wang, Y., Shen, J. and Walsh, T. (2017b) Balancing *mcr-1* expression and bacterial survival is a delicate equilibrium between essential cellular defence mechanisms. *Nature Communications* 8(1), p. 2054. doi: 10.1038/s41467-017-02149-0

Yang, QE., MacLean, C., Papkou, A., Pritchard, M., Powell, L., Thomas, D., Andrey, DO., Li, M., Spiller, B., Yang, W. and Walsh, TR. (2020) Compensatory mutations modulate the competitiveness and dynamics of plasmid-mediated colistin resistance in *Escherichia coli* clones. *The ISME Journal* 14(3), pp. 861-865. doi: 10.1038/s41396-019-0578-6

Yao, X., Doi, Y., Zeng, L., Lv, L. and Liu, JH. (2016) Carbapenem-resistant and colistin-resistant *Escherichia coli* co-producing NDM-9 and MCR-1. *The Lancet Infectious Diseases* 16(3), pp. 288-289. doi: 10.1016/S1473-3099(16)00057-8.

Yap, PS., Cheng, WH., Chang, SK., Lim, SE. and Lai, KS. (2022) MgrB Mutations and Altered Cell Permeability in Colistin Resistance in *Klebsiella pneumoniae*. *Cells* 11(19), doi: 10.3390/cells11192995

Yin, W., Li, H., Shen, Y., Liu, Z., Wang, S., Shen, Z., Zhang, R., Walsh, TR., Shen, J. and Wang, Y. (2017) Novel Plasmid-Mediated Colistin Resistance Gene *mcr-3* in *Escherichia coli*. *mBio* 8(3), pp. e00543-00517. doi:10.1128/mBio.00543-17

Yu, Z., Qin, W., Lin, J., Fang, S. and Qiu, J. (2015) Antibacterial mechanisms of polymyxin and bacterial resistance. *Biomed Res Int* 2015(679109), doi: 10.1155/2015/679109.

Zeng, D., Debabov, D., Hartsell, TL., Cano, RJ., Adams, S., Schuyler, JA., McMillan, R. and Pace, JL. (2016) Approved Glycopeptide Antibacterial Drugs: Mechanism of Action and Resistance. *Cold Spring Harbor Perspectives in Medicine* 6(12), doi: 10.1101/cshperspect.a026989

Zhang, F. and Cheng, W. (2022) The Mechanism of Bacterial Resistance and Potential Bacteriostatic Strategies. *Antibiotics* 11(9), p. 1215. doi: 10.3390/antibiotics11091215.

Zhao, J., Shen, Y., Haapasalo, M., Wang, Z. and Wang, Q. (2016) A 3D numerical study of antimicrobial persistence in heterogeneous multi-species biofilms. *Journal of Theoretical Biology* 392, pp. 83-98. https://doi.org/10.1016/j.jtbi.2015.11.010

Zheng, S., Bawazir, M., Dhall, A., Kim, HE., He, L., Heo, J. and Hwang, G. (2021) Implication of surface properties, bacterial motility, and hydrodynamic conditions on bacterial surface sensing and their initial adhesion. *Frontiers in Bioengineering and Biotechnology* 9, p. 643722. https://doi.org/10.3389/fbioe.2021.643722

Zijnge, V., van Leeuwen, MBM., Degener, JE., Abbas, F., Thurnheer, T., Gmür, R. and M. Harmsen, HJ. (2010) Oral Biofilm Architecture on Natural Teeth. *PLOS ONE* 5(2), p. e9321. doi: 10.1371/journal.pone.0009321

Zipfel, PF., Skerka, C., Kupka, D. and Luo, S. 2011. Immune escape of the human facultative pathogenic yeast *Candida albicans*: The many faces of the *Candida* Pra1 protein. *International Journal of Medical Microbiology* 301(5), pp. 423-430. doi: 10.1016/j.ijmm.2011.04.010